Insights into Anticodon Nuclease Toxicity and Rescue by tRNA Repair *in vivo*

Dissertation

der Mathematisch-Naturwissenschaftlichen Fakultät

der Eberhard Karls Universität Tübingen

zur Erlangung des Grades eines

Doktors der Naturwissenschaften

(Dr. rer. nat.)

vorgelegt von

Birthe Meineke

aus Göttingen

2011

Tag der mündlichen Qualifikation:	21. 11. 2011
Dekan:	Prof. Dr. Wolfgang Rosenstiel
1. Berichterstatter:	Prof. Dr. Thilo Stehle
2. Berichterstatter:	Stewart H. Shuman, MD, PhD

Summary

A group of cytotoxic bacterial and fungal endoribonucleases targets the anticodon loop of specific tRNAs. These anticodon nucleases (ACNases) produce 2′,3′-cyclic phosphate and 5′-hydroxyl termini at their specific cleavage sites reminiscent of the first step in metal-independent general acid-base catalysis by RNase A. Despite their similarities, ACNases share no unifying homology in their primary structures. The presently identified ACNases can be subdivided into bacterial toxin-antitoxin ACNases (VapC and colicins E5 and D), bacterial intracellular ACNases (PrrC and RloC) and fungal ACNases (subunits of *Kluyveromyces lactis* and *Pichia acaciae* killer toxins). My studies were oriented toward increasing insight into ACNase structure function-relationships and the capacity of tRNA damage repair to overcome ACNase toxicity.

Initially the $tRNA^{Glu\ (UUC)}$ specific ACNase γ-toxin of *K. lactis* had been used as a tool to study tRNA repair enzymes. In a subsequent study, the ribonuclease of γ-toxin became the focus of an extensive mutational analysis aimed to identify candidate residues for RNase A like catalysis. I investigated whether the same tRNA repair enzymes that protect *Saccharomyces cerevisiae* from γ-toxin can also protect against *Pichia acaciae* killer toxin. The ACNase subunit of this toxin (PaT) cleaves $tRNA^{Gln}$ at two possible positions. Incision at one position or nucleotide excision by cleavage at both positions depends on PaT gene dosage and *S. cerevisiae* genetic background. PaT dosage and modification state of the target tRNA also influence if rescue by repair can be successful.

After the discovery that intracellular expression of PrrC is toxic to *S. cerevisiae*, I focused on the mutational analysis of $tRNA^{Lys}$ specific *E. coli* PrrC. This was followed by characterization of the *in vivo* toxicity and the finding that expression of PrrC is fungicidal, not fungistatic. PrrC's ACNase has been proposed to reside in the C-terminal domain. The N-terminal domain of PrrC is homologous to the well-characterized nucleotide binding domain (NBD) / NTPase domain of members of the ABC superfamily. I also addressed whether the proposed domains of PrrC both contribute to ACNase activity and whether the N-terminal NBD-like domain is truly related to the ABC superfamily. Expression of separate domains is not toxic *in trans* and mutations in the predicted active site of either domain abolish PrrC activity in yeast *in vivo*. Assessing the dominant negative effect of PrrC-Ala mutants, I found evidence for *in vivo* oligomerization of PrrC.

In addition to *E. coli* PrrC, I investigated the toxicity of PrrC homologs encoded in other bacteria, in order to address whether cytotoxicity and ACNase activity are a general property of this protein family. *Streptococcus mutans* PrrC is fungicidal and bactericidal. Surprisingly, the close homolog of *E. coli* PrrC from *Neisseria meningitides* was non-toxic both in *E. coli* and yeast. Further investigation of this finding by generation of PrrC chimeras and homology-guided mutational analysis of *N. meningitides* PrrC identified the R316W gain-of-toxicity mutant. I characterized the toxicity of this mutant *in vivo* in yeast and found that it is less toxic than *E. coli* PrrC but displays the same specificity for $tRNA^{Lys}$. The R316W mutant of *N. meningitides* PrrC thus allowed the study of repair of PrrC tRNA damage *in vivo*. From these investigations of ACNase toxicity it becomes evident that *S. cerevisiae* is susceptible to tRNA damage, as its endogenous tRNA ligase Trl1 cannot counteract the tRNA damage inflicted.

New aspects of tRNA repair became apparent when archaeal, human and *E. coli* RtcB proteins were identified as RNA ligases. Archaeal and human RtcB could function in a tRNA splicing pathway. However, the biological role of bacterial RtcB remains unclear. To begin to understand the role of *E. coli* RtcB, I investigated if it can function as a ligase in yeast tRNA splicing and if it is capable of repairing ACNase tRNA damaged *in vivo*. *E. coli* RtcB is sufficient to complement lethal *TRL1* deletion in *S. cerevisiae* and it also protects from PaT ACNase toxicity in *trl1Δ* cells.

Zusammenfassung

Eine Gruppe zytotoxischer Endoribonukleases von Bakterien und Pilzen richtet sich gegen die Anticodonschleife spezifischer tRNAs. Diese Anticodonnukleasen (ACNasen) hinterlassen 2′,3′-zyklisches Phosphate and 5′-hydroxyl Termini an ihren jeweiligen Schnittstellen, die auch nach dem ersten Schritt der Metall-unabhängigen Säure-Base Katalyse von RNase A auftreten. Trotz dieser Ähnlichkeiten besteht keine vereinende Homologie unter den Primärstrukturen der ACNasen. Die derzeit bekannten ACNasen lassen sich in Toxin-Antitoxin ACNasen (VapC und Colicine E5 und D), bakterielle intrazelluläre ACNasen (PrrC und RloC) und ACNasen von Pilzen (Untereinheiten der Killertoxine von *Kluyveromyces lactis* und *Pichia acaciae*) unterteilen. Meine Promotionsstudien haben neue Einblicke in den Zusammenhang von Struktur und Funktion

von ACNasen gewährt. Zusätzlich habe ich untersucht inwiefern tRNA Reparaturenzyme die Toxizität von ACNasen überwinden können.

Die spezifisch gegen tRNA $^{Glu\ (UUU)}$ gerichtete ACNase γ-toxin von *K. lactis* wurde bereits als Hilfsmittel zum Studium von tRNA Reparaturmechanismen verwendet. In einer darauf folgenden Studie, wurde die Ribonucleaseaktivität von γ-toxin in einer ausführlichen Mutationsanalyse unterzogen, um katalytischen Aminosäurereste in RNase A-artiger Katalyse zu identifizieren. Ich habe untersucht, ob die gleichen tRNA Reparaturenyzme, welche *Saccharomyces cerevisiae* vor γ-toxin schützen, auch gegen das Killertoxin von *Pichia acaciae* wirken können. Die ACNase Untereinheit dieses Toxins (PaT) spaltet $tRNA^{Gln}$ in zwei Positionen der Anticodonschleife. Der Schnitt an einer, oder Entfernung von Nukleotiden durch Spaltung an beiden Stellen, hängt von der Gendosis PaTs als auch dem genetischen Hintergrund der PaT exprimierenden *S. cerevisiae* Zellen ab. Meine Studien zeigten, dass PaT Dosis und der Modifikationsstatus der angegriffenen tRNA auch Reparatur der tRNA beeinflusst.

Auf Basis der Entdeckung, dass intrazelluläre Expression von PrrC toxisch für *S. cerevisiea* ist, habe ich mich auf die Mutationsanalyse von *E. coli* PrrC konzentriert. Ich habe die *in vivo* Toxizität von PrrC untersucht und herausgefunden, dass PrrC Expression fungizid und nicht fungistatisch ist. Frühere Analysen der Primärstruktur von PrrC haben darauf hingewiesen, dass PrrC zwei funktionelle Domänen enthält. Die ACNase Aktivtät wurde der C-terminalen Domäne zu gewiesen. Die N-terminale Domäne PrrCs ist den Nuklotidbindedomänen (NBD)/NTPase-Domänen in Mitgliedern der ABC-Superfamilie homolog. Ich habe geprüft, ob beide Domänen zur Toxizität von PrrC beitragen und ob die NBD tatsächlich funktional mit der ABC-Superfamilie verwandt ist. Getrennte Expression der Domänen ist nicht toxisch und Mutationen in Resten der vorgeschlagenen aktiven Zentren in beiden Domänen beeinflusst PrrC Aktivität in Hefe *in vivo*. Der dominant-negative Effekt von PrrC Mutanten mit Wildtyp PrrC wies auf eine *in vivo* Oligomerisierung von PrrC hin.

Zusätzlich zu *E. coli* PrrC habe ich die Toxizität von PrrC Homologen anderer Bakterien getestet um herauszufinden, ob ACNase Aktivität allen Mitgliedern dieser Proteinfamilie eigen ist. *Streptococcus mutans* PrrC ist sowohl fungizid als auch bakterizid. Überraschenderweise hat Expression von *Neisseria meningitides* PrrC, trotz ausgeprägter Homologie mit dem *E. coli* Protein, keinen toxischen Effekt in Hefe oder *E. coli*. Genauere Untersuchung anhand von Chimären und Punktmutationen führte zur Identifizierung einer

R316W Mutation mit toxischer Aktivität. Ich habe die Toxizität dieser Mutante in Hefe *in vivo* charakterisiert und herausgefunden, dass die Spezifität mit der von *E. coli* PrrC übereinstimmt. Die Toxizität ist im Vergleich zu *E. coli* PrrC geringer. Die R316W Mutante von *N. meningitides* PrrC hat es ermöglicht die Reparatur von PrrC induzierten tRNA-Schäden zu untersuchen. Diese Studien von ACNase Toxizität verdeutlichen, dass *S. cerevisiae* für Schäden in der tRNA besonders anfällig ist, da die endogene tRNA Ligase Trl1 nicht in der Lage ist derartige Schäden zu beseitigen.

Neue Aspekte der tRNA Reparatur haben sich mit der Entdeckung von RtcB in Archaeen, Menschen und Bakterien als RNA-Ligase eröffnet. RtcB füllt eine lange bestehende Lücke im Verständnis des tRNA Splicemechanismus von Archaeen und Metazoen. Die biologische Rolle von bakteriellem RtcB ist nach wie vor unklar,. Ich habe gestestet, ob *E. coli* RtcB als Ligase Trl1 in Hefe ersetzen kann und ob es dem tRNA Schaden durch ACNasen *in vivo* entgegenwirken kann. Expression von *E. coli* RtcB komplementiert die lethale *TRL1* Deletion in *S. cerevisiae* und kann vor der Toxizität von PaT in *trl1Δ* Zellen schützen.

Table of Contents

1 Introduction

1.1 Anticodon nucleases - tRNA damage as non-self restriction and host defense

Transfer RNAs (tRNAs) deliver amino acids, the building blocks for protein synthesis, to the ribosome to translate genetic information into protein primary structure. Recent studies highlight cleavage of tRNA as a means to arrest protein synthesis in response to a variety of intra- and extra-cellular stresses e.g. starvation or reactive oxygen species, but also as a defense against viruses or non-self species (1-8). Apart from depleting the cell of functional amino-acyl-tRNA precursors for protein synthesis, it has been suggested that nicked tRNAs can also directly stall the ribosome active site (9,10). Additionally, tRNA fragments could signal to yet undiscovered downstream pathways. Cleavage of tRNA in response to stress is not limited to specific tRNA species or specific positions, although the anticodon loop is frequently targeted, likely due to its exposed position in folded tRNAs (10,11).

A unique group of toxic endoribonucleases cleaves tRNA at specific positions in the anticodon loop, usually at the wobble nucleotide (4-8). These anticodon nucleases (ACNases) are either secreted to restrict the growth of other cells, or controlled intracellularly to arrest self-growth or block virus infection. To date, seven ACNases have been described: Two are secreted fungal toxins. The other five are secreted, or intracellular, bacterial ACNases. All known ACNases produce 2′,3′-cyclic phosphate and 5′-hydroxyl termini at the cleavage site. Based on this common chemistry, mechanims similar to RNase A and RNAse T1 were suggested. The toxic activity of ACNases can be suppressed by binding to other proteins. Through these interactions, the ACNases are sequestered in a latent state. Toxic tRNA cleavage occurs only after latency is alleviated, either by displacement of the ACNase from the latent complex, or by entry of the ACNase into its target cell. Despite their common chemical mechanism, the phylogenetic distribution of functional ACNases and the lack of unifying amino acid sequence similarities suggest, that they convergently evolved to accomplish similar tasks.

1.1.1 Metal independent RNA cleavage by RNAse A and RNase T1

RNA breakage is achieved by the attack of a nucleophile on the RNA phosphodiester backbone between two nucleotides. In the simplest case, hydrolysis, the nucleophile is water. Depending on the geometry of hydrolytic attack, either the 5′ fragment, or the 3′ fragment are displaced. Thus, RNA hydrolysis yields either 5′ hydroxyl and 3′ phosphate ends, or 5′ phosphate and 3′ hydroxyl ends. When a 2’-hydroxyl acts in RNA cleavage, the products of transphosphorylation are 2′,3′-cyclic phosphate and 5′ hydroxyl fragments.

A

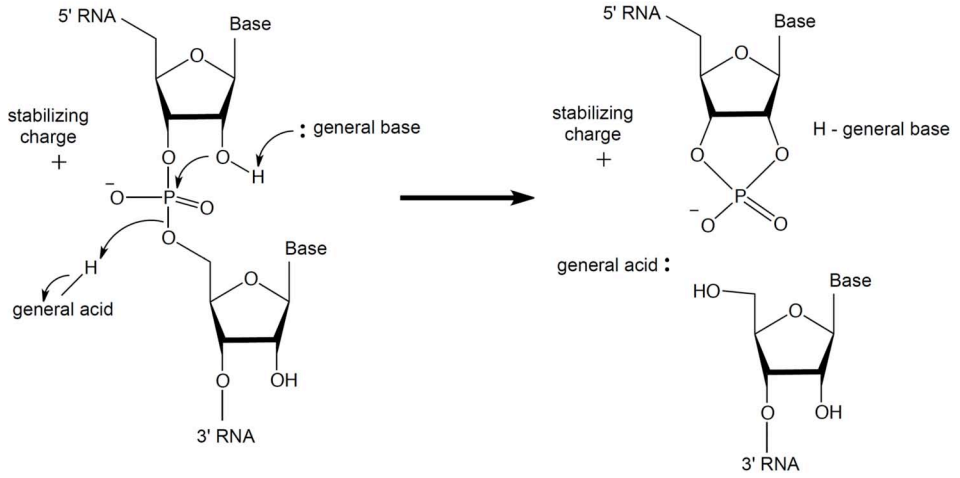

B

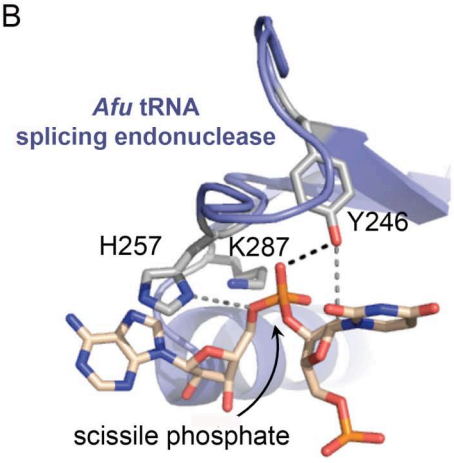

	general base	general acid	charge stabilizing
RNase A	His12	His119	Lys41
RNase T1	His 40/Glu58	His92	Arg77
Afu Sen	Tyr246	His257	Lys287
Colicin E5	Asp54?		Arg56?
Colicin D	His611	Asp614?	Lys608 or Lys610

Figure 1 – **Mechanism of metal independent tRNA cleavage**

(A) The first step of RNase A and RNase T1 catalysis, the mechanism of tRNA splicing endonucleases and the putative mechanism of anticodon nucleases. A general base activates the 2′-hydroxyl for in-line attack on the scissile phosphate to yield a 2′,3′-cyclic phosphate. The 3′ leaving group is protonated by a general acid (12). **(B)** *Left* The active site of *A. fulgidus* tRNA splicing endonuclease bound to a bulge-helix-bulge RNA (PDB 2GJW) (13). The catalytic residues and the bound dinucleotide are shown as stick models, hydrogen bonds are shown as dashed lines. *Right* Listing the identified or suggested general base, general acid and charge-stabilizing catalytic residues of RNase A, RNase T1, colicins E5 and D, and *A. fulgidus* tRNA splicing endonuclease (*Afu* Sen).

The prototypical metal-independent RNase, RNase A, follows such a transphosphorylation mechanism. RNase A specifically cleaves single stranded RNA 3′ of pyrimidine nucleotides. The RNase A mechanism has been studied in detail: His12, acting as general base, abstracts the proton from the 2′ hydroxyl group at the cleavage site ribose, facilitating the nucleophilic attack on the phosphodiester linkage. The attack proceeds in line to displace the 3′ nucleoside or oligonucleotide leaving-group which is protonated by His119, acting as general acid (Figure 1A). In a second, separate step, the resulting 2′,3′-cyclic phosphate is invariably opened to 3′ phosphate in a process that resembles the reverse transphosphorylation. Thus both His12 and His119 are returned to their initial protonation states. Both steps proceed via a pentavalent transition state that is stabilized by Lys41 (12).

RNase T1 of *Aspergillus oryzae* represents another family of metal independent RNases. RNase T1 specifically cleaves single stranded RNA 3′ of guanine nucleotides. This specificity is mediated by guanine-specific hydrogen bonds formed with the side chains and a backbone amide of three residues in RNase T1. In contrast to RNase A, RNase T1 is thought to employ a catalytic dyad to initiate the nucleophilic attack: His40, protonated at Nε, and Glu58 engage the substrate 2′-hydroxyl group in hydrogen bonds and thus polarize the nucleophile. The reaction proceeds in line as in RNase A, with His92 acting as general base and Arg77 stabilizing the transition state (Figure 1B). Like RNase A, RNAse T1 selectively opens 2′,3′-cyclic phosphate to 3′ phosphate in a second step (14). The endoribonucleases discussed below yield 2′,3′-cyclic phosphate and 5′-hydroxyl fragments as their final products. Based on this outcome, mechanisms comparable to the first step of RNase A and RNase T1 catalysis have been invoked or confirmed for them.

1.2 Bacterial anticodon nucleases

The ACNases identified in bacteria to date fall into two categories: intracellular ACNases, which arrest self-growth, and secreted ACNases, that kill other susceptible cells (non-self restriction). RNase A-like mechanisms were suggested for all but one bacterial ACNase. The exception is the VapC of *Salmonella enterica* and *Shigella flexneri,* which was recently discovered to target initiator $tRNA^{Met}$ (15). Below I will discuss the intracellular ACNases PrrC (which was the focus of my investigations), its described distant homolog RloC, and the well characterized secreted colicins E5 and D. The crystal structures solved for these colicins give insight into tRNA substrate recognition by ACNases.

1.2.1 The intracellular ACNase *E. coli* PrrC

E. coli PrrC exemplifies the group of intracellular ACNases and was the first ACNase to be described (4,16). The optional *prr* locus contains four open reading frames: the $tRNA^{Lys}$-specific ACNase PrrC and a type Ic DNA restriction-modification enzyme PrrABD (17,18). PrrABD consists of three-subunits: a DNA methylation subunit, a specificity subunit and a restriction subunit, PrrA, PrrB and PrrD respectively (19). *Eco*PrrC is involved in an arms race between *E. coli* and T4 phage (Figure 2A): in uninfected prr^+ cells *Eco*PrrC exists in a latent state bound to PrrABD, however, upon infection the phage peptide Stp inhibits the DNA restriction enzyme and frees *Eco*PrrC to induce cytotoxic tRNA damage (20-22). The tRNA damage is overcome by the tRNA repair activities of T4 phage enzymes Pnkp (polynucleotide kinase and phosphatase) and the RNA ligase Rnl1 thwarting altruistic suicide of the bacterial cells to ensure phage production (23,24). Therefore, *Eco*PrrC only ablates spreading of $rnl1^-$ or $pnkp^-$ T4 phages (4,25).

The tRNA fragments produced by *Eco*PrrC were analyzed for break position and nature of the break termini: $tRNA^{Lys}$ is broken by cleavage of a single phosphodiester bond between uridine in position 33 and the modified wobble uridine (Figure 2B). Isolated $tRNA^{Lys}$ halves from $pnkp^-$ infected cells have 2′,3′-cyclic phosphate and 5′-hydroxyl termini, while $rnl1^-$ infected cells contained $tRNA^{Lys}$ halves with 2′,3′-diol and 5′-phosphate at the break site (4). From these findings, it was derived that Pnkp phosphorylates the 5′ break terminus and dephosphorylates the cyclic 3′ end (leading to the termini found in cells infected with $rnl1^-$ phage). These ends are subsequently ligated by the RNA ligase Rnl1 (1.4.1).

Expression of plasmid-encoded *Eco*PrrC is sufficient to induce toxic ACNase activity in *E. coli* and HeLa cells (26,28). Cleavage of mammalian $tRNA^{Lys,3}$ by *Eco*PrrC was shown *in vitro* (26). *E. coli* only encodes a single isoacceptor of $tRNA^{Lys}$, which shares the UUU anticodon with mammalian $tRNA^{Lys,3}$. Eukarya additionally have a second lysine isoacceptor: $tRNA^{Lys\,(CUU)}$. *E. coli* and human $tRNA^{Lys\,(UUU)}$ isoacceptors differ, within the anticodon loop, only on the level of posttranscriptional modifications (Figure 2B). The wobble uridine at position 34 and the adenine base at position 37 are modified differently in bacteria and eukarya.

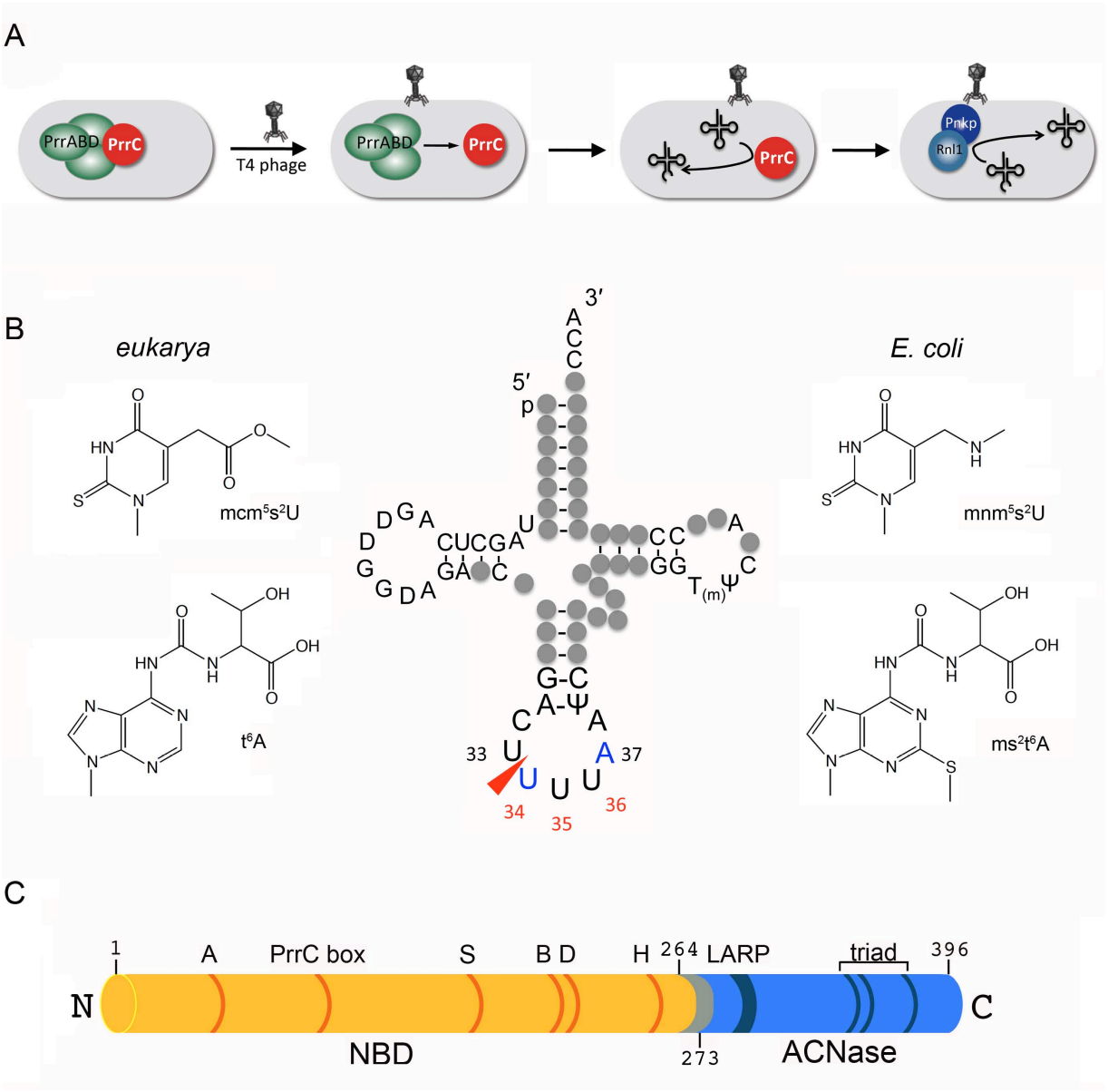

Figure 2 – **The *E. coli* anticodon nuclease PrrC**

(A) Activation of *Eco*PrrC after T4 phage infection, see text for details. (Adapted from [22]). **(B)** The *Eco*PrrC target $tRNA^{Lys}_{(UUU)}$ of *E. coli* and eukarya. Nucleotides that differ between *E. coli*, *S. cerevisiae* and human tRNA are depicted as grey circles. The UUU anticodon is numbered in red, adjacent positions are numbered in black, according to convention. Position of cleavage by *Eco*PrrC is shown as a red arrowhead. The post-transcriptional modifications of U34 and A37 (blue) are shown on the sides. (26,27). **(C)** Presumed domain structure of the *Eco*PrrC polypeptide. The putative ABC NBD-like domain (yellow) and the ABC motifs conserved in PrrC proteins (orange) lie in the N-terminal domain. PrrC shares Walker A motif (A), Walker B motif (B), signature motif (S), D-loop motif (D) and H-loop motif (H) with the ABC superfamily. Additionally, all PrrC proteins also share the PrrC box. The putative ACNase domain (blue) with the $tRNA^{Lys}$ recognition peptide (LARP) and presumed catalytic triad comprise the C-terminal domain. The two possible domain boundaries are labeled with the corresponding residue numbers.

Mature *E. coli* $tRNA^{Lys}$ contains a 5-methylaminomehtyl-2-thio-uridine (mnm^5s^2U) wobble base and a 6-threonyl-carbamoyladenosine (t^6A) in position 37, which rigidify the anticodon in A-RNA conformation (29). In eukarya, the $tRNA^{Lys\ (UUU)}$ wobble uridine is 5-methoxycarbonylmethyl-2-thio modified (mcm^5s^2) and A37 carries a 2-methylthio-6-threonylcarbamoyl (ms^2t^6) modification (Figure 2B).

Both mnm^5s^2U34 and t^6A37 modifications enhance *in vitro* cleavage of synthetic anticodon loop substrates in *Eco*PrrC containing cell extracts (30). Cleavage of such 17mer substrates shows that the anticodon sequence and t^6A37 are sufficient for *Eco*PrrC recognition. *In vitro* studies rank $mnm^5s^2U > U > C > mcm^5s^2U$ as *Eco*PrrC's wobble nucleotide preference (27). Nevertheless, *Eco*PrrC is able to cleave *in vitro* transcribed unmodified *E. coli* $tRNA^{Lys}$, as well as the hypomodified wobble uridine species in *mnmA* cells (containing mnm^5U) and *mnmE* cells (containing s^2U) (27). The same study points to an involvement of Asp287 in substrate recognition, as a D287Q mutant of *Eco*PrrC prefers $tRNA^{Lys}$ deficient of the mnm^5 modification to the natural substrate.

Activation of PrrABD-bound latent *Eco*PrrC requires the presence of DNA in the complex and the phage Stp peptide (31). GTP and dTTP nucleotides have an additional effect on the activation process. While there are indications that GTP is hydrolyzed, dTTP is interacting allosterically. Intracellular dTTP levels increase upon T4 phage infection through the activity of phage dCMP deaminase. Infections with dCMP deaminase-deficient phage leads to delayed *Eco*PrrC activation, thus dTTP is not necessary yet stimulating *Eco*PrrC activation from latency (32). Nucleotides also affect the activity of *Eco*PrrC in absence of masking PrrABD. In partially purified extracts dTTP and ATP stimulate $tRNA^{Lys}$ cleavage by *Eco*PrrC and UV-crosslinking experiments indicated binding of GTP, ATP and dTTP (31,33).

Genes encoding PrrC homologs are found in strains of distantly related bacteria in the context of *prr* operons also encoding PrrABD genes (31,33). The random distribution of *prr* loci in isolated strains of many different bacteria and a high frequency of mobile elements (e.g. transposons) flanking the operons, suggest genetic mobility of *prr* loci. To date, *Eco*PrrC is the only representative of this protein family for which a biological role has been studied and a specific RNA target identified. The 396 amino acid sequence of *Eco*PrrC contains a Walker A or P-loop motif (^{40}AFNGTGKT^{47}) towards its amino-terminus (Figure 2C) (28). Mutations in this motif affect $tRNA^{Lys}$ cleavage activity (31). Further sequence analysis showed overall similarity of *Eco*PrrC's N-terminal 2/3 (residues 1-264)

with the nucleotide-binding domain (NBD) of ATP binding-cassette (ABC) family of proteins (31,33). The motifs and their function in ABC-proteins are described in detail below (1.2.3). In light of the known structures of ABC NBDs, the domain boundary in *Eco*PrrC might lie further towards the C-terminus at Ser273 (12 amino acids after the H-loop motif) to account for a structurally conserved β-sheet (Figure 3B). The role of this putative ABC domain in ACNase catalysis is unclear.

The ACNase activity was attributed to the remaining residues 265-396 (274-396 respectively) of *Eco*PrrC (Figure 2C) (34). Random missense mutations selected for reduced ACNase activity mapped to residues 287-303 (34). As Asp287, suggested to be involved in wobble base recognition, lies in this region, residues ^{284}KYGDSNKSFSY^{294} were implied in lysine anticodon recognition (34,35). This lysine anticodon recognition peptide (LARP) motif is conserved in only a few PrrC homologs e.g. those of *Nesseria meningitidis* and *Haemophilus influenza*, it deviates in the PrrC homolog of *Streptococcus mutans* (Figure 3). This might reflect shared and differing substrate specificity compared to *E. coli* PrrC, respectively. The search for RNase A-like general acid-base catalysis candidate residues within the ACNase domain led the proposition of a putative catalytic triad, consisting of Arg320, Glu324 and His356 (33).

Self-limiting expression and inhibition of cell growth by depletion of $tRNA^{Lys}$ preclude standard methods of over-expression for protein purification of *Eco*PrrC (33,34). In expressing a hypomorphic mutant, D222E, which is less active and therefore expressed more abundantly in *E. coli*, the Kaufmann lab have isolated 45 kDa *Eco*PrrC. The presence of 2 M TMAO (trimethylamine oxide) and 2-10 μM dTTP reportedly increase protein stability. ACNase activity co-purifies with the D222E *Eco*PrrC protein. The D222E *Eco*PrrC elution volume in size-exclusion chromatography corresponds to a molecular weight of ~200 kDa, suggesting a tetrameric organization of PrrC. This result is supported by glutaraldehyde crosslinking data (33). These *Eco*PrrC homotetramers are proposed to form by dimerization of the NBD domain, in the head-to-tail fashion shown for ABC NBDs, and by parallel dimerization at the LARP motif in the ACNase domain (33,35). The proposition of parallel ACNase dimerization is based on studies where peptides with the LARP sequence could be crosslinked to RNA, *Eco*PrrC protein and themselves (35). Whether these *Eco*PrrC oliogomers are formed non-transiently or cycle through conformations analogous to ABC NBDs and how the multimeric state affects activity remains unknown.

1.2.2 RloC, a distant relative of PrrC

Database searches based on *Eco*PrrC's amino acid sequence lead to the discovery of the more distantly related RloC family of proteins. Genes encoding RloC proteins were first found as insertion in type I DNA restriction-modification loci of *Campylobacter jejuni* strains and were named "restriction linked ORF" (Rlo). However, most *rloC* genes do not actually lie within such loci. RloC proteins share the NBD motifs with PrrC proteins and also share the residues of the potential ACNase triad, however RloCs are roughly twice the size of PrrC proteins. This increase in size is due to the insertion of a Rad50-like coiled-coil domain and central CxxC zinc-binding motif. Davidov and Kaufmann expressed 804aa *Geobacillus kaustophilus* RloC in *E. coli* and studied its properties in cell extracts. Expression of plasmid-borne *Gka*RloC impairs cell growth. The phenotype is enhanced by cysteine to glycine mutations in the zinc-binding motif. This result suggests a Zn^{2+} regulation of wild type RloC. *Gka*RloC over-expression in *E. coli* leads to breakage of several tRNAs, preferentially $tRNA^{Glu}$. When extracts of *Gka*RloC expressing cells were used to cleave $tRNA^{Lys}$, the recovered fragments were not only incised, but *Gka*RloC had excised the wobble nucleotide (36). Although the biological role of RloC and its coiled-coil remain obscure, *Gka*RloC is the first described member of a new class of ACNases, related to, but distinct from PrrC proteins.

1.2.3 Homology of PrrC with ATP binding cassette proteins

The N-terminal domain of *Eco*PrrC contains primary structure motifs, conserved in PrrC homologs and the more distant family of RloC proteins, that are characteristic of ATP binding cassette (ABC) proteins (Figure 3B) (31,33,36). The nucleotide-binding domain (NBD) is the uniting feature of this large ABC-superfamily present in all three domains of life (37). The NBD couples ATP hydrolysis to a conformational change, which is relayed to other components of the respective ABC system to perform a variety of biological activities. In addition to ATP hydrolysis, adenylate kinase activity is catalyzed in the active site of at least some members of the superfamily (38).

The ABC superfamily can be divided in three main functional categories (37):

(i) Transmembrane importers e.g. HisP and MalK components of the *Salmonella enterica* histidine and *E. coli* maltose uptake systems, respectively.

(ii) Transmembrane exporters e.g. multidrug resistance (MDR) proteins like human TAP1/TAP2 and *Staphylococcus aureus* Sav1866.

(iii) Non-transporters involved in DNA repair (e.g. Rad50), mRNA translation (e.g. *S. cerevisiae* translation elongation factor Tef3) and antibiotic resistance (e.g. *Staphylococci* VgaA proteins).

ABC proteins are multidomain proteins containing other functional domains beside the NBD, present on the same polypeptide as the NBD or in separate subunits. Transporter ABCs are membrane anchored via a transmembrane domain (TMD). While in most ABC importers the NBD and TMD are independent chains, in most exporters both NBD and TMD are present on the same polypeptide chain as NBD-TMD or TMD-NBD fusions. Non-transporter ABCs can comprise more than one NBD domain on a single polypeptide chain. The NBD can also be interrupted by another functional domain, as exemplified by a coiled coil insertion in Rad50 (37).

The ABC protein family is defined by presence of Walker A or P-loop and Walker B nucleotide binding motifs, as well as the LSGGQ-consensus ABC-signature motif in the NBD. Structurally, the NBD consists of two sub-domains joined by two flexible loops: a RecA-like motor ATPase that contains the Walker A and B motifs and a α-helical subdomain containing the signature motif (helices C through F in Figure 3A) (37). In crystal structures of NBD monomers, the Walker A and B motifs are far away from the signature motif. Yet both are involved in nucleotide binding and catalysis, as NBDs form head-to-tail dimers upon ATP binding. The nucleotide is sandwiched between the Walker A and B motifs of the *cis*-protomer and signature motif of the *trans*-protomer. The first crystal structure of such a physiological dimer was solved for *Pyrococcus furiosus* Rad50 bound to non-hydrolysable AMP-PNP and a magnesium ion (39). The molecular structure of the NBD of *Methanocaldococcus jannaschii* MJ0796 bound to ATP and a sodium ion (PDB 1L2T) showed the dimerization seen for Rad50 also for ABC transporters, thus establishing a common mode of dimerization and common mechanism of ATP hydrolysis for ABC proteins (40). In the model for an ATP-driven reaction cycle, two nucleotide-free NBDs in an open conformation dimerize upon ATP binding to form a closed, catalytically active dimer (40,41). This conformational change is relayed to the “effector” domain and thereby coupled to function, e.g. transport by attached TMD or release of bound DNA. ATP hydrolysis returns the NBD protomers to the initial open conformation where ADP and phosphate are released.

A

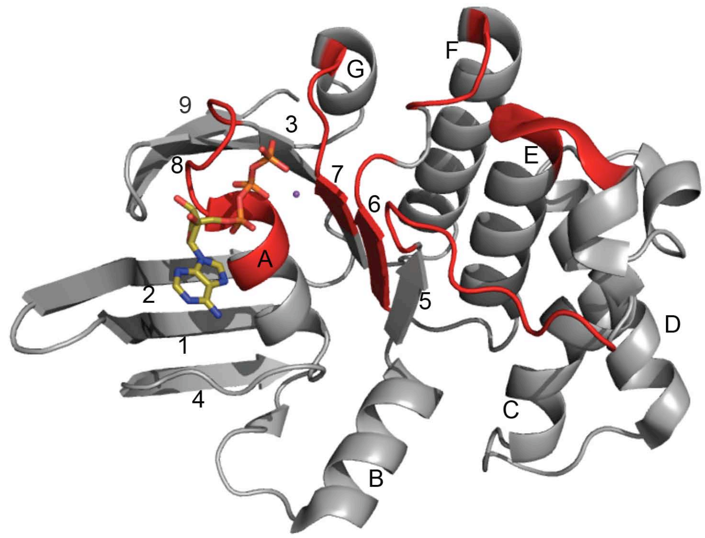

B

```
                         1              2          3        A         4
MJ0796   -----MIKLKNVTKTYKMGEEIIYALKNVNLNIKEGEFVSIMGPSGSGKSTMLNIIGCL-DKPTEGEVY 63
HisP     MMSENKLHVIDLHKRYGG----HEVLKGVSLQARAGDVISIIGSSGSGKSTFLRCINFL-EKPSEGAII 64
MalK     ---MASVQLQNVTKAWGEVVVSKDINLDIHEGEF----VVFVGPSGCGKSTLLRMIAGL-ETITSGDLF 61
                                                   Walker A
PrrC     ---MGKTLSEIAQQLSTPQKVKKTVHKEVEATRAVPKVQLIYAFNGTGKTRLSRDFKQLLESKVHDGEG 66

                             B     5                            C
MJ0796   IDN-----IKTND----LDDDELTKIRRDKIGFVFQQFNLIPL-------------LTALENVELPLIF 110
HisP     VNGQNINLVRDKDGQLKVADKNQLRLLRTRLTMVFQHFNLWSH-------------MTVLENVMEAPIQ 120
MalK     IGE---------------KRMNDTPPAERGVGMVFQSYALYPH-------------LSVAENMSFGLKL 102
                                            Q-loop
PrrC     ED-----------------EAEQSALSRKKILYYNAFTEDLFYWDNDLQEDAEPKLKVQPNSYTNWLL 116
                                         PrrC box
                D                                               E
MJ0796   KYRGAMSGEERRKRALECLKMAELEERF----------------ANHKPNQLSGGQQQRVAIARALAN- 162
HisP     VLG--LSKHDARERALKYLAKVGIDERA----------------QGKYPVHLSGGQQQRVSIARALAM- 170
MalK     AGAKKEVINQRVNQVAEVLQLAHLLD--------------------RKPKALSGGQRQRVAIGRTLVA- 150
                                                             Signature
PrrC     TLLKDLGQDSNIVRYFQRYANDKLTPHFNPDFTEITFSMERGNDERSAHIKLSKGEESNFIWSVFYTLL 185

                              6            F                 7
MJ0796   ---------------------NPPIILADEPTGALDSKT--GEKIMQLLKKLNEEDGKTVVVVTHDINV 198
HisP     ---------------------EPDVLLFDEPTSALDPELVGEVLRIMQQLA---EEGKTMVVVTHEMGF 215
MalK     ---------------------EPSVFLLDEPLSNLDAALRVQMRIEISRLHK--RLGRTMIYVTHDQVE 210
                             Walker B  D-loop                      H-loop
PrrC     DQVVTILNVADPDARETHAFDQLKYVFIDDPVSSLDDNHLIELAVNLAGLIKSSESDLKFIITTHSPIF 254

          G    8     9
MJ0796   AR-FGERIIYLKDGEVEREEKLRGFDDR----------------------------------------- 235
HisP     ARHVSSHVIFLHQGKIEEEGDPEQVFGNPQSPRLQQFLKGSLKKLEH---------------------- 262
MalK     AMTLADKIVVLDAGRVAQVGKPLELYHYPADRFVAGFIGSPKMNFLPVKVTATAIDQVQVELPMPNRQQ 266

PrrC     YNVLFNELN-GKVCYYMLES------------------------------------------------- 273
```

C

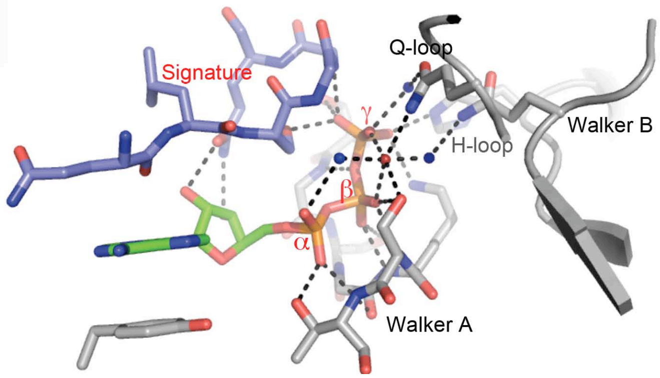

Figure 3 **– The ATP binding cassette domain**

(A) ABC transporter NBD fold exemplified by *M. jannaschii* MJ0796 (PDB 1L2T) (40). The structure of a MJ0796 monomer is shown as grey cartoon, characteristic NBD motifs are highlighted in red and bound ATP is shown as stick model together with the bound sodium ion in purple. Important secondary structure elements are numbered, β-sheets (1 through 9) and α-helices (A through G). **(B)** Manual alignment of *E. coli* PrrC to a ClustalW (43) alignment of ABC transporter NBDs of MJ0796 (accession NP_247785.1), HisP (accession 1B0U_A) and MalK (accession ZP_08356843.1). The PrrC aminos acid sequence was aligned guided by the NBD motifs. Secondary structure elements above the alignment correspond to MJ0796 in panel A. **(C)** MJ0796 active site binding ATP (PDB 1L2T), side chains are shown as stick model, the ATP phosphates are labeled. A sodium ion (red sphere) indicates the position of the active Mg^{2+}-cofactor. Side chains of the NBD motifs are shown as stick models and their interactions as dashed lines. Three water molecules in the active site are shown as blue spheres.

High-resolution crystal structures of various NBDs have been solved, allowing structural interpretation of the role of the conserved ABC motifs (Figure 3BC). The Walker A (GxxGxGKS/T consensus) and Walker B (ΦΦΦΦDE/D, Φ is a hydrophobic residue) motifs were first described by John Walker and colleagues (42) and are common NTP binding motifs, found also in many other protein families such as helicases and kinases. The Walker A motif lies in a flexible loop between the C-terminal tip of a β-strand and an α-helix. This motif is also referred to as P-loop, because its side chains and backbone functional groups make numerous contacts to β- and γ-phosphates of bound nucleotides. The C-terminal serine or threonine hydroxyl of the Walker A motif, also contacts the magnesium ion coordinated by β- and γ-phosphates (Figure 3C). (37)

In the Walker B motif, the four hydrophobic residues lie at the C-terminal end of a β-strand. The aspartate residue is conserved, however it is the adjacent glutamate or aspartate residue, which positions a water molecule to coordinate the catalytic metal ion (44). In one suggested mechanism, this Glu/Asp functions as a general base, polarizing the catalytic water. This model is supported biochemically *inter alia* by the inactivity of the MJ0796 E171Q mutant (40). The ABC signature motif (LSGGQ consensus) is located in a sharp bend between two α-helices and is contributed to the active site by the *trans*-protomer. Crucial interactions with the γ-phosphate are made by the backbone amides of the two glycines in the signature motif. The hydroxyl side chain of the serine residue also contacts the γ-phosphate. In the MJ0796 structure, the signature glutamine makes bidentate contacts to the ribose hydroxyl-groups. This is not reproduced in other crystal structures where usually only one such contacts can be seen e.g. in HlyB (PDB 1XEF) and *S. cerevisiae* Smc1 (PDB 1W1W) (40,45,46).

The Q-loop is another NBD motif, its eponymous glutamine is the only conserved residue in a loop connecting the two NBD sub-domains. The Q-loop was suggested to play

a role in relaying the conformational change induced by ATP binding to the "effector" domain by "sensing" the γ-phosphate (47). The glutamine amide contacts the γ-phosphate via a water molecule and coordinates the metal ion. At the tip of another β-strand adjacent to the Walker B β-strand lies a conserved histidine residue (H-loop motif) (37). The N-ε of this histidine contacts the γ-phosphate. The high-resolution structure of the H-loop H662A mutation of the *E. coli* HlyB NBD led to the proposition of an alternative substrate assisted model for ATPase catalysis (37,45). In this model, Q-loop Gln and H-loop His form a catalytic dyad. The histidine acts as a "linchpin" that positions the attacking water, the catalytic magnesium ion, and the γ-phosphate and also contacts the *trans*-protomer across the dimer interface. The D-loop motif, directly adjacent to the Walker B motif in the amino acid sequence, is important for dimer formation (37,40). The D-loop aspartate in this motif contacts a residue in the Walker A (conserved Ser/Asn residue directly preceding the second glycine in the consensus). The side chains preceding the D-loop, Asp, Ala and Leu in the ^{175}ALD^{177} D-loop of MJ0796, also contact the *trans*-protomer, namely at H-loop His and Q-loop Gln (40).

Another common structural element (sometimes referred to as A-loop) is an aromatic residue towards the N-terminus (Tyr11 in MJ0796) of the NBD, which, positioned at the end of a β-strand, makes π-π interactions with the base of the bound nucleotide (40,48). This unspecific interaction with the base explains on a structural level why ABC proteins have no pronounced NTP preference (49). Such residue is conserved in many transporter NBDs. However, yeast Smc1 has a lysine residue in an equivalent position suggestive of π-cation interactions (46).

In summary, NBD dimers sandwich the nucleotide between the Walker A and signature motifs, the metal ion is octahedrally coordinated by a conserved Walker A serine, the β- and γ-phosphates, the Q-loop glutamine and two water molecules bridging to the α-phosphate and a Walker B carboxylate side chain, respectively. The Walker B Glu/Asp, the Q-loop Gln and the H-loop His further interact with the γ-phosphate (Figure 3C).

PrrC proteins have conserved motifs corresponding to Walker A motif, Walker B motif, signature motif (diverging from the consensus to ^{169}LSKGE^{173} in *Eco*PrrC), D-loop and H-loop motifs (Figure 2C, Figure 3B) (33). Instead of an obvious candidate for the Q-loop motif, PrrC proteins contain a conserved motif termed "PrrC box". So far, importance for ACNase activity has only been shown for the Walker A motif (31). However, this motif is a widely distributed nucleotide-binding motif also found in other enzymes, e.g.

Pnkp's kinase moiety (1.4.1.1). Direct requirement for other NBD motifs was shown for nucleotide crosslinking of PrrC, but not for tRNA cleavage (33). Thus, PrrC's ABC-like motifs remain to be investigated in detail in order to understand if such a domain has role in ACNase activity.

1.2.4 Colicins

A second class of bacterial ACNases is encoded in the toxin-antitoxin loci of *E. coli* Col plasmids. These secreted toxins, colicins, are expressed in response to SOS-inducing signals. Colicins kill *E. coli* cells lacking a compatible Col plasmid, which also encodes an immunity protein (5,6,50). Colicins consist of three domains that each perform a distinct step in cell killing: A central receptor binding domain for recognition of the target cell, an N-terminal translocation domain that mediates passage through the periplasm and a C-terminal domain exclusively responsible for the toxicity in the cytoplasm (5,50). Four groups of colicins have been described: channel-forming colicins, inhibitors of murein synthesis, DNases and specific RNases, which were shown to arrest translation (colicins E3 - E6 and D) (6,50). While Colicins E3, E4 and E6 target 16S ribosomal RNA, colicins D and E5 have ACNase activity. The N-terminal and central domains of nuclease type colicins are conserved, but their C-terminal ribonuclease domains (CRD) are non-homologous (5,6). Although colicin E5 and D CRDs both target tRNAs and are structurally similar, they have non-overlapping target specificities. They also cleave their target tRNAs in different positions and do not share amino acid sequence similarities (5,6,51-53).

1.2.4.1 Colicin E5

The expression of colicin E5's 115 amino acid CRD, E5-CRD, is sufficient for toxicity to *E. coli* cells and can be fully inhibited by coexpression of the 108 amino acid immunity protein ImmE5. E5-CRD cleaves $tRNA^{Tyr(QUA)}$, $tRNA^{Asn(QUU)}$, $tRNA^{His(QUG)}$ and $tRNA^{Asp(QUC)}$ *in vitro* and *in vivo* (Figure 4A). The Q in the QUN sequence denotes queunine, a guanine-derived base. tRNA cleavage by colicin E5 occurs 3′ of the queunine wobble base and produces 2′,3′-cyclic phosphate and 5′-hydroxyl termini at the cleavage site. Colicin E5 substrate preference is as follows: $tRNA^{Tyr\ (QUA)}$ > $tRNA^{Asp(QUC)}$ > $tRNA^{His(QUG)}$ > $tRNA^{Asn(QUU)}$ (5). Based on the anticodon sequence of these targets, the diribonucleotide GpUp was discovered as a minimal substrate for E5-CRD *in vitro* (54).

Crystal structures have been solved for different constructs of E5-CRD: E5-CRD apo (PDB 2A8K), E5-CDR bound to its immunity protein ImmE5 (PDB 2DFX) and bound to dGpdUp (PDB 2DJH), the non-cleavable deoxy-form of the minimal substrate (52,53). E5-CRD adopts a fold reminiscent of RNase T1 (Figure 4C) (52): the E5-CRD consists of three helices and a central five-stranded antiparallel β-sheet. The β-sheet stacks on the second helix, while the first, N-terminal α-helix runs along the fifth β-strand. This fold forms a positively charged cleft where both ImmE5 and the substrate analog bind. (52,53). In the dGpdUp-bound structure E5-CRD side chains make both, ring-ring (Trp102 with G) and ring-pseudoring (Asp105 and Arg107 with U) interactions as well as hydrogen bonds similar to Watson-Crick pairing with the nucleotide bases (Figure 4E) (53). Colicin E5 substrate specificity results from this direct immitation of the codon-anticodon base pairing. When the inhibitor ImmE5 binds to the catalytic cleft of E5-CRD, it imitates in protein-protein interaction, the protein-tRNA mimicry of mRNA-tRNA base pairing (53).

Even though a nucleotide-bound structure of E5-CRD exists, its mechanism of catalysis remains unclear. Usually, histidine side chains act as general acid-base catalytic residues in the RNase A- or RNase T1-like mechanisms (1.1.1), but E5-CRD does not contain any histidines. An aspartate, as general base, and an arginine, to stabilize the transition state, were suggested to be catalytic (Figure 1B). These residues extend their side chains into the putative catalytic cleft and mutations to alanine strongly reduce cleavage activity of a stem-loop substrate (52). Yet, these side chains (Asp54 and Arg65 in the nucleotide-bound structure) are more than 10 Å away from the scissile bond in the dGpdUp-bound structure. The only charged residues contacting the phosphates in this structure are two lysines and an arginine. Mutations of these residues (R33Q and K25Q/K60Q) abolish cell killing by E5-CRD. At physiological pH both lysine and arginine side chains should be protonated and unable to act as general base (53). Thus, the catalytic mechanism of E5-CRD remains to be confirmed. Although the crystal structures of RNase T1 and E5-CRD can be superimposed and share common structural components, this comparison does not help to identify E5-CRD catalytic residues: The catalytic residues of RNase T1 are 12 - 15 Å away from the scissile phosphate of dGpdUp-bound in E5-CRD and the putative catalytic residues of colicin E5 do not reside in corresponding positions within the fold (Figure 4C).

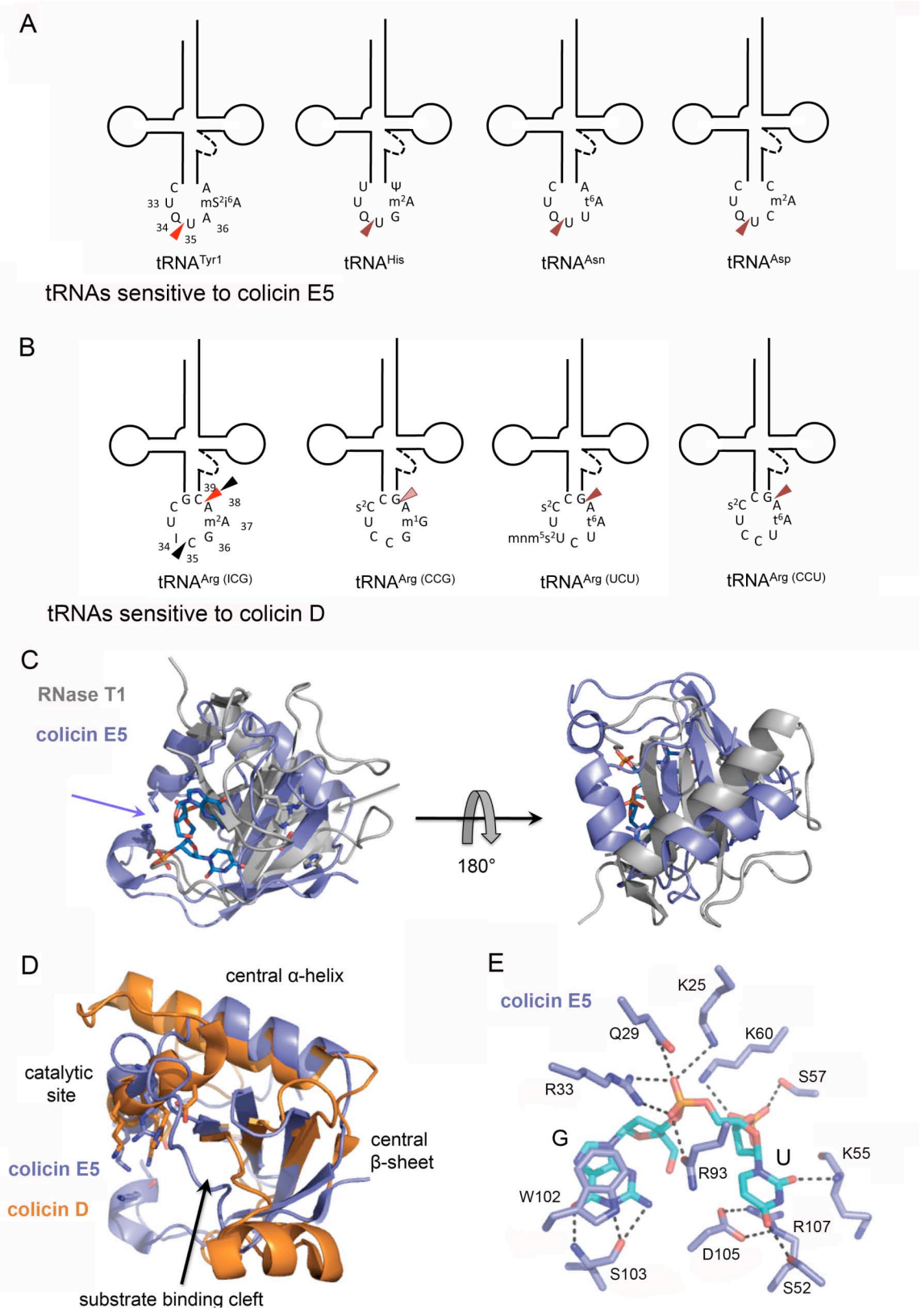

Figure 4 – **tRNA targeted by colicins E5 and D**

(Figure 4 continued)

tRNAs are depicted in their clover-leaf secondary structure, the anticodon loop nucleotides are identified. **(A)** *E. coli* tRNA species sensitive to colicin E5. Arrowheads point to the phosphodiester bond cleaved by colicin E5 *in vitro*; major species (red) and minor species (brown) (55). **(B)** *E. coli* tRNA species sensitive to colicin D. Arrowheads point to the phosphodiester bond cleaved by colicin D. *In vitro*: major species (red) and minor species (brown). *In vivo* recovered fragment (black) (55). **(C)** Superimposition (in Pymol) of dGpdUp-bound E5-CRD in blue (PDB 2DJH) with RNase T1 in grey (PDB RNT1), blue and grey arrows point to the respective active sites. (D) Superimposition (in Pymol) of dGpdUp-bound E5-CRDin blue (PDB 2DJH) with D-CRD in orange (PDB 1TFO) the catalytic site and important structural components are labeled. (E) The active site of E5-CRD. Side chains contacting the dGpdUp dinucleotide (light-blue) are labeled and interactions are shown as dashed lines (PDB 2DJH).

1.2.4.2 Colicin D

After the discovery of tRNA as the molecular target of colicin E5's nuclease, tRNA came into focus as potential target of colicin D. Full length colicin D (697 aa) cleaves tRNAs decoding for arginine, *in vivo* and *in vitro* and can be inhibited by its immunity protein ImmD. $tRNA^{Arg\ (ICG)}$ (with I for inosine) is the major substrate, but isoacceptors with CCG, CCU and UCU anticodons are also cleaved (Figure 4B). The wobble uridine of the latter is 5-methylaminomethyl-2-thio-modified (mnm^5s^2). Cleavage by colicin D was mapped to the phosphodiester bond 3′ of A 38, which is an adenosine in *E. coli* $tRNA^{Arg}$ isoacceptors. A second *in vivo* break site, 3′ to the wobble base, was identified for $tRNA^{Arg\ (ICG)}$. It has been speculated that this cleavage occurs after incision at position 38, possibly by another nuclease. tRNA fragments recovered after colicin D cleavage have 2′,3′-cyclic phosphate and 5′-hydroxyl termini. In search for catalytic residues in an RNase A-like general acid-base mechanism the four histidines in the CRD were mutated to tyrosine. Only one, H611Y, abolished colicin D toxicity, indicating His611 as putative general acid or base (6).

A crystal structure for colicin D's CRD (103 aa) in complex with ImmD was solved (PDB 1TFO). D-CRD displayed ACNase activity with all four $tRNA^{Arg}$ isoacceptors in total RNA extract *in vitro*. The D-CRD fold consists of a central anti-parallel three stranded β-sheet stacking on an α-helix. Two further α-helices flank the β-sheet. Based on their position in the putative catalytic cleft of D-CRD Asp614 and Lys608 or Lys610 were suggested to act in RNase catalysis. As seen for E5-CRD and ImmE5, ImmD blocks access to the putative active site. ImmD adopts an α-helical fold with no similarity to ImmE5. Despite the lack in primary structure similarity, the crystal structures of E5-CRD and D-CRD are superimposable (Figure 4D) (51). The catalytic His611 and the putative catalytic Arg33 of E5-CRD partially overlap in this superpostion of the E5-CRD and D-CRD structures.

Expression of colicin D-CRD or E5-CRD is toxic to *S. cerevisiae*. Both colicins target the yeast tRNA equivalents of their bacterial substrates (56,57). Of note, the colicin E5 substrate tRNAs are cleaved, but naturally have guanine rather that queunine wobble nucleotides in yeast. Also, colicin D does not cleave yeast $tRNA^{Arg\ (CCG)}$, presumably because it has a uridine in position 38 where colicin D requires adenine for activity.

1.3 Fungal secreted anticodon nucleases

Killer-strains of the yeasts *Kluyveromyces lactis* and *Pichia acaciae* harbor linear plasmids encoding for secreted killer toxins named zymocin and Pichia toxin (PaT), respectively, that arrest growth of susceptible non-self species like *S. cerevisiae* (58,59). These plasmids also encode cognate immunity proteins that protect from the respective ACNase (58,60). The molecular mechanism of toxins encoded in similar linear plasmids of *Pichia inositovora* and *Wingea robertsiae* have not been investigated (61). Zymocin and Pichia toxin are secreted as heterotrimeric proteins, yet intracellular expression in susceptible cells of the ACNase subunit, zymocin's γ-toxin and PaT's toxic subunit, is sufficient to elicit the growth arrest phenotype (Figure 5A) (58,61-63). Both killer toxins are anticodon loop specific endoribonucleases: PaT targets $tRNA^{Gln\ (UUG)}$ while γ-toxin cleaves $tRNA^{Glu\ (UUC)}$ (7,8). These target tRNA species have 5-methoxycarbonylmethyl-2-thio-uridine (mcm^5s^2U) wobble nucleotides in *S. cerevisiae* (Figure 2 and Figure 5 BC). In yeast, the mcm^5 modification is added post-transcriptionally by the acetyltransferase subunit Tot3 (also Elp3 or Hap1) within the elongator complex and, in the last step, the methyltransferase Trm9 (8,64-67). The thiolase Tuc1 thiolates the wobble uridine at position 2 (68). Trm9 deficient cells are resistant to exogenous zymocin, intra-cellular γ-toxin and PaT (7,8,67). Cells deficient in any one of the six subunits of the elongator complex are resistant to γ-toxin (69). However, the mcm^5 modification alone is not a sufficient determinant of substrate identity, as it is not only found on $tRNA^{Glu\ (UUC)}$ and $tRNA^{Gln\ (UUG)}$, but also on other tRNA species with wobble uridine in *S. cerevisiae*: $tRNA^{Lys\ (UUU)}$, $tRNA^{Gly\ (UCC)}$ and $tRNA^{Arg\ (UCU)}$ (70).

1.3.1 *Kluyveromyces lactis* γ-toxin

K. lactis zymocin toxicity has mainly been studied with the help of two classes of mutants, resistant to either exogenous zymocin or intracellular γ-toxin (71). The former type of mutants lead to the discovery of the exo-chitinase and membrane binding properties of zymocin's α- and β-subunits, respectively (58). All mutants of the latter type map to genes related to tRNA modification (71).

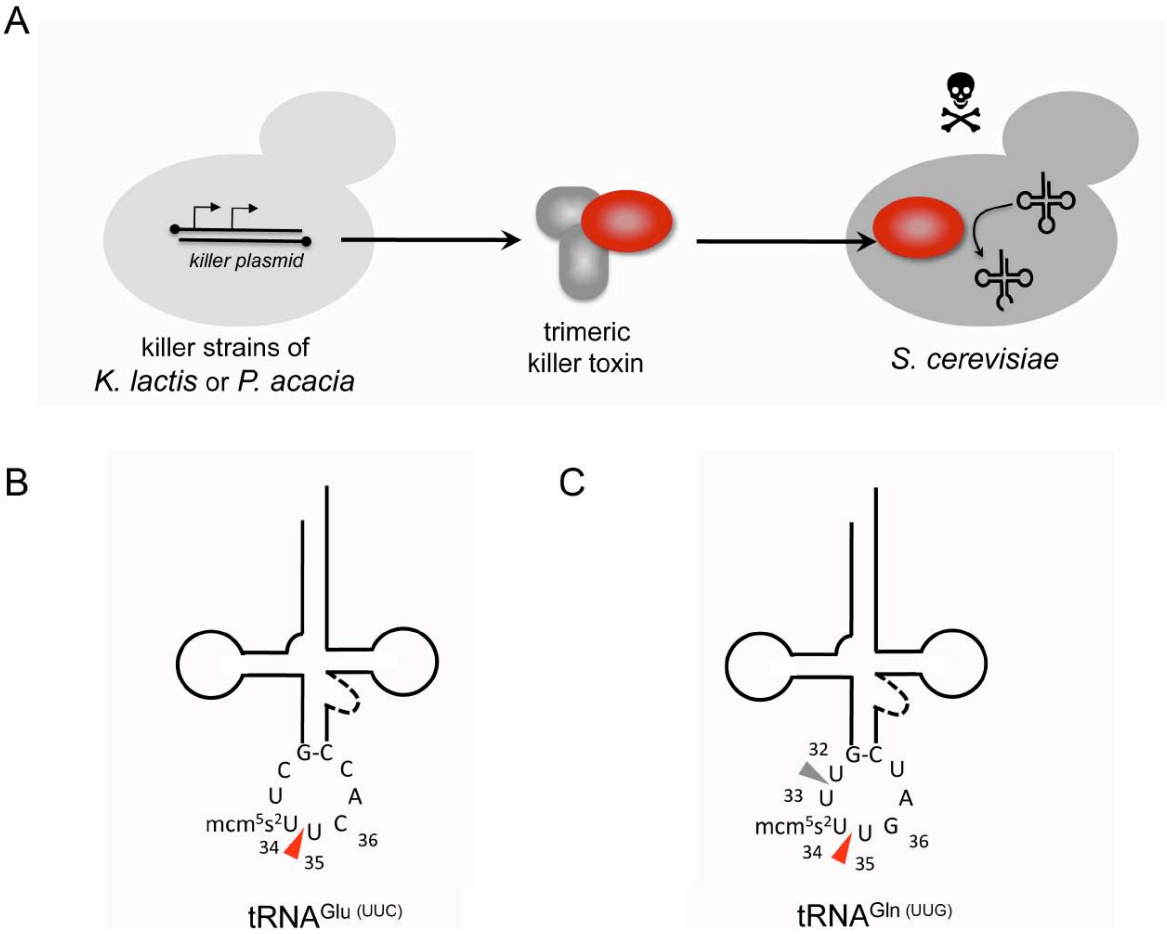

Figure 5 – **Secreted fungal anticodon nucleases of *Kluyveromyces lactis* and *Pichia acaciae***

(A) Schematic depiction of non-self restriction by the fungal killer toxins. The toxic ACNase subunit is shown in red (Modified from (73)). **(B)** $tRNA^{Glu\ (UUC)}$ targeted by γ-toxin, the position of cleavage is indicated by a red arrowhead (7, 74). **(C)** $tRNA^{Gln\ (UUG)}$ targeted by PaT, the primary position of cleavage is indicated by a red arrowhead (8). The grey arrowhead shows the alternative cleavage site when PaT is over-expressed or the wobble uridine is hypomodified.

The Byström lab have identified γ-toxin as an ACNase and mcm^5s^2 wobble modified $tRNA^{Glu\ (UUC)}$ as the relevant target in *S. cerevisiae* (7). Expression of $tRNA^{Glu\ (UUC)}$ from a high-copy plasmid confers γ-toxin resistance (72). $tRNA^{Lys\ (UUU)}$ or $tRNA^{Gln\ (UUG)}$ are minor targets of γ-toxin. High-copy expression of either or both minor targets together with

$tRNA^{Glu\ (UUC)}$ has a synergistic effect on toxin resistance (7). Purified GST-γ-toxin incises $tRNA^{Glu\ (UUC)}$ from wild type, but not *trm9Δ* or *tot3Δ* cells. *In vitro*, cleavage of $tRNA^{Lys\ (UUU)}$ and $tRNA^{Gln\ (UUG)}$ also occurs, at higher concentrations of γ-toxin. γ-toxin breaks a single phosphodiester bond, between the wobble nucleotide and the following nucleotide in position 36, and produces 2′,3′-cyclic phosphate and 5′-hydroxyl termini (7).

A study with 17mer RNA substrates corresponding to the $tRNA^{Glu\ (UUC)}$ anticodon-loop, and variations thereof, showed that γ-toxin can cleave unmodified substrate *in vitro* in presence of TMAO (7). The optimal γ-toxin substrate has the $tRNA^{Glu\ (UUC)}$ anticodon loop sequence UUCAC, wherein the first U corresponds to the wobble nucleotide. Modification to mcm^5U in this position greatly enhances γ-toxin cleavage. The 2-thio-modification of the wobble uridine has only a small positive effect on cleavage. The narrow specificity of γ-toxin is underscored by the inability to incise *E. coli* $tRNA^{Glu}$ with its fully modified innate 5-methylaminomethyl-2-thio wobble uridine (mnm^5s^2U) (60). In contrast to the more promiscuous bacterial ACNases, γ-toxin and PaT are selective for eukaryotic tRNA through their specificity for mcm^5-modified wobble uridines especially *in vivo* (7,8). Accordingly, PaT and γ-toxin are not toxic to *E. coli* and can be recombinantly over-expressed and purified.

1.3.2 *Pichia acaciae* toxin is a $tRNA^{Glu}$ ACNase

Despite overlapping substrate specificity, PaT shares no primary structure similarity with γ-toxin. The other subunits of PaT however, are homologous to zymocin's α- and β-subunits, respectively, and share their activities (59,63). $tRNA^{Gln\ (UUG)}$ is PaT's major target *in vitro* and *in vivo*. Increased levels of $tRNA^{Gln\ (UUG)}$ are sufficient to protect *S. cerevisiae* against exogenous PaT. Furthermore, intracellular expression of PaT or exogenous addition of PaT specifically reduces the levels of intracellular $tRNA^{Gln\ (UUG)}$ detected by reverse transcriptase PCR in *S. cerevisiae* cells. PaT cleavage occurs at two positions in the anticodon loop primarily 3′ of the wobble uridine and to a lesser extent 3′ of position 32 (Figure 5C). The secondary site could account for toxicity of PaT expressed from high-copy plasmids in *trm9Δ* cells and of high dosed exogenous PaT in *tot3Δ* and *tot3Δ trm9Δ* cells. Additionally, $tRNA^{Gln\ (CUG)}$ isoacceptors, as well as $tRNA^{Lys\ (UUU)}$ and $tRNA^{Glu\ (UUC)}$, can be cleaved by PaT *in vitro* (8).

1.4 tRNA damage repair

All described ACNases produce tRNA fragments with 2′,3′-cyclic phosphate and 5′-hydroxyl termini. Classical RNA ligases follow a mechanism analogous to that of DNA ligases. These enzymes require 3′-hydroxyl and 5′-phosphate ends to form a new 3′,5′-phosphodiester bond. Thus, the break sites have to be healed to a 3′-hydroxyl, by a cyclic phosphodiesterase, and to a 5′-phosphate, by a kinase, before sealing via the classical ligation pathway can occur. Such a tRNA repair pathway was first described for the T4 phage enzymes Pnkp and Rnl1 that repair PrrC ACNase damage (1.4.1) (4). The mechanisms of T4 phage Pnkp and Rnl1 are described in detail below (1.4.1.1 and 1.4.1.2). Proteins homologous to Pnkp have been identified in other bacteriophages, bacteria, eukarya and eukaryotic viruses, while ligases similar to Rnl1 are found in viruses, bacteria and eukarya (75,76). Bacterial tRNA repair systems that comprise healing and sealing activities are capable of repairing tRNA damaged by colicins *in vitro* (1.4.2). The similarity of directed tRNA breakage and dedicated repair by healing and sealing to the pathways of tRNA splicing, especially with the yeast/plant pathway, are remarkable (1.5).

1.4.1 The T4 phage tRNA repair pathway

The tRNA healing and sealing activities of T4 bacteriophage enzymes Pnkp and Rnl1 are essential for productive infection of *prr*$^{+}$ *E. coli*. The ACNase PrrC and the T4 phage tRNA repair enzymes are thus linked in discovery and biological function (4,77-79). The genes encoding Pnkp and Rnl1, *pseT* and *63*, respectively, lie in close proximity to each other in the T4 genome (77). The product of gene *63* has also been described to promote tail fiber attachment, these activities are thought to be unrelated, since RNA ligase and tail fiber attachment reactions differ in requirements and response to inhibitors (80). Coexpression of T4 Pnkp and Rnl1 in *trl1Δ* yeast cells complements the lethal deletion phenotype of yeast tRNA splicing ligase Trl1, underscoring similar outcome of phage tRNA repair and tRNA repair in yeast splicing (Figure 8) (81)

1.4.1.1 The T4 phage end-healing enzyme Pnkp

T4 Pnkp exemplifies a family of repair enzymes that heal broken RNA or DNA by converting 3′-phosphate and 5′-hydroxyl ends to 3′-hydroxyl and 5′-phosphate termini suitable for classical RNA/DNA ligases (82). Such end-healing requires two activities: a 5′ kinase and a 3′ phosphatase. In T4 Pnkp, these activities are present in separate functional domains within a 301 amino acid polypeptide (Figure 6) (83,84). The kinase activity resides in the N-terminal residues 1-148, while the phosphatase activity lies within the remaining C-terminal domain (82). Crystal structures were solved for the kinase domain (PDB 1LYI), full length Pnkp bound to ADP (PDB 1LTQ), full length Pnkp bound to desoxy-oligonucleotides (PDB 1RRC, Pnkp bound to a trinucleotide), and the homotetrameric functional quarternary structure of Pnkp (PDB 2IA5) (82,84-87). These structures show that kinase and phosphatase active sites are present in separate α/β fold domains. Full length Pnkp forms homotetramers through interaction at two separate interfaces, one in the kinase and one in the phosphatase domain (Figure 6B) (85,87). The proximity of the kinase and phosphatase active sites of two neighboring protomers could facilitate binding and processing of both ends of incised tRNA (85). Separated, both the 5′ kinase and a 3′ phosphatase domains form homodimers (82,86). Dimerization is important for phosphatase function (see below) (87).

1.4.1.1.1 Structure and mechanism of the N-terminal 5′ kinase

The N-terminal domain (residues 1-148) of Pnkp catalyzes the transfer of γ-phosphate from ATP, or other NTPs, to the 5′-hydroxyl of RNA. Other accepted substrates include double and single stranded DNA and single 3′ phosphate nucleotides (82,85,88). The kinase domain consists of a central four-stranded parallel β-sheet surrounded by four α-helices and two more α-helices at the C-terminal end of the domain (Figure 6A). The β-strand and helices form a shallow tunnel, capped by two surface loops (82,85). The fold shows that Pnkp's kinase domain belongs to the adenylate kinase superfamily (85). Site-directed mutagenesis identified five essential residues in the 5′ kinase domain: Lys15 and Ser16, found in a Walker A or P-loop motif (^{9}GCPGSGKS^{16} in Pnkp), Asp35, Arg38 and Arg126. Mutations of any one of these residues to alanine strongly reduce the specific activity of the kinase. Only in one case, S16T, activity was restored by a conservative mutation (83,84). The essential residues map to the substrate

binding tunnel in the crystal structure (Figure 6C): The Walker A motif lies in the loop between the first β-strand and first α-helix and binds ADP. Lys15 contacts the β-phosphate of bound ADP. Ser16 contacts the β-phosphate with its side chain and also interacts with the α-phosphate with its backbone amide. Arg126 also interacts with the β-phosphate, while Asp35 and Arg38 form hydrogen bonds to the substrate in the trinucleotide-bound structure (82,85,86).

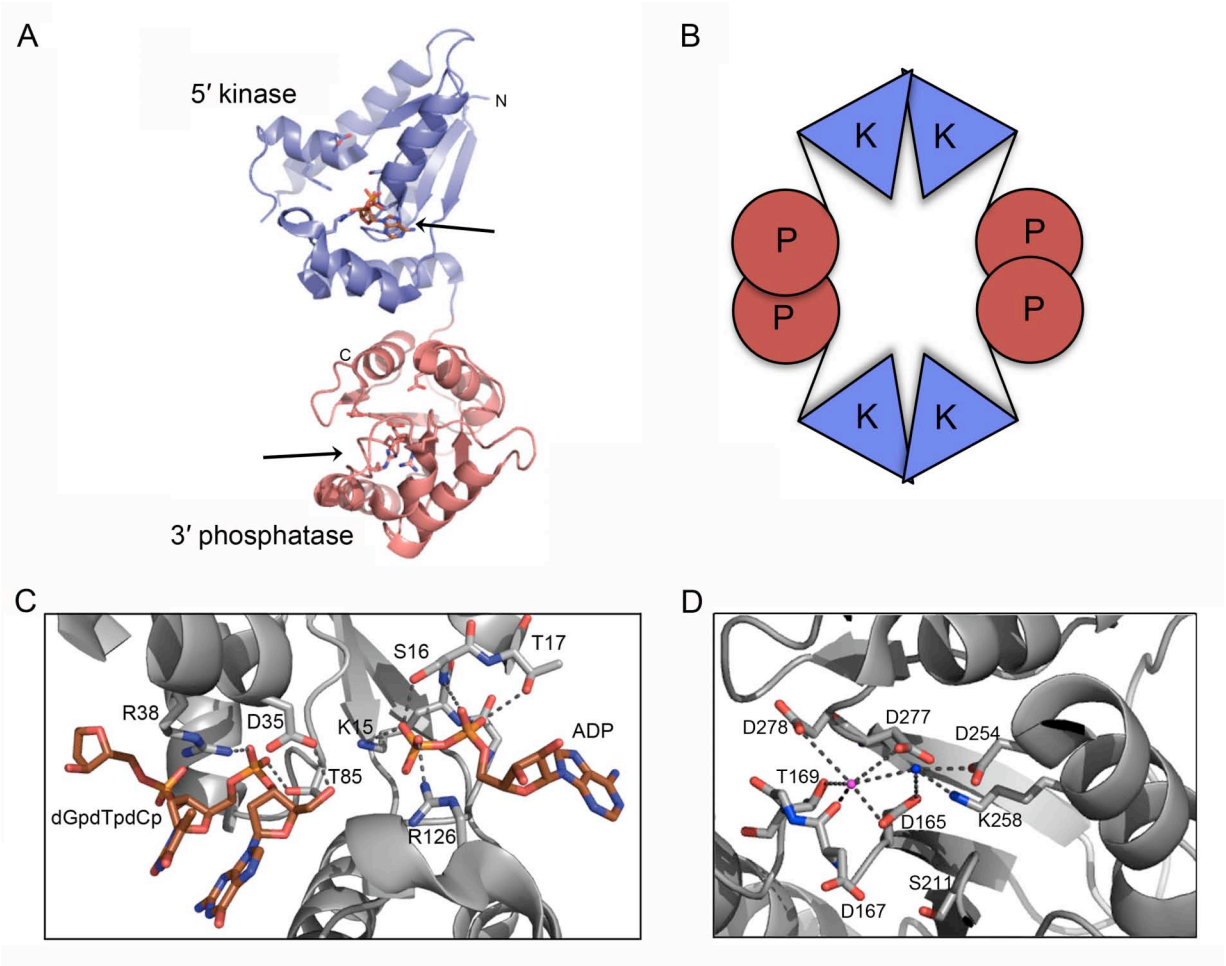

Figure 6 – **Structure and active sites of T4 Pnkp**

(A) Crystal structure of full length T4 Pnkp (PDB 1LTQ) (85) with the N-terminal 5′ kinase domain in blue and the C-terminal 3′ phosphatase domain in red. Arrows point to the respective active sites. **(B)** Schematic of the quaternary structure of T4 Pnkp. The functional tetramer is formed by interaction at kinase (K, blue) and phosphatase (P, red) interfaces. **(C)** The 5′ kinase active site of T4 Pnkp (PDB 1RRC) (86). The domain is shown as grey cartoon, active-site side chains, dGpdTpdCp trinucleotide and ADP moieties are shown as stick models, their interactions are shown as dashed lines. **(D)** The 3′ phosphatase active site of T4 Pnkp (PDB 2IA5) the domain is shown as grey cartoon (87), active-site side chains are shown as stick models, the hexagonally coordinated magnesium ion as a purple sphere and a water molecule as blue sphere, their interactions are shown as dashed lines.

1.4.1.1.2 Structure and mechanism of the C-terminal 3′ phosphatase

The C-terminal domain of Pnkp (residues 150-301) catalyzes the magnesium-dependent hydrolytic removal of a 3′ phosphate from RNA or DNA (89). An additional 2′,3′-cyclic phosphodiesterase activity was described when Pnkp was identified as a tRNA repair enzyme (4). Residues that contact the *trans*-protomer at the phosphatase dimer interface were identified in the tetrameric crystal structure (87). Pairwise mutations to alanine disrupted dimer formation at the phosphatase domain. The phosphatase activity is greatly reduced in R287A-Q295A and E292A-W294A double mutants, highlighting the importance of quaternary structure for activity.

The Pnkp phosphatase shares structural and amino acid sequence similarity with the L-2-haloacid dehalogenase (HAD) family of phosphatases (85). Members of this family are defined by a DxDxT motif (^{165}DVDGT^{169} in Pnkp), which is involved in covalent catalysis (83,87). Crystal structures of full length Pnkp show, that the phosphatase domain contains a five-stranded β-sheet, with four α-helices inserted between the strands and a second small two-stranded anti-parallel β-sheet (85). Site-directed mutagenesis identified ten essential residues in the phosphatase domain (Figure 6D): Asp165, Asp167, Arg176, Asp187, Ser211, Arg213, Asp254, Lys258, Asp277, and Asp278 (84,87). Combination of this biochemical data with information from the crystal structures led to proposition of a catalytic mechanism of the phosphatase, where Asp167 acts as general acid-base. The phosphate is transferred to Asp165 in covalent catalysis. Asp167, Thr169, Asp277 and Asp278 side chains, as well as the backbone carbonyl of Asp167 and a water molecule octahedrally coordinate the metal. Lys258 and Ser211, as well as the divalent metal and backbone amides of nearby residues were further suggested to form the oxyanion hole of the phosphatase (87).

1.4.1.2 The T4 phage RNA ligase Rnl1

1.4.1.2.1 Affiliation to the superfamily of covalent nucleotidyltransferases

T4 phage Rnl1 is a “classical” RNA ligase and belongs to the superfamily of covalent nucleotidyltransferases. The polynucleotide ligases belonging to this family join 3′-hydroxyl and 5′-phosphate ends to form a new 3′,5′-phosphodiester bond. This family includes bacterial NAD^+ dependent DNA ligases, ATP dependent DNA and RNA ligases and GTP dependent guanylyltransferases (mRNA capping enzymes) (90,91).

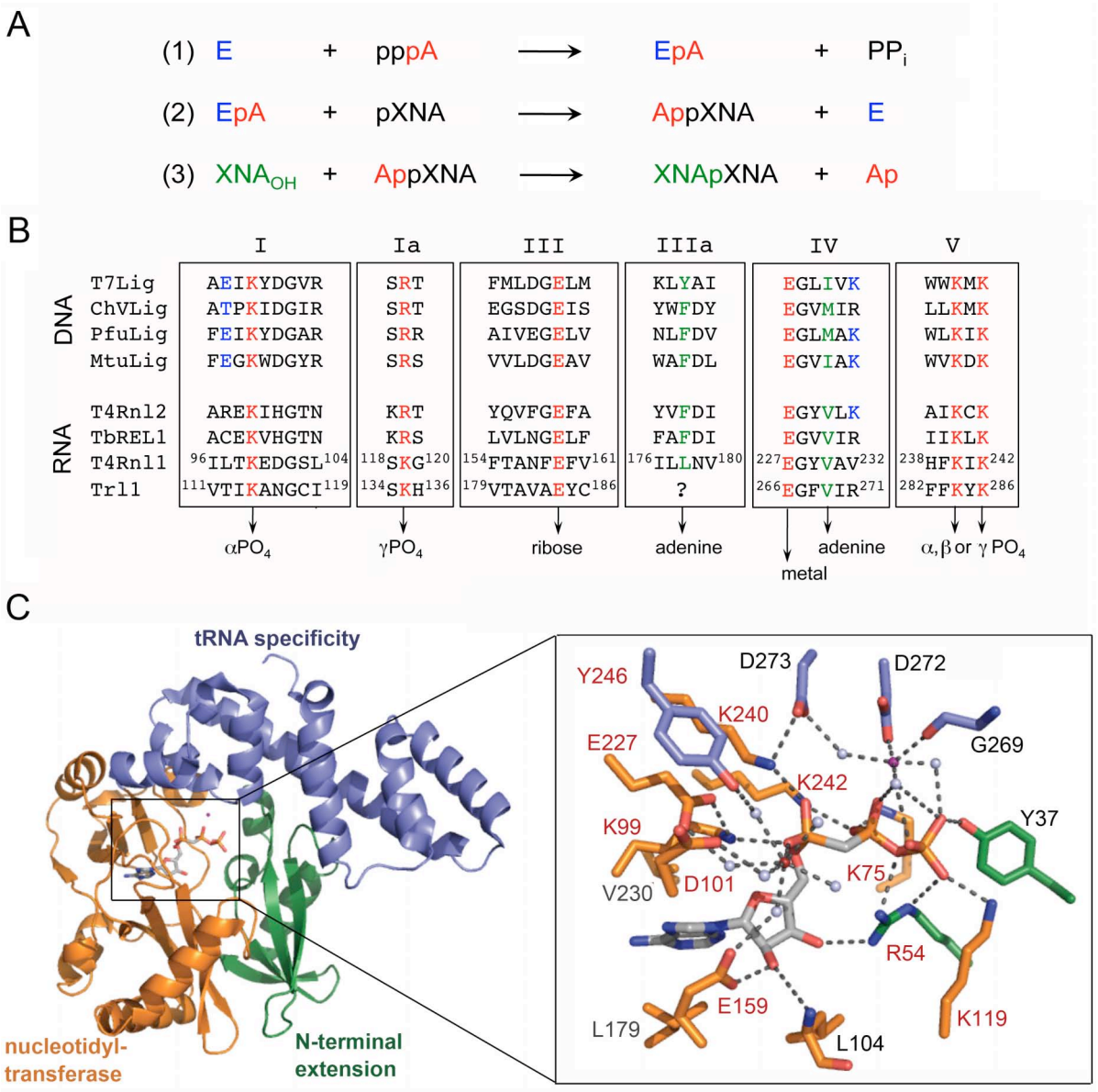

Figure 7 – **T4 Rnl1 belongs to the family of covalent nucleotidyltransferases** (next page)

(A) The three steps of ligation catalyzed by the ATP-dependent ligases of the adenylyltranseferase subfamily. In step one the adenylyl moiety from ATP (pppA) is covalently bound to the catalytic lysine residue in the enzyme (E). In step two the adenylyl is transferred from the enzyme adenylate (EpA) to the phosphorylated 5′ end of a polynucleotide (pXNA for pRNA and pDNA respectively) to form a 5′ to 5′ phosphoanhydride bond (AppXNA). In step three the new 3′ to 5′ phosphodiester bond is formed between the 3′ hydroxyl of a second polynucleotide (XNA_{OH}) and AppXNA and AMP (Ap) is released (modified after (90)). **(B)** Alignement of motifs I, Ia, III, IIIa, IV and V of members of the ATP-dependent subfamilies: DNA ligases (phage T7, *Chlorella* virus, *Pyrococcus furiosus*, *Mycobacterium tuberculosis* LigD) and RNA ligases (phage T4 Rnl2, *Trypanosoma brucei* REL1, phage T4 Rnl1, *S. cerevisiae* Trl1). For the motifs of Rnl1 and Trl1 residue numbers are given. Trl1 motif IIIa has not yet been defined. Specific contacts between conserved residues in the motifs and the nucleotide substrate or metal cofactor are indicated as seen in the Rnl1 crystal structure (panel C) (based on (90,91,97)). **(C)** The crystal structure of phage T4 Rnl1 (PDB 2C5U) (95): the core nucleotidyltransferase domain in orange, the Rnl1 specific N-terminal extension in green and the C-terminal tRNA specificity domain in blue. In the close up of the active site. Side chains contacting the AMPcPP substrate analog are shown as stick models and colored according to the domain they reside in. Residues essential for ligase activity are labeled in red, others in black. Contacts made to the nucleotide, the magnesium ion (red) or calcium ion (purple), are shown as dashed lines. Water molecules are shown as light-blue spheres.

Two subfamilies of RNA ligases exist within the superfamily, one, exemplified by T4 Rnl2, is more closely related to ATP-dependent DNA ligases (90). The other subfamily is exemplified by T4 Rnl1 and also includes bacterial tRNA repair ligases and the tRNA splicing ligases of yeasts and plants (81,92). Nucleotidyltransfer by enzymes of this family proceeds in distinct steps (90). The first step of catalysis is the transfer of a NMP moiety from a donor (NAD^+, ATP or GTP) to the ε-amine of a lysyl side chain in the active site, forming a covalent enzyme-(lysine-Nζ)-NMP intermediate. In the second step, the NMP is transferred to the phosphorylated 5′ end of a polynucleotide to form a A(5′)pp(5′)polynucleotide. DNA and RNA ligases catalyze a third step, the formation of a new 3′,5′-phosphodiester bond from the A(5′)pp(5′)polynucleotide and an acceptor polynucleotide with a 3′-hydroxyl terminus. AMP is released in this last step (Figure 7A).

Six conserved motifs (I, Ia, III, IIIa, IV and V) define covalent nucleotidyltransferases by contributing catalytic side chains to the active site (Figure 7BC). Not all essential residues are necessary in every step of ligation, but all are required for at least one of the steps. As deduced from crystal structures, the motifs have the following roles: Motif I (KxDGxR consensus) contains the lysine that forms the covalent N-P bond and a conserved aspartate, which contacts the magnesium ion cofactor bridged by a water molecule. A conserved basic residue contacting the γ-phosphate defines motif Ia. Motif III contains a conserved glutamate residue that interacts with the ribose moiety of the nucleotide, while an aromatic or aliphatic residue of motif IIIa stacks on the purine ring of the base. Motif IV contains a glutamate or aspartate residue coordinating the divalent cation cofactor and an aliphatic residue contacting the purine. One or two basic residues contacting γ- and α-phosphates, respectively, characterize motif V. The nucleotidyl-transferase domain adopts a fold consisting of two antiparallel β-sheets, that delimit the nucleotide binding cleft (90,91).

1.4.1.2.2 Structure and tRNA specificity of T4 Rnl1

The motif I lysine (Lys99) of Rnl1 was identified as essential by mutagenesis (93). More recently, homology-guided and, after report of the Rnl1 crystal structure, structure-guided mutagenesis efforts have identified all six adenylyltransferase motifs of Rnl1 (94-96). In a crystal structure of monomeric Rnl1 (374 aa), the non-hydrolysable ATP analogon AMPcPP is bound in the active site of the protein, presumably showing the

pre-step 1 conformation of the enzyme (PDB 2C5U) (95). This structure identifies three structural modules in Rnl1 (95,96):

(i) A central adenylyltransferase domain (residues 71-242), which can be superimposed on the N-terminal adenylyltransferase domain of Rnl2.

(ii) An N-terminal Rnl1 specific extension (residues 1-70).

(iii) A C-terminal domain (residues 243-374) that confers tRNA substrate specificity (76,94,95).

Eleven residues have been found to be essential by biochemical dissection of all three steps of ligation using Rnl1 mutants. Seven of the essential side chains reside in the nucleotidyltransferase motifs (Figure 7B) and can be structurally interpreted with the help of the crystal structure (Figure 7C) (94,96). In the structure, Lys99 of motif I is positioned apical to the PcP linkage of AMPcPP, aligned for in line attack. Asp101, also motif I, coordinates the bound magnesium ion bridged by a water molecule. Lys119 of motif Ia donates a hydrogen bond to the γ-phosphate. Structure-guided mutagenesis led to identification of motifs III and IIIa of Rnl1 (96): Glu159 (motif III) contacts both the 3′ oxygen of the ribose and the magnesium ion bridged by a water molecule. The essential Glu227 of motif IV coordinates the bound magnesium ion bridged by a water molecule. The two lysines, Lys240 and Lys242, of motif V interact with β- and α-phosphate, respectively. Two essential residues were identified within the N-terminal extension, establishing it as necessary for Rnl1 activity (94): Arg54 contacts the ribose at the 2′-hydroxyl, the phosphoanhydride linkage between β- and γ-phosphate and the γ-phosphate. Tyr246, in the C-terminal domain, is also coordinating the magnesium cofactor bridged by a water molecule.

Beside the nucleotidyltransferase domain, ATP- and NAD^+-dependent DNA ligases have an additional OB-domain (oligonucleotide binding). This domain consists of a five-stranded antiparallel β-sheet and an α-helix (90). Neither Rnl1 nor Rnl2 have such an OB-domain. Rather, they have their own characteristic C-terminal domains with no structural similarities to each other (95,98). The α-helical C-terminal domain of Rnl1 contains eight helices, one long helix on which the other short helices lie almost parallel to each other. Deletion of this domain does not affect RNA ligation ability, yet slows the kinetics of RNA circularization by Rnl1 (76). However, the same Rnl1 mutation abrogates ligation of tRNA halves *in vitro* and *in vivo*. This finding showed that, T4 Rnl1 is actually

much better at ligating tRNA than linear substrates, demonstrating that it is indeed foremost a tRNA repair enzyme. Rnl1 recognizes tRNAs by their characteristic fold. Deletion of the D-loop or the TΨC-loop from the tRNA structure considerably reduces ligation activity (73). Presumably, this specificity prevents the detrimental consequences of random ligation of compatible RNA fragments.

1.4.2 The bacterial Hen1/Pnkp RNA-repair cassette

Proteins with amino acid sequence homology to T4 Pnkp are encoded in other bacteriophages and also in bacterial genomes. The first bacterial Pnkp to be studied was the multidomain RNA end-healing enzyme of *Clostridium thermocellum*, *Cth*Pnkp (75). *Cth*Pnkp is an 870 amino acid polypeptide with three functional domains (Figure 8B):

(i) An N-terminal 150 amino acid kinase module that displays sequence similarity to T4 Pnkp. This segment harbors a metal- and ATP-dependent kinase, capable of phosphorylating 5′-hydroxyl termini of RNA and DNA oligonucleotides *in vitro* (75).

(ii) A central phosphatase domain, which resembles the bacteriophage λ phosphatase prototype of the dinuclear metallo-phosphatase superfamily (75). This segment of *Cth*Pnkp harbors Ni^{2+}/Mn^{2+}-dependent phosphodiesterase and phosphoesterase activities that release phosphate from 2′,3′-cyclic phosphate, 2′-phosphate and 3′-phosphate ends (75,99). Phosphate release from a 2′,3′-cyclic phosphate terminus occurs in two sequential steps, first the cyclic phosphate is opened to either 2′ phosphate or 3′ phosphate. The phosphate is subsequently released by hydrolysis. A single residue mutation, H189D, reprograms *Cth*Pnkp to a phosphodiesterase that produces only 2′ phosphate ends (100,101).

(iii) A C-terminal ~250 amino acid domain that contains counterparts of the nucleotidyl transferase motifs I, III, IV and V. *In vitro*, this segment of *Cth*Pnkp transfers an adenylyl-group from ATP to Lys531, in motif I (75). However, *Cth*Pnkp does not perform steps two and three of ligation, possibly because it lacks a substrate recognition module like the oligonucleotide binding (OB) fold of DNA ligases or the C-terminal domain of Rnl1 (75,87,90).

Homologs of *Cth*Pnkp are found in 40 bacterial species across eight different phyla (102). Bacterial genomes that encode Pnkp also encode a homolog of the 2′O-methyltransferase Hen1. The *hen1* gene lies directly upstream of *pknp* suggesting a functional association. Gene products of the *Anabaena variabilis* Hen1/Pnkp (*Ava*Hen1/Pnkp) cassette are able to repair tRNA broken by the ACNases colicin D and E5 *in vitro* (1.2.4) (103). *Ava*Hen1 and *Ava*Pnkp form an ($\alpha_2\beta_2$) heterotetramer. This oligomerization establishes a functional ligase by bringing together *Ava*Hen1's N-terminal domain and the adenylyltransferase domain of *Ava*Pnkp (103). *Cth*Hen1 (465 aa) catalyzes the transfer of a methyl-group from S-adenosyl-methionine to the 3′-terminal 2′-hydroxyl of an RNA acceptor (102,104). The 2′O-methyltransferase activity of bacterial Hen1 resides in a C-terminal domain (102,103). In repair of ACNase-induced tRNA damage, the 2′O-methylation marks the RNA repair junction and protects the repaired RNA against further site-specific cleavage *in vitro* (103). Although an *in vivo* role for this system of bacterial RNA repair has been implied, its actual role and the relevance of the methylation remain unclear. It needs to be addressed if repaired tRNA is still functional after methylation within the anticodon.

1.5 tRNA splicing

A subset of tRNA genes, in every archaeal and metazoan genome, contains intronic sequences. In tRNA maturation these introns, which are usually located in the anitcodon loop, are removed. Dedicated tRNA splicing endonucleases excises the introns from pre-tRNA molecules, tRNA splicing ligases subsequently join the fragments. The splice sites of eukaryal tRNAs are not conserved in nucleotide sequence, but begin at the second nucleotide after the anticodon, suggesting a conservation of splice site position. (105,106).

In *S. cerevisiae*, tRNA splicing occurs in three steps (Figure 8A) (105):

(i) The intron is excised by the splicing endonuclease.

(ii) The cleavage termini in the anticodon of pre-tRNA molecules are healed and sealed by the three catalytic activities of the tRNA ligase Trl1 (1.5.2.1).

(iii) Ligation by Trl1 leaves a 2′ phosphate at the newly formed 3′,5′-phosphodiester splice juction. This phosphate is transferred to NAD^+ by the tRNA 2′-phosphotransferase Tpt1.

The yeast and human tRNA splicing endonucleases are homologous to the endonucleases in archaeal tRNA splicing (1.5.2) (106,107). While the tRNA splicing ligase is conserved from yeast to plants, no equivalent of such an enzyme has been identified in archaea or metazoa, although a yeast-like tRNA splicing ligase activity has been described in HeLa cells (108). The presence of Tpt1-like proteins and 5' kinase healing activities in metazoa also suggests the existence of a yeast-like splicing pathway (109,110). The recent discovery of the "direct" RNA ligase RtcB in archaea, human, and *E. coli* highlights, that tRNA splicing in archaea and metazoa is still only incompletely understood (1.5.4) (111-113).

The similarities of pre-tRNA processing by tRNA splicing endonucleases and tRNA cleavage by ACNases are remarkable: The ribonuclease reaction follows RNase A-like catalysis and incisions are made within the anticodon-loop of tRNA in both cases. Notable is also, that T4 Pnkp and Rnl1 can functionally replace Trl1 *in vivo* and a plant Trl1 ortholog can counteract ACNase damage in yeast (1.5.3) (73,81).

1.5.1 tRNA splicing endonucleases

In the first step of eukaryal and archaeal tRNA splicing, pre-tRNAs are cleaved to yield two tRNA halves and a linear intron with 2′,3′-cyclic phosphate and 5′-hydroxyl termini (105). The archaeal and eukaryal tRNA splicing endonucleases catalyzing this reaction have evolved from a common ancestor. These endonucleases are multimers with a (pseudo-) two-fold symmetry reflected by presence of two active sites per complex, one for each splice junction. Four subfamilies have been classified: α_4 homotetramers (e.g. in *Methannococcus jannaschii*), α_2 homodimers (e.g. in *Haloferax volcanii* and *Archaeoglobus fulgidus*), $(\alpha\beta)_2$ heterodimers or $\alpha\beta\gamma\delta$ heterotetramers (in yeast and human) (105-107).

Archaeal pre-tRNAs are defined by a conserved structural bulge-helix-bulge motif, consisting of two three-nucleotide loops separated by a four-nucleotide helix, which is recognized by archaeal splicing endonucleases (105). The co-crystal structure of homodimeric *A. fulgidus* archaeal endonuclease bound to bulge-helix-bulge RNA (PDB 2GJW), together with biochemical studies, has illuminated substrate recognition and the catalytic mechanism of tRNA splicing endonucleases (13,106). The cleavage reaction has been compared to the chemistry catalyzed by RNase A. In the active site of *A. fulgidus* endonuclease Tyr246, His257 and Lys287 are positioned suggestive of an RNase A-like mechanism: Tyr246 as general base activating the ribose 2′ oxygen for in line attack on the

phosphate, Lys287 as stabilizator of the pentavalent transition state and His257 as general acid protonating the 5′ oxygen of the leaving group 3′ of the scissile bond (Figure 1B). All three of these residues are conserved, together with an arginine (Arg280 in the *A. fulgidus* enzyme), in all known tRNA splicing endonucleases (106).

The yeast splicing endonuclease (Sen) consists of four essential subunits: Sen2, Sen54, Sen15 and Sen34, and localizes to the mitochondrial outer membrane (105). A pseudo two-fold symmetry is retained in this heterotetramer, as the catalytic subunits Sen2 and Sen34, as well as the non-catalytic subunits Sen15 and Sen54 share regions of homology, respectively. The domain of homology between Sen2 and Sen34 is similar to the catalytic domains of the archaeal endonucleases. Yeast genetic experiments have shown that Sen2 and Sen34 are specifically responsible for cleavage of the 5′ splice site and 3′ splice site, respectively. The subunits of the human tRNA splicing endonuclease are homologous to the yeast proteins and have thus been designated HsSen54, HsSen2, HsSen34 and HsSen15 (107). Mutations in *HsSEN* genes cause defects in neurological development in zebrafish and have been causally linked to human pontocerebellar hypoplasia (114-116).

1.5.2 tRNA ligation in fungi and plants

1.5.2.1 Yeast tRNA splicing ligase Trl1

The yeast tRNA splicing ligase of *S. cerevisiae* (827 aa) unites three catalytic activities on one polypeptide and localizes to the cytoplasm (105). Genomic disruption of *TRL1* is lethal in yeast (117). *In vivo* complementation experiments show, that the N-terminal adenylyltransferase/ligase domain (residues 1-388), the central 5′ kinase domain (residues 389-561), and the C-terminal cyclic phosphodiesterase domain (CPD, residues 562-827) are all essential for yeast viablity. Separated healing and sealing activities can complement *trl1Δ* cells *in trans* (117). However, such a separation of ligase and CPD/kinase domains reduces overall Trl1 tRNA ligation *in vitro* by an order of magnitude (73). Trl1's ligase activity belongs to the covalent adenylyltransferase family and is related to Rnl1 (Figure 8) (94,96). *In vitro*, Trl1 is able to ligate pre-tRNA substrates incised by an archaeal tRNA splicing endonuclease, but does not catalyze intron circularization. Unlike T4 Rnl1, Trl1 does not rely on the tRNA fold, but requires a 2′-phosphate at the 3′ break site for substrate recognition (73).

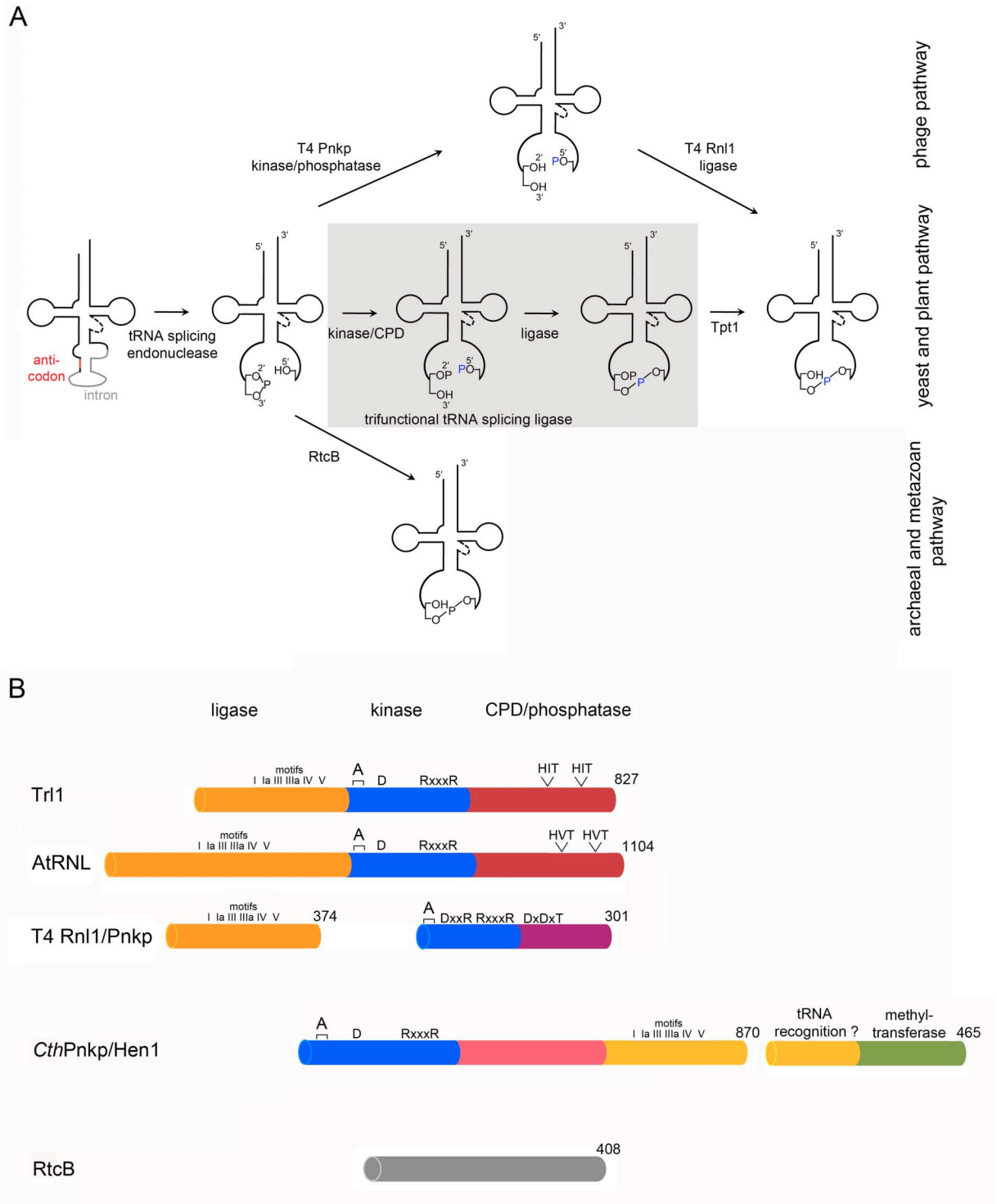

Figure 8 – **tRNA repair enzymes**

(A) Depicted are the pathways of tRNA splicing. In addition to the yeast/plant-like pathway and the direct archaeal/animal RtcB pathway, the phage pathway, as it occurs in yeast *trl1Δ* complementation, is shown. This pathway requires three activities comprised in two proteins and proceeds via 2′,3′-diol and 5′-phosphate healed intermediate. In the yeast/plant pathway healing yields 2′-phosphate, 3′-hydroxyl and 5′-phosphate ends, the 2′-phosphate is required for sealing and removed in a third step by Tpt1.

(Figure 8 – continued)

The archaeal and metazoan ligase RtcB directly ligates the ends produced by the splicing endonuclease, the phosphate in the new 3′,5′-phosphodiester bond is derived from the 2′,3′-cyclic phosphate. **(B)** Comparison of tRNA healing enzymes: Ligases are shown in orange/yellow, kinase domains in blue, phosphatases belonging to different families in different shades of red or purple, the Hen1 methyltransferase is shown in green. RtcB is shown in grey, as it has no similarity to known protein structures. Yeast Trl1 and plant AtRNL are trifunctional enzymes. Their CPD belongs to the 2H phosphoesterase family defined by two HxT motifs (HIT in Trl1, HVT in AtRNL). The ligases of Trl1 and AtRNL are similar to T4 phage Rnl1, conserved are the motifs I – V as well as the Rnl1 N-terminal extension. The 5′ kinase domains of T4 Pnkp are also conserved in Trl1 and AtRNL, containing a Walker A motif (A), a conserved essential aspartate (D) and RxxxR motif. However, the phosphatase domain of Pnkp belongs to the HAD family defined by a DxDxT motif involved in covalent catalysis. The Pnkp enzyme of *Clostridium thermocellum* also contains a Pnkp-like 5′ kinase, the phosphatase on the other hand is a metallo-phosphatase of the calcineurin family. The C-terminal adenylyltransferase domain of bacterial Pnkp and the N-terminal domain of Hen1 together form a functional ligase. Hen1 additionally contains a methyl-transferase activity.

Residues 1-376 of Trl1 define the minimal ligase domain necessary for *in vivo* and *in vitro* sealing activity (117). In the minimal ligase, Lys114 of motif I, the motif Ia residues ^{134}SKH^{136}, Glu184 defining motif III, Glu266 and Gly267 of motif IV, and the lysines (Lys284 and Lys286) of motif V are essential (Figure 7B) (96,97,117). Motif IIIa has not yet been defined for Trl1.

The 5′ kinase module of Trl1 catalyzes the transfer of the γ-phosphate of GTP to the 5-hydroxyl of the 3′ tRNA half and displays sequence similarity to the kinase domain of T4 Pnkp (96,105,117). Like the Pnkp kinase, the Trl1 kinase module contains a Walker A motif (^{398}SVIGCGKT^{405}), an essential aspartate, Asp425 (suggested to correspond to Pnkp Asp35) and a RxxxR (^{507}RVIKR^{511}) motif (Figure 8B) (117). K404A/T405A, D425A and R511A mutations in Trl1 ablate *trl1Δ* complementation. The D425A mutation also abolishes GTP dependent kinase activity *in vitro*.

The CPD activity marks the difference between the T4 phage and yeast pathway of tRNA repair. The Trl1 CPD catalyzes the opening of the 2′,3′-cyclic phosphate at the 5′ tRNA half to 3′-hydroxyl and 2′-phosphate, the latter is required for sealing by the Trl1 ligase activity (81,105). T4 Rnl1 and Pnkp can functionally replace Trl1 as tRNA splicing ligase *in vivo*, bypassing the requirement for Tpt1 (81). However, combinations of Trl1's ligase domain with T4 Pnkp fail to rescue *trl1Δ* cells. This demonstrated the requirement for 2′-phosphate at the cleavage site for sealing by Trl1. T4 Rnl1 is more promiscuous and catalyzes ligation of tRNA healed by Trl1 kinase/CPD (81).

The Trl1 CPD belongs to the 2H family of phosphoesterases defined by two HxT motifs, ^{673}HIT^{675} and ^{777}HIT^{780} in Trl1 (117,118). In crystal structures solved for other members of the 2H family, histidines and threonines of both motifs contact the phosphate oxygens in the ligand complex and the histidines are thought to catalyze hydrolysis in a

general acid-base mechanism (119). While both histidines are essential in other 2H phosphoesterases, in Trl1 only Thr675 of the first HxT, and His777 of the second HxT are required for activity *in vivo* (117,119).

Besides tRNA splicing, Trl1 is involved in unconventional mRNA splicing in the unfolded protein response (UPR) in yeast. Trl1 joins *HAC1* mRNA exons after intron-excision by the site-specific endoribonuclease activity of Ire1 (120). Ire1 spans the membrane of the endoplasmic reticulum. Upon unfolded protein stress Ire1 oligomerizes which activates the nuclease activity on the cytoplasmic membrane surface (121). Spliced *HAC1* mRNA is translated to yield the transcription factor Hac1, which upregulates expression of UPR proteins. The tRNA splicing and UPR functions of Trl1 can be separated (120). Cells expressing a Trl1 H148Y mutant are viable, this mutant is competent in pre-tRNA ligation, but inactive in *HAC1* mRNA splicing.

1.5.2.2 Plant tRNA splicing ligase

A plant RNA ligase activity, capable of pre-tRNA ligation, was first discovered in wheat germ extract (122,123). This plant tRNA ligase is able to ligate 5′-hydroxyl or 5′-phosphate termini to 5′ acceptors with 2′-phosphate, or 2′,3′-cyclic phosphate ends. After purification of the enzymatic activity, peptide sequencing allowed the identification of genes encoding for homologous proteins in *Arabidopsis* and *Oryza* genomes (92). The 1104 amino acid tRNA splicing ligase of *Arabidosis thaliana*, AtRNL, is a true ortholog of yeast Trl1, sharing all three activities and complementing *trl1Δ* yeast cells (Figure 8B) (119). *In vitro* AtRNL, like Trl1, ligates tRNA halves even when they are missing characteristic loops. However, in contrast to Trl1, the plant ligase also circularizes the spliced intron (73). The sealing (residues 1-675) and healing (residues 677-1104) domains of AtRNL can act *in trans* (73,119). These separated AtRNL domains are also active in *trl1Δ* complementation when combined with the complement Trl1 domain. Mutations of AtRNL residues corresponding to ligase motif I (K152A), ligase motif IV (E326A), kinase Walker A motif (S701A) or conserved aspartate (D726A) and the HxT motifs (T1001A and H1060A) lose activity *in vivo* (119). AtRNL can ligate spliced *HAC1* mRNA *in vitro*, yet fails to alleviate attenuation of *HAC1* translation (124). The circularized *HAC1* introns produced by AtRNL activity are degraded less efficiently than linear introns. These intron circles impede effective *HAC1* translation by binding to the spliced mRNA.

1.5.3 Repair of anticodon nuclease damage *in vivo*

The susceptibility of *S. cerevisiae* to fungal and bacterial ACNases is intriguing, given that *S. cerevisiae* Trl1 is, in principle, capable of healing and sealing the exact 2′,3′-cyclic phosphate and 5′-hydroxyl termini generated by these toxins (1.1). The portability of tRNA repair systems, i.e. the ability of either AtRNL or T4 tRNA repair enzymes to functionally replace Trl1 in yeast, made the study of ACNase damage repair in yeast possible (73,81,119). AtRNL or T4 Pnkp/Rnl1 expressing *trl1Δ* cells are rescued from γ-toxin toxicity by *in vivo* tRNA repair (73). Use of loss of function mutants of AtRNL in wild type (*TRL1*) cells showed, that it is predominantly the ligase activity of Trl1 that fails to accept γ-toxin cleaved tRNA as a substrate (73). It is possible, that Trl1 is incapable of joining completely modified broken tRNAs. However, the absolute dependence of γ-toxin the mcm^5 modification at the wobble uridine precluded the exploration of this hypothesis.

1.5.4 tRNA ligation in archaea and metazoa

An additional, different tRNA splicing pathway was described in HeLa cell extract: a ligase activity capable of circularized linear RNA substrates with 2′,3′-cyclic phosphate and 5′-hydroxyl ends (125). In this mechanism, the phosphate from the cyclic 3′ end is directly incorporated into the newly formed 3′,5′-phoshodiester. It was also postulated that mammalian tRNA splicing involves a ligase that follows such a “direct” mechanism of ligation (126). This would distinguish metazoan tRNA splicing from the yeast/plant pathway, which includes end-healing and classic ligation. With the recent identification of the direct ligase as RtcB, there is evidence for two parallel pathways of tRNA ligation in metazoa: a yeast-like pathway of tRNA-splicing and direct pre-tRNA ligation pathway.

1.5.4.1 The putative archaeal and metazoan tRNA ligase RtcB

RtcB was identified as the “direct” ligase in bacteria, archaea and humans (Figure 9A) (111-113). Human RtcB, HsRtcB, was isolated from HeLa cells based on its ability to convert 2′,3′-cyclic phosphate and 5′-hydroxyl terminated dsRNA to covalently linked hairpins (113). Silencing of HsRtcB by siRNA delayed maturation of a reporter tRNA, suggesting that HsRtcB functions as a ligase human tRNA splicing. A direct ligation activity

A

```
Pae  ------MRNIPINKINDYVWEIPPGVKPCQKVPVRIYADSVLLEKMKSDM--------------TLEQGINVGCLP 56
Pho  -------MVVPLKRIDKIRWEIP-KFDKRMRVPGRVYADEVLLEKMKNDR--------------TLEQATNVAMLP 54
Hs   MSRSYNDELQFLEKINKNCWRIKKGFVPNMQVEGVFYVNDALEKLMFEELRNACRGGGVGGFLPAMKQIGNVAALP 76
Eco  ---------------------MNYELLTTENAPVKMWTKGVPVEADARQQ-----------------LINTAKMP 37
                          :   .    ..   .:.. .  :    :                      .. :*

Pae  GIYRWSIVLPDAHQGYGFPIGGVAAIDAE--EGVISPGGIGYDINCGVRVLRTNLTEEDVRPKLKELVDTIFRLVP 130
Pho  GIYKYSIVMPDGHQGYGFPIGGVAAFDVK--EGVISPGGIGYDINCGVRLIRTNLTEKEVRPRIKQLVDTLFKNVP 128
Hs   GIVHRSIGLPDVHSGYGFAIGNMAAFDMNDPEAVVSPGGVGFDINCGVRLLRTNLDESDVQPVKEQLAQAMFDHIP 152
Eco  FIFKHIAVMPDVHLGKGSTIG-----SVIPTKGAIIPAAVGVDIGCGMNALRTALTAEDLPENLAELRQAIETAVP 108
      * :    :** * * * .**     .    :..: *..:* **.**:. :** *  .::     :* :::   :*

Pae  PGVGGTGHLRLSPSEFERVLAEGVEWAVQKG-YGWAEDMEYIEERGSWKLADPSKVSEKAKARGRDQLGTLGSGNH 205
Pho  SGVGSQGRIKLHWTQIDDVLVDGAKWAVDNG-YGWERDLERLEEGGRMEGADPEAVSQRAKQRGAPQLGSLGSGNH 203
Hs   VGVGSKGVIPMNAKDLEEALEMGVDWSLREG-YAWAEDKEHCEEYGRMLQADPNKVSARAKKRGLPQLGTLGAGNH 227
Eco  HGRTTGRCKRDKGAWENPPVNVDAKWAELEAGYQWLT----------------QKYPRFLNTNNYKHLGTLGTGNH 168
      *              :  :  ...*:  :. * *                  .  .   : ..  :**:**:***

Pae  FLEIQVVDKIYDEKIAKLFGIEREGQVVVMIHTGSRGFGHQVATDYLLIMERKMRQWGLNLPDRELAAAPLKDKVA 281
Pho  FLEVQVVDKIFDPEVAKAYGL-FEGQVVVMVHTGSRGLGHQVASDYLRIMERAIRKYRIPWPDRELVSVPFQSEEG 278
Hs   YAEIQVVDEIFNEYAAKKMGIDHKGQVCVMIHSGSRGLGHQVATDALVAMEKAMKRDKIIVNDRQLACARIASPEG 303
Eco  FIEICLDE---------------SDQVWIMLHSGSRGIGNAIGTYFIDLAQKEMQETLETLPSRDLAYFMEGTEYF 229
      : *: ::               ..** :*:*:****:*: :.:  :   :: ::.      .*:*.

Pae  EDYIKAMASAANFAWTNRHIIMHWVREAFKKVFG--SIEKVGLEVVYDVAHNIAKLEEHVVDEKGTVRKVWVHRKG 355
Pho  QRYFSAMKAAANFAWANRQMITHWVRESFQEVFKQDPEGDLGMDIVYDVAHNIGKVEEHEVD--GKRVKVIVHRKG 352
Hs   QDYLKGMAAAGNYAWVNRSSMTFLTRQAFAKVFN-TTPDDLDLHVIYDVSHNIAKVEQHVVD--GKERTLLVHRKG 376
Eco  DDYLKAVAWAQLFASLNRDAMMENVVTALQSITQKTVRQPQTLAMEEINCHHNYVQKEQHFG-----EEIYVTRKG 300
      : *:..:  *  :*  **  :   .  :: .:          : :    .*: ::: ..          : * ***

Pae  ATRAFPPGRSEIPAKYREVGQPVLIPGSMGTASWILVGTHDAMRLTFGTAPHGAGRVLSREAAIRMYPPHKVQEEM 431
Pho  ATRAFPPGHEAVPRLYRDVGQPVLIPGSMGTASYILAGTEGAMKETFGSTCHGAGRVLSRKAATRQYRGDRIRQEL 428
Hs   STRAFPPHHPLIAVDYQLTGQPVLIGGTMGTCSYVLTGTEQGMTETFGTTRHGAGRALSRAKSRRNLDFQDVLDKL 452
Eco  AVSAR-------------AGQYGIIPGSMGAKSFIVRG--LGNEESFCSCSHGAGRVMSRTKAKKLFS----VEDQ 357
      :. *              .**  :* *:**: *::: *   .   :* :  *****.:**  : :        :.

Pae  AKRGIIVRSAETEVISEEAPWAYKDVDRVVEAAHQVGFAKKVVRQRPIGVVKG 484
Pho  LNRGIYVRAASMRVVAEEAPGAYKNVDNVVKVVSEAGIAKLVARMRPIGVAKG 481
Hs   ADMGIAIRVASPKLVMEEAPESYKNVTDVVNTCHDAGISKKAIKLRPIAVIKG 505
Eco  IRATAHVECRKDAEVIDEIPMAYKDIDAVMAAQSDL--VEVIYTLRQVVCVKG 408
           :.  .   : :* * :**::  *: .  :    :     * :   **
```

B

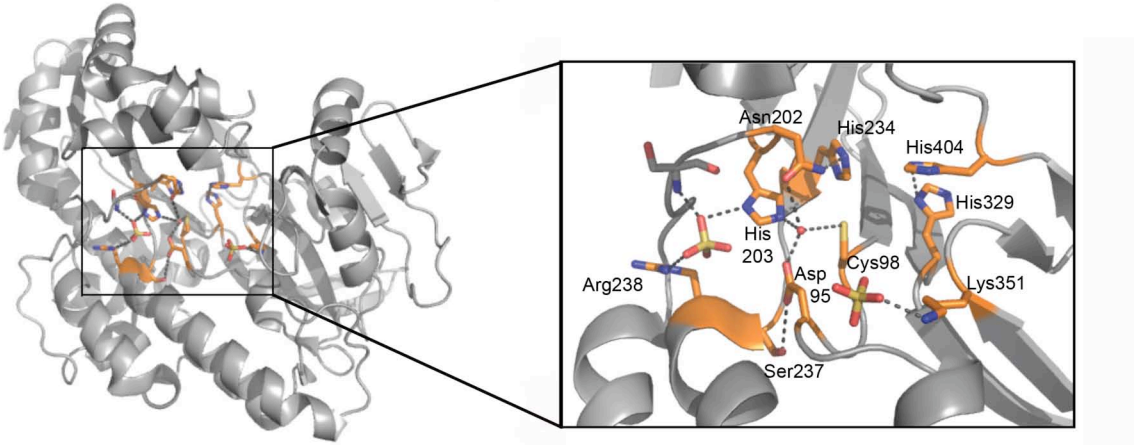

Figure 9 **– RtcB, a novel RNA ligase**

(A) Alignment of RtcB proteins from *Pyrobalcum aerophilum* (Pae, accession Q8ZY09), *Pyrococcus horikishii* (Pho, accession O59245), human (Hs, accession CAG33456) and *E. coli* (Eco, AP_004370). The alignment was generated with ClustalW (43). Residues of the putative active site are highlighted in yellow, conserved residues are labeled with an asterisk (*), similar residues with one or two dots. **(B)** The crystal structure of *Pyrococcus horikoshii* RtcB in grey with the putative active site in orange (PDB 1UC2). Residues highlighted in panel A are labeled and shown as stick models. A water molecule that might mimic a divalent metal cofactor is shown as a red sphere, interactions are shown as dashed lines.

was also detected in extracts of archaeal *Methanopyrus kandleri* and purified to homogeneity. Mass spectroscopic analysis indentified the isolated polypeptide as the 988 amino acid intein-containing precursor of an RtcB family protein. RtcB proteins encoded by other archaea were expressed recombinantely and *Pyrobalcum aerophilum* RtcB (*Pae*RtcB) was characterized further (112). *In vitro*, *Pae*RtcB ligated pre-tRNA incised by an archaeal tRNA splicing endonuclease, incorporating the phosphate from the 3′ terminus of the 5′ half. This activity was reported to be Zn^{2+} dependent, but independent of NTP addition. The phylogenetic distribution of RtcB accords with an archaeal/metazoan specific role in tRNA splicing: it is missing in most plants and fungi (111).

The crystal structure of archaeal *Pyrococcus horikoshii* RtcB shows a novel fold with no similarity to known ligases or phosphotransferases (127). *Pho*RtcB folds into a single domain, consisting of three β-sheets surrounded by 15 α-helices (PDB 1UC2). The putative active site lies in a hydrophilic pocket at the bottom of a positively charged cleft where conserved residues lie in close proximity. The structure of *Pho*RtcB does not contain metal density, however conserved residues Asp95, Cys98, Asn202 and His203 coordinate a water molecule that could mimic such a cofactor (Figure 9B).

Interestingly, RtcB proteins are also found in eubacteria. *E. coli* RtcB has an Mn^{2+}-dependent RNA ligase activity. *Eco*RtcB catalyzes resealing of 2′,3′-cyclic phosphate and 5′-hydroxyl terminated tRNAs halves generated by the fungal ACNase γ-toxin *in vitro* (111). *Eco*RtcB expression is genetically linked to expression of the RNA 3′-terminal phosphate cyclase, RtcA (128). This genetic link suggests a common pathway for RtcA and RtcB, possibly RtcA functions upstream of RtcB, and produces the 2′,3′-cyclic phosphate termini for ligation by RtcB.

2 Significance and Objective

The possible therapeutic application for tRNA damage inducing agents is exemplified by onconase of *Rana pipiens*. Onconase is a member of the RNase A super-family and exerts cytotoxicity by cleaving tRNA (129). Onconase is currently used in clinical trials as an adjuvant in lung cancer treatment (Tamir Biotechnology, Inc.). A use in cancer therapy has also been suggested for colicins, as tumor cells are more sensitive to their toxicity than normal tissue (50). Thus the circle of therapeutic candidates can be expanded to all ACNases. An interesting extension of this concept is the protection from cytotoxic tRNA damage by tRNA repair enzymes. Such a rescue has been demonstrated by coexpression of tRNA damaging *K. lactis* γ-toxin and repair enzymes *in vivo* in yeast (73). In combination, tRNA damaging toxins and compatible RNA repair mechanisms can be envisioned in new approaches to therapy. tRNA repair could selectively increase the resistance of healthy tissue against ACNase toxicity. Before putative therapeutic applications can be addressed, it is essential to understand the biological activity of different tRNA targeting enzymes and how their cytotoxicity can be modulated.

The objective of my studies was the investigation of structure-function relationships of ACNases, with *in vivo* toxicity to *S. cerevisiae* as a read-out of activity. Initially, I contributed to mutational analysis of *K. lactis* γ-toxin (3.1). After it was discovered that intracellular expression of *E. coli* PrrC is also toxic to yeast, I focused on analyzing and characterizing this ACNase activity *in vivo*. In parallel to these functional analyses, I crystallized the non-toxic mutant H356A of full length *Eco*PrrC. A PrrC crystal structure could give insight into the mechanism of the ACNase and the role of the NBD-domain. However, under all tested conditions, crystals only diffracted to 7.5 Å impeding elucidation of the molecular structure of PrrC. I tested whether homologs of PrrC encoded in other bacteria are also toxic to yeast. *Streptococcus mutans* PrrC is toxic, while the PrrC encoded in *Neisseria meningitidis*is not (3.3). I found that a single nucleotide mutation is sufficient to transform *N. meningitidis*PrrC into a toxin. I investigated the toxicity of this new ACNase in yeast *in vivo* and used it to study PrrC-inflicted tRNA damage repair (3.4). I extended the study of *in vivo* ACNase damage repair to rescue of *P. acaciae* toxicity by phage-type tRNA repair, plant/yeast-type repair and, with *E. coli* RtcB, the newly discovered direct pathway of tRNA repair (3.2 and 3.5). These *in vivo* repair studies show that T4 phage and plant tRNA repair enzymes, as well as *Eco*RtcB are able to overcome

ACNase damage, depending principally on toxin dosage and incision site. The intrinsic *S. cerevisiae* tRNA ligase Trl1, however, is incapable of such repair under any conditions tested. The therapeutic use of any ACNase may similarly exploit deficiencies of mammalian cells and malignant cell types in particular in repairing broken tRNAs.

3 Results and Discussion

3.1 Structure-activity relationships in *K. lactis* γ-toxin

Keppetipola N, Jain R, Meineke B, Diver M, Shuman S (2009)
Structure-activity relationships in *K. lactis* γ-toxin. RNA 15(6), 1036-44.

The Byström group discovered the endoribonuclease activity of *K. lactis* zymocin's γ-toxin and identified $tRNA^{Glu\ (UUC)}$ as its relevant intracellular target (7). The RNA substrate requirements for recognition by γ-toxin have been well defined by *in vitro* studies with 17mer RNA stem-loops (60). On the other hand, there was very little information about the determinants in γ-toxin that confer this specificity or which residues contribute to the active site. In order to elucidate γ-toxin function, we carried out a targeted alanine-scan of residues likely to be involved in the RNase A-like mechanism (histidine, glutamate, lysine and arginine) suggested for the ACNase (see section 1.1.1) or in binding the phosphate backbone of RNA (lysine and arginine). Mutation to alanine replaces the side chain of the targeted amino acid by an inert methyl-group, allowing insight into the functional contribution of this residue. Toxicity of intracellular γ-toxin was used as *in vivo* read-out of ACNase activity. In 25 of the 62 positions, targeted mutation to alanine ablated γ-toxin toxicity, demonstrating essential contribution of the mutated residue. In these positions, we used conservative mutations (e.g. replacing glutamate by glutamine and aspartate) to gain insight into the role of the side chain in question. Residues that could not be functionally replaced were considered strictly essential.

The alanine-scan identified γ-toxin's sole histidine, His209, as strictly essential for *in vivo* and *in vitro* activity. This result is consistent with a catalytic role as general acid or base in an RNase A-like mechanism. Of 23 lysines mutated in γ-toxin, 10 were essential for toxicity, but only Lys21 was strictly essential. Replacement of three of the 13 tested arginine residues with alanine, lysine or glutamine lead to activity loss. Four other arginines were essential, but could be functionally replaced by conservative changes. Lysine residues are involved in metal-independent RNase activity of RNase A, *A. flugidus* tRNA splicing endonuclease and colicin D (Figure 1B). An active site lysine in these enzymes contacts the scissile phosphate and stabilizes the pentavalent transition state. In RNase T1, an arginine fulfills an equivalent role (14). Outside of the active site, positively charged

lysine and arginine side chains could function in substrate binding by contacting the phosphate backbone. RNase T1 has a glutamate residue involved in general base catalysis in its active site (14). Only three of γ-toxin's 21 glutamates could not be replaced by alanine without loss of toxicity. Two of the essential residues could be replaced by Asp or Asp and Gln, respectively. A sole strictly essential glutamate, Glu9, could be involved in RNase activity.

Mutation of three of four cysteine residues in γ-toxin to alanine did not affect *in vivo* or *in vitro* activity, but allowed increased yield of soluable recombinantly expressed protein. This triple Cys to Ala γ-toxin mutant was purified using a cleavable N-terminal His_{10}-tag and sedimented as a monomer. *In vitro* experiments agree with an RNase A- or RNase T1-like mechanism, because γ-toxin cleavage of a 17mer stem-loop is metal independent and the 2′-hydroxyl at the incision site is required; stem-loops with 2′-H or 2′-F are not cleaved.

In a follow up study, my colleagues continued the mutational analysis of γ-toxin, mutating all tyrosine and aspartate residues in the primary structure and testing those Arg to Ala mutations *in vitro* that had lost toxicity *in vivo* (130). Together, the data of both studies suggest catalytic roles for His209, Glu9 and Arg151, possibly in an RNase T1 like mechanism. However, a catalytic role for Lys21 can also not be excluded at this point. Definite assignment of catalytic residues and residues recognizing the mcm^5 modification would require knowledge of γ-toxin's tertiary structure.

3.2 *In vivo* repair of tRNA damaged by *Pichia acaciae* toxin in *Saccharomyces cerevisiae*[1]

3.2.1 Introduction

The linear killer plasmid of *Pichia acaciae* encodes a secreted heterotrimeric killer toxin and a cognate immunity protein (60,62,63). Whereas the intracellular toxic subunit of Pichica toxin (PaT) shows no obvious amino acid sequence similarity to *K. lactis* γ-toxin or other ACNases, the other toxin subunits are homologous to zymocin's α- and β-subunits,

[1] The data presented in this section constitutes my contribution to a collaborative study on the *Pichia acaciae* ACNase conducted with the group of Prof. Friedhelm Meinhardt at the University of Münster. A publication combining this data with data generated in the Meinhardt lab is planned.

respectively (63). The major intracellular target of PaT is $tRNA^{Gln\ (UUG)}$, which is incised primarily 3′ of the mcm^5s^2U wobble nucleotide. Subsequent PaT cleavage at a secondary upstream site, between U32 and U33, results in excision of a dinucleotide (Figure 12) (8).

The substrate specificity of γ-toxin differs from PaT's: γ-toxin cleaves $tRNA^{Glu\ (UUC)}$ specifically 3′ of the mcm^5s^2U wobble nucleotide. PaT and γ-toxin are differently affected by hypomodification of the target wobble uridine (7,8,60). The acetyltransferase Tot3, and in the last step the methyltransferase Trm9 produce mcm^5U modified uridine wobble nucleotides in yeast (8,64-67). Disruption of either *TRM9* or *TOT3* makes *S. cerevisiae* cells resistant to exogenous zymocin or intracellular γ-toxin expression (7). Whereas *trm9Δ* cells are resistant to exogenous PaT, *trm9Δtot3Δ* and *tot3Δ* cells are sensitive. Intact mcm^5s^2U is not essential for cleavage by PaT, but incomplete modifications inhibit its ACNase activity. Intracellular expression of PaT from a high-copy plasmid is toxic to both *trm9Δ* and *tot3Δ* cells (8).

Susceptibility of *S. cerevisiae* to PaT, and all other ACNases tested in this yeast so far demonstrate that Trl1 fails to efficiently repair the inflicted tRNA damage. In contrast, plant tRNA ligase AtRNL and also the T4 tRNA repair enzymes can confer protection from γ-toxin (73). With this background, we wanted to address the following questions: Are the same tRNA repair systems able to repair tRNA damaged by PaT? Does PaT dosage and the state of the wobble base modification affect tRNA repair? Does the presence of innate Trl1 repair activities influence the repair efficiency?

3.2.2 Results

Galactose-inducible high-copy (*2μ*) and single-copy (*CEN*) plasmids were used for PaT expression in *S. cerevisiae*. Expression of PaT from a high-copy plasmid is toxic to wild type, *trm9Δ* and *tot3Δ S. cerevisiae* cells (Figure 10A) (8). Coexpression of AtRNL or T4 phage Pnkp/Rnl1 protect *trm9Δ* and *tot3Δ*, but not wild type cells from *2μ* PaT toxicity. This protective effect is strongest in *trm9Δ* cells. In contrast to γ-toxin toxicity, PaT toxicity could not be overcome in wild type cells, while both plant and phage tRNA repair can protect from PaT toxicity in cells with hypomodified tRNA.

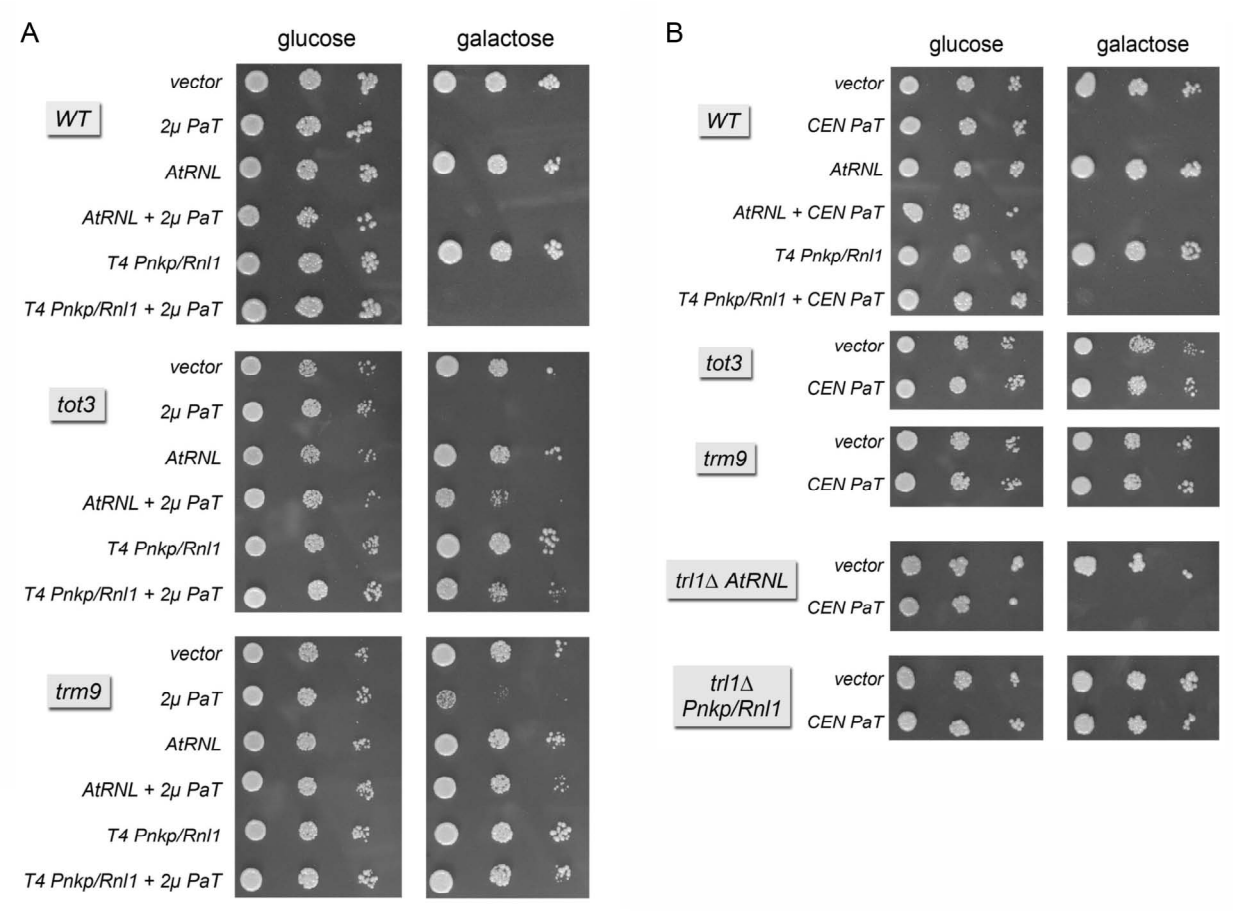

Figure 10 – **Intracellular PaT expression from a single-copy plasmid.**

Serial 10-fold dilutions of *S. cerevisiae cells* expressing PaT or an empty vector or in presence of an additional plasmid encoding AtRNL (2μ) or T4 Pnkp and Rnl1 were spotted on selective agar plates with 2% glucose or galactose. Plates were photographed after 2d (glucose) or 3d (galactose) incubation at 30°C. **(A)** PaT expression from a single copy (2μ) plasmid. **(B)** PaT expression from a high-copy (CEN) plasmid.

Expression of PaT from a single-copy (*CEN*) plasmid is also toxic to wild type *S. cerevisiae* cells, while it does not affect growth of *trm9Δ* and *tot3Δ* cells (Figure 10B). AtRNL or T4 Pnkp/Rnl1 cannot protect from *CEN* PaT toxicity in wild type cells. In *trl1Δ* cells complemented with AtRNL, *CEN* PaT is toxic, while *trl1Δ* cells with T4 Pnkp/Rnl1 are resistant. Presence of Trl1 therefore impairs phage-type repair. To discriminate whether the healing activity or the sealing activity of Trl1 interfere with Pnkp/Rnl1 mediated tRNA repair, constructs encoding either Trl1 ligase (residues 1-388) or Trl1 kinase and CPD (residues 389-827) were expressed in the presence of CEN PaT (Figure 11). Coexpression of Trl1's sealing domain phenocopies expression of the toxin in *trl1Δ*+Pnkp/Rnl1 cells. However, co-expression of Trl1's healing domain together with PaT prevents growth on galactose due to PaT toxicity.

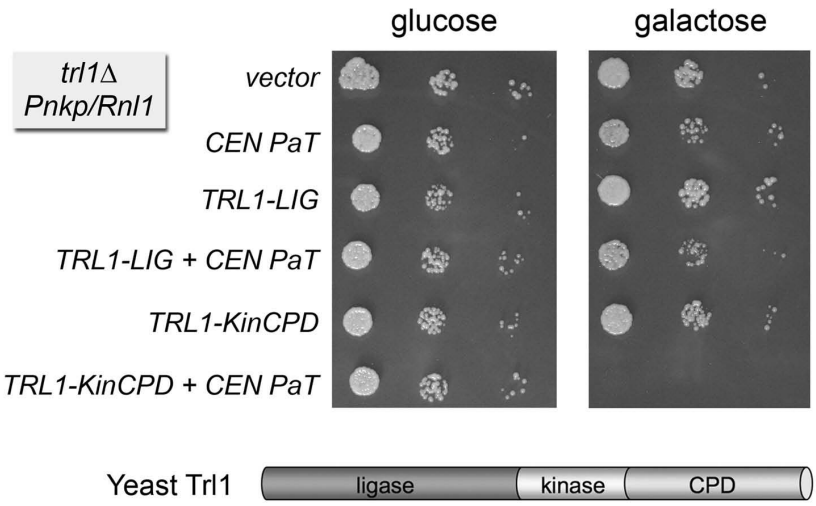

Figure 11 **– Yeast pathway tRNA healing activities preclude rescue of PaT toxicity by phage pathway repair.**
Serial 10-fold dilutions of *S. cerevisiae cells* expressing PaT or an empty vector or in presence of an additional plasmid encoding full length AtRNL or domain truncations thereof (2μ) were spotted on –Ura–His agar plates with 2% glucose or galactose. Plates were photographed after 2d (glucose) or 3d (galactose) incubation at 30°C.

3.2.3 Discussion

The following model of PaT cleavages takes the new findings on PaT *in vivo* toxicity into account (Figure 12): Low dosage of PaT is only toxic in wild type cells, but not in *tot3Δ* and *trm9Δ* (Figure 10B). This supports the interpretation, that hypomodified $tRNA^{Gln}$ is resistant to cleavage at the wobble nucleotide. tRNA cleavage in cells with high PaT dosage is toxic (Figure 10A). This toxicity cannot be alleviated by repair in wild type cells. Such irreparable damage could be due to nucleotide excision by PaT cleavage at both possible sites. When high doses of PaT are expressed in *tot3Δ* or *trm9Δ* cells, presence of either AtRNL or T4 Pnkp/Rnl1 allows growth on galactose. Therefore, $tRNA^{Gln}$ molecules are incised at only one position. Due to the hypomodification at the wobble nucleotide, cleavage occurs 5′ of position 33. Trl1 fails to protect from cleavage at the upstream site, indicating that Trl1 can only repair breaks at specific positions in the anticodon loop.

The Trl1 healing activity prevents PaT damage repair by T4 Pnkp/Rnl1 (Figure 11), as the phage tRNA repair enzymes are only sufficient to overcome tRNA damage in *trl1Δ* cells. Principally, yeast-type healing and phage-type sealing are compatible, such a combination complements *trl1Δ* (81). Yet, the temperature sensitive growth phenotype of the *trl1Δ*+Pnkp/Rnl1 strain shows, that Rnl1 is negatively affected by the 2′-phosphate yielded by Trl1's CPD activity. In PaT damage repair in wild type cells, Pnkp and Trl1

healing activities compete. By producing suboptimal substrates for Rnl1, Trl1 impedes rescue from PaT toxicity by repair.

Both PaT and γ-toxin cleave their tRNA substrates 3′ of the mcm^{5}s^{2}U wobble nucleotide in wild type cells. This raises the question of why AtRNL is capable of repairing γ-toxin damage, but fails to protect wild type cells from *CEN* PaT damage. A possible explanation for this difference is the capacity of PaT to induce breaks at a secondary site. If this secondary cleavage occurs faster and more frequently than breakage repair, PaT is toxic. This would imply different kinetics for overall tRNA damage repair by the yeast-type and the phage-type pathway. However, comparative kinetic-studies, which could validate or reject the presented explanation, have not been performed for these enzymes. It is however known, that the *in vitro* specific activity of Trl1 is more than 10 fold lower, and that of AtRNL about 50 fold lower than Rnl1's specific activity (73).

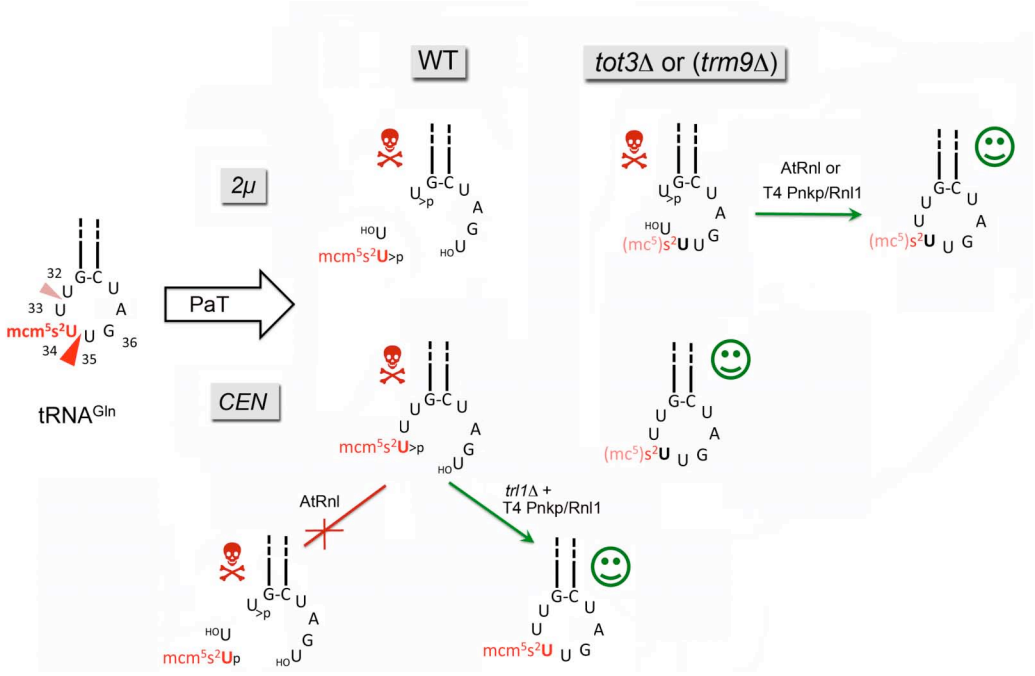

Figure 12 – **Model of dosage and modification dependent tRNA$^{Glu\ (UUG)}$ PaT cleavage in *S. cerevisiae***

Left: Arrowheads show the major (red) and minor (pink) cleavage PaT cleavage site in the anticodon loop of tRNA$^{Glu\ (UUG)}$. Center: High-copy (*2μ*) PaT expression is toxic in wild type (WT) and Trm9 or Tot3 deficient strains. While cleavage at two positions (nucleotide excision) occurring in WT cells is irreparable. Right: the damage in *trm9Δ*/*tot3Δ* can be repaired. Bottom: Single-copy (*CEN*) PaT expression is toxic only in WT cells and can be repaired only in *trl1Δ*+T4 Pnkp/Rnl1 cells.

3.2.4 Material and Methods

3.2.4.1 Expression Plasmids and *S. cerevisiae* strains

PaT was intracellularly expressed in *S. cerevisiae* in a galactose-inducible manner. The expression constructs (wherein PaT lacks the N-terminal 12-aa signal peptide) pPACBX (2µ, *URA3*) and pRS415-Gal1-PaT (CEN, *LEU2*) are described (8,131).

To generate the yeast plasmid pRS423-*TPI1*-AtRNL BamHI and SmaI restriction sites were introduced by PCR upstream of the start codon and downstream of the stop codon, respectively, of the AtRNL gene in pTPI-AtRNL (119). The BamHI/SmaI restriction digested PCR product was inserted into the corresponding sites of pRS423-*TPI1*. A *CEN HIS3* yeast expression plasmid bearing both T4 Pnkp and Rnl1 (pRS413-T4 Pnkp/Rnl1) was generated by inserting a *SLU7*-Pnkp PCR fragment into the XbaI restrition site of pRS413-*TPI1*-Rnl1 (81). The PCR reaction was performed with primers introducing XbaI restriction sites upstream of the Slu7 promoter and downstream of the stop codon of the Pnkp gene. The *TRL1* gene was cloned from pET-His_{10}Smt3-Trl1 (73) by inserting the BamHI/SalI fragment into the corresponding restriction sites of 2µ *HIS3* pRS423-*TPI1* generating pRS423-*TPI1*-Trl1. The integrity of the tRNA repair enzymes was verified by sequencing. The plasmids for separated expression of Trl1 healing (1-388) and sealing (389-827) activities have been published (73). The used strains are derivatives of W303a (*trm9Δ*, *tot3Δ, trl1Δ+T4 Pnkp/Rnl1* and *trl1Δ+AtRNL*) and have been described (64,67,73,117).

3.2.4.2 *Pichia toxin* toxicity assay

The indicated haploid *S. cerevisiae* strains were transformed with plasmid DNA using the lithium acetate method (132). Transformants were selected on appropriate selective minimal synthetic media on 2% (w/v) bacto agar plates. Cells derived from single transformants were grown at 30°C in liquid culture in selective media containing 2% glucose. The cultures were adjusted to A_{600} of 0.1 and then serially diluted in 10-fold steps in water. Aliquots (3 µl) of the dilutions were then spotted in parallel on selective agar plates containing either 2% glucose or 2% galactose. The plates were photographed after incubation at 30°C for 2 days (glucose) or 3 days (galactose).

3.3 Determinants of eukaryal cell killing by the bacterial ribotoxin PrrC

Meineke B, Schwer B, Schaffrath R, Shuman S (2011)

Determinants of eukaryal cell killing by the bacterial ribotoxin PrrC. Nucleic Acids Research 39(2), 687-700.

The greatest constraint of biochemical analysis of *E. coli* PrrC has been its self-limiting expression of the active ACNase (33). Assays for ACNase activity were performed with cell extracts of PrrC expressing cells (20,31). Possibly due to these limitations, no comprehensive structure-function analysis of PrrC has been conducted. Random and limited targeted mutagenesis has been performed. However, these efforts were always confined to small regions of the protein (31,33-35).

By testing *E. coli* PrrC and several of its homologs for toxicity in yeast (*S. cerevisiae*) we hoped to establish an easily accessible *in vivo* system for mutational analysis of PrrC. Such an assay allowed study of *Eco*PrrC, in a manner similar to our effective analysis of *K. lactis* γ-toxin. *Eco*PrrC has been shown to cleave mammalian $tRNA^{Lys\ (UUU)}$ and was thus likely to target the yeast species, too (26). After our initial experiments had shown yeast to be susceptible to PrrC, expression of colicins D and E5 was reported to be toxic to yeast (56,57). Along with *Eco*PrrC, we tested PrrC homologs of *Neisseria meningitidis*, *Streptococcus mutans* and *Xanthomonas campestris* for toxicity. The PrrC proteins encoded in *N. meningitidis* and *X. campestris* had no effect on yeast growth. *E. coli* and *Streptococcus mutans* PrrC were fungicidal in our assay. In contrast, colicins E5 and D as well as γ-toxin and PaT arrest yeast growth (7,8,56,57). This discrepancy could simply be due to higher ACNase activity of the PrrCs, differences in the experimental set-up, or result from different downstream responses. We compared the effect of galactose-inducible intracellular *Eco*PrrC and γ-toxin expression. Unlike γ-toxin, *Eco*PrrC was toxic also in *trm9Δ* and *tot3Δ* cells. *Eco*PrrC toxicity could not be rescued by overexpression of $tRNA^{Lys\ (UUU)}$ or other tRNA species tested. However, we were able to identify hypomorphic mutants of *Eco*PrrC (S219T and C386A) that are specifically rescued by increasing cellular $tRNA^{Lys\ (UUU)}$ levels. *trm9Δ* cells were resistant to the hypomorphs, showing that the modification state at the wobble uridine affects toxicity. Thus, *Eco*PrrC targets yeast $tRNA^{Lys\ (UUU)}$, but the intracellular toxicity of wild type *Eco*PrrC is to high to be affected by increased levels of substrate or suboptimal modification of the wobble base. In

fact, *in vitro* studies had placed the mcm^5s^2 modification found on eukaryal $tRNA^{Lys\ (UUU)}$ low in PrrC's list of preferred substrates (27,30).

Guided by amino acid sequence homology between different bacterial PrrCs we performed an extended alanine-scan of PrrC by targeting:

(i) All histidines, which might be involved in RNase A-like ACNase catalysis,

(ii) Conserved glutamate, lysine, serine, asparagine and arginine residues in the putative ACNase domain

(iii) Conserved residues in or around the putative ABC motifs as well as alternative aspartate/glutamate pairs that might comprise a Walker B motif.

A total of 53 alanine-mutations were tested for galactose-inducible toxicity. In 33 cases the mutation allowed growth, i.e. abolished toxicity, and the mutated residue was deemed essential. Subsequently, conservative mutations were introduced at each of the essential positions (e.g. lysine was replaced by arginine and glutamine). It is noteworthy that all residues targeted within ABC motifs were essential, for the first time providing evidence that the entire NBD-like domain, and not only the Walker A/P-loop, is necessary for PrrC activity. Expression of the domains (residues 1-264 and 265-396) in *trans* failed to elicit toxicity.

Within the ACNase domain, the results of the alanine-scan were interpreted in light of the known mechanisms of RNase A and RNAse T1. All five histidines tested in the ACNase domain were strictly essential for *E. coli* PrrC toxicity. However, only three of them, His295, His315 and His356 are conserved in the toxic *S. mutans* homolog. Two lysines were targeted in the putative ACNase, yet one was non-essential for toxicity and the other does not have a counterpart in *S. mutans* PrrC, arguing against their involvement in catalysis. In contrast, both Arg320 and Arg349 could be catalytic. They were strictly essential and are conserved in *S. mutans* PrrC. The Kaufman lab implicate Arg320, Glu324 and His356 in catalysis (33). Mutations of these residues had no activity in previously reported ACNase assays, while H295N and H315A retained at least some activity. However, no alternative arginines or lysines were tested in that study. Also, Tyr294 was not considered to be catalytic even though their results show a Y294F mutant to be ACNase dead, which would agree with a role as general base as was reported for *A. fulgidus* tRNA splicing endoribonuclease (Figure 1B) (13).

Dimer formation is necessary for productive ATPase activity of ABC domains (details 1.2.3) and purified *Eco*PrrC D222E has been reported to form tetramers (33). If

ABC-like dimerization is necessary for PrrC toxicity in yeast, overexpression of a mutant with a defective NBD active site could sequester wild type PrrC in a non-toxic dimer. Such a dominant-negative effect is exactly what we observe with all non-toxic alanine-mutants in the NBD-domain. At the same time, non-toxic alanine-mutants in the ACNase domain do not affect wild type PrrC toxicity. These results support a model wherein PrrC activity requires dimerization of two active N-terminal domains. The dimerization reported for the C-terminal domain seems not to require two functional ACNase domains or might not be needed for tRNA cleavage. None of the other single-incision anticodon loop targeting ribonucleases are known to require dimerization (35).

3.4 Determinants of the cytotoxicity of PrrC anticodon nuclease and its amelioration by tRNA repair

Meineke B and Shuman S (2012)

Determinants of the cytotoxicity of PrrC anticodon nuclease and its amelioration by tRNA repair. RNA 18 (published online ahead of print 2011)

When expressed in *S. cerevisiae* (yeast) the PrrCs of *E. coli* (*Eco*PrrC) and *S. mutans* are toxic. In contrast, expression of *N. meningitidis* PrrC (*Nme*PrrC) is not toxic in yeast, despite 57% amino acid sequence identity with the *E. coli* protein. This striking difference is maintained when we tested the same set of PrrC proteins for toxicity in *E. coli*, arguing against a more stringent substrate specificity of *Nme*PrrC for bacterial tRNA. To identify the determinants that make *Eco*PrrC expression toxic and *Nme*PrrC innocuous we generated “domain-swap” chimeras, which pointed us towards the ACNase domain for further investigation. Site-directed mutagenesis, guided by the differences between toxic and non-toxic PrrCs identified a single residue, gain-of-toxicity mutant of *Nme*PrrC: R316W. Further characterization of this mutant showed that it phenocopied the previously described *Eco*PrrC hypomorphs: *Nme*PrrC R316W is toxic to both wild type and *tot3Δ* cells, but *trm9Δ* cells and wild type cell with increased $tRNA^{Lys\ (UUU)}$ levels are resistant. Interestingly, *Nme*PrrC is the only close homolog of *Eco*PrrC that does not have a tryptophan at this position.

ACNase damage repair has been studied with γ-toxin *in vivo* (73). We tested whether tRNA repair enzymes can protect yeast cells from PrrC toxicity. In this regard, T4

Pnkp and Rnl1 are of special interest as they repair tRNA damaged by PrrC to allow productive phage infection in *prr*$^{+}$ *E. coli* (20). *Eco*PrrC toxicity cannot be counteracted by tRNA repair in yeast, possibly due to higher activity. We proceeded to investigate *in vivo* repair of *NmeR316W*PrrC damage and found the T4 phage system and AtRNL capable of repair. In contrast to γ-toxin damage repair, not only Trl1 ligase activity, but also Trl1 5′ kinase, fails to process the broken tRNA (73). The difference could be due to the different cleavage site of the ACNases: γ-toxin cleaves $tRNA^{Glu\ (UUC)}$ directly after the mcm^5s^2U wobble nucleotide, while PrrC cleaves before such a nucleotide in $tRNA^{Lys\ (UUU)}$ (Figure 2B and Figure 5B). Thus, Trl1 5′ kinase encounters the bulky and obstructive modification only after incision by PrrC, not after cleavage by γ-toxin.

The mutational analysis of the nuclease domain of *Eco*PrrC was extended focusing on the putative $tRNA^{Lys}$ anticodon recognition motif LARP ^{284}KYGDSNSFSY^{294}. This motif had been described to play a role in tRNA recognition as mutants within the motif alter PrrC's substrate specificity (34, 35). The LARP motif is found only in a subset of PrrC proteins e.g. in *Nme*PrrC, but is not conserved in *Smu*PrrC (only 3/11 identical residues). Thus, the motif is unlikely to be a decisive determinant of toxicity. We found Asp287 and Ser288, but not Asn289, be essential for *Eco*PrrC toxicity in yeast, by replacing these residues with alanine. We further analyzed the structure-function relationships at Asp287 by replacing this residue with aspartate, glutamate, lysine, tyrosine, histidine and glutamine. The D287E, D287N, D287H, and D287Q mutants were fully toxic.

The total of 15 essential residues identified in the nuclease domain of *Eco*PrrC in this study and previously (3.3) were further analyzed. These mutants were tested for galactose-inducible toxicity to yeast when expressed from high-copy plasmids. This increase in gene-dosage lead to a regain of partial or full toxicity in six mutants: S288A, H297A, K299A, N321A, N352, and H381A. Among the remaining, absolutely essential residues six potentially catalytic residues emerge: three histidines (His295, His315, His365), two arginines (Arg320, Arg349) and Glu324. These findings are consistent with the catalytic triad proposed by the Kaufman lab (33), but raise the possibility of a catalytic role for additional residues.

3.5 RtcB, a novel RNA ligase, can catalyze tRNA splicing and *HAC1* mRNA splicing *in vivo*

Tanaka N, Meineke B, Shuman S (2011)

RtcB, a novel RNA ligase, can catalyze tRNA splicing and *HAC1* mRNA splicing *in vivo*. The Journal of Biological Chemistry 286 (35), 30253–30257

Human, archaeal and *E. coli* RtcB proteins were recently identified as direct RNA ligases (Figure 9A) (111,113,124). All of them are capable of ligating pre-tRNAs or stem-loops with 2′,3′-cyclic phosphate and 5′-hydroxyl termini *in vitro*. *Eco*RtcB is also able to ligate stem-loops incised by γ-toxin *in vitro*. Knock-down of human RtcB reduces levels of mature reporter tRNAs, further linking RtcB to tRNA splicing. However, there is no experimental evidence that RtcB is directly responsible for ligation of pre-tRNAs *in vivo*. To fill this gap, we expressed *Eco*RtcB from a high-copy plasmid in *S. cerevisiae* and tested for complementation of *trl1Δ* lethality. *Eco*RtcB expression allows growth of *trl1Δ* cells, confirming that *Eco*RtcB is a true tRNA repair enzyme. This is underscored by *Eco*RtcB's ability to repair PaT toxicity in *trl1Δ* cells *in vivo*. This ACNase damage repair of *Eco*RtcB also highlights the different mechanism of ligation, as AtRNL fails to repair this damage (3.2 for details). Like the T4 phage and plant/yeast RNA repair systems *Eco*RtcB is capable of splicing *HAC1* mRNA *in vitro*.

*Eco*RtcB has been characterized previously *in vitro* (111): The RNA stem-loop ligation activity of RtcB is manganese-dependent and does not require ATP for activity. Here we show that RtcB can ligate stem-loops with 2′,3′-cyclic phosphate RNA halves to DNA or RNA, as long as their 5′ terminus is not phosphorylated. Such 5′ phosphorylation is required for both phage and yeast/plant tRNA repair pathways. The incompatibility of RtcB's mechanism with 5′ phosphorylated 3′ halves explains the failure of PaT damage repair in presence of active Trl1.

Site-directed mutagenesis based on the available crystal structure of *P. horikoshii* RtcB identifies Asp75, Cys78, Asn167, His168, His185, Arg189, Lys298, His337 and Arg341 essential for *Eco*RtcB *in vitro* and *in vivo* in *trl1Δ* complementation in yeast. The biological function of RtcB in bacteria remains to be determined.

4 References

1. Lee, S.R. and Collins, K. (2005) Starvation-induced cleavage of the tRNA anticodon loop in Tetrahymena thermophila. *J Biol Chem*, 280, 42744-42749.

2. Thompson, D.M., Lu, C., Green, P.J. and Parker, R. (2008) tRNA cleavage is a conserved response to oxidative stress in eukaryotes. *RNA*, 14, 2095-2103.

3. Li, Y., Luo, J., Zhou, H., Liao, J.Y., Ma, L.M., Chen, Y.Q. and Qu, L.H. (2008) Stress-induced tRNA-derived RNAs: a novel class of small RNAs in the primitive eukaryote Giardia lamblia. *Nucleic Acids Res*, 36, 6048-6055.

4. Amitsur, M., Levitz, R. and Kaufmann, G. (1987) Bacteriophage T4 anticodon nuclease, polynucleotide kinase and RNA ligase reprocess the host lysine tRNA. *EMBO J*, 6, 2499-2503.

5. Ogawa, T., Tomita, K., Ueda, T., Watanabe, K., Uozumi, T. and Masaki, H. (1999) A cytotoxic ribonuclease targeting specific transfer RNA anticodons. *Science*, 283, 2097-2100.

6. Tomita, K., Ogawa, T., Uozumi, T., Watanabe, K. and Masaki, H. (2000) A cytotoxic ribonuclease which specifically cleaves four isoaccepting arginine tRNAs at their anticodon loops. *Proc Natl Acad Sci U S A*, 97, 8278-8283.

7. Lu, J., Huang, B., Esberg, A., Johansson, M.J. and Bystrom, A.S. (2005) The Kluyveromyces lactis gamma-toxin targets tRNA anticodons. *RNA*, 11, 1648-1654.

8. Klassen, R., Paluszynski, J.P., Wemhoff, S., Pfeiffer, A., Fricke, J. and Meinhardt, F. (2008) The primary target of the killer toxin from Pichia acaciae is tRNA(Gln). *Mol Microbiol*, 69, 681-697.

9. Zhang, S., Sun, L. and Kragler, F. (2009) The phloem-delivered RNA pool contains small noncoding RNAs and interferes with translation. *Plant Physiol*, 150, 378-387.

10. Thompson, D.M. and Parker, R. (2009) Stressing out over tRNA cleavage. *Cell*, 138, 215-219.

11. Phizicky, E.M. and Hopper, A.K. (2010) tRNA biology charges to the front. *Genes Dev*, 24, 1832-1860.

12. Raines, R.T. (1998) Ribonuclease A. *Chem Rev*, 98, 1045-1066.

13. Xue, S., Calvin, K. and Li, H. (2006) RNA recognition and cleavage by a splicing endonuclease. *Science*, 312, 906-910.

14. Steyaert, J. (1997) A decade of protein engineering on ribonuclease T1--atomic dissection of the enzyme-substrate interactions. *Eur J Biochem*, 247, 1-11.

15. Winther, K.S. and Gerdes, K. (2011) Enteric virulence associated protein VapC inhibits translation by cleavage of initiator tRNA. *Proc Natl Acad Sci U S A*, 108, 7403-7407.

16. David, M., Borasio, G.D. and Kaufmann, G. (1982) T4 bacteriophage-coded polynucleotide kinase and RNA ligase are involved in host tRNA alteration or repair. *Virology*, 123, 480-483.

17. Levitz, R., Chapman, D., Amitsur, M., Green, R., Snyder, L. and Kaufmann, G. (1990) The optional E. coli prr locus encodes a latent form of phage T4-induced anticodon nuclease. *EMBO J*, 9, 1383-1389.

18. Linder, P., Doelz, R., Gubler, M. and Bickle, T.A. (1990) An anticodon nuclease gene inserted into a hsd region encoding a type I DNA restriction system. *Nucleic Acids Res*, 18, 7170.

19. Tyndall, C., Meister, J. and Bickle, T.A. (1994) The Escherichia coli prr region encodes a functional type IC DNA restriction system closely integrated with an anticodon nuclease gene. *J Mol Biol*, 237, 266-274.

20. Amitsur, M., Morad, I. and Kaufmann, G. (1989) In vitro reconstitution of anticodon nuclease from components encoded by phage T4 and Escherichia coli CTr5X. *EMBO J*, 8, 2411-2415.

21. Penner, M., Morad, I., Snyder, L. and Kaufmann, G. (1995) Phage T4-coded Stp: double-edged effector of coupled DNA and tRNA-restriction systems. *J Mol Biol*, 249, 857-868.

22. Kaufmann, G. (2000) Anticodon nucleases. *Trends Biochem Sci*, 25, 70-74.

23. Novogrodsky, A. and Hurwitz, J. (1966) The enzymatic phosphorylation of ribonucleic acid and deoxyribonucleic acid. I. Phosphorylation at 5'-hydroxyl termini. *J Biol Chem*, 241, 2923-2932.

24. Silber, R., Malathi, V.G. and Hurwitz, J. (1972) Purification and properties of bacteriophage T4-induced RNA ligase. *Proc Natl Acad Sci U S A*, 69, 3009-3013.

25. Sirotkin, K., Cooley, W., Runnels, J. and Snyder, L.R. (1978) A role in true-late gene expression for the T4 bacteriophage 5' polynucleotide kinase 3' phosphatase. *J Mol Biol*, 123, 221-233.

26. Shterman, N., Elroy-Stein, O., Morad, I., Amitsur, M. and Kaufmann, G. (1995) Cleavage of the HIV replication primer tRNALys,3 in human cells expressing bacterial anticodon nuclease. *Nucleic Acids Res*, 23, 1744-1749.

27. Jiang, Y., Meidler, R., Amitsur, M. and Kaufmann, G. (2001) Specific interaction between anticodon nuclease and the tRNA(Lys) wobble base. *J Mol Biol*, 305, 377-388.

28. Morad, I., Chapman-Shimshoni, D., Amitsur, M. and Kaufmann, G. (1993) Functional expression and properties of the tRNA(Lys)-specific core anticodon nuclease encoded by Escherichia coli prrC. *J Biol Chem*, 268, 26842-26849.

29. Sundaram, M., Durant, P.C. and Davis, D.R. (2000) Hypermodified nucleosides in the anticodon of tRNA(Lys) stabilize a canonical U-turn structure. *Biochemistry*, 39, 15652.

30. Jiang, Y., Blanga, S., Amitsur, M., Meidler, R., Krivosheyev, E., Sundaram, M., Bajji, A.C., Davis, D.R. and Kaufmann, G. (2002) Structural features of tRNALys favored by anticodon nuclease as inferred from reactivities of anticodon stem and loop substrate analogs. *J Biol Chem*, 277, 3836-3841.

31. Amitsur, M., Benjamin, S., Rosner, R., Chapman-Shimshoni, D., Meidler, R., Blanga, S. and Kaufmann, G. (2003) Bacteriophage T4-encoded Stp can be replaced as activator of anticodon nuclease by a normal host cell metabolite. *Mol Microbiol*, 50, 129-143.

32. Klaiman, D. and Kaufmann, G. (2011) Phage T4-induced dTTP accretion bolsters a tRNase-based host defense. *Virology*, 414, 97-101.

33. Blanga-Kanfi, S., Amitsur, M., Azem, A. and Kaufmann, G. (2006) PrrC-anticodon nuclease: functional organization of a prototypical bacterial restriction RNase. *Nucleic Acids Res*, 34, 3209-3219.

34. Meidler, R., Morad, I., Amitsur, M., Inokuchi, H. and Kaufmann, G. (1999) Detection of anticodon nuclease residues involved in tRNALys cleavage specificity. *J Mol Biol*, 287, 499-510.

35. Klaiman, D., Amitsur, M., Blanga-Kanfi, S., Chai, M., Davis, D.R. and Kaufmann, G. (2007) Parallel dimerization of a PrrC-anticodon nuclease region implicated in tRNALys recognition. *Nucleic Acids Res*, 35, 4704-4714.

36. Davidov, E. and Kaufmann, G. (2008) RloC: a wobble nucleotide-excising and zinc-responsive bacterial tRNase. *Mol Microbiol*, 69, 1560-1574.

37. Davidson, A.L., Dassa, E., Orelle, C. and Chen, J. (2008) Structure, function, and evolution of bacterial ATP-binding cassette systems. *Microbiol Mol Biol Rev*, 72, 317-364, table of contents.

38. Lammens, A. and Hopfner, K.P. (2010) Structural basis for adenylate kinase activity in ABC ATPases. *J Mol Biol*, 401, 265-273.

39. Hopfner, K.P., Karcher, A., Shin, D.S., Craig, L., Arthur, L.M., Carney, J.P. and Tainer, J.A. (2000) Structural biology of Rad50 ATPase: ATP-driven conformational control in DNA double-strand break repair and the ABC-ATPase superfamily. *Cell*, 101, 789-800.

40. Smith, P.C., Karpowich, N., Millen, L., Moody, J.E., Rosen, J., Thomas, P.J. and Hunt, J.F. (2002) ATP binding to the motor domain from an ABC transporter drives formation of a nucleotide sandwich dimer. *Mol Cell*, 10, 139-149.

41. Hopfner, K.P. and Tainer, J.A. (2003) Rad50/SMC proteins and ABC transporters: unifying concepts from high-resolution structures. *Curr Opin Struct Biol*, 13, 249-255.

42. Walker, J.E., Saraste, M., Runswick, M.J. and Gay, N.J. (1982) Distantly related sequences in the alpha- and beta-subunits of ATP synthase, myosin, kinases and other ATP-requiring enzymes and a common nucleotide binding fold. *EMBO J*, 1, 945-951.

43. Thompson, J.D., Gibson, T.J. and Higgins, D.G. (2002) Multiple sequence alignment using ClustalW and ClustalX. *Curr Protoc Bioinformatics*, Chapter 2, Unit 2 3.

44. Gaudet, R. and Wiley, D.C. (2001) Structure of the ABC ATPase domain of human TAP1, the transporter associated with antigen processing. *EMBO J*, 20, 4964-4972.

45. Zaitseva, J., Jenewein, S., Jumpertz, T., Holland, I.B. and Schmitt, L. (2005) H662 is the linchpin of ATP hydrolysis in the nucleotide-binding domain of the ABC transporter HlyB. *EMBO J*, 24, 1901-1910.

46. Haering, C.H., Schoffnegger, D., Nishino, T., Helmhart, W., Nasmyth, K. and Lowe, J. (2004) Structure and stability of cohesin's Smc1-kleisin interaction. *Mol Cell*, 15, 951-964.

47. Diederichs, K., Diez, J., Greller, G., Muller, C., Breed, J., Schnell, C., Vonrhein, C., Boos, W. and Welte, W. (2000) Crystal structure of MalK, the ATPase subunit of the trehalose/maltose ABC transporter of the archaeon Thermococcus litoralis. *EMBO J*, 19, 5951-5961.

48. Ambudkar, S.V., Kim, I.W., Xia, D. and Sauna, Z.E. (2006) The A-loop, a novel conserved aromatic acid subdomain upstream of the Walker A motif in ABC transporters, is critical for ATP binding. *FEBS Lett*, 580, 1049-1055.

49. Schmitt, L. and Tampe, R. (2002) Structure and mechanism of ABC transporters. *Curr Opin Struct Biol*, 12, 754-760.

50. Lancaster, L.E., Wintermeyer, W. and Rodnina, M.V. (2007) Colicins and their potential in cancer treatment. *Blood Cells Mol Dis*, 38, 15-18.

51. Yajima, S., Nakanishi, K., Takahashi, K., Ogawa, T., Hidaka, M., Kezuka, Y., Nonaka, T., Ohsawa, K. and Masaki, H. (2004) Relation between tRNase activity and the structure of colicin D according to X-ray crystallography. *Biochem Biophys Res Commun*, 322, 966-973.

52. Lin, Y.L., Elias, Y. and Huang, R.H. (2005) Structural and mutational studies of the catalytic domain of colicin E5: a tRNA-specific ribonuclease. *Biochemistry*, 44, 10494-10500.

53. Yajima, S., Inoue, S., Ogawa, T., Nonaka, T., Ohsawa, K. and Masaki, H. (2006) Structural basis for sequence-dependent recognition of colicin E5 tRNase by mimicking the mRNA-tRNA interaction. *Nucleic Acids Res*, 34, 6074-6082.

54. Ogawa, T., Inoue, S., Yajima, S., Hidaka, M. and Masaki, H. (2006) Sequence-specific recognition of colicin E5, a tRNA-targeting ribonuclease. *Nucleic Acids Res*, 34, 6065-6073.

55. Masaki, H. and Ogawa, T. (2002) The modes of action of colicins E5 and D, and related cytotoxic tRNases. *Biochimie*, 84, 433-438.

56. Shigematsu, M., Ogawa, T., Kido, A., Kitamoto, H.K., Hidaka, M. and Masaki, H. (2009) Cellular and transcriptional responses of yeast to the cleavage of cytosolic tRNAs induced by colicin D. *Yeast*, 26, 663-673.

57. Ogawa, T., Hidaka, M., Kohno, K. and Masaki, H. (2009) Colicin E5 ribonuclease domain cleaves Saccharomyces cerevisiae tRNAs leading to impairment of the cell growth. *J Biochem*, 145, 461-466.

58. Stark, M.J., Boyd, A., Mileham, A.J. and Romanos, M.A. (1990) The plasmid-encoded killer system of Kluyveromyces lactis: a review. *Yeast*, 6, 1-29.

59. Bolen, P.L., Eastman, E.M., Cihak, P.L. and Hayman, G.T. (1994) Isolation and sequence analysis of a gene from the linear DNA plasmid pPacl-2 of Pichia acaciae

that shows similarity to a killer toxin gene of Kluyveromyces lactis. *Yeast*, 10, 403-414.

60. Paluszynski, J.P., Klassen, R. and Meinhardt, F. (2007) Pichia acaciae killer system: genetic analysis of toxin immunity. *Appl Environ Microbiol*, 73, 4373-4378.

61. Klassen, R., Teichert, S. and Meinhardt, F. (2004) Novel yeast killer toxins provoke S-phase arrest and DNA damage checkpoint activation. *Mol Microbiol*, 53, 263-273.

62. Butler, A.R., Porter, M. and Stark, M.J. (1991) Intracellular expression of Kluyveromyces lactis toxin gamma subunit mimics treatment with exogenous toxin and distinguishes two classes of toxin-resistant mutant. *Yeast*, 7, 617-625.

63. McCracken, D.A., Martin, V.J., Stark, M.J. and Bolen, P.L. (1994) The linear-plasmid-encoded toxin produced by the yeast Pichia acaciae: characterization and comparison with the toxin of Kluyveromyces lactis. *Microbiology*, 140 (Pt 2), 425-431.

64. Huang, B., Johansson, M.J. and Bystrom, A.S. (2005) An early step in wobble uridine tRNA modification requires the Elongator complex. *RNA*, 11, 424-436.

65. Jablonowski, D., Frohloff, F., Fichtner, L., Stark, M.J. and Schaffrath, R. (2001) Kluyveromyces lactis zymocin mode of action is linked to RNA polymerase II function via Elongator. *Mol Microbiol*, 42, 1095-1105.

66. Kalhor, H.R. and Clarke, S. (2003) Novel methyltransferase for modified uridine residues at the wobble position of tRNA. *Mol Cell Biol*, 23, 9283-9292.

67. Jablonowski, D., Zink, S., Mehlgarten, C., Daum, G. and Schaffrath, R. (2006) tRNAGlu wobble uridine methylation by Trm9 identifies Elongator's key role for zymocin-induced cell death in yeast. *Mol Microbiol*, 59, 677-688.

68. Bjork, G.R., Huang, B., Persson, O.P. and Bystrom, A.S. (2007) A conserved modified wobble nucleoside (mcm5s2U) in lysyl-tRNA is required for viability in yeast. *RNA*, 13, 1245-1255.

69. Frohloff, F., Fichtner, L., Jablonowski, D., Breunig, K.D. and Schaffrath, R. (2001) Saccharomyces cerevisiae Elongator mutations confer resistance to the Kluyveromyces lactis zymocin. *EMBO J*, 20, 1993-2003.

70. Johansson, M.J., Esberg, A., Huang, B., Bjork, G.R. and Bystrom, A.S. (2008) Eukaryotic wobble uridine modifications promote a functionally redundant decoding system. *Mol Cell Biol*, 28, 3301-3312.

71. Jablonowski, D. and Schaffrath, R. (2007) Zymocin, a composite chitinase and tRNase killer toxin from yeast. *Biochem Soc Trans*, 35, 1533-1537.

72. Butler, A.R., White, J.H., Folawiyo, Y., Edlin, A., Gardiner, D. and Stark, M.J. (1994) Two Saccharomyces cerevisiae genes which control sensitivity to G1 arrest induced by Kluyveromyces lactis toxin. *Mol Cell Biol*, 14, 6306-6316.

73. Nandakumar, J., Schwer, B., Schaffrath, R. and Shuman, S. (2008) RNA repair: an antidote to cytotoxic eukaryal RNA damage. *Mol Cell*, 31, 278-286.

74. Lu, J., Esberg, A., Huang, B. and Bystrom, A.S. (2008) Kluyveromyces lactis gamma-toxin, a ribonuclease that recognizes the anticodon stem loop of tRNA. *Nucleic Acids Res*, 36, 1072-1080.

75. Martins, A. and Shuman, S. (2005) An end-healing enzyme from Clostridium thermocellum with 5' kinase, 2',3' phosphatase, and adenylyltransferase activities. *RNA*, 11, 1271-1280.

76. Wang, L.K., Nandakumar, J., Schwer, B. and Shuman, S. (2007) The C-terminal domain of T4 RNA ligase 1 confers specificity for tRNA repair. *RNA*, 13, 1235-1244.

77. Depew, R.E. and Cozzarelli, N.R. (1974) Genetics and physiology of bacteriophage T4 3'-phosphatase: evidence for involvement of the enzyme in T4 DNA metabolism. *J Virol*, 13, 888-897.

78. Runnels, J.M., Soltis, D., Hey, T. and Snyder, L. (1982) Genetic and physiological studies of the role of the RNA ligase of bacteriophage T4. *J Mol Biol*, 154, 273-286.

79. Jabbar, M.A. and Snyder, L. (1984) Genetic and physiological studies of an Escherichia coli locus that restricts polynucleotide kinase- and RNA ligase-deficient mutants of bacteriophage T4. *J Virol*, 51, 522-529.

80. Snopek, T.J., Wood, W.B., Conley, M.P., Chen, P. and Cozzarelli, N.R. (1977) Bacteriophage T4 RNA ligase is gene 63 product, the protein that promotes tail fiber attachment to the baseplate. *Proc Natl Acad Sci U S A*, 74, 3355-3359.

81. Schwer, B., Sawaya, R., Ho, C.K. and Shuman, S. (2004) Portability and fidelity of RNA-repair systems. *Proc Natl Acad Sci U S A*, 101, 2788-2793.

82. Wang, L.K., Lima, C.D. and Shuman, S. (2002) Structure and mechanism of T4 polynucleotide kinase: an RNA repair enzyme. *EMBO J*, 21, 3873-3880.

83. Wang, L.K. and Shuman, S. (2001) Domain structure and mutational analysis of T4 polynucleotide kinase. *J Biol Chem*, 276, 26868-26874.

84. Wang, L.K. and Shuman, S. (2002) Mutational analysis defines the 5'-kinase and 3'-phosphatase active sites of T4 polynucleotide kinase. *Nucleic Acids Res*, 30, 1073-1080.

85. Galburt, E.A., Pelletier, J., Wilson, G. and Stoddard, B.L. (2002) Structure of a tRNA repair enzyme and molecular biology workhorse: T4 polynucleotide kinase. *Structure*, 10, 1249-1260.

86. Eastberg, J.H., Pelletier, J. and Stoddard, B.L. (2004) Recognition of DNA substrates by T4 bacteriophage polynucleotide kinase. *Nucleic Acids Res*, 32, 653-660.

87. Zhu, H., Smith, P., Wang, L.K. and Shuman, S. (2007) Structure-function analysis of the 3' phosphatase component of T4 polynucleotide kinase/phosphatase. *Virology*, 366, 126-136.

88. Richardson, C.C. (1965) Phosphorylation of nucleic acid by an enzyme from T4 bacteriophage-infected Escherichia coli. *Proc Natl Acad Sci U S A*, 54, 158-165.

89. Becker, A. and Hurwitz, J. (1967) The enzymatic cleavage of phosphate termini from polynucleotides. *J Biol Chem*, 242, 936-950.

90. Shuman, S. and Lima, C.D. (2004) The polynucleotide ligase and RNA capping enzyme superfamily of covalent nucleotidyltransferases. *Curr Opin Struct Biol*, 14, 757-764.

91. Shuman, S. (2009) DNA ligases: progress and prospects. *J Biol Chem*, 284, 17365-17369.

92. Englert, M. and Beier, H. (2005) Plant tRNA ligases are multifunctional enzymes that have diverged in sequence and substrate specificity from RNA ligases of other phylogenetic origins. *Nucleic Acids Res*, 33, 388-399.

93. Heaphy, S., Singh, M. and Gait, M.J. (1987) Effect of single amino acid changes in the region of the adenylylation site of T4 RNA ligase. *Biochemistry*, 26, 1688-1696.

94. Wang, L.K., Ho, C.K., Pei, Y. and Shuman, S. (2003) Mutational analysis of bacteriophage T4 RNA ligase 1. Different functional groups are required for the nucleotidyl transfer and phosphodiester bond formation steps of the ligation reaction. *J Biol Chem*, 278, 29454-29462.

95. El Omari, K., Ren, J., Bird, L.E., Bona, M.K., Klarmann, G., LeGrice, S.F. and Stammers, D.K. (2006) Molecular architecture and ligand recognition determinants for T4 RNA ligase. *J Biol Chem*, 281, 1573-1579.

96. Wang, L.K., Schwer, B. and Shuman, S. (2006) Structure-guided mutational analysis of T4 RNA ligase 1. *RNA*, 12, 2126-2134.

97. Wang, L.K. and Shuman, S. (2005) Structure-function analysis of yeast tRNA ligase. *RNA*, 11, 966-975.

98. Ho, C.K., Wang, L.K., Lima, C.D. and Shuman, S. (2004) Structure and mechanism of RNA ligase. *Structure*, 12, 327-339.

99. Keppetipola, N. and Shuman, S. (2006) Mechanism of the phosphatase component of Clostridium thermocellum polynucleotide kinase-phosphatase. *RNA*, 12, 73-82.

100. Keppetipola, N., Nandakumar, J. and Shuman, S. (2007) Reprogramming the tRNA-splicing activity of a bacterial RNA repair enzyme. *Nucleic Acids Res*, 35, 3624-3630.

101. Keppetipola, N. and Shuman, S. (2007) Characterization of the 2',3' cyclic phosphodiesterase activities of Clostridium thermocellum polynucleotide kinase-phosphatase and bacteriophage lambda phosphatase. *Nucleic Acids Res*, 35, 7721-7732.

102. Jain, R. and Shuman, S. (2010) Bacterial Hen1 is a 3' terminal RNA ribose 2'-O-methyltransferase component of a bacterial RNA repair cassette. *RNA*, 16, 316-323.

103. Chan, C.M., Zhou, C. and Huang, R.H. (2009) Reconstituting bacterial RNA repair and modification in vitro. *Science*, 326, 247.

104. Jain, R. and Shuman, S. (2011) Active site mapping and substrate specificity of bacterial Hen1, a manganese-dependent 3' terminal RNA ribose 2'O-methyltransferase. *RNA*, 17, 429-438.

105. Abelson, J., Trotta, C.R. and Li, H. (1998) tRNA splicing. *J Biol Chem*, 273, 12685-12688.

106. Calvin, K. and Li, H. (2008) RNA-splicing endonuclease structure and function. *Cell Mol Life Sci*, 65, 1176-1185.

107. Paushkin, S.V., Patel, M., Furia, B.S., Peltz, S.W. and Trotta, C.R. (2004) Identification of a human endonuclease complex reveals a link between tRNA splicing and pre-mRNA 3' end formation. *Cell*, 117, 311-321.

108. Zillmann, M., Gorovsky, M.A. and Phizicky, E.M. (1991) Conserved mechanism of tRNA splicing in eukaryotes. *Mol Cell Biol*, 11, 5410-5416.

109. Weitzer, S. and Martinez, J. (2007) The human RNA kinase hClp1 is active on 3' transfer RNA exons and short interfering RNAs. *Nature*, 447, 222-226.

110. Zillmann, M., Gorovsky, M.A. and Phizicky, E.M. (1992) HeLa cells contain a 2'-phosphate-specific phosphotransferase similar to a yeast enzyme implicated in tRNA splicing. *J Biol Chem*, 267, 10289-10294.

111. Tanaka, N. and Shuman, S. (2011) RtcB Is the RNA Ligase Component of an Escherichia coli RNA Repair Operon. *J Biol Chem*, 286, 7727-7731.

112. Englert, M., Sheppard, K., Aslanian, A., Yates, J.R., 3rd and Soll, D. (2011) Archaeal 3'-phosphate RNA splicing ligase characterization identifies the missing component in tRNA maturation. *Proc Natl Acad Sci U S A*, 108, 1290-1295.

113. Popow, J., Englert, M., Weitzer, S., Schleiffer, A., Mierzwa, B., Mechtler, K., Trowitzsch, S., Will, C.L., Luhrmann, R., Soll, D. *et al.* (2011) HSPC117 is the essential subunit of a human tRNA splicing ligase complex. *Science*, 331, 760-764.

114. Bailey, K.A. and Aldinger, K.A. (2009) Mutations in the tRNA splicing endonuclease complex cause pontocerebellar hypoplasia. *Clin Genet*, 75, 427-428.

115. Namavar, Y., Chitayat, D., Barth, P.G., van Ruissen, F., de Wissel, M.B., Poll-The, B.T., Silver, R. and Baas, F. (2011) TSEN54 mutations cause pontocerebellar hypoplasia type 5. *Eur J Hum Genet*, 19, 724-726.

116. Kasher, P.R., Namavar, Y., van Tijn, P., Fluiter, K., Sizarov, A., Kamermans, M., Grierson, A.J., Zivkovic, D. and Baas, F. (2011) Impairment of the tRNA-splicing endonuclease subunit 54 (tsen54) gene causes neurological abnormalities and larval death in zebrafish models of pontocerebellar hypoplasia. *Hum Mol Genet*, 20, 1574-1584.

117. Sawaya, R., Schwer, B. and Shuman, S. (2003) Genetic and biochemical analysis of the functional domains of yeast tRNA ligase. *J Biol Chem*, 278, 43928-43938.

118. Mazumder, R., Iyer, L.M., Vasudevan, S. and Aravind, L. (2002) Detection of novel members, structure-function analysis and evolutionary classification of the 2H phosphoesterase superfamily. *Nucleic Acids Res*, 30, 5229-5243.

119. Wang, L.K., Schwer, B., Englert, M., Beier, H. and Shuman, S. (2006) Structure-function analysis of the kinase-CPD domain of yeast tRNA ligase (Trl1) and requirements for complementation of tRNA splicing by a plant Trl1 homolog. *Nucleic Acids Res*, 34, 517-527.

120. Sidrauski, C., Cox, J.S. and Walter, P. (1996) tRNA ligase is required for regulated mRNA splicing in the unfolded protein response. *Cell*, 87, 405-413.

121. Sidrauski, C. and Walter, P. (1997) The transmembrane kinase Ire1p is a site-specific endonuclease that initiates mRNA splicing in the unfolded protein response. *Cell*, 90, 1031-1039.

122. Konarska, M., Filipowicz, W. and Gross, H.J. (1982) RNA ligation via 2'-phosphomonoester, 3'5'-phosphodiester linkage: requirement of 2',3'-cyclic phosphate termini and involvement of a 5'-hydroxyl polynucleotide kinase. *Proc Natl Acad Sci U S A*, 79, 1474-1478.

123. Schwartz, R.C., Greer, C.L., Gegenheimer, P. and Abelson, J. (1983) Enzymatic mechanism of an RNA ligase from wheat germ. *J Biol Chem*, 258, 8374-8383.

124. Mori, T., Ogasawara, C., Inada, T., Englert, M., Beier, H., Takezawa, M., Endo, T. and Yoshihisa, T. (2010) Dual functions of yeast tRNA ligase in the unfolded protein response: unconventional cytoplasmic splicing of HAC1 pre-mRNA is not sufficient to release translational attenuation. *Mol Biol Cell*, 21, 3722-3734.

125. Filipowicz, W., Konarska, M., Gross, H.J. and Shatkin, A.J. (1983) RNA 3'-terminal phosphate cyclase activity and RNA ligation in HeLa cell extract. *Nucleic Acids Res*, 11, 1405-1418.

126. Filipowicz, W. and Shatkin, A.J. (1983) Origin of splice junction phosphate in tRNAs processed by HeLa cell extract. *Cell*, 32, 547-557.

127. Okada, C., Maegawa, Y., Yao, M. and Tanaka, I. (2006) Crystal structure of an RtcB homolog protein (PH1602-extein protein) from Pyrococcus horikoshii reveals a novel fold. *Proteins*, 63, 1119-1122.

128. Genschik, P., Drabikowski, K. and Filipowicz, W. (1998) Characterization of the Escherichia coli RNA 3'-terminal phosphate cyclase and its sigma54-regulated operon. *J Biol Chem*, 273, 25516-25526.

129. Saxena, S.K., Sirdeshmukh, R., Ardelt, W., Mikulski, S.M., Shogen, K. and Youle, R.J. (2002) Entry into cells and selective degradation of tRNAs by a cytotoxic member of the RNase A family. *J Biol Chem*, 277, 15142-15146.

130. Jain, R., Poulos, M.G., Gros, J., Chakravarty, A.K. and Shuman, S. (2011) Substrate specificity and mutational analysis of Kluyveromyces lactis γ-toxin, a eukaryal tRNA anticodon nuclease. *RNA*, 17, 1336-1343.

131. Tanaka, N., Meineke, B. and Shuman, S. (2011) RtcB, a novel RNA ligase, can catalyze tRNA splicing and HAC1 mRNA splicing in vivo. *J Biol Chem*. 286, 30253-30257

132. Schiestl, R.H. and Gietz, R.D. (1989) High efficiency transformation of intact yeast cells using single stranded nucleic acids as a carrier. *Curr Genet*, 16, 339-346.

5 Appendix

5.1 Abbreviations

aa	amino acid
ABC	ATP-binding cassette
ACNase	anticodon nuclease
ADP	adenosin diphosphate
AMP	adenosin monophosphate
ATP	adenosin triphosphate
CPD	Cyclic phosphodiesterase
CRD	C-terminal ribonuclease domain
DNA	deoxyribonucleic acid
dTTP	2′ -deoxy-thymidine triphosphate
GST	glutathin S-transferase
GTP	guanosin triphosphate
HAD	L-2-haloacid dehalogenase
LARP	lysine anticodon recognition peptide
mcm^5	5-methoxycarbonylmethyl
mnm^5	5-methylaminomethyl
mRNA	messenger RNA
ms^2t^6	2-mehtylthio-6-threonylcarbamoyl
NAD	nicotinamide adenine dinucleotide
NBD	nucleotide binding domain
NMP	nucleotide monophosphate
NTP	nucleotide triphosphate
NTPase	nucleotide triphosphatase
OB fold	oligonucleotide binding fold
ORF	open reading frame
PaT	*Pichia acaciae* toxin
PDB	protein database
RNA	ribonucleic acid
RNase	ribonuclease
s^2	2-thio
t^6	6-threonylcarbamoyl
TMAO	trimethylamine oxide
TMD	transmembrane domain
tRNA	transfer RNA
UPR	unfolded protein response

5.2 *Curriculum vitae*

Date and place of birth

March 19, 1983 in Göttingen

Academic career

Feb 2008 – Dec 2011	Visiting graduate student with Stewart Shuman, MD, PhD, at the Sloan-Kettering Institute in New York, USA. Thesis supervision by Prof. Dr. Thilo Stehle, IFIB, Tübingen University
2002 – 2007	**Biochemistry** studies (degree: Diplom) at Tübingen University
Nov 2007	Receipt of degree certificate **Diplom Biochemikerin** (*final grade 1.2*)
Mar 2007 - Nov 2007	Diploma thesis with Prof. Dr. Doron Rapaport at the IFIB, Tübingen "*Investigating Mcr1p sorting in yeast mitochondria*" (*grade 1.0*)
09/2005 – 02/2006	ERASMUS student at the Université de la Méditerrannée, Aix-Marseille II, France, laboratory rotations
Oct 2004	"Vordiplom" in biochemistry *(grade average 1.3)*

Education

2002	Abitur (*grade average 1.4*).
1995 – 2002	Felix-Klein Gymnasium, Göttingen
1999 – 2000	Bexley Highschool, Bexley, Ohio, USA
1993 – 1995	Orientierungsstufe Nord, Göttingen
1989 – 1993	Hainbundschule, Göttingen

Awards

"Diplom-/Master-Preis" award sponsored by the GBM

(German society for biochemistry and molecular biology)

Publications

Meineke B, Engl G, Kemper C, Vasiljev-Neumeyer A, Paulitschke H, Rapaport D.

"The outer membrane form of the mitochondrial protein Mcr1 follows a TOM-independent membrane insertion pathway" FEBS Lett. 2008 Mar 19;582(6):855-60.

Keppetipola N, Jain R, Meineke B, Diver M, Shuman S

"Structure-activity relationships in K. lactis γ-toxin" RNA 2009 Jun;15(6):1036-44

Meineke B, Schwer B, Schaffrath, Shuman S

"Determinants of eukaryal cell killing by the bacterial ribotoxin PrrC" Nucleic Acids Research 2011 Jan;39(2):687-700

Tanaka N, Meineke B, Shuman S

"RtcB, a novel RNA ligase, can catalyze tRNA splicing and HAC1 mRNA splicing in vivo" The Journal of Biochemistry, 2011, Sep;286(35), 30253-30257

Meineke B, Shuman S

"Determinants of PrrC tRNA anticodon nuclease cytotoxicity and its amelioration by tRNA repair" RNA 2012, 18 (published online Nov, 2011)

5.3 Acknowledgements

I would like to thank Stewart Shuman for giving me the opportunity to do my PhD research in his lab. Stewart is an experienced supervisor and I am lucky to have benefitted from his vast scientific knowledge and expertise. I appreciate the freedom I had to independently pursue my project, knowing that guidance would always be available if needed.

I would like to thank Thilo Stehle for agreeing to be my thesis advisor in Tübingen and enabling me to come to New York for my PhD studies.

Special thanks go to my lab. The atmosphere in the lab has always been friendly and supportive. In short you guys are fun to work with! Special thanks to Naoko, for letting contribute to one of her many publications this year. I really enjoyed working on RtcB. Thanks also to Paul, who has put up with me while crystallizing PrrC, its not over yet… I would like to thank Niroshika Keppetipola and Ruchi Jain for their help at the outset of my project. Thanks to everyone else who is or was in the lab: Mihaela, Murari, Anupam, Ray, Jonathan, Peihong, Barbara, Julien, Ushati, Delphine, Pravin, Poulami, Heather, Hui, Mike, Li Kai and Luda.

Special thanks to Poulami, Ushati, Anupam, Paul, Claire, Disan and Simon for critically reading my thesis drafts, you have spared me many mistakes.

Ganz besonderer Dank gilt meiner Familie und Simon. Ihr habt an mich geglaubt und mich durch jahrelanges gut Zureden unterstützt.

Structure–activity relationships in *Kluyveromyces lactis* γ-toxin, a eukaryal tRNA anticodon nuclease

NIROSHIKA KEPPETIPOLA, RUCHI JAIN, BIRTHE MEINEKE, MELINDA DIVER, and STEWART SHUMAN
Molecular Biology Program, Sloan-Kettering Institute, New York, New York, 10065 USA

ABSTRACT

tRNA anticodon damage inflicted by secreted ribotoxins such as *Kluyveromyces lactis* γ-toxin and bacterial colicins underlies a rudimentary innate immune system that distinguishes self from nonself species. The intracellular expression of γ-toxin (a 232-amino acid polypeptide) arrests the growth of *Saccharomyces cerevisiae* by incising a single RNA phosphodiester 3′ of the modified wobble base of $tRNA^{Glu}$. Fungal γ-toxin bears no primary structure similarity to any known nuclease and has no plausible homologs in the protein database. To gain insight to γ-toxin's mechanism, we tested the effects of alanine mutations at 62 basic, acidic, and polar amino acids on ribotoxin activity in vivo. We thereby identified 22 essential residues, including 10 lysines, seven arginines, three glutamates, one cysteine, and one histidine (His209, the only histidine present in γ-toxin). Structure–activity relations were gleaned from the effects of 44 conservative substitutions. Recombinant tag-free γ-toxin, a monomeric protein, incised an oligonucleotide corresponding to the anticodon stem–loop of $tRNA^{Glu}$ at a single phosphodiester 3′ of the wobble uridine. The anticodon nuclease was metal independent. RNA cleavage was abolished by ribose 2′-H and 2′-F modifications of the wobble uridine. Mutating His209 to alanine, glutamine, or asparagine abolished nuclease activity. We propose that γ-toxin catalyzes an RNase A-like transesterification reaction that relies on His209 and a second nonhistidine side chain as general acid–base catalysts.

Keywords: RNA damage; general acid–base catalysis; innate immune system

INTRODUCTION

Target-specific endoribonuclease toxins (''ribotoxins'') of bacteria and fungi play important roles in defending the organism against nonself species or viruses (for review, see Masaki and Ogawa 2002; Lacadena et al. 2007) and as mediators of programmed cell death (Nariya and Inouye 2008). Secreted ribotoxins comprise an RNA-based innate immune system in which killing or growth arrest of the ''foreign'' cell that takes up the toxin relies on that cell's inability to repair the toxin-induced damage to essential RNAs. Other ribotoxins are maintained intracellularly in a latent state until the nuclease is activated by stress or virus infection (Amitsur et al. 2003). Transfer RNAs figure prominently as the specific targets of bacterial ribotoxins, exemplified by the bacterial tRNA anticodon nucleases PrrC (and its homolog RloC), colicin D, and colicin E5 (Ogawa et al. 1999; Tomita et al. 2000; Graille et al. 2004; Blanga-Kanfi et al. 2006; Davidoff and Kaufmann 2008). PrrC and colicin E5 incise specific tRNAs at a single phosphodiester flanking the wobble base (position 34) of the anticodon via a transesterification reaction that yields 2′,3′ cyclic phosphate and 5′-OH ends. Their target preferences are determined by base modifications within the anticodon loop. The specificity of colicin E5 for Tyr, His, Asn, and Asp tRNAs is dictated by presence of the wobble base queosine (Yajima et al. 2006). PrrC cleaves at the mnm^5s^2U (5-methylaminomethyl-2-thiouridine) wobble base of $tRNA^{Lys}$, aided by recognition of the t^6A (6-threonylcarbamoyl adenosine) nucleoside at position 37 (Jiang et al. 2002).

Fungi also produce and secrete tRNA-directed ribotoxins (Lin et al. 2005; Lu et al. 2005, 2008; Jablonowski et al. 2006; Klassen et al. 2008). *Kluyveromyces lactis* and *Pichia acaciae* harbor cytoplasmic episomes, called ''killer'' plasmids, that encode secreted protein toxins known as zymocin and PaT, respectively (Stark and Boyd 1986; Klassen et al. 2004; Jablonowski and Schaffrath 2007). Zymocin is a heterotrimer of α, β, and γ subunits that arrests growth of the non-self-yeast species *Saccharomyces cerevisiae* by exposure from without. The α and β subunits interact with the target cell surface to effect the transport of the γ subunit

Reprint requests to: Stewart Shuman, Molecular Biology Program, Sloan-Kettering Institute, New York, NY 10065, USA; e-mail: s-shuman@ski.mskcc.org; fax: (212) 772-8410.

Article published online ahead of print. Article and publication date are at http://www.rnajournal.org/cgi/doi/10.1261/rna.1637809.

(the toxin) into the cytoplasm of the target cell. Induced expression in *S. cerevisiae* of only the γ-toxin polypeptide suffices to arrest cell growth (Butler et al. 1991). γ-toxin is an anticodon nuclease that specifically cleaves $tRNA^{Glu}$ at a single phosphodiester 3′ of the modified wobble base mcm^5s^2U (5-methoxycarbonylmethyl-2-thiouridine) of the UUC anticodon to generate 2′,3′ cyclic phosphate and 5′-OH termini at the break site. γ-toxin can cleave the two other yeast tRNAs (Gln and Lys) that have an mcm^5s^2U wobble base, albeit less efficiently than it incises $tRNA^{Glu}$, which is γ-toxin's principal target in vivo. γ-toxin arrests yeast growth by depleting the pool of functional $tRNA^{Glu}$ and its toxicity can be ameliorated by overexpression of $tRNA^{Glu}$ (Lu et al. 2005; Jablonowski et al. 2006). The mcm^5s^2U modification is required for tRNA cleavage by γ-toxin; yeast mutants that lack any of the enzymes responsible for synthesizing the mcm^5 moiety are resistant to exogenous zymocin and endogenous γ-toxin (Huang et al. 2005; Lu et al. 2005; Jablonowski et al. 2006). Resistance to γ-toxin can be achieved as well by expression of heterologous tRNA repair enzymes that heal and seal the ends of the broken anticodon loop (Nandakumar et al. 2008).

The *Pichia acaciae* toxin (PaT) also cleaves yeast tRNAs that contain a modified mcm^5s^2U wobble base (Klassen et al. 2008). Whereas the tRNase subunit of PaT can break all three mcm^5s^2U-containing yeast tRNAs in vitro, its toxicity in vivo is attributed to specific cleavage and depletion of $tRNA^{Gln}$, insofar as PaT toxicity can be reversed by overexpression of $tRNA^{Gln}$, but not $tRNA^{Glu}$ (Klassen et al. 2008). Although PaT and γ-toxin are functionally analogous and have overlapping tRNase activities, PaT's cytotoxicity in *S. cerevisiae* is less stringently dependent than γ-toxin's on the presence of the mcm^5-modified wobble uridine in the target tRNA (Klassen et al. 2008).

Perhaps the most remarkable features of the two known fungal tRNA anticodon nucleases is that they have no discernible primary structure similarity to one another, to any of the bacterial tRNA ribotoxins, or to any known ribonucleases or phosphotransferases. Indeed, *K. lactis* γ-toxin is effectively sui generis with respect to any known protein or predicted polypeptide in public databases. The goal of this study was to delineate structure–activity relations for γ-toxin that might illuminate its active site and catalytic mechanism. Initial efforts in this direction by Jablonowski et al. (2006) entailed selection in *S. cerevisiae* of nontoxic mutants of γ-toxin from a pool of randomly mutagenized plasmid clones. Although they identified nine different inactive mutants, the results were not immediately informative, because the inactive proteins contained either: (1) multiple missense changes; or (2) single missense changes that were drastic structurally (e.g., charge inversions or ionic-hydrophobic swaps). Here we conducted a systematic alanine scan of 62 residues of the intracellular form of *K. lactis* γ-toxin (Fig. 1A), covering 28% of the nonalanine side chains, focusing on the functional groups likely to be involved in catalysis or RNA recognition. We identified 22 essential residues and determined their relevant properties by introducing conservative substitutions. Biochemical characterization of recombinant γ-toxin highlighted its RNase A-like chemical mechanism and a likely role of His209 in catalysis of transesterification.

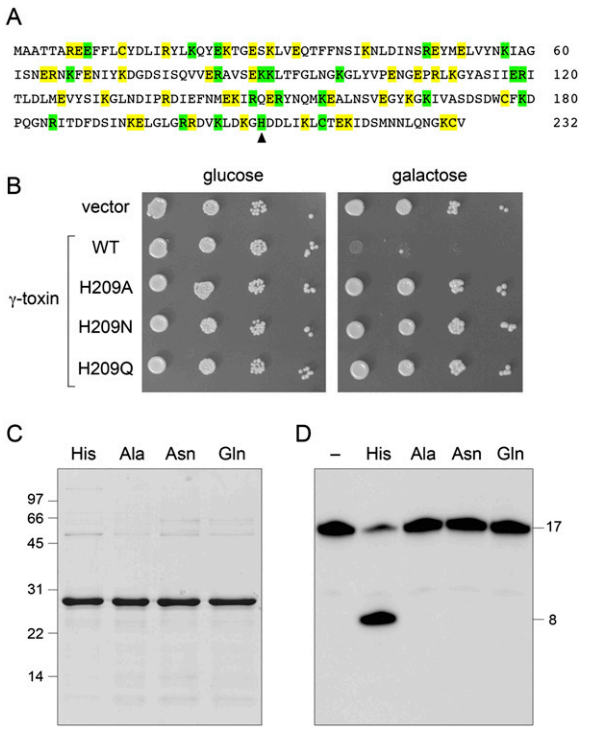

FIGURE 1. Mutational analysis of γ-toxin and essential catalytic role of His209. (*A*) The amino acid sequence of the intracellular version of *K. lactis* γ-toxin used in this study is shown. The amino acids subjected to alanine scanning are highlighted in green (essential residues) and yellow (nonessential residues). The lone histidine is denoted by an arrowhead. (*B*) Aliquots of serial dilutions of *S. cerevisiae* cells with a plasmid-borne galactose-regulated wild-type (WT) γ-toxin gene or *H209A*, *H209N*, or *H209Q* mutants thereof were spotted on glucose- or galactose-containing agar medium, in parallel with cells bearing an empty plasmid vector. The plates were photographed after incubation at 30°C for 2 d (glucose) or 3 d (galactose). (*C*) Aliquots (3 μg) of the recombinant tag-free γ-toxin C13A-C177A-C231A polypeptides were analyzed by SDS-PAGE. The Coomassie-blue-stained gel is shown. The amino acid at position 209 is indicated *above* each lane. The positions and sizes (in kDa) of marker polypeptides are indicated on the *left*. (*D*) Anticodon nuclease reaction mixtures (10 μL) containing 20 mM Tris-HCl (pH 7.5), 2 M TMAO, 200 fmol 5′ ^{32}P-labeled 17-mer stem–loop RNA (see Fig. 2D), and 200 fmol of the indicated γ-toxin preparations were incubated at 4°C for 30 min. Enzyme was omitted from the control reaction in lane "–." The products were analyzed by denaturing PAGE. An autoradiograph of the gel is shown, with the sizes (in nucleotides) of the substrate and product indicated on the *right*.

RESULTS AND DISCUSSION

Mutagenesis strategy

The biological activity of γ-toxin was assayed using an *S. cerevisiae* strain containing a galactose-inducible γ-toxin

expression cassette on a centromeric plasmid. In the presence of glucose, γ-toxin expression is suppressed and yeast cells grow normally. In the presence of galactose, γ-toxin is produced and growth is arrested (Fig. 1B). We tested the effects of 62 single alanine mutations on galactose-dependent toxicity. The residues targeted for alanine scanning (Fig. 1A) were ones we deemed most likely to be involved in catalysis of phosphoryl transfer (histidine, lysine, arginine, glutamate, cysteine) or RNA binding (lysine, arginine), based on general principles and the specific mechanisms of other well-studied ribonucleases that generate 2′,3′ cyclic phosphodiesters, such as RNase A, RNase T1, colicin E5, and tRNA splicing endonuclease (Steyaert 1997; Raines 1998; Xue et al. 2006; Yajima et al. 2006).

Forty of the alanine mutations did not affect toxicity in vivo (Table 1). The inessential functional groups are highlighted in yellow in the primary structure of the intracellular γ-toxin polypeptide (Fig. 1A). They include three cysteines, 18 glutamates, 13 lysines, and six arginines. By contrast, 22 of the alanine mutations inactivated γ-toxin and thereby allowed yeast cells to grow on medium containing galactose (Fig. 1; Table 1). The 22 essential amino acid side chains are highlighted in green in Figure 1A. They include the sole histidine in the γ-toxin polypeptide (His209), 10 lysines, seven arginines, three glutamates, and one cysteine. We proceeded to determine structure–activity relationships for each of the 22 essential residues by testing the effects of 44 conservative side chains substitutions: histidine was replaced by glutamine and asparagine; arginine was changed to lysine and glutamine; lysine was substituted by arginine and glutamine; glutamate was mutated to glutamine and aspartate; and cysteine was changed to serine and histidine. The results are summarized in Table 1 and are discussed below.

TABLE 1. Mutational effects on γ-toxin activity in vivo

γ-Toxin allele	Toxicity	γ-Toxin allele	Toxicity
WT	Yes	R7A	Yes
H209A	No	R18A	Yes
H209Q	No	R48A	No
H209N	No	R48K	Yes
C13A	Yes	R48Q	No
C177A	Yes	R65A	Yes
C216A	No	R84A	No
C216S	No	R84K	No
C216H	No	R84Q	No
C231A	Yes	R109A	Yes
C13A-C177A-C231A	Yes	R119A	No
K21A	No	R119K	Yes
K21Q	No	R119Q	Yes
K21R	No	R138A	Yes
K25A	Yes	R148A	No
K30A	Yes	R148K	No
K41A	Yes	R148Q	No
K57A	No	R151A	No
K57Q	No	R151K	No
K57R	Yes	R151Q	No
K67A	No	R185A	No
K67R	No	R185K	±
K67Q	Yes	R185Q	±
K73A	Yes	R200A	No
K89A	No	R200K	Yes
K89Q	Yes	R200Q	No
K89R	Yes	R201A	Yes
K90A	No	E8A	Yes
K90Q	No	E9A	No
K90R	Yes	E9Q	No
K98A	No	E9D	No
K98Q	No	E24A	No
K98R	Yes	E24Q	No
K111A	Yes	E24D	Yes
K131A	Yes	E28A	Yes
K146A	Yes	E33A	Yes
K156A	No	E49A	Yes
K156Q	No	E52A	Yes
K156R	Yes	E64A	Yes
K166A	Yes	E69A	Yes
K168A	No	E83A	Yes
K168Q	No	E88A	Yes
K168R	Yes	E104A	Yes
K179A	No	E107A	Yes
K179Q	No	E118A	No
K179R	Yes	E118Q	Yes
K194A	Yes	E118D	Yes
K204A	No	E126A	Yes
K204Q	No	E145A	Yes
K204R	Yes	E150A	Yes
K207A	Yes	E157A	Yes
K214A	Yes	E163A	Yes
K219A	Yes	E195A	Yes
K230A	Yes	E218A	Yes

A lone essential histidine

The "classical" mechanism of RNA cleavage by transesterification exemplified in RNase A relies on two histidine side chains that serve, respectively, as: (1) a general base catalyst that abstracts a proton from the attacking ribose 2′-OH, and (2) a general acid catalyst that donates a proton to the ribose 5′-O leaving group (Raines 1998). *K. lactis* γ-toxin is instantly distinguished from RNase A in that it has only one histidine side chain (His209) in the active intracellular form of the enzyme (Fig. 1A). We find that His209 is essential for cytotoxicity in yeast. Whereas wild-type γ-toxin arrested growth in galactose, the H209A, H209Q, and H209N mutants did not (Fig. 1B). Asparagine and glutamine can, in principle, mimic the hydrogen-bonding properties of the histidine Nδ and Nε atoms, respectively, but cannot serve as proton donors or acceptors. These findings are consistent with His209 being functionally analogous to one of the histidine catalysts in RNase A.

We note that Jablonowski et al. (2006) had previously isolated a nontoxic mutant of γ-toxin with three missense changes: Y152C, H209T, and L226I. Our results point to the H209T change as the likely cause of the loss of function.

Essential lysines

Structural and functional studies of RNase A highlight a single essential lysine that interacts with the scissile phosphodiester and stabilizes the pentacoordinate transition state (Raines 1998). (A glutamine side chain in RNase A also donates a hydrogen bond to the scissile phosphodiester.) By contrast, the RNase A-like *Rana catesbeiana* ribotoxin uses two lysines to coordinate the scissile phosphodiester (Leu et al. 2003). Lysine can also serve as a general acid to expel a 5′-OH polynucleotide leaving group, for example, during the DNA cleavage transesterification reaction catalyzed by topoisomerase IB (Krogh and Shuman 2000). A similar role for lysine in RNA transesterification is suggested by the crystal structure of substrate-bound colicin E5, a remarkable endoribonuclease that has no histidine side chain and instead relies on an active site composed of one arginine, one glutamine, and two lysines (one of which coordinates the O5′ leaving atom) (Yajima et al. 2006). The imputed active site of colicin D contains one histidine and two lysines (Graille et al. 2004; Yajima et al. 2004). The active site of RNA-bound tRNA splicing endonuclease is composed of one histidine and one lysine, plus a tyrosine (Xue et al. 2006). Lysines can also coordinate RNA phosphates flanking the scissile phosphodiester (Yajima et al. 2006).

The present alanine scan of γ-toxin pinpointed 10 of the 23 lysines as essential for activity in vivo. Conservative mutational effects highlighted four types of essential lysines (Table 1). In only one case, Lys21, was the lysine side chain strictly essential, i.e., neither arginine nor glutamine was active in lieu of Lys21. In seven instances (Lys57, Lys90, Lys98, Lys156, Lys168, Lys179, and Lys204), arginine substitutions restored activity in vivo, whereas glutamine did not, implicating positive charge as the key property of these eight residues. At Lys67, activity was restored by glutamine, but not by arginine, suggesting the importance of hydrogen bonding by Lys67. Only in the case of Lys89 was activity revived by either arginine or glutamine; we surmise that hydrogen bonding is the relevant feature at Lys89. Based on these results, we speculate that Lys21 is the best candidate to act as a "missing" nonhistidine general acid, assuming that His209 is a general base, because it alone cannot be replaced by arginine. (Arginine has a predicted pK_a value of 12.5 versus a lysine pK_a of 10.5, which might limit its efficacy as a general acid.) The other essential lysines that can be substituted by arginine include plausible candidates to either: (1) contact the scissile phosphodiester in $tRNA^{Glu}$; (2) contact flanking or remote phosphodiesters in the folded tRNA structure; (3) contribute to recognition of the modified wobble base; or (4) stabilize the protein fold, for example, via salt bridges.

Essential arginines

Arginines classically play a role in ground-state binding and transition-state stabilization during phosphoryl transfer reactions by making bidentate contacts to the phosphate oxygens. Two arginines serve this role during DNA transesterification by topoisomerase IB (Tian et al. 2005). Several of the transesterifying ribonucleases with known structures assimilate a catalytic arginine in their active sites. For example, the colicin E5 active site includes a single arginine that coordinates both nonbridging oxygens of the scissile phosphodiester (Yajima et al. 2006). The active site of RNase T1 also has a single arginine that contacts the scissile phosphodiester (Zegers et al. 1998). By contrast, the active site of barnase includes two arginines (and a lysine) that contact the scissile phosphodiester (Buckle and Fersht 1994).

Here we found that seven of the 13 arginines in γ-toxin were essential for activity in vivo. Conservative mutational effects highlighted three classes of essential arginines (Table 1). Arg84, Arg148, and Arg151 were strictly essential and could not be functionally replaced by either lysine or glutamine. Thus, these three residues are candidates for an essential role by virtue of bidentate phosphate contacts, either at the cleavage site, or remotely on the tRNA backbone (Xue et al. 2006). Arginine is also a plausible candidate to recognize the modified wobble base, via bidentate hydrogen bonds to the uracil O4 and/or mcm5 oxygen atoms. Of course, the mutational findings at Arg84, Arg148, and Arg151 could also be explained if one or more of these arginines make bidentate salt bridges to glutamate or aspartate side chains that are essential for proper protein folding. We note that the earlier report of a nontoxic double-mutant with I45M and R151K changes (Jablonowski et al. 2006) can now be interpreted as the consequence of the R151K single change, which sufficed here to ablate activity in vivo.

Two of the arginines—Arg48 and Arg200—could be replaced functionally by lysine but not glutamine, thus testifying to the sufficiency of positive charge at these positions. These residues are good candidates to make electrostatic contacts to the tRNA backbone. In the case of Arg119, activity was restored by either lysine or glutamine, implying that neutral hydrogen bonding capacity is the relevant property of Arg119. Similar results pertained at Arg185, although the galactose-dependent growth arrest elicited by the R185K and R185Q mutants was not as strong as seen with wild-type γ-toxin.

Critical glutamates

RNase T1 and barnase exemplify the catalytic role of a glutamate in RNA transesterification enzymology. The active site of RNase T1 is composed of two histidines, one arginine, and one glutamate that contact the scissile phosphate and are critical for activity (Steyaert 1997). The prevailing model for the RNase T1 reaction posits that one of the histidines acts as a general acid to expel the leaving group. The role of general base is imputed to the glutamate, assisted by the second histidine residue (Steyaert 1997;

Loverix and Steyaert 2001). Barnase relies on a single histidine general acid; a single glutamate is proposed to act as the general base (Buckle and Fersht 1994).

Our alanine scan of γ-toxin identified three out of 21 glutamates as essential for toxicity. (Note that the "hit-rate" in the alanine scan was much lower for glutamate than for the basic residues arginine and lysine.) Toxicity was restored when Glu118 was replaced conservatively by either glutamine or aspartate (Table 1), signifying that hydrogen-bonding capacity is the pertinent property of this residue and effectively excluding Glu118 as a candidate general base. Glu9 was strictly essential; neither glutamine nor aspartate revived activity. Thus, Glu9 could be a candidate general base, assuming that His209 is the general acid of γ-toxin. Activity was restored when Glu24 was changed to aspartate but not glutamine, indicating that an acidic residue sufficed. Of course, our data do not discriminate between a catalytic role for Glu9 and Glu24 versus a structural role, for example, in forming a salt bridge to an arginine.

Our data do bear on the previous isolation of nontoxic mutants bearing single missense changes at either Glu49 (to lysine) or Glu145 (to phenylalanine). Given our findings that alanine mutations at Glu49 and Glu145 do not affect toxicity in the same assay employed by Jablonowski et al. (2006), we conclude that the loss of toxicity they observed reflects the drastic consequences of charge inversion or an acidic-to-hydrophobic transition, rather than any functional requirement for these two glutamates per se.

A lone essential cysteine

The tertiary structure and stability of RNase A are enforced by four intramolecular cysteine-disulfide bonds. The full-length secreted form of *K. lactis* γ-toxin contains six cysteines, two of which are located within the N-terminal signal peptide. Of the four cysteines present in the active intracellular version of γ-toxin, three were deemed nonessential (Cys13, Cys177, and Cys231), because single alanine substitutions did not affect toxicity in *S. cerevisiae*. These results might be rationalized if one putative intramolecular disulfide linkage sufficed for activity. To address this point, we simultaneously changed all three nonessential cysteines to alanine and found that the C13A-C177A-C231A mutant was active in vivo (Table 1). Because this mutant contains only one remaining cysteine (the essential Cys216), we conclude that formation of intramolecular disulfides (if it does occur) is not important for γ-toxin activity in this assay format. Conservative replacement of Cys216 with either serine or histidine failed to revive activity (Table 1), signifying that a sulfhydryl is specifically required at this position. Any of several roles can be envisioned for a cysteine, including interaction with the mcm^5s^2U wobble base or a role in proton transfer during the transesterification step.

Recombinant γ-toxin

Investigators in the Byström laboratory have produced *K. lactis* γ-toxin in bacteria as a GST-fusion, isolated the recombinant protein by glutathione-affinity chromatography, and demonstrated its anticodon nuclease activity in vitro (Lu et al. 2005). Our aim here was to produce a tag-free version of γ-toxin in order to avoid the issue of forced dimerization by the GST-domain. Thus, we produced γ-toxin in bacteria as a His_{10}Smt3 fusion, a method that allows facile cleavage of the tag by the Smt3-specific protease Ulp1 (Mossessova and Lima 2000). Initial attempts to make the wild-type polypeptide in *E. coli* resulted in substantial protein accumulation, albeit exclusively in an insoluble form. Because γ-toxin is naturally a secreted protein and has multiple cysteines within the intracellular domain lacking the signal sequence used presently, we considered the prospect that the bacterial version might misfold or aggregate because of inappropriate disulfide formation, either intermolecularly or intramolecularly. To preclude intramolecular disulfides, and to try to lessen the risk of intermolecular aggregations, we attempted to express in bacteria the triple cysteine-to-alanine mutant, C13A-C177A-C231A, that we found to be active in vivo in yeast. This version of His_{10}Smt3-(γ-toxin) was sufficiently soluble to allow its purification by Ni-affinity chromatography, followed by tag cleavage and separation of the tag-free γ-toxin from His_{10}Smt3, yielding a predominant 27-kDa γ-toxin polypeptide (Fig. 1C).

To monitor the nuclease activity of γ-toxin, we employed a minimized synthetic 17-mer RNA oligonucleotide substrate corresponding to the anticodon stem–loop of $tRNA^{Glu}$ (Fig. 2D). Lu et al. (2008) have shown that this RNA, although lacking the modified mcm^5s^2U wobble base, is nonetheless incised by γ-toxin at the correct phosphodiester 3′ of the first uridine of the UUC anticodon. Inspired by the prior report (Jiang et al. 2001) that bacterial PrrC gained activity in cleaving unmodified tRNA anticodons in the presence of high concentrations of trimethylamine oxide (TMAO), Lu et al. (2008) found that TMAO had a similar effect on γ-toxin, enabling it to cleave the unmodified version of the $tRNA^{Glu}$ anticodon stem–loop. The conditions employed by Lu et al. (2008) to study the model tRNase reaction were notable for the low reaction temperature and the inclusion of 10 mM $MgCl_2$ in the reaction mixture. When we assayed our recombinant γ-toxin preparation under such conditions, we observed site-specific breakage of the 5′ ^{32}P-labeled stem–loop RNA to yield a single radiolabeled product (Fig. 2A). We were immediately interested in whether a divalent cation was required for the RNA cleavage reaction catalyzed by γ-toxin, especially given that RNase A and other 2′,3′ cyclic phosphate-forming endoribonucleases typically do not rely on a catalytic metal ion. We found that not

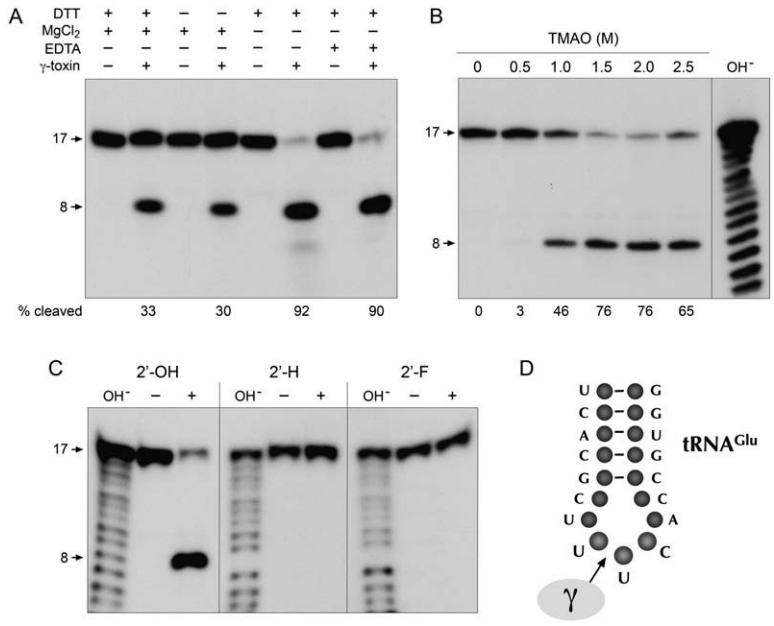

FIGURE 2. Requirements for anticodon nuclease activity in vitro. (*A*) Nuclease reaction mixtures (10 μL) containing 20 mM Tris-HCl (pH 7.5), 2 M TMAO, and 200 fmol 5′ ^{32}P-labeled 17-mer RNA (depicted in *D*) were supplemented with either 1 mM DTT, 10 mM $MgCl_2$, 10 mM EDTA, or 5 pmol γ-toxin where indicated by "+" and then incubated at 4°C for 30 min. The products were analyzed by denaturing PAGE and visualized by autoradiography. The extents of RNA cleavage are indicated *below* the lanes. (*B*) Reaction mixtures (10 μL) containing 20 mM Tris-HCl (pH 7.5), 200 fmol 5′ ^{32}P-labeled 17-mer RNA, 50 fmol γ-toxin, and TMAO as specified were incubated at 4°C for 30 min. The products were analyzed by denaturing PAGE in parallel with a size marker ladder generated by partial alkaline hydrolysis of the 5′ ^{32}P-labeled 17-mer RNA (lane OH^-). An autoradiogram of the gel is shown. (*C*) Reaction mixtures (10 μL) containing 20 mM Tris-HCl (pH 7.5), 2 M TMAO, 200 fmol 5′ ^{32}P-labeled 17-mer RNA with a ribose at the wobble nucleoside (2′-OH) (*left*), with a deoxyribose at the wobble nucleoside (2′-H) (*middle*), or with a 2′-fluoro sugar at the wobble nucleoside (2′-F) (*right*), and 100 fmol γ-toxin (lanes +) were incubated at 4°C for 30 min. Enzyme was omitted from control reactions in lanes –. The reaction products were analyzed by denaturing PAGE in parallel with size marker ladders generated by partial alkaline hydrolysis of the respective 5′ ^{32}P-labeled 17-mer RNAs (lanes OH^-). An autoradiogram of the gel is shown. (*D*) The 17-mer RNA oligonucleotide substrate corresponding to the anticodon stem–loop of $tRNA^{Glu}$ is shown. The site of cleavage by γ-toxin 3′ of the wobble base of the $tRNA^{Glu}$ anticodon nucleoside is indicated by the arrow.

only was magnesium not required for tRNase activity, its omission significantly enhanced the extent of anticodon breakage (Fig. 2A). The increased activity was maintained in the presence of 10 mM EDTA, arguing against an essential role for a divalent metal in the anticodon nuclease activity of γ-toxin. We infer that γ-toxin employs an RNase A-like metal-independent transesterification mechanism reliant primarily on general acid base catalysis and transition-state stabilization by purely enzymic functional groups (Raines 1998). Further assays of model substrate cleavage were therefore performed in the absence of magnesium. In agreement with Lu et al. (2008), we found that cleavage of the synthetic 17-mer RNA was stimulated strongly by TMAO; whereas virtually no cleavage product was detected in the absence of TMAO or in the presence of 0.5 M TMAO, the 17-mer was efficiently converted to a single incised product at 1.5 to 2.5 M TMAO (Fig. 2B). Polyacrylamide gel electrophoresis (PAGE) analysis in parallel with a partial alkaline digest of the 5′ ^{32}P-labeled 17-mer substrate verified that the cleavage product corresponds to an 8-mer formed by incision 3′ of the unmodified wobble U (Fig. 2B). The extent of RNA cleavage was proportional to input γ-toxin in the range of 0.1–5 nM concentration and attained a maximum of 90% substrate consumption at saturating enzyme (Fig. 3A). From the slope of the titration curve, we estimated that 3 fmol of RNA stem–loop was cleaved per fmol of input γ-toxin. The incised product accumulated steadily with reaction time at an RNA:enzyme ratio of 2:1, again attaining an endpoint of 91% cleavage (Fig. 3B).

The quaternary structure of tag-free γ-toxin was gauged by zonal velocity sedimentation in a 15%–30% glycerol gradient. Marker proteins catalase (native size 248 kDa), bovine serum albumin (BSA) (66 kDa), and cytochrome *c* (12 kDa) were included as internal standards in the gradient. The anticodon RNase activity profile paralleled the abundance of the γ-toxin polypeptide (calculated mass 27 kDa), which sedimented as a discrete peak (fractions 26–30) between cytochrome *c* and BSA, albeit closer to cytochrome *c* (Fig. 3C). An S value of 2.4 was calculated for γ-toxin by interpolation to a linear plot of the S values of the internal standards versus peak fraction number (not shown). We surmise from these results that γ-toxin is a monomer in solution.

Effect of ribose 2′ modifications at the scissile phosphodiester

Lu et al. (2008) showed that cleavage by γ-toxin of the minimized 17-mer anticodon stem–loop substrate is stringently dependent on the anticodon loop sequence $U^{34}U^{35}C^{36}A^{37}$ derived from wild-type $tRNA^{Glu}$. Any single base change within the UUCA element abolished tRNase activity. Here we extended the analysis of γ-toxin substrate specificity by testing the effects of pentose sugar modifications at the scissile U^{34} phosphodiester. Synthetic 17-mer oligonucleotides (20 nM) containing either 2′-deoxy (2′-H) or 2′-fluoro (2′-F) nucleosides in lieu of the 2′-OH ribonucleoside at the wobble U position were reacted with γ-toxin (10 nM) (Fig. 2C). The salient findings were

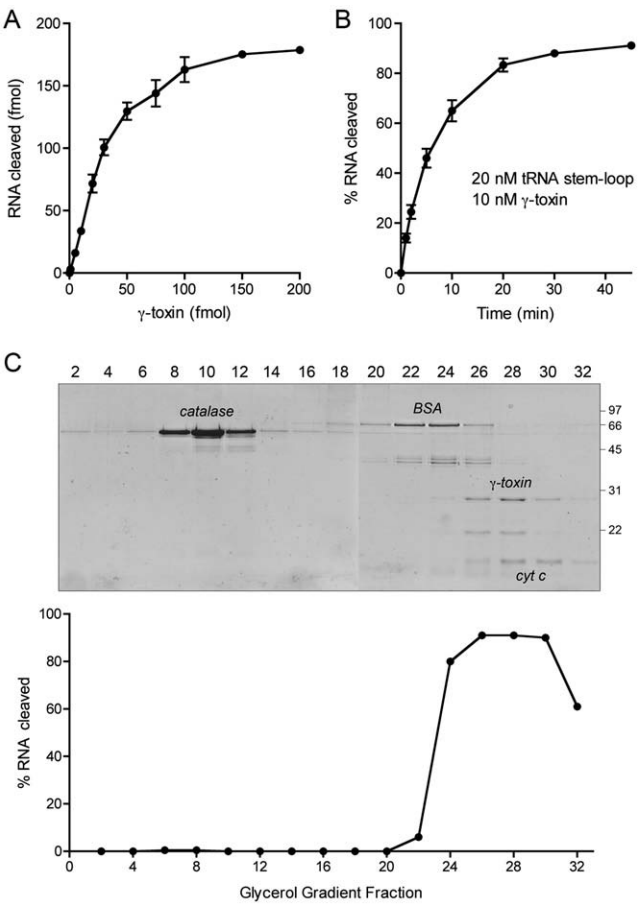

FIGURE 3. γ-toxin catalyzes multiple turnovers and sediments as a monomer. (*A*) Reaction mixtures (10 μL) containing 20 mM Tris-HCl (pH 7.5), 2 M TMAO, 200 fmol ^{32}P-labeled 17-mer RNA, and increasing amounts of γ-toxin as specified were incubated at 4°C for 30 min. The extents of RNA cleavage are plotted as a function of input γ-toxin. Each datum is an average of three separate titration experiments ± SEM. (*B*) A reaction mixture (90 μL) containing 20 mM Tris-HCl (pH 7.5), 2 M TMAO, and 20 nM ^{32}P-labeled 17-mer RNA, and 10 nM γ-toxin was incubated at 4°C. Aliquots (10 μL) were withdrawn at the times specified and quenched with formamide-EDTA. The extents of RNA cleavage are plotted as a function of time. Each datum is an average of three separate experiments ± SEM. (*C*) Aliquots (15 μL) of even-numbered glycerol gradient fractions were analyzed by SDS-PAGE (*top*). The Coomassie-blue stained gel is shown. The γ-toxin, catalase, BSA, and cytochrome *c* polypeptides are indicated. Molecular weight calibration for the PAGE analysis (kDa) is indicated at *right*. Reaction mixtures (10 μL) containing 20 mM Tris-HCl (pH 7.5), 2 M TMAO, 20 nM ^{32}P-labeled 17-mer RNA, and 1 μL of the even-numbered glycerol gradient fractions were incubated at 4°C for 10 min (*bottom*). The extents of RNA cleavage are plotted.

that (1) the 2′-H and 2′-F substrates were refractory to cleavage at the phosphodiester flanking the wobble base under conditions where 90% of the unmodified RNA was cleaved; and (2) prevention of RNA scission at the "normal" site did not precipitate the use of alternative cleavage sites within the anticodon loop. There was no detectable cleavage of the 2′-H and 2′-F substrates even when the concentration of γ-toxin was increased to 200 nM (i.e., a 10-fold excess over the RNA substrate; not shown). These results underscore the essential role of the ribose O2′ atom as the nucleophile for the transesterification reaction.

Single-turnover RNA cleavage

We measured the kinetics of cleavage of 20 nM RNA stem–loop at stoichiometric or superstoichiometric levels of enzyme, varying the concentration of γ-toxin from 20 to 200 nM. The kinetic profiles fit well to a single exponential with a common endpoint of 91% RNA cleavage (Fig. 4A). The cleavage rate increased steadily with enzyme concentration, signifying that initial binding of γ-toxin to the RNA substrate was rate limiting. A plot of the observed cleavage rate constants versus enzyme concentration fit well to a hyperbolic one-site binding model (Fig. 4B), from which we derived a K_d value of 400 nM and a k_{cat} of 6.5 min^{-1}.

His209 is required for anticodon RNase activity in vitro

Missense mutations of His209 were introduced into the vector used to express the active C13A-C177A-C231A variant of γ-toxin in *E. coli*. The H209A, H209Q, and H209N proteins were purified from soluble bacterial extracts in parallel with the "wild-type" H209 protein (Fig. 1C). The salient findings were that the alanine, glutamine, and asparagine mutations abolished anticodon nuclease activity with the synthetic stem–loop substrate (Fig. 1D), suggesting that His209 is required for transesterification per se, rather than recognition of the modified wobble base or the tRNA fold.

Concluding remarks

Here we conducted a systematic in vivo structure–function analysis of a eukaryal tRNA anticodon nuclease. The identification of 22 essential side chains by alanine-scanning, the clarification of structure–activity relations by conservative substitutions, and the analysis of the requirements for RNA incision in vitro engender plausible ideas about the catalytic mechanism, especially the role of His209. The solution to the puzzle of how γ-toxin assembles its active site and specifically recognizes its tRNA target, and whether it has any structural similarities to other RNases, will ultimately hinge on crystallizing the protein, alone and in complex with RNA. The capacity to preclude catalysis by single-atom modifications of the RNA or single conservative mutations of the toxin may facilitate such structural studies.

MATERIALS AND METHODS

Inducible expression of γ-toxin in budding yeast

The *S. cerevisiae* strain used in this study is a haploid derivative of W303 transformed with plasmid pLF16 (*CEN LEU2*

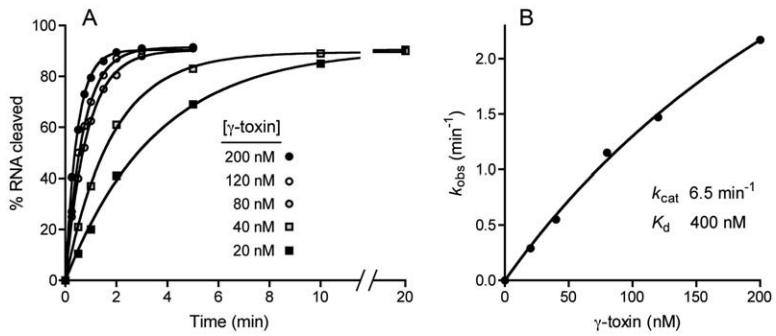

FIGURE 4. Kinetics of single-turnover RNA cleavage. (*A*) Reaction mixtures (100 μL) containing 20 mM Tris-HCl (pH 7.5), 2 M TMAO, 20 nM ^{32}P-labeled 17-mer RNA, and 20, 40, 80, 120, or 200 nM γ-toxin were incubated at 4°C. Aliquots (10 μL) were withdrawn at the times specified and quenched with formamide-EDTA. The extent of RNA cleavage is plotted as a function of time for each enzyme concentration. Nonlinear regression curve fitting to a single exponential was performed in Prism. The apparent rate constants derived thereby are plotted in *B* as a function of γ-toxin concentration. k_{cat} and K_d values were obtained by nonlinear regression curve fitting to a hyperbolic one-site binding model in Prism.

UASGAL-γ-toxin), which allows for galactose-inducible, glucose-repressible expression of an intracellular 232-amino acid version of *K. lactis* γ-toxin that lacks the N-terminal 17- amino acid signal peptide (Jablonowski et al. 2006). The "wild-type" γ-toxin open reading frame in pLF16 encodes a polypeptide that differs from the original NCBI database entry (accession YP_001648056) at two positions, such that residues 127 and 141 in pLF16 are valine and glutamate, respectively, rather than isoleucine and lysine. These polymorphisms are functionally benign, insofar as the γ-toxin encoded on pLF16 is active in vivo and in vitro (vide supra). Missense mutations were introduced into the γ-toxin gene of pLF16 via two-stage overlap extension PCR. The inserts were sequenced completely to verify the absence of unwanted coding changes. The mutated pLF16 plasmids were transformed into yeast in parallel with the wild-type pLF16. Leu$^+$ transformants were selected on glucose-containing medium lacking leucine. Cultures were grown in selective liquid media at 30°C, adjusted to A_{600} of 0.1, and then diluted serially in 10-fold increments. Aliquots (3 μL) of each dilution were spotted on glucose-containing and galactose-containing agar plates, which were incubated at 30°C.

Recombinant γ-toxin from bacteria

The gene encoding the intracellular γ-toxin C13A-C177A-C231A protein was excised from pLF16 with endonucleases NdeI and SalI and inserted between the NdeI and SalI sites in pET23a. This plasmid was used as the template to PCR-amplify the open reading frame with primers that introduced a BamHI site 5′ of the start codon and a XhoI site 3′ of the stop codon. The PCR product was inserted into pET28-His$_{10}$Smt3 to generate a phage T7 RNA polymerase-driven expression vector encoding the **γ**-toxin C13A-C177A-C231A polypeptide fused to an N-terminal His$_{10}$Smt3 tag. Missense mutations H209A, H209Q, and H209N were introduced into **γ**-toxin-(C13A-C177A-C231A) gene by two-stage overlap extension PCR. The pET28 plasmid inserts were sequenced completely to verify the intended coding sequence. The pET28-His$_{10}$Smt3-(γ-toxin) plasmids were transformed into *E. coli* BL21(DE3)-RIL. Cultures (1 L) amplified from single transformants were grown at 37°C in Luria-Bertani medium containing 0.05 mg/mL kanamycin until the A_{600} reached ~0.6. The cultures were adjusted to 0.2 mM isopropyl-β-D-thiogalactopyranoside and 2% (v/v) ethanol and then incubated at 17°C for 6 h with constant shaking. Cells were harvested by centrifugation, and the pellets were stored at −80°C. All subsequent procedures were performed at 4°C. Thawed bacteria were resuspended in 50 mL of buffer A (50 mM Tris-HCl at pH 7.5, 0.5 M NaCl, 10% sucrose). Cell lysis was achieved by the addition of lysozyme, phenylmethanesulphonylfluoride, and Triton X-100 to final concentrations of 1 mg/mL, 0.2 mM, and 0.1%, respectively. The lysates were sonicated to reduce viscosity, and insoluble material was removed by centrifugation. The soluble extracts were applied to 4-mL columns of Ni-nitrilotriacetic acid-agarose (Qiagen) that had been equilibrated with buffer A containing 0.1% Triton X-100. The columns were washed with buffer B (50 mM Tris-HCl at pH 8.0, 0.25 M NaCl, 0.05% Triton X-100, 10% glycerol) containing 50 mM imidazole and eluted with buffer B containing 500 mM imidazole. The polypeptide compositions of the column fractions were monitored by SDS-PAGE. The peak fractions containing the His$_{10}$Smt3-(γ-toxin) polypeptide were pooled and supplemented with the Smt3-specific protease Ulp1 to attain a His$_{10}$Smt3-(γ-toxin):Ulp1 ratio of 200:1. The mixtures were dialyzed overnight against buffer C (50 mM Tris-HCl at pH 7.5, 0.25 M NaCl, 0.05% Triton X-100, 10% glycerol). The dialysates were applied to 4-mL nickel-agarose columns equilibrated with buffer C. Tag-free γ-toxin was recovered in the flow-through fractions. The γ-toxin preparations were dialyzed against buffer D (50 mM Tris-HCl at pH 7.5, 0.25 M NaCl, 2 mM DTT, 5 mM EDTA, 0.05% Triton X-100, 10% glycerol) and stored at −80°C. Protein concentrations were determined by using the Bio-Rad dye reagent with bovine serum albumin as the standard. The yield of γ-toxin was ~2 mg from a 1 L bacterial culture.

Anticodon nuclease assay

Reaction mixtures containing 20 mM Tris-HCl (pH 7.5), 2 M TMAO, 20 nM 5′ ^{32}P-labeled 17-mer stem–loop RNA (see Fig. 2D), and γ-toxin and other components as specified were incubated at 4°C. The reactions were quenched by adding 10 μL of 90% formamide, 50 mM EDTA. The samples were heated at 95°C for 1 min and then analyzed by electrophoresis through a 15-cm 24% polyacrylamide gel containing 8 M urea in 0.5× TBE (45 mM Tris-borate, 1.2 mM EDTA) at 12 W for ~90 min. The radiolabeled products were visualized by autoradiography, and the extents of RNA cleavage were quantified by scanning the gel with a Fujix BAS2500 imager. The 5′ ^{32}P-labeled RNA ladders used to size the cleavage product were prepared by incubating aliquots of the 5′ ^{32}P-labeled 17-mer RNAs in a solution of 40 mM $NaHCO_3$, 60 mM Na_2CO_3 (pH 10.2) for 12 min at 95°C. The partially cleaved RNAs were then stored at −20°C.

Materials

RNA oligonucleotides used as substrates in anticodon nuclease assays were purchased from Dharmacon. The RNAs were deprotected according to the vendor's instructions and 5′ ^{32}P-labeled by reaction with T4 polynucleotide kinase and [γ^{32}P]ATP (Amersham). The labeled RNA was purified by preparative gel electrophoresis and stored at −20°C. TMAO was purchased from Sigma.

Received March 8, 2009; accepted March 27, 2009.

REFERENCES

Amitsur, M., Benjamin, S., Rosner, R., Chapman-Shimshoni, D., Meidler, R., Blanga, S., and Kaufmann, G. 2003. Bacteriophage T4-encoded Stp can be replaced as activator of anticodon nuclease by a normal host cell metabolite. *Mol. Microbiol.* **50:** 129–143.

Blanga-Kanfi, S., Amitsur, M., Azem, A., and Kaufmann, G. 2006. PrrC-anticodon nuclease: Functional organization of a prototypal bacterial restriction RNase. *Nucleic Acids Res.* **34:** 3209–3219.

Buckle, A.M. and Fersht, A.R. 1994. Subsite binding in an RNase: Structure of a barnase-tetranucleotide complex at 1.76-Å resolution. *Biochemistry* **33:** 1644–1653.

Butler, A.R., Porter, M., and Stark, M.J. 1991. Intracellular expression of *Kluyveromyces lactis* toxin gamma subunit mimics treatment with exogenous toxin and distinguishes two classes of toxin-resistant mutant. *Yeast* **7:** 617–625.

Davidoff, E. and Kaufmann, G. 2008. RloC: A wobble nucleotide-excising and zinc-responsive bacterial tRNase. *Mol. Microbiol.* **69:** 1560–1574.

Graille, M., Mora, L., Buckingham, R.H., van Tilbeurgh, H., and de Zamaroczy, M. 2004. Structural inhibition of the colicin D tRNase by the tRNA-mimicking immunity protein. *EMBO J.* **23:** 1474–1482.

Huang, B., Johansson, M.J.O., and Byström, A.S. 2005. An early step in wobble tRNA modification requires the elongator complex. *RNA* **11:** 424–436.

Jablonowski, D. and Schaffrath, R. 2007. Zymocin, a composite chitinase and tRNase killer toxin from yeast. *Biochem. Soc. Trans.* **35:** 1533–1537.

Jablonowski, D., Zink, S., Mehlgarten, C., Daum, G., and Schaffrath, R. 2006. tRNA^{Glu} wobble uridine methylation by Trm9 identifies elongator's key role for zymocin-induced cell death in yeast. *Mol. Microbiol.* **59:** 677–688.

Jiang, Y., Meidler, R., Amitsur, M., and Kaufmann, G. 2001. Specific interactions between anticodon nuclease and the tRNA^{Lys} wobble base. *J. Mol. Biol.* **305:** 377–388.

Jiang, Y., Blanga, S., Amitsur, M., Meidler, R., Krivosheyev, E., Sundaram, M., Bajii, A., Davis, D.R., and Kaufmann, G. 2002. Structural features of tRNA^{Lys} favored by anticodon nuclease as inferred from reactivities of anticodon stem and loop substrate analogs. *J. Biol. Chem.* **277:** 3826–3841.

Klassen, R., Teichert, S., and Meinhardt, F. 2004. Novel yeast killer toxins provoke S-phase arrest and DNA damage checkpoint activation. *Mol. Microbiol.* **53:** 263–273.

Klassen, R., Paluszynski, J.P., Emhoff, S., Pfeiffer, A., Fricke, J., and Meinhardt, F. 2008. The primary target of the killer toxin from *Pichia acaciae* is tRNA^{Gln}. *Mol. Microbiol.* **69:** 681–697.

Krogh, B.O. and Shuman, S. 2000. Catalytic mechanism of DNA topoisomerase IB. *Mol. Cell* **5:** 1035–1041.

Lacadena, J., Alvarez-Garcia, E., Carreras-Sangrà, N., Herrero-Galán, E., Alegre-Cebollada, J., García-Ortega, L., Oñaderra, M., Gavilanes, J.G., and Martínez del Pozo, A. 2007. Fungal ribotoxins: Molecular dissection of a family of natural killers. *FEMS Microbiol. Rev.* **31:** 212–237.

Leu, Y.J., Chern, S.S., Wang, S.C., Hsiao, Y.Y., Amiraslanov, I., Liaw, Y.C., and Liao, Y.D. 2003. Residues involved in the catalysis, base specificity, and cytotoxicity of ribonuclease from *Rana catesbeiana* based upon mutagenesis and x-ray crystallography. *J. Biol. Chem.* **278:** 7300–7309.

Lin, Y.L., Elias, Y., and Huang, R.H. 2005. Structural and mutational studies of the catalytic domain of colicin E5: A tRNA-specific ribonuclease. *Biochemistry* **44:** 10494–10500.

Loverix, S. and Steyaert, J. 2001. Deciphering the mechanism of RNase T1. *Methods Enzymol.* **341:** 305–323.

Lu, J., Huang, B., Esberg, A., Johanson, M., and Byström, A.S. 2005. The *Kluyveromyces lactis* γ-toxin targets tRNA anticodons. *RNA* **11:** 1648–1654.

Lu, J., Esberg, A., Huang, B., and Byström, A.S. 2008. The *Kluyveromyces lactis* γ-toxin, a ribonuclease that recognizes the anticodon stem–loop of tRNA. *Nucleic Acids Res.* **36:** 1072–1080.

Masaki, H. and Ogawa, T. 2002. The modes of action of colicins E5 and D, and related cytotoxic tRNases. *Biochimie* **84:** 433–438.

Mossessova, E. and Lima, C.D. 2000. Ulp1-SUMO crystal structure and genetic analysis reveal conserved interactions and a regulatory element essential for cell growth in yeast. *Mol. Cell* **5:** 865–876.

Nandakumar, J., Schwer, B., Schaffrath, R., and Shuman, S. 2008. RNA repair: An antidote to cytotoxic eukaryal RNA damage. *Mol. Cell* **31:** 278–286.

Nariya, H. and Inouye, M. 2008. MazF, an mRNA interferase, mediates programmed cell death during multicellular *Myxococcus* development. *Cell* **132:** 55–66.

Ogawa, T., Tomita, K., Ueda, T., Watanabe, K., Uozumi, T., and Masaki, H. 1999. A cytotoxic ribonuclease targeting specific tRNA anticodons. *Science* **283:** 2097–2100.

Raines, R.T. 1998. Ribonuclease A. *Chem. Rev.* **98:** 1045–1065.

Stark, M.J.R. and Boyd, A. 1986. The killer toxin of *Kluyveromyces lactis*: Characterization of the toxin subunits and identification of the genes which encode them. *EMBO J.* **5:** 1995–2002.

Steyaert, J. 1997. A decade of protein engineering on ribonuclease T1: Atomic dissection of the enzyme–substrate interactions. *Eur. J. Biochem.* **247:** 1–11.

Tian, L., Claeboe, C.D., Hecht, S.M., and Shuman, S. 2005. Mechanistic plasticity of DNA topoisomerase IB: Phosphate electrostatics dictate the need for a catalytic arginine. *Structure* **13:** 513–520.

Tomita, K., Ogawa, T., Uozumi, T., Watanabe, K., and Masaki, H. 2000. A cytotoxic ribonuclease which specifically cleaves four isoaccepting arginine tRNAs at their anticodon loops. *Proc. Natl. Acad. Sci.* **97:** 8278–8283.

Xue, S., Calvin, K., and Li, H. 2006. RNA recognition and cleavage by a splicing endonuclease. *Science* **312:** 906–910.

Yajima, S., Nakanishi, K., Takahashi, K., Ogawa, T., Hidaka, M., Kezuka, Y., Nonaka, T., Ohsawa, K., and Masaki, H. 2004. Relation between tRNase activity and the structure of colicin D according to X-ray crystallography. *Biochem. Biophys. Res. Commun.* **322:** 966–973.

Yajima, S., Inoue, S., Ogawa, T., Nonaka, T., Ohsawa, K., and Masaki, H. 2006. Structural basis for sequence-dependent recognition of colicin E5 tRNase by mimicking the mRNA–tRNA interaction. *Nucleic Acids Res.* **34:** 6074–6082.

Zegers, I., Loris, R., Dehollander, G., Haikal, A.F., Poortmans, F., Steyaert, J., and Wyns, L. 1998. Hydrolysis of a slow cyclic thiophosphate substrate of RNase T1 analyzed by time-resolved crystallography. *Nat. Struct. Biol.* **5:** 280–283.

Published online 19 September 2010 *Nucleic Acids Research, 2011, Vol. 39, No. 2* ***687–700***
doi:10.1093/nar/gkq831

Determinants of eukaryal cell killing by the bacterial ribotoxin PrrC

Birthe Meineke[1], Beate Schwer[2], Raffael Schaffrath[3] and Stewart Shuman[1,*]

[1]Molecular Biology Program, Sloan-Kettering Institute, [2]Department of Microbiology and Immunology, Weill Cornell Medical College, New York, NY 10065 USA and [3]Department of Genetics, University of Leicester, Leicester, LE1 7RH, UK

Received July 31, 2010; Revised August 31, 2010; Accepted September 3, 2010

ABSTRACT

tRNA damage inflicted by the *Escherichia coli* anticodon nuclease PrrC (*Eco*PrrC) underlies an antiviral response to phage T4 infection. PrrC homologs are present in many bacterial proteomes, though their biological activities are uncharted. PrrCs consist of two domains: an N-terminal NTPase module related to the ABC family and a distinctive C-terminal ribonuclease module. In this article, we report that the expression of *Eco*PrrC in budding yeast is fungicidal, signifying that PrrC is toxic in a eukaryon in the absence of other bacterial or viral proteins. Whereas *Streptococcus* PrrC is also toxic in yeast, *Neisseria* and *Xanthomonas* PrrCs are not. Via analysis of the effects of 118 mutations on *Eco*PrrC toxicity in yeast, we identified 22 essential residues in the NTPase domain and 11 in the nuclease domain. Overexpressing PrrCs with mutations in the NTPase active site ameliorated the toxicity of wild-type *Eco*PrrC. Our findings support a model in which *Eco*PrrC toxicity is contingent on head-to-tail dimerization of the NTPase domains to form two composite NTP phosphohydrolase sites. Comparisons of *Eco*PrrC activity in a variety of yeast genetic backgrounds, and the rescuing effects of tRNA overexpression, implicate $tRNA^{Lys(UUU)}$ as a target of *Eco*PrrC toxicity in yeast.

INTRODUCTION

Transfer RNAs are essential components of the translation machinery; they are also vulnerable targets for bacterial and fungal endoribonuclease toxins (ribotoxins) that incise specific tRNA anticodons and arrest cell growth. Secreted tRNA ribotoxins, such as bacterial colicins D and E5, *Kluyveromyces lactis* γ-toxin and *Pichia acaciae* toxin, provide a means to discriminate self from non-self species and suppress growth of the latter (1–5). Intracellular ribotoxins are normally maintained in a latent state, but are activated in response to cellular stress or viral infection (6–8).

The *Escherichia coli* PrrC anticodon nuclease (ACNase) represents an RNA-based intracellular innate immune system of host defense against a foreign invader (6). PrrC is maintained in a latent state by association with the host DNA restriction-modification enzyme encoded by the *prrA*, *prrB* and *prrD* ORFs of the *E. coli prr* operon (9,10). The PrrC ACNase is activated by a virus-encoded protein, Stp, synthesized early during bacteriophage T4 infection (11–13). Active PrrC incises $tRNA^{Lys}$ at a single site in the anticodon loop, 5′ of the modified wobble uridine (mnm^5s^2U), to generate a 2′,3′-cyclic phosphate and a 5′-OH at the broken ends. Unopposed depletion of $tRNA^{Lys}$ interdicts synthesis of viral late proteins and prevents spread of the virus through the population. However, the phage thwarts the RNA-damaging host defense by encoding an RNA repair system, consisting of T4 polynucleotide kinase-phosphatase (Pnkp) and T4 RNA ligase 1 (Rnl1), that heals and seals the broken tRNA ends (14). tRNA restriction as a defense mechanism against phages is seemingly widespread in the bacterial domain, insofar as: (i) PrrC homologs are present in many diverse bacteria; and (ii) RNA repair enzymes are encoded by viruses other than T4 (15).

E. coli PrrC (*Eco*PrrC) is the only member of the large PrrC-like family for which a biological role (antiviral host defense) and a specific RNA target have been defined. *Eco*PrrC is a 396-aa polypeptide composed of two putative domains: an N-terminal nucleoside triphosphate phosphohydrolase (NTPase) module (aa 1–264) related to the ABC transporter family and a C-terminal 'nuclease' module (aa 265–396) that has no apparent similarity to any known nuclease or tRNA-binding protein. Gabriel Kaufmann's laboratory has reported that: (i) active *Eco*PrrC is a homo-oligomeric complex; (ii) *Eco*PrrC nuclease activity is triggered by GTP hydrolysis and activated allosterically by dTTP; (iii) $tRNA^{Lys}$ is the

*To whom correspondence should be addressed. Tel: +1 212 639 7145; Fax: +1 212 717 3623; Email: s-shuman@ski.mskcc.org

specific target of *Eco*PrrC *in vivo* and (iv) *Eco*PrrC activity is influenced by base modifications in the tRNA anticodon loop (16–19).

Davidov and Kaufmann (20) recently identified *Geobacillus kaustophilus* RloC (*Gka*RloC) as the exemplar of a distinct subfamily of bacterial PrrC-like ribotoxins, in which the NTPase domain contains a large modular insert with a putative coiled-coil/zinc-hook structure reminiscent of Rad50. *Gka*RloC incises the anticodon loop of $tRNA^{Glu}$ and to a lesser extent $tRNA^{Lys}$, $tRNA^{Arg}$ and $tRNA^{Gln}$, when expressed in *E. coli* cells. In contrast to *Eco*PrrC, which merely nicks the tRNA backbone, *Gka*RloC performs two nuclease reactions on either side of the wobble uridine of a $tRNA^{Lys}$ substrate, leaving 2′,3′-cyclic phosphate and 5′-OH termini at each cleavage site. The net result is excision of the wobble nucleoside, which effectively precludes regeneration of a functional tRNA by a T4-like RNA-repair system.

Biochemical and structural studies of *Eco*PrrC have been hindered by the self-limiting capacity for expression of active PrrC in bacteria (i.e. PrrC curtails bacterial protein synthesis). Nonetheless, the Kaufmann laboratory has identified several functionally important components of the *Eco*PrrC protein, by surveying for mutations that affect PrrC toxicity in *E. coli* or assaying ACNase activity in extracts of *E. coli* expressing PrrC mutants (18,19,21). We and others have exploited budding yeast *Saccharomyces cerevisiae* as a surrogate system to study the effects of intracellular expression of tRNA anticodon nucleases, e.g. γ-toxin, colicin D, colicin E5 (22–24). Here we apply this strategy to *Eco*PrrC and PrrC homologs from other bacteria. We find that *Eco*PrrC is toxic to yeast cells, as is *Streptococcus mutans* PrrC (*Smu*PrrC). In contrast, the *Neisseria meningitidis* (*Nme*) and *Xanthomonas campestris* (*Xca*) PrrCs are nontoxic. We gained new insights to structure–function relationships in the PrrC family via an extensive mutational analysis of *Eco*PrrC. Comparisons of PrrC activity in a variety of yeast genetic backgrounds implicate $tRNA^{Lys}$ as a relevant target of *Eco*PrrC toxicity in a eukaryon, as it is in bacteria, notwithstanding the differences in the anticodon base-modification profiles of eukaryal and bacterial $tRNA^{Lys}$. We discuss possible therapeutic niches for enzymatic ribotoxins in eukarya.

MATERIALS AND METHODS

PrrC expression plasmids

The *E. coli prrC* gene was inserted into yeast plasmid YCplac111 (*CEN LEU2*) under the transcriptional control of a *GAL1* promoter to yield pYC-EcoPrrC. The amino acid sequence of the plasmid-encoded 396-aa *Eco*PrrC polypeptide is shown in Figure 2A. Missense mutations were introduced in the *prrC* gene in pYC-EcoPrrC by two-stage overlap extension PCR with mutagenic primers. The *prrC* ORF was sequenced in each case to verify the intended coding change and exclude the acquisition of unwanted coding changes during amplification and cloning. EcoRI/SalI fragments containing *GAL1-prrC-Ala* expression cassettes were excised from pYC-EcoPrrC-Ala and inserted into multicopy yeast plasmid pRS423 (2 μ *HIS3*).

The genes encoding PrrC homologs from *Neisseria meningitidis* (accession NP_273873), *Streptococcus mutans* (accession NP_721301) and *Xanthomonas campestris* (accession NP_635858) were amplified by PCR from genomic DNAs obtained from ATCC. The sense-strand PCR primers were designed to introduce an NdeI site at the translation start codon. The antisense primers introduced a SalI site downstream of the stop codon. The PCR products were digested with NdeI and SalI and inserted between the corresponding sites in pYC-EcoPrrC in lieu of the EcoPrrC fragment. Sequencing of the inserts in the resulting pYC-NmePrrC, pYC-SmuPrrC and pYC-XcaPrrC plasmids verified that no coding changes had been introduced during amplification and cloning.

tRNA expression plasmids

The 2 μ *URA3* plasmids bearing the yeast genes for $tRNA^{Glu(UUC)}$, $tRNA^{Lys(UUU)}$, $tRNA^{Gln(UUG)}$, $tRNA^{Arg(UCU)}$, $tRNA^{Gly(UCC)}$, $tRNA^{Leu(UAA)}$ and $tRNA^{Tyr(GUA)}$ are described (25). A 2 μ *URA3* $tRNA^{Lys(CUU)}$ plasmid was constructed by PCR amplifying a 1-kb fragment of *S. cerevisiae* chromosome III genomic DNA containing this tRNA gene and inserting it between BamHI and SalI sites in YEplac195 to generate pLysCUU. A KpnI/BglII fragment containing the $tRNA^{Lys(UUU)}$ gene was then inserted between KpnI and BamHI site of pLysCUU to generate pLysCUU/UUU bearing both $tRNA^{Lys}$ isoacceptors. The sequences of the tRNA inserts were verified for each of the new constructs used in this study.

PrrC toxicity assays

The haploid *S. cerevisiae* strain W303 was used in all experiments unless specified otherwise. The *trm9*Δ and *tot3*Δ derivatives of W303 are described (25,26). Yeast cells were transformed with plasmid DNAs by using the lithium acetate method (27). Transformants were selected on appropriate selective minimal synthetic media on 2% (w/v) bacto agar plates.

Toxicity of the plasmid-encoded PrrC proteins was gauged as follows. Cells derived from single transformants were grown at 30°C in liquid culture in selective media containing 2% glucose. The cultures were adjusted to A_{600} of 0.1 and then diluted in water in serial 5-fold decrements. Aliquots (3 μl) of the dilutions were then spotted in parallel on selective agar plates containing either 2% glucose or 2% galactose. The plates were photographed after incubation at 30°C for 2 (glucose) or 3 days (galactose).

Alternatively, the growth and viability of yeast cells bearing *CEN LEU2* PrrC plasmids were monitored in liquid cultures as follows. Cells derived from single transformants were grown overnight at 30°C in SD–Leu medium containing 2% raffinose. The cultures were adjusted to A_{600} of 0.1 by dilution into –Leu media containing either 2% glucose or 2% galactose (time 0). The

cultures were then incubated at 30°C with constant shaking and A_{600} was monitored at 3-h intervals. Viable cell counts were determined by withdrawing aliquots at 3 h intervals, diluting them 1:50 in water, and then plating 10, 100 and 250 µl of this sample on SD–Leu agar plates containing 2% glucose. Colonies were counted after incubation for 2 days at 30°C.

Dominant negative effects of PrrC-Ala mutants

Yeast cells were cotransformed with pYC-EcoPrrC (*CEN LEU2*) or the empty *CEN* vector and each of 15 pRS-EcoPrrC-Ala plasmids (2 µ *HIS3*) encoding nontoxic *Eco*PrrC mutants or the empty 2 µ vector. Cells derived from single transformants were grown at 30°C in liquid culture in SD–Leu–His medium containing 2% glucose. The cultures were adjusted to A_{600} of 0.1 and then diluted in water in serial 5-fold decrements. Aliquots (3 µl) of the dilutions were then spotted in parallel on –Leu–His agar plates containing either 2% glucose or 2% galactose. The plates were photographed after incubation at 30°C for 2 (glucose) or 3 days (galactose). Alternatively, the growth of yeast cells bearing pYC-EcoPrrC and pRS-EcoPrrC-Ala (or empty vector controls) was monitored in liquid cultures. Cells derived from single transformants were grown at 30°C in SD–Leu–His medium containing 2% raffinose until A_{600} reached ~2. Aliquots of the cultures were then diluted with SD–Leu–His medium containing 2% galactose to an A_{600} of 0.1. The cultures were incubated at 30°C with constant shaking for 18 h, at which time A_{600} was measured.

RESULTS AND DISCUSSION

Induced expression of *E. coli PrrC* in budding yeast is toxic

We installed the *E. coli prrC* gene in yeast on a *CEN* plasmid under the control of a glucose-repressed/galactose-induced *GAL1* promoter. Galactose induction of PrrC production suppressed yeast growth on agar medium (Figure 1A) and in liquid culture (Figure 1B). By analyzing yeast survival after transient galactose induction and return to glucose, we found that PrrC expression was profoundly fungicidal (Figure 1C). The number of viable cells in the yeast culture decreased by 19-fold within 3 h of *Eco*PrrC induction, by 350-fold after 9 h and by 550-fold after 12 h (Figure 1C). Control experiments verified that *CEN prrC* yeast cells grew as well as cells bearing the empty *CEN* vector on glucose-containing agar and liquid media (Figure 1A and B). These results showed that *Eco*PrrC is an effective toxin in a eukaryal cell, in the absence of any other bacterial or bacteriophage proteins, including the DNA restriction enzyme with

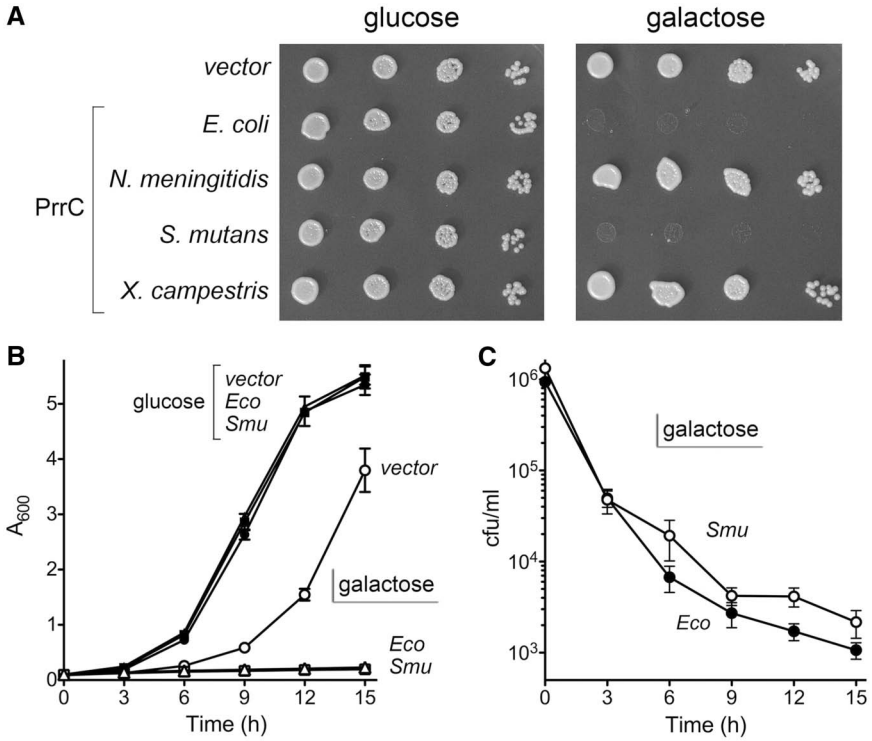

Figure 1. Induced expression of *Eco*PrrC and *Smu*PrrC is toxic to *S. cerevisiae*. (**A**) Serial 5-fold dilutions of yeast cells bearing a *CEN* plasmid encoding the indicated galactose-regulated *prrC* gene or an empty *CEN* vector were spotted on –Leu agar plates containing 2% glucose or galactose as specified. (**B**) Growth of liquid cultures of yeast cells bearing *Eco*PrrC or *Smu*PrrC plasmids or the empty vector was monitored by determining A_{600} at serial times after transfer from raffinose medium to media containing glucose or galactose. Each datum is the average of three independent growth experiments ±SEM. (**C**) Viable cell counts of liquid cultures of yeast cells bearing a *Eco*PrrC or *Smu*PrrC plasmid were determined immediately prior to (time 0) and at serial 3-h intervals after galactose induction, by plating aliquots on –Leu agar containing 2% glucose. Each datum is the average of three independent galactose-induction experiments ±SEM.

which it interacts in *E. coli* and the phage Stp protein that triggers PrrC activity during virus infection.

Remarkably, not all bacterial PrrCs are created equal in this respect. *Nme*- and *Xca*PrrC were nontoxic in yeast, while *Smu*PrrC was toxic (Figure 1A). Like *Eco*PrrC, *Smu*PrrC arrested yeast growth in liquid medium (Figure 1B) and was fungicidal after transient galactose induction and return to glucose (Figure 1C). We infer from these results that the toxic *Eco* and *Smu* PrrC proteins can incise essential target RNAs in yeast cells. The failure of *Nme*PrrC to arrest yeast growth was surprising to us, insofar as the nontoxic *Nme*PrrC protein has a significantly higher degree of amino acid identity (57%) with the *Eco*PrrC polypeptide than does *Smu*PrrC (42%). It is conceivable that: (i) *Nme*PrrC and *Xca*PrrC are nontoxic in yeast because they lack RNase activity, or (ii) *Nme*PrrC and *Xca*PrrC are *bona fide* ribotoxins, but their targets are not present in budding yeast (or are present but not essential for yeast growth). With respect to the latter issue, we tested the effects of induced expression of the four PrrCs on the growth of *E. coli* and found that the results were concordant those observed in yeast. Namely, *Eco*PrrC and *Smu*PrrC were toxic to *E. coli*, whereas *Nme*PrrC and *Xca*PrrC were not (data not shown). Thus, it is not simply a matter of the eukaryal milieu that masks an underlying ribotoxin activity of *Nme*PrrC and *Xca*PrrC. We surmise that members of the PrrC family differ with respect to their biological activity, which could reflect distinctive RNA target specificities and/or reliance on unique coactivators, e.g. if *Nme*PrrC and *Xca*PrrC require additional proteins from the cognate bacterium to manifest their RNase functions.

Structure-function analysis of *Eco*PrrC by alanine-scanning

The toxicity elicited by *Eco*PrrC expression in yeast affords a convenient assay to probe structure-activity relations. Our aim in this study was to map the amino acid functional groups of *Eco*PrrC required for cytotoxicity via alanine-scanning guided by a primary structure alignment of the *Eco*, *Nme* and *Smu* PrrC proteins (Figure 2A). We tested 53 *Eco*PrrC-Ala mutants for galactose-induced toxicity (Table 1). We thereby identified 20 nonessential residues (colored yellow in Figure 2A) and 33 essential residues (colored green in Figure 2A). In the case of nonessential residues such as His23, Lys238 and Lys325, their replacement by alanine still allowed for virtually complete growth inhibition on galactose-containing medium (Figure 2B). The *Eco*PrrC-C386A mutant also retained cytoxicity, albeit with very faint growth of the expressing yeast cells on galactose agar (Figure 2B), suggesting that C386A might be a hypomorph (see below.) Essential PrrC residues were those—like His295, Arg320, Arg349 and His356 in the C-terminal domain—at which alanine changes eliminated toxicity and permitted growth on galactose that was similar to that of the vector control (Figure 2B). Among the essential residues in the N-terminal domain were the five PrrC counterparts (Lys46, Thr47, Asp215, Asp216 and His251) of the constituents of the conserved NTP-binding site of the ABC transporter NTPases (28). We infer that NTP binding/hydrolysis is essential for *Eco*PrrC toxicity in yeast. The collection of 33 essential PrrC residues (22 in the N-domain and 11 in the C-domain) included six histidines, five lysines, three arginines, six aspartates, five asparagines, three glutamates, two threonines, two serines and a tryptophan (Table 1).

Structure–activity relationships at essential residues in the NTPase domain

We proceeded to determine structure–activity relationships for each of the 22 essential residues in the NTPase domain by testing the effects of 43 conservative substitutions. The results are summarized in Table 1 and discussed below, wherever possible, in light of structures of the homologous motor domains of ABC-family NTPases bound to nucleotide and a divalent cation cofactor (28–31).

The PrrC NTPase domain contains a consensus Walker A-box motif (AxxGxGKT[47]) found in many nucleotide-dependent phosphotransferases. The A-box is situated between the first β-strand and the first α-helix of the NTPase module and forms a classical P-loop structure in which the main-chain amide nitrogens and the signature lysine side chain (Lys46 in PrrC) coordinate the NTP phosphate oxygens (Supplementary Figure S1). The signature threonine/serine side chain vicinal to the lysine (Thr47 in PrrC) coordinates the divalent cation cofactor that bridges the β and γ phosphates (Supplementary Figure S1). Lys46 and Thr47 were both essential for PrrC toxicity, according to the alanine scan. Lys46 was strictly essential, insofar as neither arginine nor glutamine was active in its stead. Thr47 was also strictly essential; neither serine not valine could sustain *Eco*PrrC toxicity in yeast, implying that, in addition to the imputed coordination of magnesium by Thr-Oγ, the Thr47-Cγ makes an important contact as well. [In the case of human CFTR ABC protein (pdb 2PZE; 31), the equivalent A-box threonine makes a close van der Waals contact to the metal-binding aspartate of the Walker B-box.] The *Eco*PrrC Arg48 side chain flanking the A-box was also strictly essential for toxicity in yeast; neither lysine nor glutamine was functional. It is possible that Arg48 engages in bidentate hydrogen bonding or ionic interactions that lysine does not sustain. Arg48 is conserved in *Nme*PrrC and *Smu*PrrC, but is replaced by glutamine in *Xca*PrrC (Figure 2A).

The ABC proteins are homodimers, arranged head-to-tail, with two composite NTPase active sites formed by motifs derived from the *cis* protomer (which provides the A-box and B-box) and the *trans* protomer, which interacts with the P-loop of the *cis* protomer and also directly coordinates the NTP γ phosphate (Supplementary Figure S1). The *Eco*PrrC peptide segment ^{215}DDPVSSLDDNH^{225}, which embraces eight essential side chains, is composed of two distinct ABC motifs that form the active site: a Walker B-box (YVFIDD^{216}) derived from the *cis* protomer and a 'D loop' motif (SSLD^{222} in *Eco*PrrC) derived from the

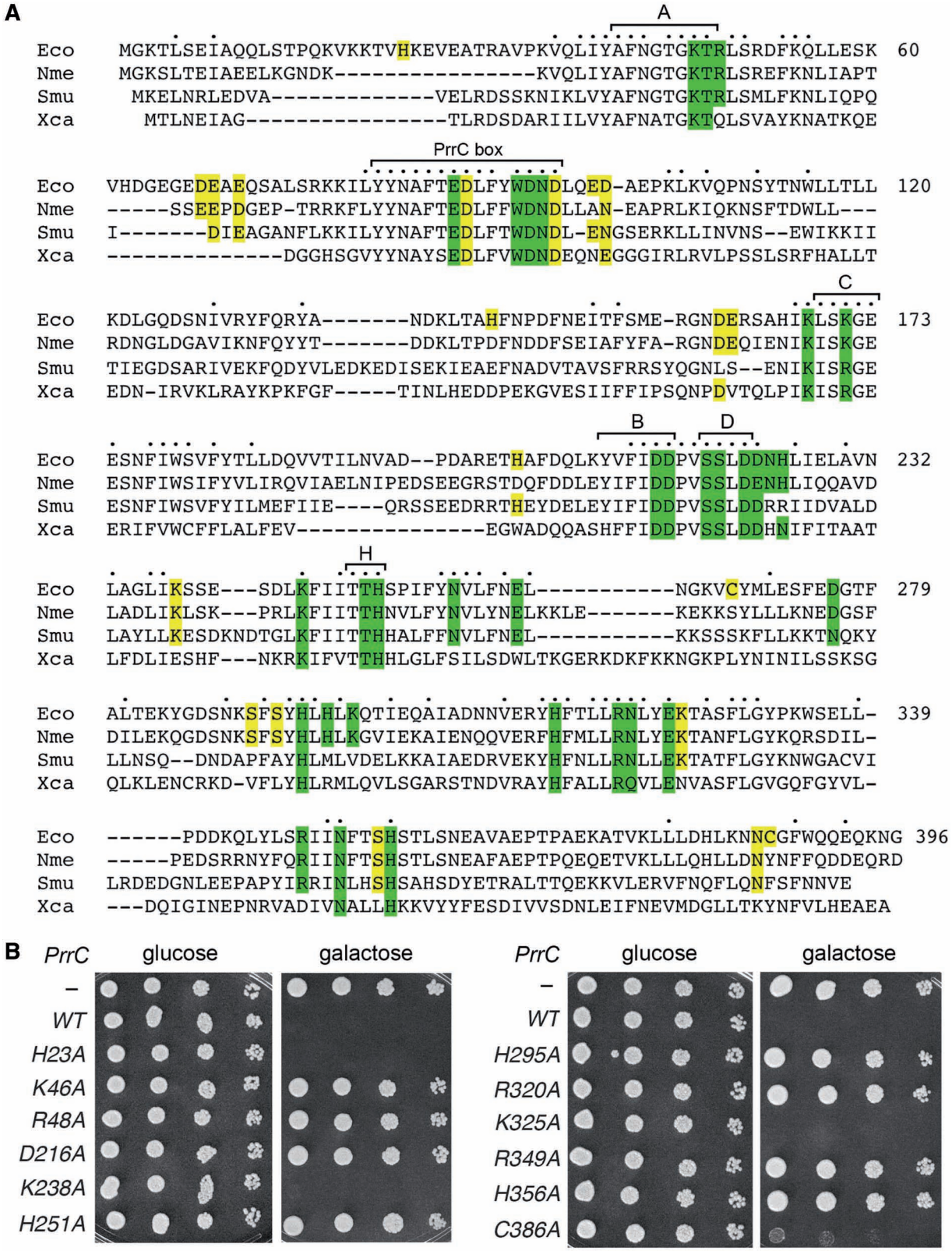

Figure 2. Homology-guided alanine-scanning mutagenesis of *Eco*PrrC. (**A**) The amino acid sequence of *Eco*PrrC is aligned to sequences of the *Nme*PrrC, *Smu*PrrC, and *Xca*PrrC proteins. Positions of side-chain identify/similarity in all four proteins are indicated by a filled black circle above the alignment. The conserved peptide motifs of the N-terminal NTPase domain are demarcated by brackets. The 54 amino acids targeted in the alanine scan are highlighted. Residues defined as essential for yeast toxicity by the alanine scan are shaded green; nonessential residues are shaded yellow. (**B**) Exemplary toxicity tests for wild-type *Eco*PrrC and EcoPrrC-Ala mutants are shown, in which serial 5-fold dilutions of yeast cells bearing the indicated *CEN GAL1-prrC* plasmid were spotted on –Leu agar plates containing 2% glucose or galactose as specified.

Table 1. Mutational effects on PrrC ribotoxin activity in yeast

PrrC allele	Toxicity	PrrC allele	Toxicity	PrrC allele	Toxicity	PrrC allele	Toxicity
WT	++	E162A	++	K238A	++	H315A	–
H23A	++	K168A	–	K245A	–	H315N	–
K46A	–	K168R	–	K245R	++	H315Q	–
K46R	–	K168Q	–	K245Q	–	R320A	–
K46Q	–	K171A	–	T250A	–	R320K	–
T47A	–	K171R	++	T250S	–	R320Q	–
T47S	–	K171Q	–	H251A	–	N321A	–
T47V	–	H204A	++	H251N	–	N321Q	–
R48A	–	D215A	–	H251Q	–	N321D	–
R48K	–	D215E	–	N257A	–	E324A	–
R48Q	–	D215N	–	N257Q	++	E324D	–
D68A	++	D216A	–	N257D	–	E324Q	–
E69A	++	D216E	–	E262A	–	K325A	++
E71A	++	D216N	–	E262Q	–	R349A	–
E88A	–	S219A	–	E262D	++	R349K	–
E88D	–	S219T	++	C268A	++	R349Q	–
E88Q	++	S219C	++	D276A	–	N352A	–
D89A	++	S220A	–	D276N	–	N352D	–
W93A	–	S220T	–	D276E	–	N352Q	++
W93Y	–	S220C	–	S291A	++	S355A	++
W93H	–	D222A	–	S293A	++	H356A	–
D94A	–	D222E	–	H295A	–	H356N	–
D94E	–	D222N	–	H295N	–	H356Q	–
D94N	–	D223A	–	H295Q	–	N385A	++
N95A	–	D223E	++	H297A	–	C386A	++
N95Q	–	D223N	–	H297N	–		
N95D	–	N224A	–	H297Q	–		
D96A	++	N224Q	++	K299A	–		
E99A	++	N224D	–	K299R	–		
D100A	++	H225A	–	K299Q	–		
H144A	++	H225N	++				
D161A	++	H225Q	–				

trans protomer (Supplementary Figure S1). The B-box provides two key carboxylates to the phosphohydrolase active site. The proximal aspartate is a component of the metal coordination complex. The vicinal Asp/Glu coordinates the water nucleophile. The corresponding Asp215 and Asp216 residues in *Eco*PrrC were both strictly essential; neither could be functionally substituted with asparagine or glutamate, signifying that a carboxylate is essential at both positions and that the putative PrrC active site cannot accommodate the longer main-chain to the carboxylate linker of Glu versus Asp.

In the ABC family, the eponymous aspartate side chain of the D loop caps an α-helix and makes a cross-protomer hydrogen bond with a phosphate-binding main chain amide of the A-box (Supplementary Figure S1). We find that the D loop Asp222 residue of *Eco*PrrC was essential and irreplaceable by Asn or Glu (Table 1). The two serines preceding the D loop aspartate were both essential for PrrC toxicity, but they displayed different structure-activity relations. Toxicity was restored when Ser219 was replaced by threonine or cysteine, signifying that hydrogen bonding of the Oγ atom is the functionally relevant property at this position and the extra methyl group of threonine is benign. The equivalent D loop serine in ABC proteins Sav1866 and HylB donates a hydrogen bond to the main-chain carbonyl of the essential B-box acidic residue located three residues upstream (corresponding to *Eco*PrrC Asp216) (30,31) (Supplementary Figure S1). We surmise that PrrC Ser219 plays a structural role in stabilizing the conformation of the loop that contains the contiguous B and D motifs. At Ser220 of *Eco*PrrC, the S220T and S220C mutants were inactive *in vivo* (Table 1), which suggests a tight steric constraint on the Ser220 side chain that does not tolerate the extra bulk of the threonine-Cγ or even the larger atomic radius of the cysteine-Sγ versus serine-Oγ. The essential Asp223, Asn224 and His225 residues flanking the *Eco*PrrC D loop are not generally conserved among ABC proteins. We conclude that the carboxylate functional group is the pertinent property at position 223, because the D223E mutant was toxic in yeast while D223N was nontoxic (Table 1). Asp223 is conserved as Asp/Glu in the *Smu*, *Nme* and *Xca* PrrCs (Figure 2A). At Asn224, the amide group was critical for function, i.e. glutamine restored toxicity while aspartate did not. At His225, asparagine supported PrrC activity though glutamine did not, which suggests that hydrogen bonding by His225-Nδ is the relevant property of this residue.

The KFIITTH^{251} motif of *Eco*PrrC that spans three essential side chains is the counterpart of the conserved 'H loop' motif of ABC-type NTPases (also called the 'switch' motif). The H loop connects a β-strand to an α-helix. The signature histidine donates a hydrogen bond to an NTP γ phosphate oxygen (28) that would stabilize the phosphohydrolase transition state. The H loop His251 of *Eco*PrrC is strictly essential for its activity *in vivo*,

insofar as the H251N and H251Q mutants were nontoxic (Table 1). The vicinal threonine-Oγ (corresponding to Thr250 in PrrC) makes a hydrogen bond to the main-chain amide of the H loop residue on the carboxyl side of the histidine (28) and thereby stabilizes the loop conformation. Loss of toxicity of the T250S mutant indicated that threonine is strictly essential in this position. The upstream Lys245 is essential for *Eco*PrrC and conserved in other PrrC homologs (albeit not in other ABC proteins). Positive charge appeared to suffice at this position, because K245R was active in yeast whereas K245Q was not (Table 1). Two important residues downstream of the H loop in *Eco*PrrC, Asn257 and Glu262, are conserved in *Nme*PrrC and *Smu*PrrC, but not in *Xca*PrrC or ABC proteins generally. The amide group of Asn257 is the key property, because mutant N257Q was toxic in yeast, whereas N257D was inactive (Table 1). At Glu262, the carboxylate was critical, i.e. E262D was toxic while E262Q was not. The C loop motif of ABC proteins (also called the ABC-signature motif) is conserved in *Eco*PrrC as ^{173}LSKGE (Figure 2A). A C loop derived from the *trans* protomer packs closely against the nucleoside and γ phosphate of the NTP substrate. The C loop and the A box P-loop of the *cis* protomer together form an oxyanion hole for the NTP γ phosphate (Supplementary Figure S1). Here we found that Lys171 within the C loop and Lys168 immediately preceding the loop were both essential for *Eco*PrrC toxicity. These two lysine residues are conserved among the PrrC homologs (Figure 2A), but they displayed different structure–activity relations. Whereas Lys168 was strictly essential (i.e. arginine and glutamine rendered PrrC nontoxic), Lys171 could be replaced functionally by arginine, but not glutamine, signifying that positive charge sufficed for activity at this position. The ABC protein Sav1866 has a lysine at the position corresponding to Lys168 in PrrC; the Sav1866 structure shows that the lysine packs over the adenine base of the bound NTP, with which it makes multiple van der Waals contacts (31; pdb 2ONJ).

Finally, we identified four essential residues (Glu88, Trp93, Asp94 and Asn95) within the *Eco*PrrC segment ^{82}YYNAFYEDLFYWDND^{96} of the NTPase domain that has been dubbed the 'PrrC box' by the Kaufmann laboratory (19) in light of its strong conservation among bacterial PrrC homologs (Figure 2A). There is little primary structure similarity between the PrrC box and the corresponding segments of ABC proteins, though it is possible that the PrrC box is a divergent analog of the ABC Q-loop motif. The Q loop is a mobile hinge that is sensitive to the presence of NTP and metal ligands. The eponymous glutamine side chain of the Q loop (e.g. Gln90 in the MJ0796 protein) makes direct contacts with metal and the nucleophilic water in the phosphohydrolase active site (28). Replacing PrrC box residue Glu88 with glutamine supported toxicity in yeast, whereas aspartate did not. This result signifies that hydrogen bonding, not negative charge, is the key property of this residue and that the distance from the main-chain to the terminal functional group of Glu/Gln is critical, accounting for why retraction of this distance in aspartate leads to loss of PrrC activity. Trp93 appeared to be strictly essential, in that function was not revived by installation of alternative aromatic (tyrosine) or planar hydrogen bonding (histidine) residues (Table 1). The flanking Asp94 and Asn95 residues were also strictly essential, i.e. the respective conservative mutants D94E, D94N, N95Q and N95D were nontoxic (Table 1).

Structure–activity relationships at essential residues in the nuclease domain

The C-terminal nuclease domains of PrrC and RloC proteins have no discernible primary structure similarity to any other tRNA ribotoxins, or to any known ribonucleases, phosphotransferases or tRNA-binding proteins. The Kaufmann laboratory has proposed two functional components of the *Eco*PrrC nuclease domain: (i) a triad comprising Arg320, Glu324 and His356 that they implicate in chemical catalysis of transesterification at the wobble nucleotide to generate 2′,3′-cyclic phosphate and 5′-OH product strands (19); and (ii) a putative lysine anticodon recognizing peptide (LARP) motif, ^{284}KYGDSNKSFSY^{294} (33). The Arg–Glu–His triad is conserved among PrrC and RloC homologs, consistent with a catalytic function. In contrast, the LARP motif, mutations of which affect the tRNA substrate preference of *Eco*PrrC (16,17), is found only in a subset of PrrC proteins and is absent from RloC (20,33). Thus it is conceivable that LARP is a *bona fide* determinant of the target specificity of a subset of PrrC proteins that contains this motif. However, LARP is unlikely be the decisive factor with respect to yeast toxicity of bacterial PrrCs, insofar as the *Eco*PrrC LARP is well conserved (10/11 identical residues) in *Nme*PrrC, which is not toxic in yeast, yet LARP is not conserved (3/11 identical residues) in *Smu*PrrC, which is toxic in yeast (Figure 2A). Two alanine mutations in the *Eco*PrrC LARP motif tested presently (at Ser291 and Ser293, which are conserved in *Nme*PrrC) had no effect on cytotoxicity in yeast.

In mutagenizing the nuclease domain, we adopted an agnostic view and mainly targeted residues we deemed most likely to be involved in catalysis of phosphoryl transfer (histidine, lysine, arginine, glutamate) or RNA binding (lysine, arginine), based on general principles and the specific mechanisms of other well-studied ribonucleases that generate 2′,3′-cyclic phosphodiesters: e.g. RNase A, RNase T1, colicin E5 and tRNA splicing endonuclease (34–37). Our alanine scan identified 11 essential amino acids in the nuclease domain, at which we assessed structure-activity relationships with 22 conservative mutations. The results are summarized in Table 1 and discussed below in light of the catalytic mechanisms and structures of analogous ribonucleases that leave 2′,3′-cyclic phosphate and 5′-OH ends.

The 'classical' mechanism of RNA cleavage by transesterification exemplified in RNase A relies on two histidine side chains that serve, respectively, as: (i) a general base catalyst that abstracts a proton from the attacking ribose 2′-OH, and (ii) a general acid catalyst that donates a proton to the ribose 5′-OH leaving group (34). We replaced His295, His297, His315 and His356 in the

*Eco*PrrC nuclease domain with alanine, glutamine and asparagine and found that each histidine was strictly essential for toxicity (Table 1). Three of them—His295, His315 and His356—are conserved among PrrC homologs, and are therefore plausible candidates for a catalytic role, possibly as acid–base catalysts. Two of these three histidines (His295 and His356) are also conserved in RloC (20). In contrast, His297, though retained as histidine in nontoxic *Nme*PrrC, is replaced by methionine in the toxic *Smu*PrrC protein (Figure 2A), a scenario that makes it unlikely that His297 acts as a general acid–base catalyst.

Structural and functional studies of RNase A highlight a single essential lysine that interacts with the scissile phosphodiester and stabilizes the pentacoordinate transition state (34). None of the nine lysines in the nuclease domain of *Eco*PrrC is conserved in all three of the other PrrC homologs aligned in Figure 2A. Of the two lysines that we chose for the alanine scan, Lys325 was unessential and Lys299 was essential. PrrC was nontoxic when Lys299 was replaced conservatively by arginine or glutamine (Table 1). Yet, because this lysine is replaced by a valine and leucine in *Smu*PrrC and *Xca*PrrC, we think it unlikely that Lys299 plays a direct catalytic role in *Eco*PrrC.

Arginines classically play a role in ground-state binding and transition-state stabilization during phosphoryl transfer reactions by making bidentate contacts to the phosphate oxygens. Several of the transesterifying ribonucleases with known structures assimilate a catalytic arginine in their active sites. For example, the colicin E5 active site includes an arginine that coordinates both nonbridging oxygens of the scissile phosphodiester (37). The active site of RNase T1 also has an arginine that contacts the scissile phosphodiester (38). The active site of barnase includes two arginines that contact the scissile phosphodiester (39). Here we identified two arginines in the nuclease domain (Arg320 and Arg349) as strictly essential for *Eco*PrrC toxicity, i.e. Ala, Lys and Gln mutants thereof were inactive (Table 1). Both of these arginines are conserved in the toxic *Smu*PrrC homolog (Figure 2A) and in RloC (18) and are therefore plausible candidates for a catalytic role.

Glu324 was strictly essential for *Eco*PrrC toxicity (Table 1). This position is conserved as glutamate in the *Nme*, *Smu* and *Xca* homologs (Figure 2A) and also in RloC. Glutamate acts as a general base catalyst of RNA transesterification by RNase T1 and barnase (35,39,40).

We identified two essential asparagines in the *Eco*PrrC nuclease domain. Asn321 was strictly essential (Ala, Gln and Asp mutants were inactive; Table 1). This residue is conserved as Asn or Gln among PrrC homologs (Figure 2A). At Asn352, the Ala and Asp changes eliminated toxicity, but the conservative N352Q mutant retained toxicity. This result attests to the importance of the amide functional group at position 352 and tolerance by *Eco*PrrC of the longer main-chain to amide distance in Gln versus Asn. Asn352 is conserved as Asn in PrrC homologs (Figure 2A) and in RloC (18).

In sum, our mutational study of the nuclease domain verifies the importance of several residues studied by Kaufmann and colleagues (19), while identifying new candidate constituents of the active site and establishing structure–activity relationships for each of 11 essential residues. A definitive interpretation of the mutational data awaits an atomic structure of the nuclease domain.

*Eco*PrrC is toxic in the absence of a modified tRNA mcm^{5}U wobble base

The target specificity of many tRNA anticodon nucleases is achieved via recognition of modified nucleobases in the anticodon loop, especially the wobble base. For example, colicin E5 cleaves bacterial $tRNA^{Tyr}$, $tRNA^{His}$, $tRNA^{Asn}$ and $tRNA^{Asp}$ that contain the wobble base queosine (37). *K. lactis* γ-toxin specifically cleaves yeast $tRNA^{Glu(UUC)}$ containing the modified wobble base mcm^{5}s^{2}U (5-methoxycarbonylmethyl-2-thiouridine; Figure 3C) (3,4). *Pichia acaciae* toxin (PaT) exerts its toxicity by incising a different yeast tRNA containing the mcm^{5}s^{2}U wobble base: $tRNA^{Gln(UUG)}$ (5).

*Eco*PrrC incises bacterial $tRNA^{Lys(UUU)}$ at a single phosphodiester 5′ of the modified wobble base mnm^{5}s^{2}U (5-methylaminomethyl-2-thiouridine) (16) (Figure 3C). The mnm^{5}U wobble modification does not exist in eukaryal tRNAs, which instead have mcm^{5}s^{2}U in their $tRNA^{Lys(UUU)}$ (and also in $tRNA^{Glu}$ and $tRNA^{Gln}$). *Kluyveromyces lactis* γ-toxin requires the mcm^{5}s^{2}U modification in its $tRNA^{Glu}$ target, such that yeast *tot3*Δ(*elp3*Δ) and *trm9*Δ mutants, which either fail to modify the C5 atom or fail to add the terminal methyl group (Figure 3C), are resistant to γ-toxin's effects (41). Consequently, galactose-induced intracellular expression of γ-toxin, which prevents growth of wild-type *S. cerevisiae*, had no effect on the growth of *tot3*Δ and *trm9*Δ cells (Figure 3A). In contrast, we found that *Eco*PrrC was toxic to *tot3*Δ and *trm9*Δ cells (Figure 3A). Thus, we infer that: (i) the target specificity of PrrC in yeast differs from that of γ-toxin; and (ii) if PrrC exerts its toxicity in yeast by cleaving $tRNA^{Lys}$, then it does so without strict need for the mcm^{5}s^{2}U wobble modification.

Is yeast $tRNA^{Lys}$ a target of *Eco*PrrC?

If an intracellular ribotoxin exerts its effect by breaking a specific cellular RNA target, then one might expect to reverse the toxicity by overexpressing the RNA target. This is demonstrated nicely for *K. lactis* γ-toxin, whereby overexpression of its specific target $tRNA^{Glu(UUC)}$ protects yeast from toxin-induced growth arrest (25) (Figure 3B). Here we screened various yeast tRNAs on multicopy 2μ plasmids for their ability to protect yeast from the toxicity of *Eco*PrrC. Increased gene dosage of $tRNA^{Glu(UUC)}$ afforded no protection from *Eco*PrrC, but neither did overexpression of the presumptive target $tRNA^{Lys(UUU)}$, the isoacceptor $tRNA^{Lys(CUU)}$ or a combination of both $tRNA^{Lys(UUU)}$ and $tRNA^{Lys(CUU)}$ (Figure 3B). High-copy plasmids expressing other tRNAs with wobble uridines ($tRNA^{Gln}$, $tRNA^{Arg}$, $tRNA^{Leu}$ or $tRNA^{Gly}$) or $tRNA^{Tyr(GUA)}$ were also ineffective (data not shown). Several possibilities come to mind to explain the negative results of the tRNA rescue experiment: (i) $tRNA^{Lys}$ is not a PrrC target in yeast; (ii) $tRNA^{Lys}$ is a PrrC target, but so are

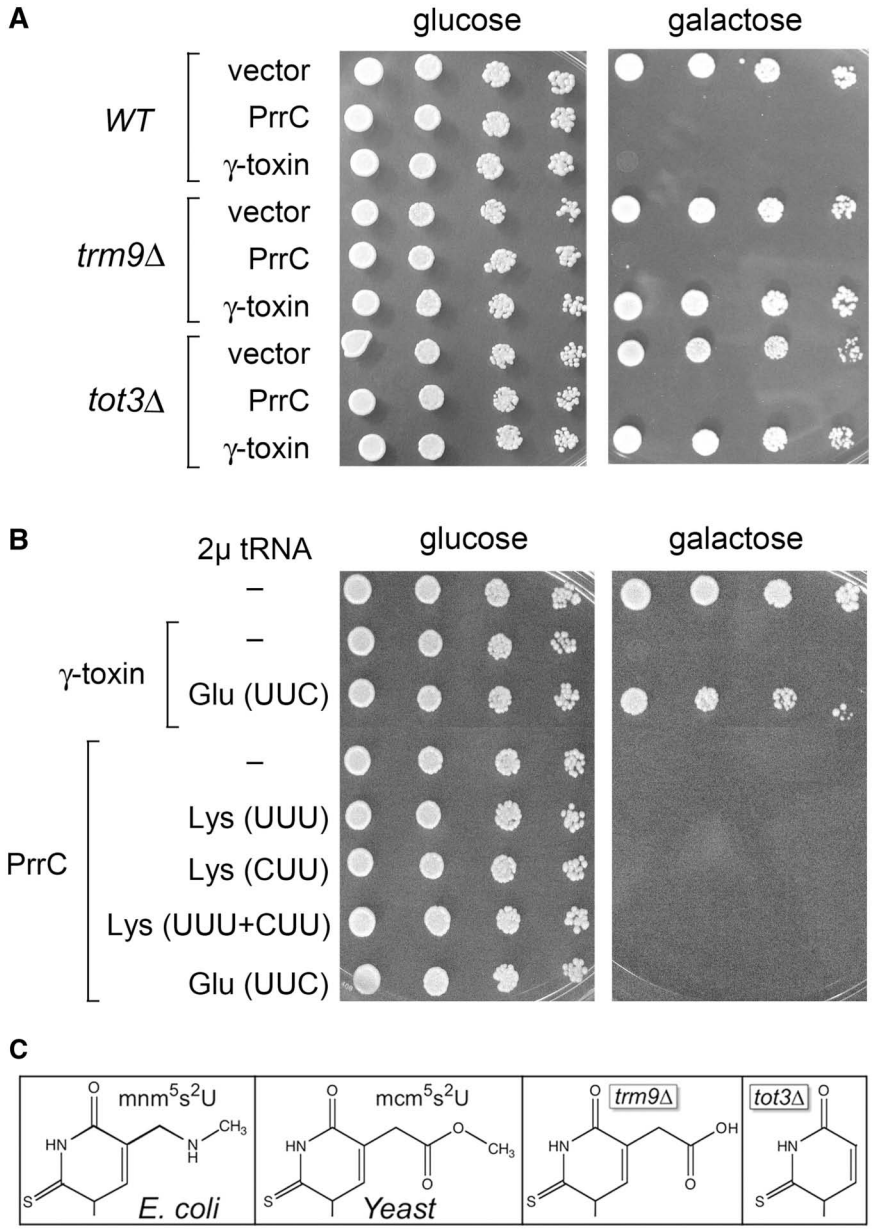

Figure 3. *Eco*PrrC is toxic in the absence of a modified tRNA mcm^{5}U wobble base. (**A**) Serial 5-fold dilutions of wild-type (WT), *trm9*Δ, and *tot3*Δ yeast cells bearing a *CEN* plasmid encoding galactose-regulated *Eco*PrrC or *K. lactis* γ-toxin were spotted on –Leu agar plates containing 2% glucose or galactose as specified. (**B**) Serial dilutions of wild-type yeast cells bearing a *CEN* plasmid encoding galactose-regulated *Eco*PrrC or *K. lactis* γ-toxin plus a 2 μ plasmid carrying the indicated yeast tRNA genes were spotted on –Leu–Ura agar plates containing glucose or galactose. (**C**) Structures of the wobble uridine modifications found in tRNA$^{Lys(UUU)}$ of *E. coli* (mnm^{5}s^{2}U), wild-type yeast (mcm^{5}s^{2}U) and yeast mutants *trm9*Δ (cm^{5}s^{2}U; 5-carboxymethyl-2-thiouridine) and *tot3*Δ (s^{2}U; 2-thiouridine).

other essential yeast RNAs or (iii) tRNA^{Lys} is the principal PrrC target, but the level of anticodon nuclease activity in the PrrC-producing yeast cells is sufficient to cleave the target tRNA pool even when the tRNA gene is present in high copy.

To interrogate the third option, we surveyed several of our collection of 'active' PrrC mutants for rescue of toxicity by increased tRNA^{Lys} gene dosage. We focused especially on two possibly hypomorphic mutants, C386A and S219T, that were clearly toxic, but reliably yielded faint spots when cells bearing the *CEN prrC-C386A* and *prrC-S219T* plasmids were plated on galactose agar at low dilution. We found that overexpression of tRNA$^{Lys(UUU)}$ partially protected yeast cells from the toxic effect of both of these PrrC mutants, whereas overexpression of tRNA$^{Lys(CUU)}$ or tRNA$^{Glu(UUC)}$ did not (Figure 4A). This instructive result indicated that tRNA$^{Lys(UUU)}$ is a physiologic target of PrrC toxicity in yeast, as it is in *E. coli*.

The inferred hypomorphic quality of *Eco*PrrC S219T and C386A was reinforced by the results of experiment shown in Figure 4B, wherein we analyzed their effect on growth of *trm9*Δ cells. Whereas wild-type *Eco*PrrC was profoundly toxic in *trm9*Δ, neither of the mutants

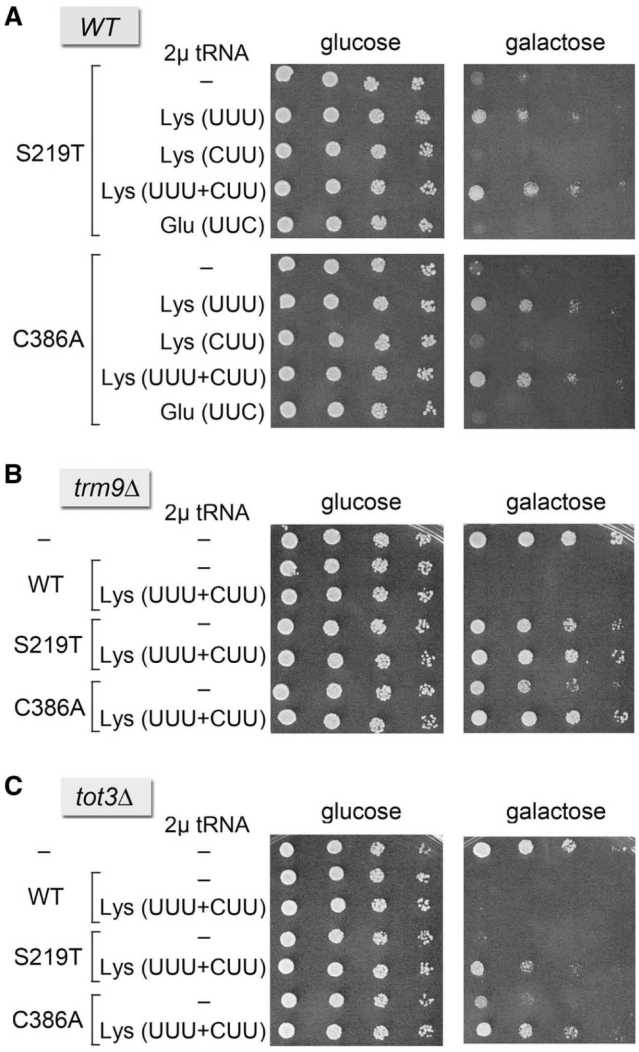

Figure 4. Rescue of *Eco*PrrC S219T and C386A toxicity by 2μ $tRNA^{Lys(UUU)}$. (**A**) Serial dilutions of wild-type yeast cells bearing a *CEN* plasmid encoding galactose-regulated *Eco*PrrC mutants S219T or C386A plus a 2μ plasmid carrying the indicated yeast tRNA genes (or an empty 2μ vector, denoted by a dash) were spotted on –Leu–Ura agar plates containing glucose or galactose. (**B**) Serial dilutions of yeast *trm9*Δ cells bearing a *CEN* plasmid encoding galactose-regulated wild-type *Eco*PrrC or mutants S219T or C386A plus a 2μ plasmid carrying the indicated yeast tRNA genes (or an empty 2μ vector, denoted by a dash) were spotted on agar plates containing glucose or galactose. (**C**) Serial dilutions of yeast *tot3*Δ cells bearing a *CEN* plasmid encoding galactose-regulated wild-type *Eco*PrrC or mutants S219T or C386A plus a 2μ plasmid carrying the indicated yeast tRNA genes (or an empty 2μ vector, denoted by a dash) were spotted on agar plates containing glucose or galactose.

prevented growth of the *trm9*Δ cells on galactose. Rather, they had a modest effect on growth rate, as gauged by colony size compared to the vector control (Figure 4B). Moreover, while the toxicity of wild-type *Eco*PrrC in *trm9*Δ cells was unabated by increased dosage of $tRNA^{Lys}$, the same maneuver sufficed to reverse the slow-growth phenotypes of the S219T and C386A mutants (Figure 4B). In contrast, the yeast *tot3*Δ mutation *per se* afforded no protection against the toxic effect of the S219T mutant, and only minimally protection against C386A (evident at low dilution), notwithstanding that partial protection of *tot3*Δ cells against both mutants was still conferred by $tRNA^{Lys}$ overexpression (Figure 4C).

We surmise from these experiments that: (i) *Eco*PrrC can target a wobble uridine with either bacterial mnm^5 or eukaryal mcm^5 modifications *in vivo*; and (ii) *Eco*PrrC can also target a wobble uridine with no modifications at the C5 atom (*tot3*Δ). However, an incompletely modified eukaryal wobble uridine lacking the terminal methyl group (*trm9*Δ; Figure 3C) is relatively resistant *in vivo* to *Eco*PrrC S219T and C386A. Our findings resonate with *in vitro* studies from the Kaufmann laboratory (16,17) that showed a hierarchy of wobble base-modification effects on the cleavage of anticodon stem-loop structures by extracts of *E. coli* expressing a different hypomorphic *Eco*PrrC mutant (D222E). The order of wobble U preferences was: $mnm^5s^2U > s^2U > mcm^5s^2U$.

Dominant negative effects of PrrC mutants

PrrC and RloC are the only known ribotoxins with an ABC-like NTPase domain. Whereas the present mutational scan of the *Eco*PrrC NTPase fortified the conclusion that NTP binding and/or hydrolysis are essential for PrrC toxicity, the mechanism by which the PrrC NTPase activates the PrrC nuclease is unknown. It has been suggested that one role of NTPase domain could be the regulation the nuclease-masking interaction PrrC with the EcoPrrI DNA restriction enzyme (18). This would not be a factor in yeast toxicity studied presently. Structural studies of other ABC domains highlight the general theme that formation or stability of the head-to-tail ABC dimer is influenced by NTP occupancy of the phosphohydrolase active site. If it is true for PrrC that NTP binding acts as an allosteric switch, then the key issue is whether the NTP switch activates the nuclease directly (by inducing an active state of the inherently latent nuclease domain) or indirectly (by relieving the constitutively repressive effects of the NTPase domain on an inherently competent nuclease domain).

One prediction of a purely anti-repression model is that removal of the NTPase domain might lead to a constitutively active nuclease. However, this was not the case in yeast, insofar as we found that induced expression of the isolated C-terminal nuclease domain of *Eco*PrrC had no effect on cell growth, even when the nuclease domain was expressed from a multicopy 2μ plasmid (data not shown). In addition, we found that induced coexpression of the *Eco*PrrC NTPase and nuclease domains in *trans* (from separate genes on *CEN* or 2μ plasmids) also had no effect on yeast growth (data not shown). We surmised from these results that the NTPase and nuclease domains must be linked in *cis* for *Eco*PrrC to exert its toxicity in yeast.

A plausible direct activation model invokes NTP-triggered dimerization of the NTPase domain to yield a PrrC quaternary structure in which the previously latent nuclease module is now functional for tRNA target recognition and scission. One prediction of an obligatory oligomerization model is that overexpression of inactive

mutants of PrrC might dampen the activity of wild-type PrrC, by forcing the assembly of defective hetero-oligomers via mass action. We evaluated this scenario by installing several of our nontoxic *prrC*-Ala alleles on 2 μ plasmids under the control of a *GAL1* promoter. After verifying that these mutants were nontoxic when the 2 μ plasmid-bearing cells were plated on galactose-containing agar (Figure 5A; PrrC–), we tested them for a dominant-negative effect on the galactose-induced growth arrest caused by wild-type *Eco*PrrC on a *CEN* plasmid (Figure 5A; PrrC+). Spotting tests revealed distinct levels of effects exerted by overexpression of the mutants in *trans*. For example, mutants K46A, T250A and H251A in the NTPase domain partially suppressed the toxicity of wild-type *Eco*PrrC and allowed the cells to form colonies on galactose agar, albeit smaller colonies than the 'PrrC–' controls (Figure 5A). In contrast, mutants H315A, R320A and E324A in the nuclease domain had essentially no impact on the toxicity of wild-type *Eco*PrrC (Figure 5A).

To quantify the dominant negative effect, we grew liquid cultures of yeast strains bearing a *CEN* wild-type *Eco*PrrC plasmid (or empty *CEN* control) plus 2 μ plasmids expressing 15 different nontoxic PrrC-Ala mutants (or an empty 2 μ vector control). Equal aliquots of cells from the cultures were then transferred to liquid medium containing galactose to induce PrrC expression. Measurement of A_{600} after overnight growth in galactose ± wild-type *Eco*PrrC revealed that the PrrC–culture bearing the empty 2 μ vector had grown to saturation (A_{600} > 4.0), while the PrrC+ culture was arrested completely (A_{600} 0.26; compare black and white bars in Figure 5B, 'vector'). Six of the PrrC mutants (H295A, H315A, R320A, E324A, R349A and H356A) had little or no impact on the toxicity of wild-type PrrC, i.e. cells expressing these mutant alone grew to saturation in galactose (A_{600} > 4.0), whereas cells coexpressing wild-type PrrC grew to A_{600} of 0.3–0.6 (Figure 5). In contrast, the toxicity of wild-type PrrC was clearly ameliorated in cells overexpressing mutants K46A, T47A, R48A, K168A, D215A, D216A, S220A, T250A and H251A, such that the cultures grew to A_{600} values of 1–2 (Figure 5B). It was most striking that all of the dominant negative mutations were in the putative active-site motifs of the NTPase domain, whereas the mutations that did not have a negative effect in *trans* were all in located in the nuclease domain.

These results are consistent with a model for the physical organization of the active *Eco*PrrC toxin, in which: (i) antiparallel head-to-tail dimerization of the NTPase domain is required for PrrC toxicity in yeast; and (ii) toxicity requires two fully functional NTP-binding phosphohydrolase active sites (Figure 6A). Consequently, the dominant negative effect of the NTPase mutants results from the formation of mixed dimers in which one of the active sites is defective (Figure 6B). In contrast, we infer that just one active nuclease module suffices for PrrC toxicity in yeast, provided that proper dimerization has occurred, thereby accounting for why overexpression of PrrC with a nuclease-inactivating mutation (but an intact NTPase domain) does not diminish the toxicity of wild-type *Eco*PrrC (Figure 6C). (A caveat to this interpretation of the absence of dominant negative effects of the nuclease mutants is that we have not directly gauged the steady-state levels of the mutant PrrC proteins expressed in yeast from the 2 μ plasmids. Thus we cannot exclude a scenario in which all of the mutations surveyed in the nuclease domain destabilize PrrC in yeast while none of the mutations in the NTPase domain have this effect.) The model in Figure 6 focuses on dimerization as a key quaternary-structure trigger, but is equally adaptable to alternative

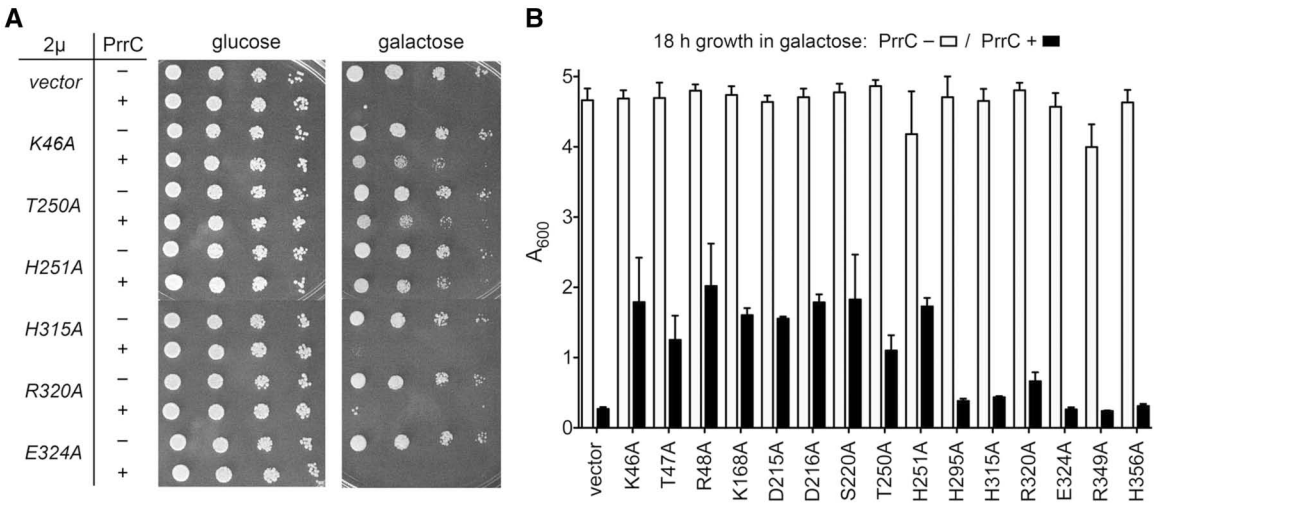

Figure 5. Dominant negative effects of PrrC-Ala mutants. (**A**) Serial dilutions of yeast cells bearing a *CEN* plasmid encoding wild-type *Eco*PrrC (PrrC+) or the empty *CEN* vector (PrrC–) plus a 2 μ plasmid encoding the indicated PrrC-Ala mutants (or the empty 2 μ vector) were spotted on –Leu–His agar plates containing glucose or galactose. (**B**) Yeast cells bearing a *CEN* plasmid encoding wild-type *Eco*PrrC (PrrC+) or the empty *CEN* vector (PrrC–) plus a 2 μ plasmid encoding the indicated PrrC-Ala mutants (or the empty 2 μ vector) were inoculated into SD–Leu–His medium containing 2% galactose to attain an A_{600} of 0.1. The cultures were incubated at 30°C for 18 h, at which time A_{600} was measured. Each datum is the average of three independent galactose-induction experiments ± SEM.

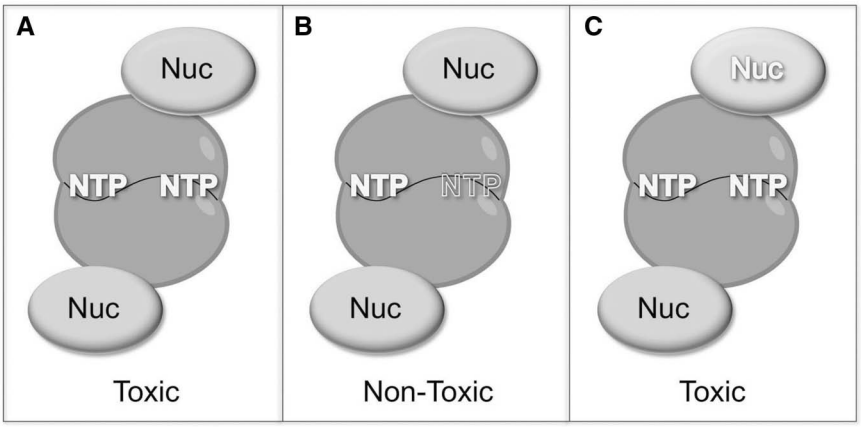

Figure 6. Model for oligomeric domain organization in *Eco*PrrC in light of mutational data and dominant negative effects of NTPase mutations. (**A**) Toxicity of wild-type *Eco*PrrC is contingent on head-to-tail dimerization of the ABC-like NTPase domains and the consequent formation of two composite NTP phosphohydrolase active sites ('NTP' in white bold type), which in turn activates the C-terminal nuclease domains ('Nuc' in black). (**B**) A mixed PrrC dimer of one wild-type protomer and one NTPase-defective protomer ('NTP' in gray) is nontoxic, because only one of the two composite NTPase sites is intact. (**C**) A mixed dimer of one wild-type protomer and one nuclease-defective protomer ('Nuc' in black) is toxic, because it is able to execute the proposed dual NTP-dependent activation of the one intact nuclease module.

oligomerization models, variously invoking hexameric or tetrameric states of *Eco*PrrC (18,19,33), wherein all NTPase sites, but not necessarily all nuclease sites, must be intact to exert toxicity.

CONCLUSIONS

Programmed RNA damage is a common feature of cellular responses to virus infection, whether it be tRNA restriction by PrrC in *E. coli* (14) or innate immune signaling via RNase L-damaged RNAs in mammalian cells (42). There is also a growing consensus that programmed RNA damage—especially tRNA damage—is a common feature of eukaryal cellular stress responses, wherein the broken tRNAs molecules *per se* can have a signaling role at levels of tRNA damage that do not significantly deplete the pool of the tRNA target (43–51). This suggests a possible therapeutic niche for enzymatic and chemical ribotoxins, predicated either on: (i) depleting an essential RNA or (ii) eliciting an 'RNA damage response' (e.g. reduced and altered protein synthesis, altered gene expression, cell-cycle arrest, apoptosis, etc.) analogous to DNA damage responses. As an example of the former mode, Kaufmann *et al*. have suggested PrrC as a means of interdicting HIV infection via depletion of the pool of human $tRNA^{Lys}$ that serves as primer for HIV reverse transcriptase (17,52).

Cytotoxic ribonucleases from bacteria and eukarya exemplify a new modality of cancer therapy (53). Onconase, an RNase A-like ribonuclease elaborated by frogs, has been studied extensively as an anticancer agent (54). Onconase cytoxicity is facilitated by its ready uptake by mammalian cells, its resistance to the cellular RNase inhibitor protein and its induction of damage to tRNAs in human tumor cells (55). Bacterial tRNA ribotoxins have much higher selectivity for specific tRNA target sites than does Onconase. The present demonstration that PrrC is fungicidal in yeast, together with recent reports that colicins D and E5 are also growth suppressive in yeast (22,23), suggest practical applications for bacterial tRNA anticodon nucleases in eukarya. Because fungi appear not to have an endogenous RNA repair system capable of rectifying the tRNA anticodon breaks (56), they would be vulnerable to ribotoxins as antifungals, provided one could devise a way to modify the toxin to promote its cellular uptake. Cancer cells might also be sensitized to tRNA ribotoxins, alone or in combination with other chemotherapeutics.

SUPPLEMENTARY DATA

Supplementary Data are available at NAR Online.

ACKNOWLEDGEMENTS

We thank Gabriel Kaufmann for providing a clone of the *E. coli prrC* gene and Sabrina Zink for constructing the pYC-EcoPrrC plasmid for galactose-inducible *Eco*PrrC expression in yeast.

FUNDING

National Institutes of Health (grant GM42498) to S.S. S.S. is an American Cancer Society Research Professor. Funding for open access charge: National Institutes of Health (grant GM42498).

Conflict of interest statement. None declared.

REFERENCES

1. Ogawa,T., Tomita,K., Ueda,T., Watanabe,K., Uozumi,T. and Masaki,H. (1999) A cytotoxic ribonuclease targeting specific tRNA anticodons. *Science*, **283**, 2097–2100.

2. Tomita,K., Ogawa,T., Uozumi,T., Watanabe,K. and Masaki,H. (2000) A cytotoxic ribonuclease which specifically cleaves four isoaccepting arginine tRNAs at their anticodon loops. *Proc. Natl Acad. Sci. USA*, **97**, 8278–8283.
3. Lu,J., Huang,B., Esberg,A., Johanson,M. and Byström,A.S. (2005) The *Kluyveromyces lactis* gamma-toxin targets tRNA anticodons. *RNA*, **11**, 1648–1654.
4. Lu,J., Esberg,A., Huang,B. and Byström,A.S. (2008) The *Kluyveromyces lactis* γ-toxin, a ribonuclease that recognizes the anticodon stem loop of tRNA. *Nucleic Acids Res.*, **36**, 1072–1080.
5. Klassen,R., Paluszynski,J.P., Emhoff,S., Pfeiffer,A., Fricke,J. and Meinhardt,F. (2008) The primary target of the killer toxin from *Pichia acaciae* is $tRNA^{Gln}$. *Mol. Microbiol.*, **69**, 681–697.
6. Kaufmann,G. (2000) Anticodon nucleases. *TIBS*, **25**, 70–74.
7. Condon,C. (2006) Shutdown decay of mRNA. *Mol. Microbiol.*, **61**, 573–583.
8. Nariya,H. and Inouye,M. (2008) MazF, an mRNA interferase, mediates programmed cell death during multicellular *Myxococcus* development. *Cell*, **132**, 55–66.
9. Levitz,R., Chapman,D., Amitsur,M., Green,R., Snyder,L. and Kaufmann,G. (1990) The optional *E. coli prr* locus encodes a latent form of phage T4-induced anticodon nuclease. *EMBO J.*, **9**, 1383–1389.
10. Tyndall,C., Meister,J. and Bickle,T.A. (1994) The *Escherichia coli prr* region encodes a functional type IC DNA restriction system closely integrated with an anticodon nuclease gene. *J. Mol. Biol.*, **237**, 266–274.
11. Amitsur,M., Morad,I. and Kaufmann,G. (1989) *In vitro* reconstitution of anticodon nuclease from components encoded by phage T4 and *Escherichia coli* CTr5X. *EMBO J.*, **8**, 2411–2415.
12. Amitsur,M., Morad,I., Chapman-Shimshoni,D. and Kaufmann,G. (1992) HSD restriction-modification proteins partake in latent anticodon nuclease. *EMBO J.*, **11**, 3129–3134.
13. Penner,M., Morad,I., Snyder,L. and Kaufmann,G. (1995) Phage T4-coded Stp: double-edged effector of coupled DNA and tRNA-restriction systems. *J. Mol. Biol.*, **249**, 857–868.
14. Amitsur,M., Levitz,R. and Kaufman,G. (1987) Bacteriophage T4 anticodon nuclease, polynucleotide kinase, and RNA ligase reprocess the host lysine tRNA. *EMBO J.*, **6**, 2499–2503.
15. Zhu,H., Yin,S. and Shuman,S. (2004) Characterization of polynucleotide kinase/phosphatase enzymes from mycobacteriophages Omega and Cjw1 and vibriophage KVP40. *J. Biol. Chem.*, **279**, 26358–26369.
16. Jiang,Y., Mediler,R., Amitsur,M. and Kaufmann,G. (2001) Specific interaction between anticodon nuclease and the $tRNA^{Lys}$ wobble base. *J. Mol. Biol.*, **305**, 377–388.
17. Jiang,Y., Blanga,S., Amitsur,M., Meidler,R., Krivosheyev,E., Sundaram,M., Bajii,A., Davis,D.R. and Kaufmann,G. (2002) Structural features of $tRNA^{Lys}$ favored by anticodon nuclease as inferred from reactivities of anticodon stem and loop substrate analogs. *J. Biol. Chem.*, **277**, 3826–3841.
18. Amitsur,M., Banjamin,S., Rosner,R., Chapman-Shimshoni,D., Meidler,R., Blanga,S. and Kaufmann,G. (2003) Bacteriophage T4-encoded Stp can be replaced as activator of anticodon nuclease by a normal host cell metabolite. *Mol. Microbiol.*, **50**, 129–143.
19. Blanga-Kanfi,S., Amitsur,M., Azem,A. and Kaufmann,G. (2006) PrrC-anticodon nuclease: functional organization of a prototypical bacteria restriction RNase. *Nucleic Acids Res.*, **34**, 3209–3219.
20. Davidov,E. and Kaufmann,G. (2008) RloC: a wobble nucleotide-excising and zinc-responsive bacterial tRNase. *Mol. Microbiol.*, **69**, 1560–1574.
21. Meidler,R., Morad,I., Amitsur,M., Inokuchi,H. and Kaufmann,G. (1999) Detection of anticodon nuclease residues involved in $tRNA^{Lys}$ cleavage specificity. *J. Mol. Biol.*, **287**, 499–510.
22. Ogawa,T., Hidaka,M., Kohno,K. and Masaki,H. (2009) Colicin E5 ribonuclease domain cleaves *Saccharomyces cerevisiae* tRNAs leading to impairment of the cell growth. *J. Biochem.*, **145**, 461–466.
23. Shigematsu,M., Ogawa,T., Kido,A., Kitamoto,H.K., Hidaka,M. and Masaki,H. (2009) Cellular and transcriptional responses of yeast to the cleavage of cytosolic tRNAs by colicin D. *Yeast*, **26**, 663–673.
24. Keppetipola,N., Jain,R., Meineke,B., Diver,M. and Shuman,S. (2009) Structure-activity relationships in *Kluyveromyces lactis* γ-toxin, a eukaryal tRNA anticodon nuclease. *RNA*, **15**, 1036–1044.
25. Jablonowski,D., Zink,S., Mehlgarten,C., Daum,G. and Schaffrath,R. (2006) $tRNA^{Glu}$ wobble uridine methylation by Trm9 identifies Elongator's key role for zymocin-induced cell death in yeast. *Mol. Microbiol.*, **59**, 677–688.
26. Huang,B., Johansson,M.J.O. and Byström,A. (2005) An early step in wobble uridine tRNA modification requires the Elongator complex. *RNA*, **11**, 424–436.
27. Schiestl,R.H. and Gietz,R.D. (1989) High efficiency transformation of intact yeast cells using single stranded nucleic acids as a carrier. *Curr Genet.*, **16**, 339–346.
28. Smith,P.C., Karpowich,N., Millen,L., Moody,J.E., Rosen,J., Thomas,P.J. and Hunt,J.F. (2002) ATP binding to the motor domain of a ABC transporter drives formation of a nucleotide sandwich dimer. *Mol. Cell.*, **10**, 139–149.
29. Zaitseva,J., Jenewein,S., Jumpertz,T., Holland,I.B. and Schmitt,L. (2005) A structural analysis of asymmetry required tor catalytic activity of an ABC-ATPase domain dimer. *EMBO J.*, **25**, 3432–3443.
30. Zaitseva,J., Oswald,C., Jumpertz,T., Jenewein,S., Wiedenmann,A., Holland,I.B. and Schmitt,L. (2006) H662 is the lynchpin of ATP hydrolysis in the nucleotide-binding domain of the ABC transporter HlyB. *EMBO J.*, **24**, 1901–1910.
31. Dawson,R.J.P. and Locher,K.P. (2007) Structure of the multidrug ABC transporter Sav1866 from *Staphylococcus aureus* in complex with AMPPNP. *FEBS Lett.*, **581**, 935–938.
32. Atwell,S., Brouillette,C.G., Conners,K., Emtage,S., Gheyi,T., Guggino,W.B., Hendle,J., Hunt,J.F., Lewis,H.A., Lu,F. *et al.* (2010) Structures of a minimal human CFTR first nucleotide-binding domain as a monomer, head-to-tail homodimer, and pathogenic mutant. *Protein Eng. Des. Sel.*, **23**, 375–384.
33. Klaiman,D., Amitsur,M., Blanga-Kanfi,S., Chai,M., Davis,D.R. and Kaufmann,G. (2007) Parallel dimerization of a PrrC-anticodon nuclease region implicated in $tRNA^{Lys}$ recognition. *Nucleic Acids Res.*, **35**, 4704–4714.
34. Raines,R.T. (1998) Ribonuclease A. *Chem Rev.*, **98**, 1045–1065.
35. Steyaert,J. (1997) A decade of protein engineering on ribonuclease T1: atomic dissection of the enzyme-substrate interactions. *Eur. J. Biochem.*, **247**, 1–11.
36. Xue,S., Calvin,K. and Li,H. (2006) RNA recognition and cleavage by a splicing endonuclease. *Science*, **312**, 906–910.
37. Yajima,S., Inoue,S., Ogawa,T., Nonaka,T., Ohsawa,K. and Masaki,H. (2006) Structural basis for sequence-dependent recognition of colicin E5 tRNase by mimicking the mRNA-tRNA interaction. *Nucleic Acids Res.*, **34**, 6074–6082.
38. Zegers,I., Loris,R., Dehollander,G., Haikal,A.F., Poortmans,F., Steyaert,J. and Wyns,L. (1998) Hydrolysis of a slow cyclic thiophosphate substrate of RNase T1 analyzed by time-resolved crystallography. *Nature Struct. Biol.*, **5**, 280–283.
39. Buckle,A.M. and Fersht,A.R. (1994) Subsite binding in an RNase: structure of a barnase-tetranucleotide complex at 1.76-Å resolution. *Biochemistry*, **33**, 1644–1653.
40. Loverix,S. and Steyaert,J. (2001) Deciphering the mechanism of RNase T1. *Meth. Enzymol.*, **341**, 305–323.
41. Jablonowski,D. and Schaffrath,R. (2007) Zymocin, a composite chitinase and tRNase killer toxin from yeast. *Biochem. Soc. Trans.*, **35**, 1533–1537.
42. Sadler,A.J. and Williams,B.R. (2008) Interferon-inducible antiviral effectors. *Nat. Rev. Immunol.*, **8**, 559–568.
43. Lee,S.R. and Collins,K. (2005) Starvation-induced cleavage of the tRNA anticodon loop in *Tetrahymena thermophila*. *J. Biol. Chem.*, **280**, 42744–42749.
44. Li,Y., Zhou,H., Liao,J.Y., Ma,L.M., Chen,Y.Q. and Qu,L.H. (2008) Stress-induced tRNA-derived RNAs: a novel class of small RNAs in the primitive eukaryote *Giardia lamblia*. *Nucleic Acids Res.*, **36**, 6048–6055.
45. Thompson,D.M., Lu,C., Green,P.J. and Parker,R. (2008) tRNA cleavage is a conserved response to oxidative stress in eukaryotes. *RNA*, **14**, 2095–2103.

46. Thompson,D.M. and Parker,R. (2009) The RNase Rny1p cleaves tRNAs and promotes cell death during oxidative stress in *Saccharomyces cerevisiae*. *J. Cell Biol.*, **185**, 43–50.
47. Fu,H., Feng,J., Liu,Q., Sun,F., Tie,Y., Zhu,J., Xing,R., Sun,Z. and Zheng,X. (2009) Stress induces tRNA cleavage by angiogenin in mammalian cells. *FEBS Lett.*, **583**, 437–442.
48. Yamasaki,S., Ivanov,P., Gu,G. and Anderson,P. (2009) Angiogenin cleaves tRNA and promotes stress-induced translational repression. *J. Cell Biol.*, **185**, 35–42.
49. Emara,M.M., Ivanov,P., Hickman,T., Dawra,N., Tosdale,S., Kedersha,N., Hu,G.F. and Anderson,P. (2010) Angiogenin-induced tRNA-derived stress-induced RNA promote stress-induced stress granule assembly. *J. Biol. Chem.*, **285**, 20959–10968.
50. Garcia-Silva,M.R., Frugier,M., Tosar,J.P., Correa-Dominguez,A., Ronalte-Alves,L., Parodi-Talice,A., Robira,C., Robello,C., Goldenberg,S., Cayota,A. *et al.* (2010) A population of tRNA-derived small RNAs is actively produced in *Trypanosoma cruzi* and recruited to specific cytoplasmic granules. *Mol. Biochem. Parisitol.*, **171**, 64–73.
51. Thompson,D.M. and Parker,R. (2009) Stressing out over tRNA cleavage. *Cell*, **138**, 215–219.
52. Shterman,N., Elroy-Stein,O., Morad,I., Amitsur,M. and Kaufmann,G. (1995) Cleavage of the HIV replication primer $tRNA^{Lys3,3}$ in human cells expressing bacterial anticodon nuclease. *Nucleic Acids Res.*, **23**, 1744–1749.
53. Makarov,A.A., Kolchinsky,A. and Ilinskaya,O.N. (2008) Binase and other microbial RNases as potential anticancer agents. *BioEssays*, **30**, 781–790.
54. Ardelt,W., Ardelt,B. and Darzynkiewicz,Z. (2009) Ribonucleases as potential modalities in anticancer therapy. *Eur. J. Pharmacol.*, **625**, 181–189.
55. Saxena,S.K., Sirdeshmukh,R., Ardelt,W., Mikulski,S.M., Shogen,K. and Youle,R.J. (2002) Entry into cells and selective degradation of tRNAs by a cytotoxic member of the RNase A family. *J. Biol. Chem.*, **277**, 15142–15146.
56. Nandakumar,J., Schwer,B., Schaffrath,R. and Shuman,S. (2008) RNA repair: an antidote to cytotoxic eukaryal RNA damage. *Mol. Cell*, **31**, 278–286.

Supplemental Figure 1

Determinants of Eukaryal Cell Killing by the Bacterial Ribotoxin PrrC

Birthe Meineke, Beate Schwer, Raffael Schaffrath, and Stewart Shuman

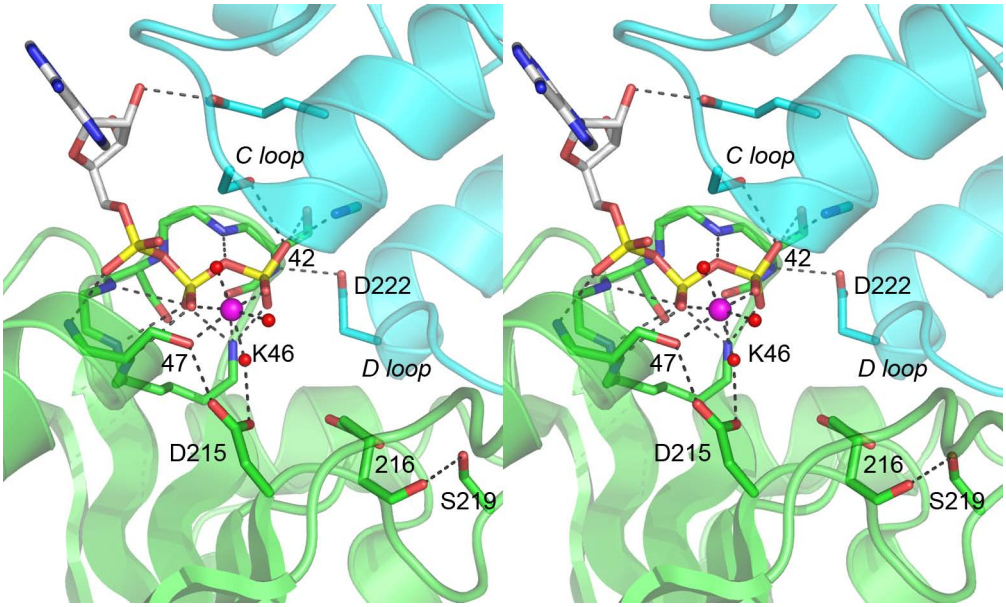

Figure S1. ***Composite active site of an ABC NTPase homodimer***. Stereo view of the NTPase active site in the crystal structure of the H662A mutant of ABC transporter HlyB in complex with ATP (stick model with grey carbons) and magnesium (magenta sphere) (pdb id: 1XEF). The phosphohydrolase active site of the homodimeric enzyme is a composite of structural elements derived from a *cis* protomer (colored green) that provides the Walker A and B motifs and a *trans* protomer (colored cyan) that provides the D loop and C loop motifs. Ionic and hydrogen bonding interactions are denoted by dashed lines. Waters are rendered as red spheres. The amino acid numbering refers to the equivalent positions in the NTPase domain of *Eco*PrrC.

Determinants of the cytotoxicity of PrrC anticodon nuclease and its amelioration by tRNA repair

BIRTHE MEINEKE and STEWART SHUMAN[1]
Molecular Biology Program, Sloan-Kettering Institute, New York, New York 10065, USA

ABSTRACT

Breakage of $tRNA^{Lys(UUU)}$ by the *Escherichia coli* anticodon nuclease PrrC (*Eco*PrrC) underlies a host antiviral response to phage T4 infection that is ultimately thwarted by a virus-encoded RNA repair system. PrrC homologs are prevalent in other bacteria, but their activities and substrates are not defined. We find that induced expression of *Eco*PrrC is toxic in *Saccharomyces cerevisiae* and *E. coli*, whereas the *Neisseria meningitidis* PrrC (*Nme*PrrC) is not. PrrCs consist of an N-terminal NTPase module and a C-terminal nuclease module. Domain swaps identified the *Eco*PrrC nuclease domain as decisive for toxicity when linked to either the *Eco* or *Nme* NTPase. Indeed, a single arginine-to-tryptophan change in the *Nme*PrrC nuclease domain (R316W) educed a gain-of-function and rendered *Nme*PrrC toxic to yeast, with genetic evidence for $tRNA^{Lys(UUU)}$ being the relevant target. The reciprocal Trp-to-Arg change in *Eco*PrrC (W335R) abolished its toxicity. Further mutagenesis of the *Eco*PrrC nuclease domain highlighted an ensemble of 15 essential residues and distinguished between hypomorphic alleles and potential nuclease-nulls. We report that the RNA repair phase of the bacterial virus-host dynamic is also portable to yeast, where coexpression of the T4 enzymes Pnkp and Rnl1 ameliorated the toxicity of *Nme*PrrC-R316W. Plant tRNA ligase AtRNL also countered *Nme*PrrC-R316W toxicity, in a manner that depended on AtRNL's 5′-kinase and ligase functions.

Keywords: RNA ligase; polynucleotide kinase-phosphatase; ribotoxin; tRNA breakage; wobble uridine modification

INTRODUCTION

The *Escherichia coli* tRNA anticodon nuclease PrrC (*Eco*PrrC) mediates an RNA-damaging innate immune response to bacteriophage T4 infection (Kaufmann 2000). The normally latent *Eco*PrrC nuclease is switched on by the virus-encoded Stp peptide synthesized early during T4 infection (Amitsur et al. 1989, 1992; Penner et al. 1995). The activated form of *Eco*PrrC incises the $tRNA^{Lys(UUU)}$ anticodon loop at a single site 5′ of the wobble uridine, leaving 2′,3′ cyclic phosphate and 5′-OH ends at the break. Ensuing depletion of functional $tRNA^{Lys}$ blocks the synthesis of T4 late proteins and prevents spread of the virus through the bacterial population. However, phage T4 thwarts the host cell's defense strategy by encoding a tRNA repair system, consisting of polynucleotide kinase-phosphatase (Pnkp) and RNA ligase 1 (Rnl1), that heals and seals the broken tRNA ends (Amitsur et al. 1987).

*Eco*PrrC consists of two domains: an N-terminal nucleoside triphosphate phosphohydrolase (NTPase) module (aa 1–264) related to the ABC transporter NTPase family and a distinctive C-terminal ribonuclease module (aa 265–396) that has no apparent similarity to any known nuclease or tRNA binding protein (Kaufmann 2000; Blanga-Kanfi et al. 2006). PrrC homologs are present in the proteomes of many other bacteria, though their biological activities and RNA targets are uncharted. We reported recently that the ribotoxicity of bacterial PrrC is portable to eukarya. Specifically, we found that induced expression of *Eco*PrrC in budding yeast cells is fungicidal, signifying that *Eco*PrrC is toxic in a eukaryon in the absence of any other bacterial or viral proteins (Meineke et al. 2011). Testing for rescue of toxicity by increased tRNA gene dosage implicated $tRNA^{Lys(UUU)}$ as an *Eco*PrrC target in yeast. An extensive survey of the effects of alanine and conservative mutations on *Eco*PrrC toxicity in yeast identified 22 essential residues in the NTPase domain and 11 in the nuclease domain and delineated structure-function relationships at each essential position (Meineke et al. 2011). Overexpressing PrrCs with inactivating mutations in the NTPase active site ameliorated the toxicity of wild-type *Eco*PrrC; these dominant

[1]**Corresponding author.**
E-mail s-shuman@ski.mskcc.org.
Article published online ahead of print. Article and publication date are at http://www.rnajournal.org/cgi/doi/10.1261/rna.030171.111.

negative effects were not observed with PrrCs containing inactivating mutations in the nuclease domain. Our findings, building on the elegant studies of *Eco*PrrC by Gabi Kaufmann and colleagues (Meidler et al. 1999; Jiang et al. 2001, 2002; Amitsur et al. 2003; Blanga-Kanfi et al. 2006), support a model in which *Eco*PrrC toxicity is contingent on head-to-tail dimerization of the ABC-like NTPase domains and the consequent formation of two composite NTP phosphohydrolase active sites, which in turn activates the nuclease domains in *cis*, only one of which needs be functional.

Remarkably, not all bacterial PrrCs are created equal with respect to their activity in yeast, e.g., *Streptococcus mutans* PrrC (*Smu*PrrC) is toxic in yeast, whereas *Neisseria meningitidis* (*Nme*PrrC) is benign (Meineke et al. 2011). The failure of *Nme*PrrC to arrest yeast growth was surprising to us, insofar as the nontoxic *Nme*PrrC protein has a significantly higher degree of amino acid identity (57%) with the *Eco*PrrC polypeptide than does the toxic *Smu*PrrC (42%). It is conceivable that (1) *Nme*PrrC is nontoxic in yeast because it lacks RNase activity; (2) *Nme*PrrC is a bonafide ribotoxin, but its target is not present in budding yeast (or is present but not essential for yeast growth); or (3) *Nme*PrrC requires additional proteins (or activating metabolites) from the cognate bacterium to manifest its RNase functions.

In the present study, we explored this issue by studying a series of chimeric PrrCs. Domain swaps established that the *Eco*PrrC nuclease module is decisive for yeast toxicity when linked to either the *Eco* or *Nme* NTPase domain. Inspection of the primary structure differences between the nuclease domains of toxic (*Eco* and *Smu*) and nontoxic (*Nme*) PrrCs highlighted potential candidate toxicity determinants that we queried by mutating individual side chains in *Nme*PrrC to their counterparts in *Eco*PrrC. We thereby identified a single amino acid change in *Nme*PrrC (arginine to tryptophan) that elicited a gain-of-function and rendered it toxic to yeast. The reciprocal Trp to Arg change at the corresponding residue in *Eco*PrrC ablated its toxicity in yeast. From the results of tRNA rescue experiments and the effects of genetic manipulation of the wobble uridine modification on the activity of the ''enabled'' *Nme*PrrC-R316W mutant, we surmised that $tRNA^{Lys(UUU)}$ is the relevant target for the *Nme*PrrC-R316W ribotoxin.

We extended these findings by showing that the RNA repair phase of the bacterial tRNA restriction-repair host-virus dynamic is also portable to yeast, where coexpression of the T4 enzymes Pnkp and Rnl1 ameliorated the toxicity of *Nme*PrrC-R316W. Expression of plant tRNA ligase in yeast also countered *Nme*PrrC-R316W toxicity. Our findings, in conjunction with earlier studies (Nandakumar et al. 2008), offer proof of principle for the ability of RNA repair to modulate the effects of programmed tRNA damage in eukarya.

RESULTS

Domain swaps between *Eco*PrrC and *Nme*PrrC implicate the nuclease domain as the source of species-variation in PrrC toxicity

The *E. coli* and *N. meningitidis prrC* genes were introduced into yeast on *CEN* plasmids under the control of a glucose-repressed/galactose-inducible *GAL1* promoter. *Eco*PrrC induction inhibited yeast growth on agar medium containing galactose, whereas *Nme*PrrC induction had no effect on cell growth (Fig. 1). An inference from these results is that *Eco*PrrC can incise essential target RNAs in yeast, but *Nme*PrrC cannot.

Turning to the question of why *Nme*PrrC is nontoxic, we performed reciprocal domain swap experiments, in which the N-terminal NTPase domain of *Eco*PrrC (aa 1–264) was fused to the C-terminal nuclease domain of *Nme*PrrC (aa 246–380) and the *Nme*PrrC NTPase domain (aa 1–245) was joined to the *Eco*PrrC nuclease module (aa 265–396) (Fig. 1). The N-*Nme*/*Eco*-C chimera was clearly toxic in yeast, while the N-*Eco*/*Nme*-C hybrid was not (Fig. 1). However, the very faint growth of the *Nme*/*Eco*PrrC-expressing yeast cells on galactose agar seen with the more concentrated cell spottings (Fig. 1) suggested that the *Nme*/*Eco* hybrid is a genetic hypomorph vis à vis *Eco*PrrC (see below). We conclude that the *Eco*PrrC nuclease module is decisive for yeast toxicity when linked to either the *Eco* or *Nme* NTPase domain.

To see if the differential toxicity of bacterial PrrCs also obtains in a bacterium, we tested the effects of induced expression of the *Eco, Smu,* and *Nme* PrrCs and the *Eco*/*Nme* and *Nme*/*Eco* chimeras, on the growth of *E. coli*. The respective *prrC* genes were introduced into *E. coli* Top10 cells on pBAD plasmids under the control an arabinose-inducible promoter. Serial dilutions of *E. coli* pBAD-*prrC*

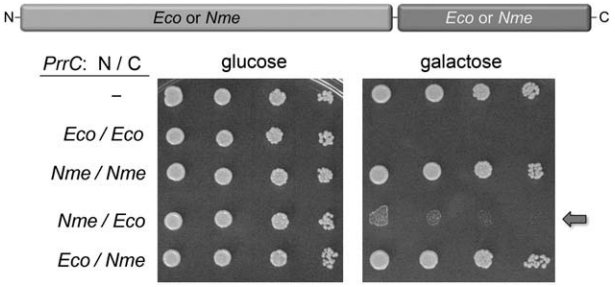

FIGURE 1. Domain swaps between toxic *Eco*PrrC and nontoxic *Nme*PrrC. Bacterial PrrC proteins consist of an N-terminal NTPase domain fused to a C-terminal nuclease domain, as shown. *Eco*PrrC and *Nme*PrrC, and domain-swapped PrrCs (N-*Eco*/*Nme*-C and N-*Nme*/*Eco*-C), were tested for their effects on the growth of *S. cerevisiae*. Serial fivefold dilutions of yeast cells bearing a *CEN* plasmid encoding the indicated galactose-regulated *prrC* gene or an empty *CEN* vector (–) were spotted on –Leu agar plates containing glucose or galactose as specified.

cultures grown in LB medium were plated on LB agar (*prrC* expression repressed) or LB agar with 0.2% arabinose (*prrC* expression induced). The results showed that *Eco*PrrC and *Smu*PrrC were toxic to *E. coli*, whereas *Nme*PrrC was not (Fig. 2). The *Nme*/*Eco* hybrid inhibited growth of *E. coli* on arabinose agar, albeit not as profoundly as wild-type *Eco*PrrC, as indicated by the tiny colony size of *Nme*/*Eco*PrrC-expressing bacteria (Fig. 2). In contrast, arabinose induction of the *Eco*/*Nme*PrrC hybrid had no effect on *E. coli* growth (Fig. 2). We surmise from the results shown in Figures 1 and 2 that it is not simply the case that the eukaryal milieu masks an intrinsic ribotoxin activity of *Nme*PrrC and the *Eco*/*Nme* hybrid. Rather, it seems that members of the PrrC family differ with respect to their biological activity, which could reflect distinctive RNA target specificities and/or reliance on unique species-specific coactivators. It is pertinent to note that, whereas *Eco*PrrC targets $tRNA^{Lys(UUU)}$ in *E. coli* and yeast, the imputed ribotoxicity and possible RNA targets of *Nme*PrrC are tabula rasa, even in *Neisseria*.

We next examined the effects of transient expression of the toxic *Eco* and *Smu* PrrCs on *E. coli* survival. The *Eco*PrrC and *Smu*PrrC expression plasmids had no effect on the rate of bacterial growth in liquid medium lacking arabinose, i.e., compared to the growth of control bacteria carrying the empty vector (Supplemental Fig. S1A). In contrast, the growth of bacteria carrying the *Eco* and *Smu* PrrC plasmids was arrested by 3 to 4 h after transfer to arabinose-containing medium, an effect not seen with bacteria carrying the empty vector (Supplemental Fig. S1A). By analyzing bacterial survival after transient arabinose induction in liquid medium and return to control medium, we found that *Eco*PrrC expression was bacteriostatic, i.e., the number of viable bacteria in the culture was stable for the 5-h interval of arabinose exposure. (Supplemental Fig. S1B). In contrast, *Smu*PrrC was bactericidal, eliciting a 240-fold decrement in the viable cell count by 3 h of SmuPrrC induction (Supplemental Fig. S1B). We noted progressive recovery of viability at 4 and 5 h post-induction of *Smu*PrrC, suggesting the outgrowth of survivors. The instructive point here is that the cytostatic effect of *Eco*PrrC expression in *E. coli* contrasts with its cytocidal properties in budding yeast (Meineke et al. 2011), as opposed to *Smu*PrrC expression, which is cytocidal in bacteria and yeast.

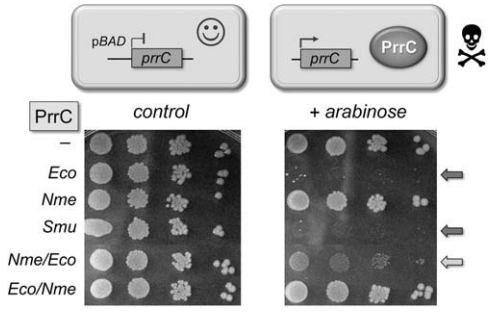

FIGURE 2. The nuclease domain is an exchangeable determinant of PrrC toxicity in *E. coli*. Serial dilutions of *E. coli* cells bearing a pBAD plasmid encoding the indicated arabinose-regulated *prrC* gene or an empty vector were spotted on LB-ampicillin agar plates with or without arabinose. When grown on control medium lacking arabinose, *prrC* expression is switched off, and the bacteria grow normally. When grown on medium containing 0.2% arabinose, the *prrC* expression is turned on, and if the PrrC ribotoxin is active, bacterial growth is arrested (absence of colonies) or slowed (presence of tiny colonies).

Species-specific toxicity determinants in the PrrC nuclease domain

To vet the hypothesis that the PrrC nuclease domain harbors key determinants of RNA target specificity, we attempted to coax the nontoxic *Nme*PrrC to become toxic in yeast. Our search for gain-of-function mutations was guided by alignment of the nuclease domains of the *Eco*, *Smu*, and *Nme* PrrCs, which highlighted seven "deviant" amino acids in nontoxic *Nme*PrrC that we changed to the "consensus" equivalents present in the toxic *Eco*PrrC and *Smu*PrrC proteins, individually or as a pairwise change in vicinal residues (Fig. 3A). We found that five of the *Nme*PrrC mutants (N309S, E322D, Q354K, D366N, and E288A-N289D) remained nontoxic in yeast. In contrast, the *Nme*PrrC R316W mutant was enabled by a single amino acid substitution to arrest the growth of yeast cells on medium containing galactose (Fig. 3B). Thus, a gain-of-function was achieved. In a similar vein, we were able to convert the nontoxic *Eco*/*Nme* PrrC chimera (Fig. 1) into an active ribotoxin in yeast by the equivalent Arg-to-Trp mutation in its *Nme*-derived nuclease domain (data not shown).

If the identity of this amino acid as tryptophan is decisive as a toxicity determinant in PrrC, then we might expect mutation of Trp335 in *Eco*PrrC to diminish or eliminate its ribotoxicity. Indeed, changing Trp335 to arginine (to mimic the side chain in *Nme*PrrC) abolished the toxicity of *Eco*PrrC in yeast (Fig. 3C). Similar loss-of-function effects were elicited by changing Trp335 to alanine (which truncates the side chain at the β-carbon) or by conservative substitutions with other γ-branched aromatic amino acids (tyrosine, phenylalanine, or histidine) (Fig. 3C). Thus, tryptophan is strictly essential at this position for the ribotoxicity of *Eco*PrrC in yeast.

We compared the severity of the yeast growth arrest triggered by the two gain-of-function mutants—*Nme*R316W and *Eco/Nme*RW—to that of the active *Nme/Eco* chimeric PrrC. By analyzing yeast survival after transient galactose induction and return to glucose, we found that *Eco/NmeRW* expression was fungicidal; the number of viable cells in the yeast culture decreased by a factor of 20 after 15 h of induction (Supplemental Fig. S2). In contrast, expression of the *Nme*R316W and *Nme/Eco* PrrC proteins was effectively

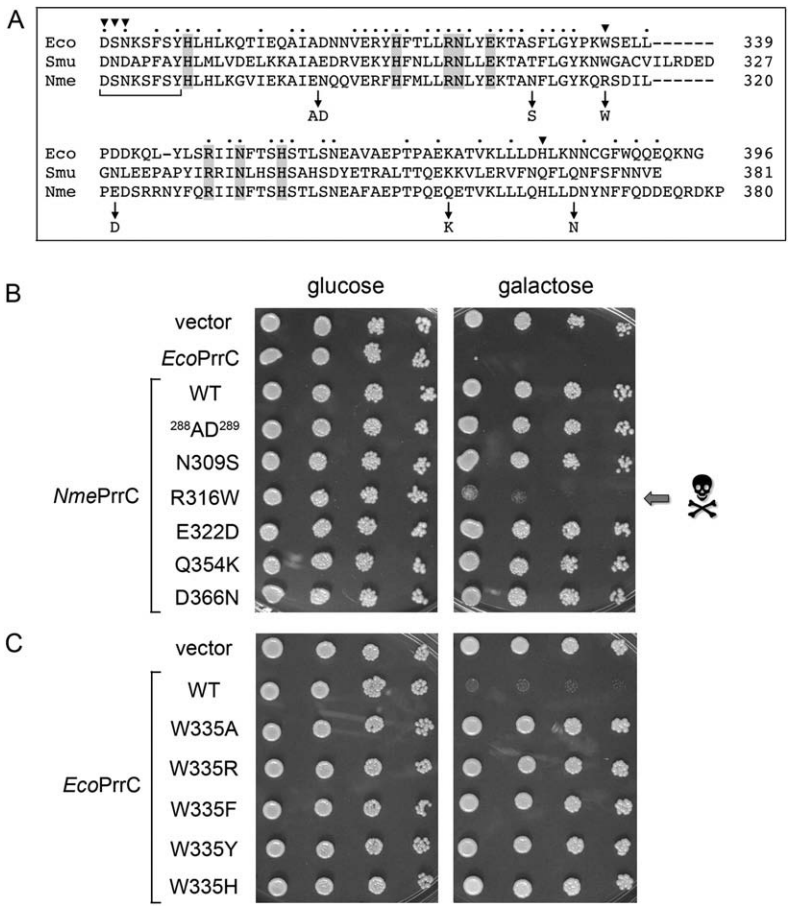

FIGURE 3. A gain-of-function mutation renders *Nme*PrrC toxic to yeast. (*A*) The amino acid sequence of the nuclease domain of *Eco*PrrC is aligned to the homologous segments of *Smu*PrrC and *Nme*PrrC. Positions of side-chain identity/similarity in all three proteins are indicated by • *above* the alignment. The eight conserved residues defined previously as essential for yeast toxicity are shaded gray. Positions of side chain variation between the nontoxic *Nme*PrrC and the toxic *Eco* and *Smu* PrrCs are indicated by arrows *below* the alignment, which specify the *Nme*PrrC mutations tested for gain-of-toxicity in yeast. The LARP motif is demarcated by the bracket *below* the sequences. *Eco*PrrC residues subjected to mutational analysis in the present study are indicated by ▼. (*B*) Serial fivefold dilutions of yeast cells bearing a *CEN* plasmid encoding the indicated galactose-regulated *prrC* gene or an empty *CEN* vector were spotted on –Leu agar plates containing glucose or galactose as specified. (*C*) Toxicity tests for wild-type *Eco*PrrC and the indicated W335 mutants are shown.

cytostatic, i.e., viable cell counts increased less than threefold over 15 h in galactose-containing medium (Supplemental Fig. S2).

Overexpression of yeast tRNA$^{Lys(UUU)}$ blunts the toxicity of *Nme*R316W

If an intracellular ribotoxin exerts its effect by breaking a specific cellular RNA target, then one might expect to reverse the toxicity by overexpressing the RNA target (Jablonowski et al. 2006). We found that a multicopy 2μ plasmid carrying the yeast gene for tRNA$^{Lys(UUU)}$ protected yeast cells from the toxic effects of the gain-of-function mutant *Nme*R316W (Fig. 4, top panel). In contrast, 2μ plasmids bearing genes encoding either the isoacceptor tRNA$^{Lys(CUU)}$ or various other yeast tRNAs (tRNA^{Glu}, tRNA^{Gln}, tRNA^{Arg}, tRNA^{Tyr}, tRNA^{Leu}, or tRNA^{Gly}) had no effect on *Nme*R316W toxicity (data not shown). This instructive result indicated that tRNA$^{Lys(UUU)}$ is a target of *Nme*R316W in yeast. The same tRNA rescue profile was seen previously for two toxic hypomorphs of *Eco*PrrC (Meineke et al. 2011). We surmise that a latent tRNA$^{Lys(UUU)}$ anticodon nuclease activity of *Nme*PrrC is revived by the R316W mutation.

Influence of wobble uridine modifications on the toxicity of *Nme*R316W

*Eco*PrrC incises bacterial tRNA$^{Lys(UUU)}$ at a single phosphodiester 5′ of the modified wobble base mnm^{5}s^{2}U (5-methylaminomethyl-2-thiouridine) (Jiang et al. 2001). The mnm^{5}U wobble modification does not exist in eukaryal tRNAs, which have mcm^{5}s^{2}U (5-methoxycarbonylmethyl-2-thiouridine) instead (Fig. 4). Some tRNA anticodon nucleases rely on the modified wobble base as a target specificity determinant. For example, *K. lactis* γ-toxin requires the mcm^{5}U modification in its tRNA^{Glu} target, such that yeast *elp3*Δ and *trm9*Δ mutants, which either fail to modify the C5 atom or fail to add the terminal methyl group (Fig. 4), are resistant to γ-toxin's effects (Lu et al. 2005, 2008; Jablonowski and Schaffrath 2007). Here we found that *Nme*R316W was toxic to *elp3*Δ cells and that this toxicity was reversed by overexpressing tRNA$^{Lys(UUU)}$ (Fig. 4, middle panel), which signifies that *Nme*R316W can target tRNA with a wobble uridine with no modifications at the C5 atom. In contrast, *Nme*R316W did not prevent growth of the *trm9*Δ cells on galactose; rather it had only a slight effect on growth, as gauged by colony size compared to the vector control, and this slight effect was reversed by 2μ tRNA$^{Lys(UUU)}$ (Fig. 4, bottom panel). We noted similar effects of the yeast *elp3*Δ and *trm9*Δ mutations on the ribotoxin activities of two *Eco*PrrC hypomorphs: S219T and C386A (Meineke et al. 2011). Our findings suggest that *Nme*R316W has gained both the activity and target specificity of *Eco*PrrC in yeast, albeit at the level of a hypomorphic *Eco*PrrC variant.

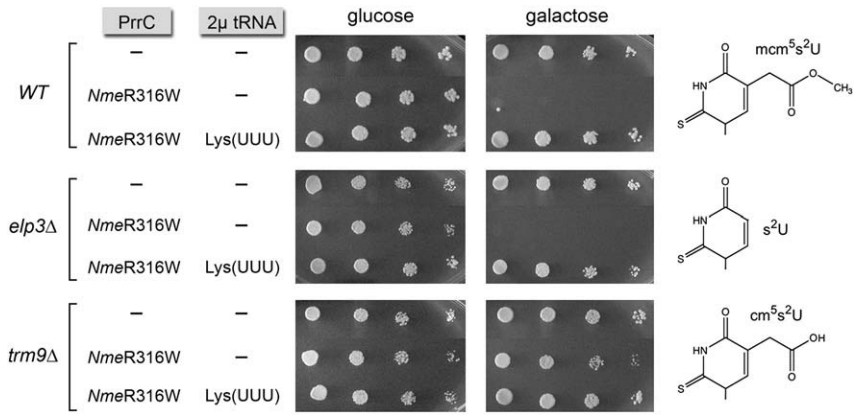

FIGURE 4. Rescue of *Nme*PrrC-R316W toxicity by 2μ $tRNA^{Lys(UUU)}$ and effect of wobble U modification on toxicity. Serial fivefold dilutions of wild-type (WT), *elp3*Δ, and *trm9*Δ yeast cells bearing a *CEN* plasmid encoding galactose-regulated *Nme*PrrC-R316W or the empty *CEN* vector (–) plus a 2μ plasmid carrying the $tRNA^{Lys(UUU)}$ gene or an empty 2μ vector (–) were spotted on –Leu–Ura agar plates containing glucose or galactose. The structures of the wobble uridine modifications found in $tRNA^{Lys(UUU)}$ of wild-type yeast (mcm^5s^2U), and yeast mutants *elp3*Δ (s^2U; 2-thiouridine) and *trm9*Δ (cm^5s^2U; 5-carboxymethyl-2-thiouridine), are shown at *right*.

Heterologous RNA repair enzymes ameliorate the toxicity of *Nme*R316W

Yeast cells are susceptible to tRNA ribotoxins because the endogenous yeast tRNA ligase is unable to rectify the break in the anticodon loop of the tRNAs targeted by the ribotoxin. However, expression of plant or phage T4 tRNA repair enzymes protect yeast from growth arrest by *K. lactis* γ-toxin because they are able to reverse the damage inflicted in the anticodon loop of $tRNA^{Glu(UUC)}$ (Nandakumar et al. 2008). Given that the native function of the T4 RNA repair system is to neutralize the PrrC-driven antiviral response (Amitsur et al. 1987), it was of interest to us to see whether importing phage and plant tRNA repair enzymes into yeast might protect a eukaryon against PrrC's toxicity. Our initial experiments showed that neither plant tRNA ligase (AtRNL) nor T4 Rnl1+Pnkp were able to overcome galactose-induced *Eco*PrrC growth arrest (data not shown). We considered two potential explanations for the negative outcome: (1) that the heterologous repair enzymes were inherently unable to fix the PrrC-induced damage to yeast $tRNA^{Lys(UUU)}$; or (2) that the level of tRNA incision activity of *Eco*PrrC after galactose induction was too vigorous to be offset by the activities of the heterologous repair systems, i.e., the RNA repair system loses an uphill battle against relentless tRNA cleavage. In the latter case, we might expect that dialing back on the strength of the PrrC activity, by expressing a hypomorphic version of the ribotoxin, might tip the dynamic in favor of RNA repair. Indeed, this is what we observed when the *Nme*R316W variant was induced in yeast cells expressing heterologous repair enzymes (Fig. 5).

In this experiment, we introduced *CEN* plasmids expressing Rnl1 and Pnkp into a yeast strain bearing the galactose-regulated *Nme*R316W expression plasmid and then tested growth under toxin-off and toxin-on conditions. For comparison, we also tested the effects of overexpressing the yeast tRNA ligase Trl1 (by introducing a 2μ plasmid bearing *TRL1* under the control of a constitutive yeast *TPI1* promoter) and the plant tRNA ligase AtRNL (delivered on a 2μ plasmid and driven by the *TPI1* promoter). Whereas control cells and 2μ *TRL1* cells did not thrive on medium containing galactose, the phage tRNA repair system and plant AtRNL allowed cell growth (Fig. 5). It is apparent from the colony size that the phage tRNA repair system is more salutary than AtRNL and that neither repair system restored growth on galactose to the level of control cells that lack the *Nme*R316W expression cassette (Fig. 5). This result underscores the theme (Nandakumar et al. 2008) that a repair-based cure of ribotoxicity may be incomplete in the face of constitutive RNA damage.

The observation that plant tRNA ligase rescues cells from *Nme*PrrC-R316W growth arrest while yeast tRNA ligase does not suggests that there are intrinsic differences in the ability of the plant and yeast systems to repair the broken $tRNA^{Lys(UUU)}$ anticodon loop. To probe the roles of the

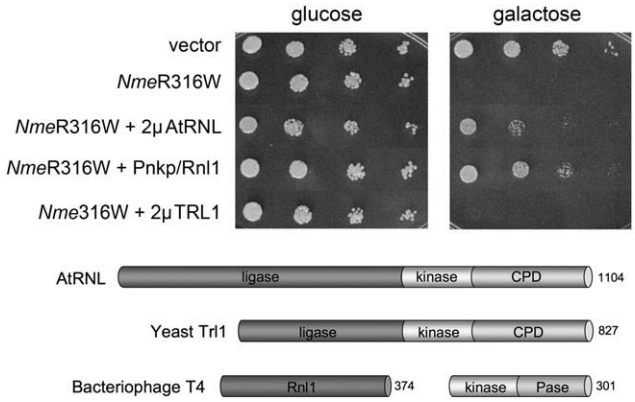

FIGURE 5. Rescue of *Nme*PrrC-R316W toxicity by tRNA repair enzymes. (*Top* panel) Growth of yeast cells bearing a *CEN* plasmid encoding galactose-regulated *Nme*PrrC-R316W or the empty *CEN* vector (–) and either a 2μ *TPI1-AtRNL* plasmid, a 2μ *TPI1-TRL1* plasmid, or a *CEN* plasmid expressing T4 Pnkp and Rnl1 as specified was assessed by spotting serial fivefold dilutions to minimal synthetic agar medium containing glucose or galactose. (*Bottom* panel) The tRNA ligases of plant (AtRNL) and yeast (Trl1) are composed of three discrete catalytic domains: an N-terminal ligase module; a central 5′-OH polynucleotide kinase module; and a C-terminal RNA 2′,3′ cyclic phosphodiesterase (CPD) module. The phage T4 tRNA repair system consists of separate sealing (Rnl1) and healing (Pnkp) enzymes.

three catalytic activities of AtRNL, we tested a collection of mutant AtRNL alleles bearing lethal alanine mutations in the active sites that specifically ablate the ligase (K152A or E326A), kinase (S701A or D726A), or CPD (T1001A or H1060A) functions (Fig. 6; Wang et al. 2006). The wild-type, kinase-dead, ligase-dead, and CPD-dead AtRNL proteins were expressed from 2μ plasmids in yeast cells bearing the *Nme*R316W plasmid and tested in parallel for growth on glucose and galactose media (Fig. 6). None of the AtRNL-Ala mutations affected growth on glucose because tRNA splicing activity is provided by the endogenous Trl1 enzyme. However, these mutations had disparate effects on yeast growth on galactose, depending on which catalytic activity was affected. The CPD activity of AtRNL was not required to confer *Nme*R316W resistance, insofar as the CPD-dead alleles could rescue growth on galactose, albeit not as effectively as wild-type AtRNL (Fig. 6). We surmise that the endogenous level of yeast Trl1 CPD suffices to heal the 2′,3′ cyclic phosphate end of broken $tRNA^{Lys}$. In contrast, the two ligase-dead and the two kinase-dead AtRNL mutants failed to protect against *Nme*R316W (Fig. 6). Thus, the ligase and 5′ kinase activities of AtRNL are essential for *Nme*R316W resistance.

These enzymatic requirements for AtRNL repair of PrrC damage in vivo are different from what was observed for AtRNL rescue of $tRNA^{Glu}$ damage by *K. lactis* γ-toxin. Protection against γ-toxin required the ligase activity but was unaffected by the kinase-dead mutations (Nandakumar et al. 2008). We envision that these differences might be attributable to the fact that PrrC and γ-toxin incise the anticodon loop on opposite sides of the mcm^5s^2U wobble nucleoside in their respective tRNA targets. γ-toxin cleaves on the 3′ side of the wobble nucleoside to form a mcm^5s^2U–2′,3′-cyclic phosphate end that, when hydrolyzed by the CPD activity of Trl1 or AtRNL, will yield an mcm^5s^2U–3′OH, 2′-PO_4 end. It was proposed that (1) the Trl1 ligase domain is hindered from sealing γ-toxin-incised $tRNA^{Glu}$ by the presence of the bulky mcm^5s^2U base at the 3′-OH, 2′-PO_4 end; (2) the unmodified 5′-OH nucleoside at the γ-toxin incision site in $tRNA^{Glu}$ can be phosphorylated by either the Trl1 or AtRNL kinase domains, accounting for the ability of kinase-dead AtRNL to rescue growth on galactose; and (3) the capacity of AtRNL to rectify γ-toxin damage is a unique property of its ligase domain, which is apparently adept at sealing the broken tRNA with a bulky mcm^5s^2U base at the 3′-OH, 2′-PO_4 end (Nandakumar et al. 2008). Extending that line of reasoning to PrrC, which incises on the 5′ side of the wobble nucleoside to yield an unmodified 2′,3′ cyclic phosphate terminus and a 5′-OH mcm^5s^2U terminus, leads to the following speculations: (1) The Trl1 kinase module is ineffective at phosphorylating the bulky 5′-OH mcm^5s^2U nucleoside, whereas the AtRNL kinase is competent to do so; and (2) the Trl1 ligase domain is ineffective at sealing the healed 5′-PO_4 end with a bulky mcm^5s^2U nucleoside, whereas the AtRNL ligase is competent to do so. Nothing is known as yet concerning the structural features of the yeast and plant ligases that dictate their differential healing and sealing of base-modified RNA breaks.

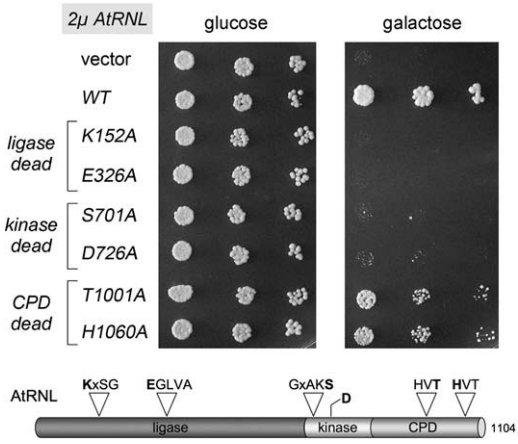

FIGURE 6. RNA sealing and 5′ healing activities of AtRNL dictate resistance to PrrC. (*Top* panel) Growth of yeast cells bearing a *CEN* plasmid encoding galactose-regulated *Nme*PrrC-R316W or the empty *CEN* vector (–) and either an empty 2μ *HIS3* vector or a 2μ *HIS3 TPI1-AtRNL* plasmid encoding wild-type plant tRNA ligase or the indicated ligase-dead, kinase-dead, or CPD-dead mutant was assessed by spotting serial fivefold dilutions to minimal synthetic agar medium containing glucose or galactose. The galactose plate was photographed after 4 d of incubation at 30°C. (*Bottom* panel) AtRNL mutants. The positions of the covalent adenylylation motif (KxxG) and the metal-binding motif (EGxxx) at the ligase active site, the P-loop motif GxxK(S/T) at the kinase active site, and the two HxT motifs that comprise the CPD active site are depicted *above* the AtRNL polypeptide. The sites of enzyme-inactivating alanine mutations in the AtRNL active sites are highlighted in bold.

Further mutational analysis of the *Eco*PrrC nuclease domain

Our previous study of the effects of alanine and conservative mutations on *Eco*PrrC toxicity in yeast identified 11 essential residues in the C-terminal nuclease domain. Here, we identified Trp335 as an additional essential constituent of *Eco*PrrC (Fig. 3C). To extend the structure-function analysis of the nuclease domain, we initiated a new round of alanine and conservative mutagenesis, focusing mainly on a putative lysine anticodon recognizing peptide (LARP) motif, ^{284}KYGDSNKSFSY^{294}, that had been the subject of studies by the Kaufmann lab (Klaiman et al. 2007). The LARP motif (denoted by bracket in Fig. 3A), mutations of which affect the tRNA substrate preference of *Eco*PrrC (Jiang et al. 2001, 2002), is found only in a subset of PrrC proteins (Klaiman et al. 2007; Davidov and Kaufmann 2008). It is speculated that LARP is a determinant of the target specificity of those PrrC proteins that contain the motif. However, LARP may not be the decisive factor with respect to yeast toxicity of bacterial PrrCs, insofar as the *Eco*PrrC LARP is not conserved (only 3/11 identical residues) in *Smu*PrrC, which is toxic in yeast. We reported previously

that two alanine mutations in the *Eco*PrrC LARP motif (at Ser291 and Ser293, which are conserved in *Nme*PrrC) (Fig. 3A) had no effect on cytotoxicity in yeast (Meineke et al. 2011).

Here we introduced alanine in lieu of *Eco*PrrC LARP motif residues Asp287, Ser288, and Asn289, and also at the distal residue His381 (Fig. 3A, targeted positions denoted by ▼). The mutant alleles were inserted into *CEN* plasmids under *GAL*-control. Tests of yeast growth on glucose and galactose showed that the D287A, S288A, and H381A mutants were nontoxic, whereas N289A retained toxicity (Fig. 7; and data not shown). Substituting His381 conservatively with glutamine and asparagine also rendered *Eco*PrrC nontoxic in yeast (data not shown). Thus, His381 joins four other histidines in the nuclease domain (His295, His297, His315, and His356) as strictly essential for *Eco*PrrC toxicity in yeast (Meineke et al. 2011). Because His381 is replaced by glutamine in the toxic *Smu*PrrC protein (Fig. 3A), we suspect that His381 is not acting as general acid-base catalyst of RNA transesterification. Replacing the essential LARP motif residue Ser288 with asparagine restored toxicity to *Eco*PrrC (data not shown); note that asparagine is naturally present at the equivalent position of *Smu*PrrC. These findings suggest that the hydrogen bonding capacity of Ser288 is pertinent for PrrC activity in yeast.

We were especially interested in structure-activity relations at the essential Asp287, in light of prior suggestions

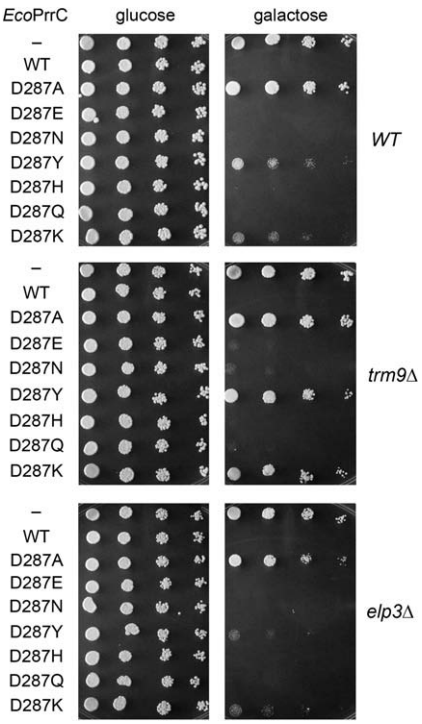

FIGURE 7. Mutational analysis of *Eco*PrrC Asp287. Serial fivefold dilutions of wild-type (WT), *elp3*Δ, and *trm9*Δ yeast cells bearing a *CEN* plasmid encoding galactose-regulated *Eco*PrrCs as specified were spotted on –Leu agar plates containing glucose or galactose.

that this residue is a target specificity determinant (Meidler et al. 1999; Jiang et al. 2001, 2002). Thus, we replaced Asp287 conservatively with glutamate and asparagine and nonconservatively with tyrosine, histidine, glutamine, and lysine (Fig. 7). The D287E, D287N, D287H, and D287Q mutants displayed full galactose-dependent toxicity in yeast (Fig. 7, top panel), suggesting that hydrogen-bonding might be the key property of this side chain. Certainly, the results exclude a strict requirement for negative charge at this position. On the other hand, the D287Y and D287K mutants were partially inhibitory to yeast growth, insofar as the yeast cells expressing these variants grew on galactose agar but formed tiny colonies compared to D287A-expressing cells or the vector control (Fig. 7, top panel). We surmise that charge inversion (in D287K) or increased side chain bulk (in D287Y) at this position exert negative effects on *Eco*PrrC function in yeast.

The Kaufmann lab had shown that missense mutations at Asp287 alter the tRNA cleavage preferences of PrrC in vivo when expressed in *E. coli* and/or in vitro, e.g., such that particular Asp287 mutants are either more or less fastidious regarding the impact of wobble base modifications (Jiang et al. 2001, 2002). In this light, we compared the effects of induced expression of Asp287A mutants in yeast cells that have the wild-type mcm^5s^2U wobble modification versus *elp3*Δ and *trm9*Δ cells that lack all or part of the mcm^5 moiety (Fig. 7). The salient findings were as follows: (1) PrrC mutants D287Y and D897K were less toxic in *trm9*Δ cells than in wild-type or *elp3*Δ cells; and (2) other nonalanine Asp287 mutants retained toxicity in all three strain backgrounds (Fig. 7). The findings fortify our inferences from the analysis of *Nme*R316W toxicity (Fig. 4) that hypomorphic PrrC variants have diminished ability to inflict damage at an incompletely modified cm^5s^2U wobble nucleoside.

Restoration of the toxicity of a subset of PrrC nuclease domain mutants by increased gene dosage

We have now identified a total of 15 residues in the nuclease domain of *Eco*PrrC that are essential for toxicity in yeast. This module has no discernible primary structure similarity to any known ribonucleases or tRNA-binding proteins, which makes it difficult to guess which essential residues might be directly involved in catalysis versus substrate recognition, PrrC folding/stability, etc. As discussed above, the mutational analysis readily identified PrrC hypomorphs that retained toxicity in yeast when expressed from a *CEN* plasmid but were either amenable to alleviation of toxicity by co-expression of RNA repair enzymes (unlike wild-type PrrC) or were affected in their toxicity by the status of the wobble uridine modification (also unlike wild-type PrrC). Other PrrC hypomorphs (e.g., D287K) were simply less inhibitory to yeast growth than wild-type PrrC when expressed from a *CEN* plasmid.

Taking this one step further, we reasoned that (1) the collection of 15 PrrC-Ala mutants in the nuclease domain that were deemed nontoxic when expressed from *CEN* plasmids might include additional, more severely affected hypomorphs; (2) some of these putative hypomorphs might regain their toxicity when expressed from a multicopy 2μ plasmid; and (3) recovery of toxicity by overexpression of a particular mutant would weigh against the mutated residue being strictly essential for catalysis.

To evaluate this scenario, we transferred the 15 $_{GAL}$-*prrC-Ala* expression cassettes to 2μ plasmids, introduced them into *Saccharomyces cerevisiae*, and tested the transformants for galactose-dependent toxicity (Table 1). Two of the originally nontoxic mutants regained full toxicity at high gene dosage (scored as ++ in Table 1): These were H297A and K299A. Three other mutants—S288A in the LARP motif, N352A, and His381A—regained partial activity (scored as + in Table 1). We surmise that these six side chains are unlikely to be directly catalytic. We presume that the set of nine EcoPrrC-Ala mutants that did not regain toxicity at high gene dosage encompasses bonafide constituents of the nuclease active site. Among the candidate active site residues are three strictly essential and conserved histidines (His295, His315, His356), two strictly essential and conserved arginines (Arg320 and Arg349), and one strictly essential and conserved glutamate (Glu324). The Kaufmann lab had proposed that Arg320, Glu324, and His356 comprise a catalytic triad that they implicate in chemical catalysis of transesterification at the wobble nucleotide to generate 2′,3′ cyclic phosphate and 5′-OH product strands (Blanga-Kanfi et al. 2006). Our results are consistent with their model but raise the prospect that additional residues might play a catalytic role. Of course, a definitive interpretation of the mutational data awaits an atomic structure of the nuclease domain.

TABLE 1. High gene dosage can restore toxicity of certain defective PrrC nuclease domain mutants

2μ PrrC	Toxicity on galactose
D267A	–
D287A	–
S288A	+
H295A	–
H297A	++
K299A	++
H315A	–
R320A	–
N321A	+
E324A	–
W335A	–
R349A	–
N352A	+
H356A	–
H381A	+

DISCUSSION

Programmed tRNA damage by site-specific endoribonucleases is a shared feature of cellular stress responses and self-nonself discrimination in a wide range of prokaryal and eukaryal taxa. tRNA anticodon breakage results in inhibition of protein synthesis, either by depletion of the pool of specific tRNA isoacceptors or by a mechanism by which the broken tRNA fragments per se can have a signaling role without significantly depleting the pool of the tRNA target (Thompson and Parker 2009; Ivanov et al. 2011 and references therein). *E. coli* PrrC was the first example of an intracellular tRNA restriction endonuclease. The activity of PrrC is normally suppressed by its association with its cognate "antitoxin," a type I DNA restriction-modification enzyme (*Eco*prrI) encoded by neighboring ORFs in the *prr* operon (Levitz et al. 1990; Tyndall et al. 1994). tRNA ribotoxins have distinctive target specificities as follows: *E. coli* PrrC for $tRNA^{Lys(UUU)}$ (Amitsur et al. 1987; Jiang et al. 2001, 2002); colicin E5 for Tyr, His, Asn, and Asp tRNAs (Ogawa et al. 1999); colicin D for $tRNA^{Arg}$ (Tomita et al. 2000); enterobacterial VapC for $tRNA^{fmet}$ (Winther and Gerdes 2011); *K. lactis* γ-toxin for $tRNA^{Glu(UUC)}$ (Lu et al. 2005, 2008); and *Pichia acaciae* toxin for $tRNA^{Gln(UUG)}$ (Klassen et al. 2008). The findings that the cytotoxic effects of *Eco*PrrC, colicin E5, and colicin D are portable to budding yeast (Ogawa et al. 2009; Shigematsu et al. 2009; Meineke et al. 2011) attest that eukaryal tRNAs are vulnerable to attack by bacterial anticodon nucleases. Suppression of *EcoPrrC* toxicity in yeast by overexpression of $tRNA^{Lys(UUU)}$ indicates that PrrC exerts toxicity via the homologous tRNA substrate in bacteria and eukarya, notwithstanding their differences in $tRNA^{Lys}$ anticodon modifications.

PrrC homologs are dispersed widely among bacterial taxa, but virtually nothing is known about the biological functions and target specificities of these PrrC proteins. Nonetheless, our initial assumption was that all bacterial PrrC proteins are RNA endonucleases. Thus, it was surprising that *Nme*PrrC, which is among the closest homologs of *Eco*PrrC, displayed no toxicity when expressed in yeast, even though the more distantly related *Smu*PrrC protein was fungicidal. The lack of toxicity of *Nme*PrrC in *E. coli* and the results of our domain-swap experiments, in which the source of the PrrC nuclease domain emerged as the decisive factor for toxicity in yeast or *E. coli*, raised the prospect that either (1) *Nme*PrrC is an active ribotoxin, but its RNA target is not present in *E. coli* or yeast; or (2) *Nme*PrrC is not an active ribotoxin. With the former model in mind, we attempted to convert the nontoxic *Nme*PrrC into a toxic derivative by screening for missense gain-of-function mutants. Remarkably, this succeeded with a single nucleotide change, of an AGG codon to a TGG codon, that replaced an Arg in *Nme*PrrC with a Trp residue found at the equivalent position of *Eco*PrrC. Because the gain-of-function *Nme*R316W mutant exerted its toxicity via $tRNA^{Lys(UUU)}$ and because any mutation of the tryptophan

abolished *Eco*PrrC toxicity, we thought we might have identified an essential species-specific determinant of PrrC target specificity.

A simpler alternative scenario was suggested to us by Gabi Kaufmann, in which *Nme*PrrC has mutated to a nontoxic variant under selection pressure. The pressure arises because the *prr* operon of *N. meningitidis* MC58 (the source of the *Nme*PrrC gene) has degenerated by the acquisition of premature stops and frameshifts in the NMB0831 gene that would otherwise encode the HsdS(PrrB) subunit of the restriction-modification complex that keeps *E. coli* PrrC in an inactive state. The *Neisseria* operon also has a gene encoding an IS30-family transposase inserted into the ORF that would otherwise encode the HsdR(PrrD) subunit of the restriction-modification complex. These genetic changes would seem to ablate the antitoxin that normally exerts a brake on PrrC's nuclease. In order to survive this loss, the bacterium can be expected to acquire an inactivating mutation in the PrrC anticodon nuclease. We agree with this evolutionary sequence as the likely explanation for the lack of toxicity of *Nme*PrrC. What is remarkable is that the toxicity of *Nme*PrrC can be reconstituted by a single missense change. A key lesson from these experiments is that not all PrrC homologs can be presumed to have anticodon nuclease activity. The combination of yeast toxicity assays and domain swaps affords a useful genetic strategy to assess ribotoxicity and species variations in PrrC biological activity, especially with PrrCs encoded by taxa that are not tractable genetically.

tRNA repair as an antidote to ribotoxic tRNA damage is a well-established component of the virus-host dynamic during T4 infection of *prr*$^+$ *E. coli* (Amitsur et al. 1987). We had shown previously that RNA repair enzymes can also protect yeast against growth arrest caused by *K. lactis* γ-toxin (Nandakumar et al. 2008). Here we extend the paradigm of RNA repair to PrrC-mediated eukaryal cytotoxicity, which can be ameliorated by either the phage T4 RNA repair system (Pnkp plus Rnl1) or plant AtRNL. In light of evidence that tRNA damage can trigger strong cellular responses, including inhibition of protein synthesis, nonlethal growth arrest, and cell death, we envision that RNA repair might play a role in tuning the severity of RNA damage or in recovering from its effects.

MATERIALS AND METHODS

Yeast expression plasmids

Yeast *CEN LEU2* plasmids containing the *Eco*PrrC, *Smu*PrrC, or *Nme*PrrC ORFs under the transcriptional control of a *GAL1* promoter were described previously (Meineke et al. 2011). Domain swaps and missense mutations were introduced in the *prrC* genes by two-stage overlap extension PCR with fusogenic or mutagenic primers. The *prrC* ORF was sequenced in each case to verify the intended hybrid junctions or coding change and exclude the acquisition of unwanted coding changes during amplification and cloning. EcoRI/SalI fragments containing $_{GAL1}$-*prrC-Ala* expression cassettes were excised from the respective *CEN* plasmids and inserted into the multicopy yeast plasmid pRS423 (2μ *HIS3*). Yeast 2μ *URA3* plasmids bearing yeast tRNA genes were as described (Jablonowski et al. 2006; Meineke et al. 2011). RNA repair plasmids pRS423-TPI1-AtRNL (2μ *HIS3*) and pRS423-TPI1-TRL1 (2μ *HIS3*) carry the plant and yeast tRNA ligase genes, respectively, under the transcriptional control of the yeast *TPI1* promoter. RNA repair plasmid pRS413-Pnkp/Rnl1 (*CEN HIS3*) vector expresses phage T4 Pnkp under the control of the yeast *SLU7* promoter and T4 Rnl1 under the control of the yeast *TPI1* promoter.

Arabinose-inducible PrrC expression plasmids

The *Eco*PrrC, *Smu*PrrC, *Nme*PrrC, and chimeric PrrC open reading frames were amplified by PCR from their respective yeast *CEN* plasmids using a sense-strand primer that introduced an NheI site immediately 5′ of the translation start codon. The PCR products were digested with NheI and SalI and inserted between the corresponding restriction sites of the bacterial expression plasmid pBAD18. The *prrC* ORF was sequenced in each case to verify the intended coding sequence.

PrrC yeast toxicity assays

Yeast cells were transformed with PrrC plasmid DNAs, and transformants were selected on appropriate minimal synthetic media on 2% (w/v) Bacto agar plates. Toxicity of the plasmid-encoded PrrC proteins was gauged as described (Meineke et al. 2011). Cells derived from single transformants were grown at 30°C in liquid culture in selective media containing 2% glucose. The cultures were adjusted to A_{600} of 0.1 and then diluted in water in serial fivefold decrements. Aliquots (3 μL) of the dilutions were then spotted in parallel on selective agar plates containing either 2% glucose or 2% galactose. The plates were photographed after incubation at 30°C for 2 d (glucose) or 3 d (galactose) unless specified otherwise.

PrrC bacterial toxicity assays

Top10 cells (*araABD*$^-$, Invitrogen) were transformed with pBAD-PrrC plasmids. Cells derived from single ampicillin-resistant colonies were grown in LB medium containing 200 μg/mL ampicillin for 4 h at 37°C. The cultures were adjusted to attain A_{600} of 0.025 and then diluted in 20-fold decrements in water. Aliquots (3 μL) of the dilutions were spotted in parallel on LB agar plates containing 100 μg/mL ampicillin with or without 0.2% L-arabinose. The plates were photographed after incubation for 24 h at 37°C.

SUPPLEMENTAL MATERIAL

Supplemental material is available for this article.

ACKNOWLEDGMENTS

This research was supported by NIH grant GM42498. S.S. is an American Cancer Society Research Professor.

Received August 30, 2011; accepted October 10, 2011.

REFERENCES

Amitsur M, Levitz R, Kaufman G. 1987. Bacteriophage T4 anticodon nuclease, polynucleotide kinase, and RNA ligase reprocess the host lysine tRNA. *EMBO J* **6:** 2499–2503.

Amitsur M, Morad I, Kaufmann G. 1989. *In vitro* reconstitution of anticodon nuclease from components encoded by phage T4 and *Escherichia coli* CTr5X. *EMBO J* **8:** 2411–2415.

Amitsur M, Morad I, Chapman-Shimshoni D, Kaufmann G. 1992. HSD restriction–modification proteins partake in latent anticodon nuclease. *EMBO J* **11:** 3129–3134.

Amitsur M, Benjamin S, Rosner R, Chapman-Shimshoni D, Meidler R, Blanga S, Kaufmann G. 2003. Bacteriophage T4-encoded Stp can be replaced as activator of anticodon nuclease by a normal host cell metabolite. *Mol Microbiol* **50:** 129–143.

Blanga-Kanfi S, Amitsur M, Azem A, Kaufmann G. 2006. PrrC-anticodon nuclease: Functional organization of a prototypical bacteria restriction RNase. *Nucleic Acids Res* **34:** 3209–3219.

Davidov E, Kaufmann G. 2008. RloC: A wobble nucleotide-excising and zinc-responsive bacterial tRNase. *Mol Microbiol* **69:** 1560–1574.

Ivanov P, Emara MM, Villen J, Gygi SP, Anderson P. 2011. Angiogenin-induced tRNA fragments inhibit translation initiation. *Mol Cell* **43:** 613–623.

Jablonowski D, Schaffrath R. 2007. Zymocin, a composite chitinase and tRNase killer toxin from yeast. *Biochem Soc Trans* **35:** 1533–1537.

Jablonowski D, Zink S, Mehlgarten C, Daum G, Schaffrath R. 2006. $tRNA^{Glu}$ wobble uridine methylation by Trm9 identifies Elongator's key role for zymocin-induced cell death in yeast. *Mol Microbiol* **59:** 677–688.

Jiang Y, Mediler R, Amitsur M, Kaufmann G. 2001. Specific interaction between anticodon nuclease and the $tRNA^{Lys}$ wobble base. *J Mol Biol* **305:** 377–388.

Jiang Y, Blanga S, Amitsur M, Meidler R, Krivosheyev E, Sundaram M, Bajii A, Davis DR, Kaufmann G. 2002. Structural features of $tRNA^{Lys}$ favored by anticodon nuclease as inferred from reactivities of anticodon stem and loop substrate analogs. *J Biol Chem* **277:** 3836–3841.

Kaufmann G. 2000. Anticodon nucleases. *Trends Biochem Sci* **25:** 70–74.

Klaiman D, Amitsur M, Blanga-Kanfi S, Chai M, Davis DR, Kaufmann G. 2007. Parallel dimerization of a PrrC-anticodon nuclease region implicated in $tRNA^{Lys}$ recognition. *Nucleic Acids Res* **35:** 4704–4714.

Klassen R, Paluszynski JP, Emhoff S, Pfeiffer A, Fricke J, Meinhardt F. 2008. The primary target of the killer toxin from *Pichia acaciae* is $tRNA^{Gln}$. *Mol Microbiol* **69:** 681–697.

Levitz R, Chapman D, Amitsur M, Green R, Snyder L, Kaufmann G. 1990. The optional *E. coli prr* locus encodes a latent form of phage T4-induced anticodon nuclease. *EMBO J* **9:** 1383–1389.

Lu J, Huang B, Esberg A, Johanson MJO, Byström AS. 2005. The *Kluyveromyces lactis* γ-toxin targets tRNA anticodons. *RNA* **11:** 1648–1654.

Lu J, Esberg A, Huang B, Byström AS. 2008. *Kluyveromyces lactis* γ-toxin, a ribonuclease that recognizes the anticodon stem loop of tRNA. *Nucleic Acids Res* **36:** 1072–1080.

Meidler R, Morad I, Amitsur M, Inokuchi H, Kaufmann G. 1999. Detection of anticodon nuclease residues involved in $tRNA^{Lys}$ cleavage specificity. *J Mol Biol* **287:** 499–510.

Meineke B, Schwer B, Schaffrath R, Shuman S. 2011. Determinants of eukaryal cell killing by the bacterial ribotoxin PrrC. *Nucleic Acids Res* **39:** 687–700.

Nandakumar J, Schwer B, Schaffrath R, Shuman S. 2008. RNA repair: An antidote to cytotoxic eukaryal RNA damage. *Mol Cell* **31:** 278–286.

Ogawa T, Tomita K, Ueda T, Watanabe K, Uozumi T, Masaki H. 1999. A cytotoxic ribonuclease targeting specific tRNA anticodons. *Science* **283:** 2097–2100.

Ogawa T, Hidaka M, Kohno K, Masaki H. 2009. Colicin E5 ribonuclease domain cleaves *Saccharomyces cerevisiae* tRNAs leading to impairment of the cell growth. *J Biochem* **145:** 461–466.

Penner M, Morad I, Snyder L, Kaufmann G. 1995. Phage T4-coded Stp: Double-edged effector of coupled DNA and tRNA-restriction systems. *J Mol Biol* **249:** 857–868.

Shigematsu M, Ogawa T, Kido A, Kitamoto HK, Hidaka M, Masaki H. 2009. Cellular and transcriptional responses of yeast to the cleavage of cytosolic tRNAs by colicin D. *Yeast* **26:** 663–673.

Thompson DM, Parker R. 2009. Stressing out over tRNA cleavage. *Cell* **138:** 215–219.

Tomita K, Ogawa T, Uozumi T, Watanabe K, Masaki H. 2000. A cytotoxic ribonuclease which specifically cleaves four isoaccepting arginine tRNAs at their anticodon loops. *Proc Natl Acad Sci* **97:** 8278–8283.

Tyndall C, Meister J, Bickle TA. 1994. The *Escherichia coli prr* region encodes a functional type IC DNA restriction system closely integrated with an anticodon nuclease gene. *J Mol Biol* **237:** 266–274.

Wang LK, Schwer B, Englert M, Beier H, Shuman S. 2006. Structure–function analysis of the kinase-CPD domain of yeast tRNA ligase (Trl1) and requirements for complementation of tRNA splicing by a plant Trl1 homolog. *Nucleic Acids Res* **34:** 517–527.

Winther KS, Gerdes K. 2011. Enteric virulence associated protein VapC inhibits translation by cleavage of initiator tRNA. *Proc Natl Acad Sci* **108:** 7403–7407.

Supplemental Material

Determinants of the cytotoxicity of PrrC anticodon nuclease and its amelioration by tRNA repair

Birthe Meineke and Stewart Shuman

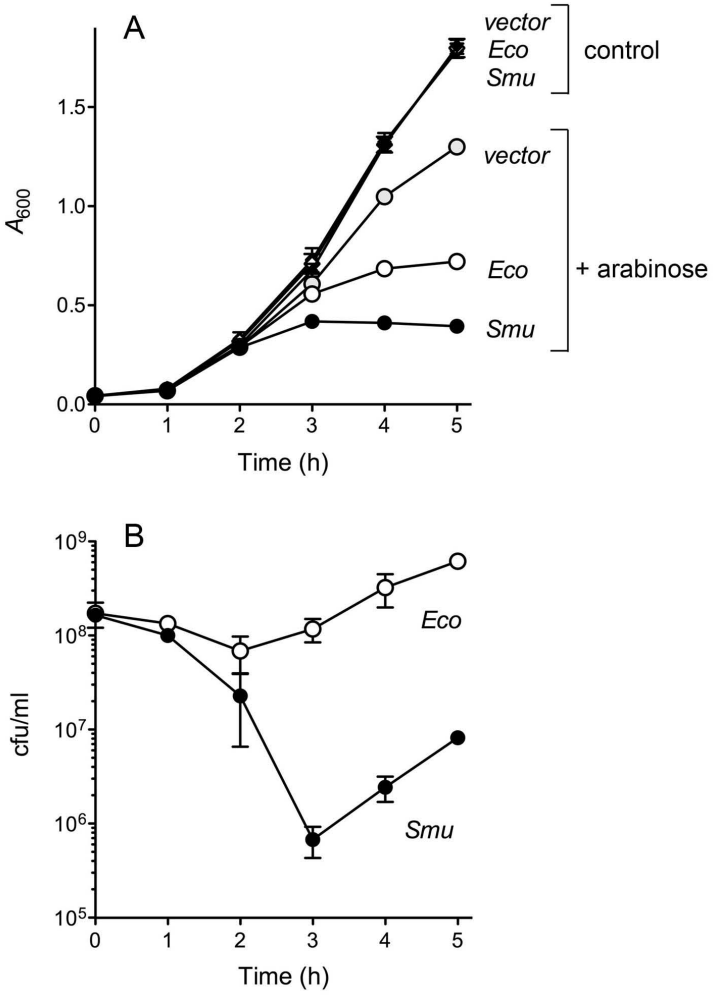

Figure S1. **Bacteriostatic *versus* bactericidal effects of *Eco* and *Smu* PrrC expression in *E. coli***.

(A) Growth of liquid cultures of *E. coli* cells bearing the empty pBAD vector, pBAD-*Eco*PrrC, or pBAD-*Smu*PrrC was monitored by determining A_{600} at hourly intervals after transfer to fresh LB-ampicillin medium (control) or LB-ampicillin medium containing 0.2% arabinose. Each datum is the average of three independent growth experiments ±SEM. (B) Viable cell counts of liquid cultures of *E. coli* cells bearing pBAD-*Eco*PrrC or pBAD-*Smu*PrrC were determined immediately prior to (time 0) and at hourly intervals after transfer to medium containing 0.2% arabinose. Colony counts were assayed by plating diluted aliquots of the cultures on LB-ampicillin agar. Each datum is the average of three independent arabinose-induction experiments ±SEM.

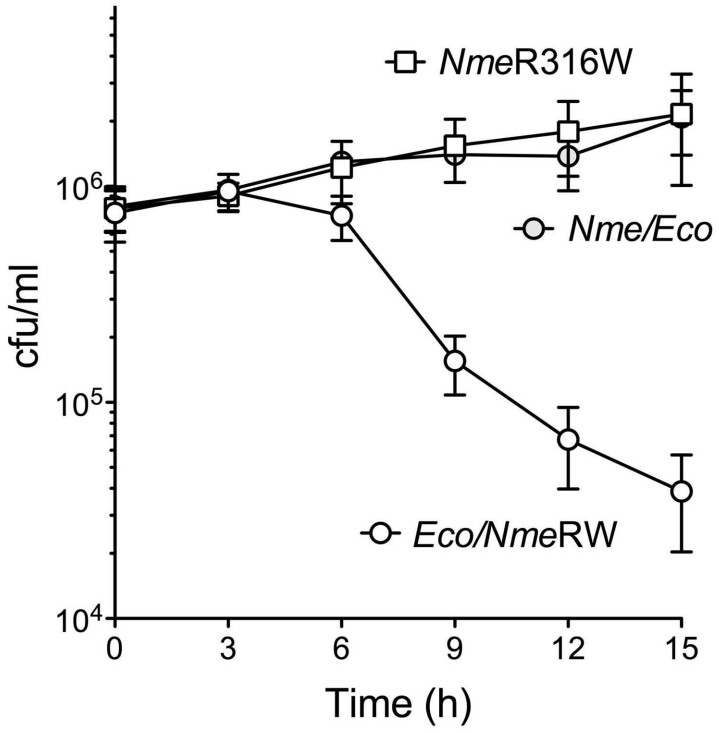

Figure S2. **Cytocidal versus cytostatic effects of expressing gain-of-function versions of *Neisseria* PrrC in budding yeast**. Viable cell counts of liquid cultures of yeast cells bearing *NmeR316W, Nme/Eco,* or *Eco/NmeRW* PrrC expression plasmids were determined immediately prior to (time 0) and at serial 3 h intervals after galactose induction, by plating aliquots on –Leu agar containing 2% glucose. Each datum is the average of three independent galactose-induction experiments ±SEM.

This paper is available online at www.jbc.org

THE JOURNAL OF BIOLOGICAL CHEMISTRY VOL. 286, NO. 35, pp. 30253–30257, September 2, 2011

RtcB, a Novel RNA Ligase, Can Catalyze tRNA Splicing and *HAC1* mRNA Splicing *in Vivo*[*][S]

Received for publication, June 22, 2011
Published, JBC Papers in Press, July 11, 2011, DOI 10.1074/jbc.C111.274597

Naoko Tanaka, Birthe Meineke, and Stewart Shuman[1]

From the Molecular Biology Program, Sloan-Kettering Institute, New York, New York 10065

RtcB enzymes are novel RNA ligases that join 2′,3′-cyclic phosphate and 5′-OH ends. The phylogenetic distribution of RtcB points to its candidacy as a tRNA splicing/repair enzyme. Here we show that *Escherichia coli* RtcB is competent and sufficient for tRNA splicing *in vivo* by virtue of its ability to complement growth of yeast cells that lack the endogenous "healing/sealing-type" tRNA ligase Trl1. RtcB also protects yeast *trl1*Δ cells against a fungal ribotoxin that incises the anticodon loop of cellular tRNAs. Moreover, RtcB can replace Trl1 as the catalyst of *HAC1* mRNA splicing during the unfolded protein response. Thus, RtcB is a *bona fide* RNA repair enzyme with broad physiological actions. Biochemical analysis of RtcB highlights the uniqueness of its active site and catalytic mechanism. Our findings draw attention to tRNA ligase as a promising drug target.

Escherichia coli RtcB exemplifies a new family of RNA ligases that directly seal 2′,3′-cyclic phosphate and 5′-OH ends (1–3). Direct ligation is thought to be the main pathway of tRNA splicing in animals and archaea (4–6). By contrast, yeast and plants rely on a different mechanism of tRNA splicing in which the broken 3′ and 5′ ends are healed (converted to a 3′-OH/2′-PO_4 and 5′-PO_4, respectively) and then sealed by a classical ATP-dependent RNA ligase (7) (see Fig. 1). RNA ligases of the RtcB family are present in metazoa and protozoa, but not in fungi and plants. RtcB homologs purified from archaeal and mammalian cells can seal broken tRNA halves and are thereby imputed to be the catalysts of archaeal and mammalian tRNA splicing (2, 3). However, this scenario is complicated by the existence of a yeast/plant-like tRNA splicing pathway in mammalian cells (8–12) and of analogous yeast-like RNA repair enzymes in many archaeal taxa (13–16). Definitive genetic evidence that RtcB is the sole essential agent of the repair phase of mammalian or archaeal tRNA splicing is lacking, and the available genetic evidence concerning the healing-sealing pathway in animals is equivocal. Genetic ablation of a murine homolog of a yeast-like pathway component Tpt1 (the enzyme that removes the 2′-phosphate at the splice junction; see Fig. 1) has no discernible phenotype (17), suggesting that the mammalian yeast-like pathway either is functionally redundant with direct ligation or is non-contributory to mammalian tRNA splicing. By contrast, siRNA-directed depletion of the mammalian RNA 5′-kinase (an ortholog of the kinase domain of yeast/plant tRNA ligase) elicited a defect in tRNA splicing *in vitro* (10). However, siRNA-directed depletion of mammalian RtcB was also reported to inhibit ligation of tRNA halves in cell extracts and to delay tRNA splicing in living cells (3). These findings leave unresolved the following key issues: (i) whether RtcB can suffice for tRNA splicing as the only source of tRNA ligase activity in a eukaryal cell and (ii) whether RtcB can perform other RNA repair functions *in vivo*. Here we address these questions by using budding yeast as a surrogate genetic model for tRNA splicing and RNA repair by heterologous enzymes (7).

EXPERIMENTAL PROCEDURES

Expression Plasmids—The bacterial plasmid pET28b-His_{10}Smt3-RtcB encodes wild-type *E. coli* RtcB fused to an N-terminal His_{10}Smt3 tag (1). Missense mutations were introduced into the RtcB ORF by two-stage overlap extension PCR. The RtcB inserts were sequenced to confirm the desired mutations and exclude the acquisition of unwanted coding changes. The wild-type and mutated RtcB ORFs were excised from their respective pET plasmids and inserted into the yeast vector pRS423 (2μ *HIS3*) wherein RtcB expression is under the control of the yeast *TPI1* promoter. The yeast p(*CEN LEU2* $_{GAL1}$PaT) plasmid for galactose-inducible expression of intracellular *Pichia acaciae* toxin (PaT)[2] lacking the N-terminal 12-amino acid signal peptide was constructed by excising an NdeI/SalI fragment containing the PaT ORF from plasmid pPACBX (18) (a gift of Roland Klassen and Friedhelm Meinhardt) and inserting it into pRS415 (*CEN LEU2*) between *GAL1* promoter and terminator elements.

RtcB Purification—The wild-type and mutant pET28b-His_{10}Smt3-RtcB plasmids were transformed into *E. coli* BL21-CodonPlus(DE3). Induction of RtcB expression, preparation of soluble lysates, recovery of the His_{10}Smt3-RtcB proteins by nickel-agarose chromatography, excision of the tags by treatment with the Smt3-specifc protease Ulp1, and separation of the tag-free RtcB proteins from His_{10}Smt3 by a second round of nickel-agarose chromatography were performed as described (1). Protein concentrations were determined by using the Bio-Rad dye reagent with BSA as the standard. The polypeptide compositions of the RtcB preparations were analyzed by SDS-PAGE (supplemental Figs. S1 and S2).

RNA Repair Substrates—A synthetic RNA oligonucleotide R30 containing the anticodon stem-loop of yeast $tRNA^{Glu(UUC)}$ was 5′ ^{32}P-labeled by reaction with T4 Pnkp and [γ-^{32}P]ATP. R30 was then cleaved 3′ of the wobble uridine by reaction with *Kluyveromyces lactis* γ-toxin (1). The ^{32}P-labeled R19>p strand with a 2′,3′ cyclic phosphate end (5′-pUGGCUCCGAUAUCACGCUU>p) was purified by preparative PAGE. Oligo-

* This work was supported, in whole or in part, by National Institutes of Health Grant GM46330 (to S. S.).

[S] The on-line version of this article (available at http://www.jbc.org) contains supplemental Figs. S1 and S2.

[1] To whom correspondence should be addressed. E-mail: s-shuman@ski.mskcc.org.

[2] The abbreviations used are: PaT, *P. acaciae* toxin; UPR, unfolded protein response.

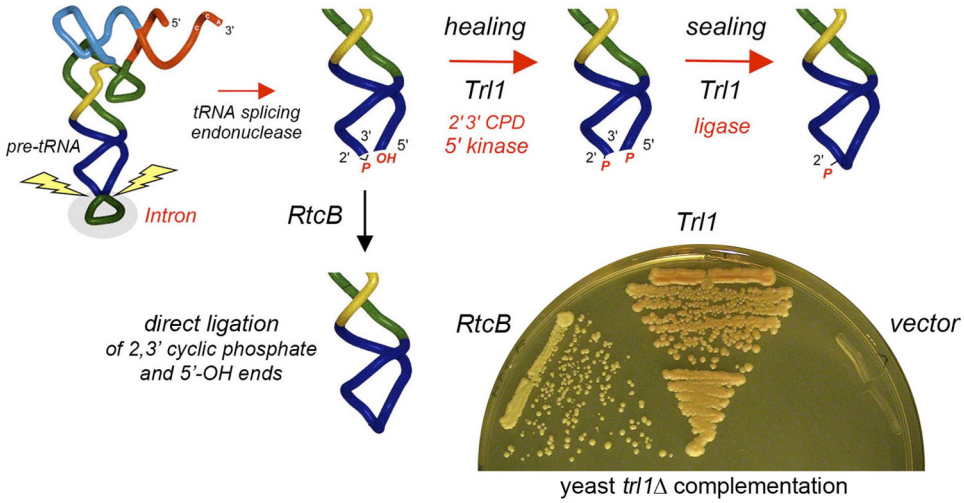

FIGURE 1. **RtcB can perform eukaryal tRNA splicing *in vivo*.** The two pathways of tRNA splicing, via end-healing and end-sealing in yeast and plants (catalyzed in *S. cerevisiae* by the tRNA ligase Trl1) or via direct ligation in animals and archaea (where RtcB is a putative catalyst), are shown. The capacity of *E. coli* RtcB to complement an *S. cerevisiae trl1*Δ mutant was assayed by plasmid shuffle. Yeast *trl1*Δ p(*CEN URA3 TRL1*) cells transformed with a 2μ *HIS3* plasmid (vector control) or 2μ *HIS3* plasmids encoding Trl1 or RtcB under the control of a yeast *TPI1* promoter were selected for histidine prototrophy and then streaked on agar medium containing 0.75 mg/ml 5-fluoroorotic acid (a drug that selects against the *URA3 TRL1* plasmid). The plate was photographed after 3 days at 30 °C.

nucleotide $_{HO}$R20 (5′-$_{HO}$UCACCGUGGUAUCGGAGCGC) was employed to form a broken tRNA-like stem-loop (see Fig. 4) by mixture with the 5′ ^{32}P-labeled R19 single strand at an R20:R19 ratio of 10:1. To test the RNA requirements for the RtcB ligation reaction, the ^{32}P-labeled R19>p strand was also annealed to a synonymous deoxyuridine-containing $_{HO}$D20 oligonucleotide to form a broken RNA-DNA hybrid stem-loop (see Fig. 5).

Alternative stem-loop RNA repair substrates with a 3′-OH end at the break site (see Fig. 5) were prepared using a synthetic R19$_{OH}$ oligonucleotide that had been 5′ ^{32}P-labeled and then purified by PAGE. The labeled R19$_{OH}$ oligonucleotide was annealed to a 10-fold excess of unlabeled D20 and R20 strands.

RNA repair substrates with a 5′-PO$_4$ at the break site (see Fig. 5) were formed by annealing radiolabeled R19>p or R19$_{OH}$ strands to a 10-fold excess of cold pR20 strand. The pRNA strand was generated by enzymatic phosphorylation of $_{HO}$R20 using T4 Pnkp and cold ATP and then purified by PAGE.

RESULTS AND DISCUSSION

Here we interrogated the tRNA repair function of *E. coli* RtcB *in vivo* by complementation of a lethal deletion of the *TRL1* gene encoding the tRNA ligase of *Saccharomyces cerevisiae* (7). Yeast Trl1 is a trifunctional tRNA repair enzyme (with 5′-OH kinase, 2′,3′ cyclic phosphodiesterase, and ATP-dependent RNA ligase activities) that heals and seals the broken tRNA halves with 2′,3′ cyclic phosphate and 5′-OH ends generated by incision of pre-tRNAs at the exon-intron junctions (Fig. 1). *E. coli* RtcB is a monofunctional ligase that directly joins 2′,3′ cyclic phosphate and 5′-OH ends (1) (Fig. 1). We expressed the 408-amino acid *E. coli* RtcB protein in *S. cerevisiae* under the control of a constitutive promoter on a 2μ plasmid and demonstrated by plasmid shuffle that RtcB could indeed sustain growth of a *trl1*Δ strain (Fig. 1). These results prove that RtcB is able and sufficient to perform the essential repair steps of eukaryal tRNA splicing *in vivo*.

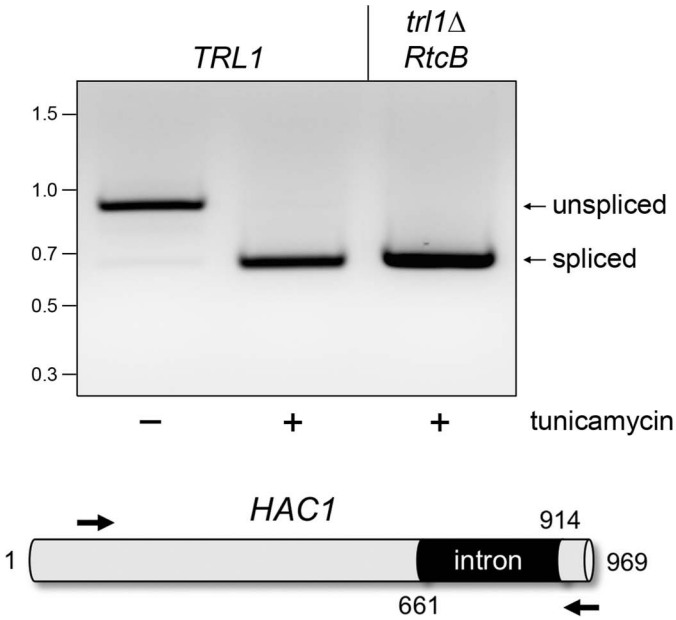

FIGURE 2. **RtcB can perform *HAC1* mRNA splicing in the unfolded protein response.** The unprocessed yeast *HAC1* open reading frame, containing a 252-nucleotide intron, is depicted at the *bottom*. To gauge *HAC1* mRNA splicing, cultures (10 ml) of *S. cerevisiae trl1*Δ p(2μ *HIS3 TRL1*) and *trl1*Δ p(2μ *HIS3 RtcB*) cells were grown at 30 °C in YPD media until the A_{600} reached 0.6. The cultures were split into 5-ml aliquots, one of which was adjusted to 1.5 μg/ml tunicamycin to induce endoplasmic reticulum stress. One hour later, the cells were harvested by centrifugation. Total RNA was isolated by using a yeast RNA purification kit (Epicentre Biotechnologies). *HAC1* transcripts were detected by RT-PCR using primers flanking the intron. The cDNAs were synthesized by using the SuperScript III system (Invitrogen) with 1.0 μg of total RNA as template and 0.1 μM of *HAC1*-specific antisense primer (5′-dCATGAAGTGATGAAGAAATCATTCAATTC; complementary to nucleotides 940–968). The cDNAs were amplified by 22 cycles of PCR with Herculase (Stratagene) using the antisense primer and a sense-strand primer (5′-dCCAAGGAAAAGAGCCAAGACAAAAGAGG; corresponding to nucleotides 82–109). The RT-PCR products were analyzed by 1.4% agarose gel electrophoresis. A negative image of the ethidium bromide-stained gel is shown. The positions and sizes (in bp) of marker dsDNAs are indicated at *left*. The predicted sizes of the unspliced and spliced *HAC1* RT-PCR products are 886 and 634 bp, respectively.

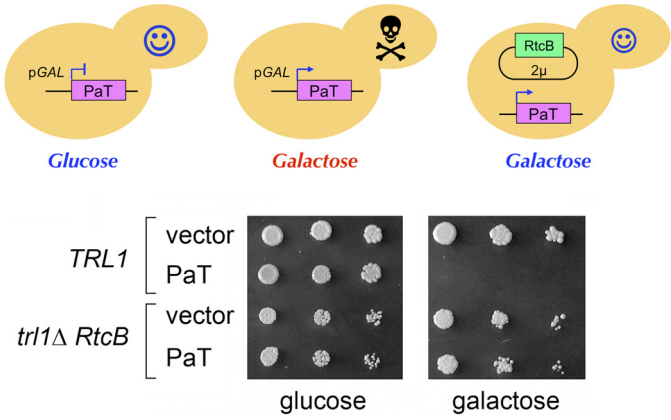

FIGURE 3. **RtcB protects cells from cytotoxic tRNA damage.** *Top*, schematic depiction of yeast cells harboring $_{GAL1}$PaT in the presence of glucose or galactose as the carbon source. The *right-most cell* expresses RtcB in lieu of Trl1. *Bottom*, *S. cerevisiae TRL1* and *trl1Δ RtcB* cells were transformed either with a *CEN LEU2* $_{GAL1}$PaT plasmid or with an empty *CEN LEU2* vector. Cultures derived from single Leu$^+$ colonies were grown in SD−Leu medium at 37 °C. After adjustment to A_{600} of 0.1, aliquots (3 μl) of serial 5-fold dilutions of the cells were spotted on −Leu agar plates containing either 2% glucose or 2% galactose. The plates were photographed after incubation for 3 days (glucose) or 4 days (galactose) at 37 °C.

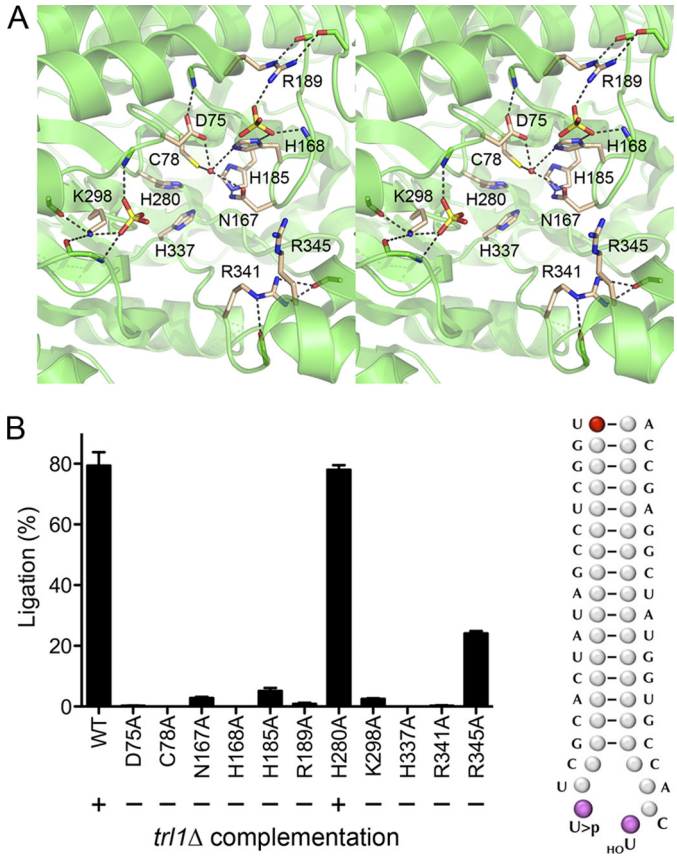

FIGURE 4. **Structure-guided mapping of the RtcB active site.** *Top*, stereo view of the putative active site pocket of *P. horikoshii* RtcB (from Protein Data Bank (PDB) 1UC2). The conserved amino acid residues that were subjected to alanine scanning in *E. coli* RtcB are shown as stick models with *beige carbons* and are labeled according to their *E. coli* RtcB equivalents. Two sulfate anions bound to RtcB are rendered as stick models. A water molecule that could plausibly mimic the metal cofactor is depicted as a *red sphere*. Ionic and hydrogen-bonding interactions are denoted by *dashed lines*. *Bottom*, RNA ligase reaction mixtures (10 μl) containing 50 mM Tris-HCl (pH 8.0), 2 mM $MnCl_2$, 100 μM GTP, 100 nM of 5′-^{32}P-labeled broken RNA stem-loop substrate (depicted at *right*), and 2 μM wild-type RtcB or RtcB-Ala mutants (see supplemental Fig. S1) were incubated for 30 min at 37 °C. The reactions were quenched by adding 10 μl of 40 mM EDTA/95% formamide, and the products were analyzed by electrophoresis through a 20% polyacrylamide gel containing 7 M urea in 45 mM Tris borate, 1.25 mM EDTA. The extents of conversion of the radiolabeled 19-mer substrate strand into sealed 39-mer product (% ligation) were quantified by scanning the gel with a Fuji Film BAS-2500 imager. Each datum in the bar graph is the average of three separate ligation experiments ±S.E. The *RtcB-Ala* ORFs were cloned into yeast 2μ plasmids under the control of the *TPI1* promoter and tested for *trl1Δ* complementation as described in the legend for Fig. 1. The results are summarized below the graph.

The discovery that the healing and sealing activities of yeast Trl1 are also responsible for unconventional splicing of the *HAC1* mRNA in the yeast unfolded protein response (UPR) pathway (19, 20) extended the RNA repair paradigm to mRNA metabolism. Endoplasmic reticulum stress induces the Ire1 endonuclease to cleave *HAC1* mRNA at two sites, which liberates a 252-nucleotide intron (Fig. 2) and leaves 2′,3′ cyclic phosphate and 5′-OH termini on the proximal and distal exons, respectively. Healing and sealing of the exons by Trl1 creates a new open reading frame encoding an active Hac1 transcription factor. The mammalian UPR entails stress-induced Ire1 cleavage and unconventional splicing of the *XBP1* mRNA (21), but the enzyme responsible for sealing the broken *XBP1* transcript is not known. Here we tested the capacity of RtcB to execute unconventional mRNA splicing during the yeast UPR. Yeast *TRL1* cells exposed to tunicamycin shifted their *HAC1* mRNA profile, as assayed by RT-PCR with primers flanking the intron, whereby the intron-containing long form was replaced by a spliced short form (Fig. 2). Sequencing of the isolated RT-PCR products confirmed their identity as unspliced and spliced *HAC1* cDNAs, respectively. Yeast *trl1Δ* cells reliant on RtcB as their source of tRNA ligase were proficient in generating the spliced *HAC1* RNA in the presence of tunicamycin (Fig. 2), signifying that RtcB is competent for mRNA splicing in the eukaryal UPR. Sequencing of the RT-PCR product verified that the Ire1 endonuclease cleavage sites were ligated faithfully.

Another manifestation of tRNA repair is the capacity to protect cells from the cytotoxicity inflicted by tRNA-specific ribotoxins that incise the anticodon loop by a transesterification mechanism that leaves 2′,3′ cyclic phosphate and 5′-OH termini at the broken tRNA ends (22, 23). PaT is a secreted fungal defense molecule that penetrates *S. cerevisiae* cells and, upon accessing the cytoplasm, breaks the anticodon loop of $tRNA^{Gln(UUG)}$. Consequent depletion of the $tRNA^{Gln(UUG)}$ pool arrests yeast growth (18). Galactose-induced expression in *S. cerevisiae* of an intracellular form of PaT recapitulates its toxicity (18). The salient finding here was that replacing yeast Trl1 with RtcB as the source of tRNA ligase protected *S. cerevisiae* from PaT-mediated growth inhibition (Fig. 3). Taken together, these experiments establish that RtcB is a tRNA/mRNA repair enzyme with broad physiological actions.

The RtcB sealing reaction is posited to entail nucleophilic attack by the O5′ nucleophile on the cyclic phosphate, with expulsion of the ribose O2′. Our initial findings that RtcB is manganese-dependent (1) indicated that sealing is not merely reversal of the metal-independent cleavage transesterification mechanism used by tRNA splicing endoribonuclease and tRNA-damaging anticodon nucleases. Manganese might pro-

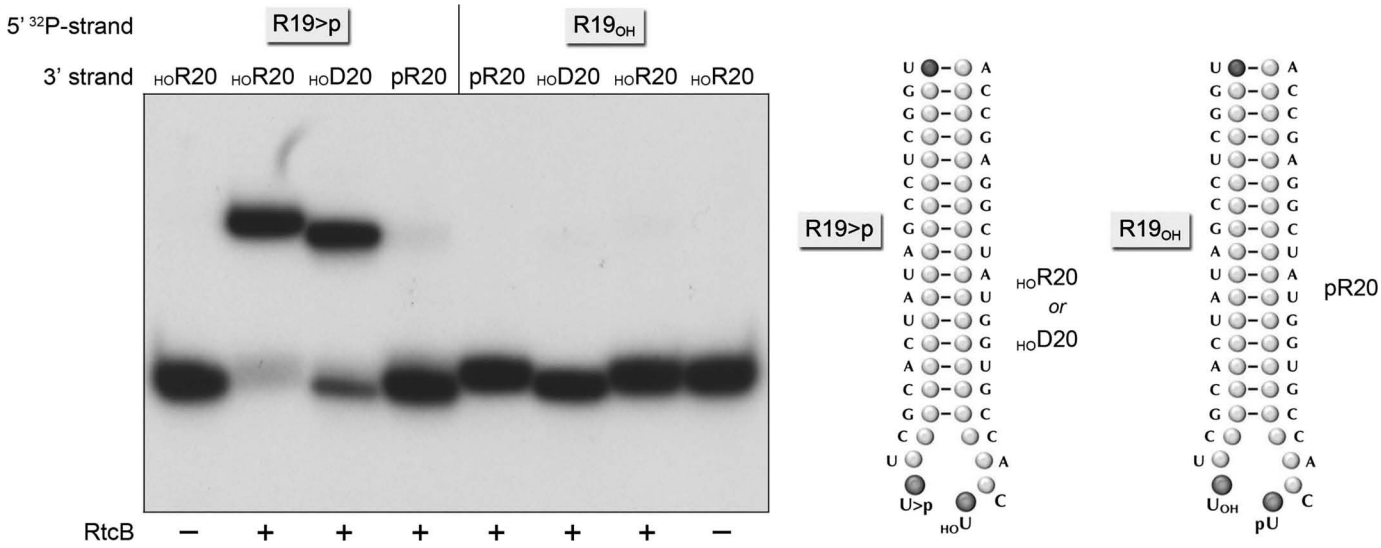

FIGURE 5. **RtcB substrate specificity.** Reaction mixtures (10 μl) containing 50 mM Tris-HCl (pH 8.0), 2 mM $MnCl_2$, 100 μM GTP, 100 nM of 5′-^{32}P-labeled broken stem-loop substrates (illustrated at *right*) with 2′,3′ cyclic or 3′-OH ends on the proximal R19 strand and 5′-OH or 5′-PO_4 ends on the distal 20-mer strand (as specified above the lanes), and 1 μM RtcB (where indicated by +) were incubated for 30 min at 37 °C. The products were analyzed by denaturing PAGE and visualized by autoradiography.

mote RtcB catalysis by coordinating the O5′ nucleophile to lower its pK_a and/or engaging the cyclic phosphate oxygens to stabilize the transition state. The mechanistic novelty of RtcB is underscored by the crystal structure of the RtcB homolog from *Pyrococcus horikoshii* (24) (Fig. 4). RtcB has a distinctive tertiary structure with no similarity to any known ligases or phosphotransferases. RtcB has a deep and wide hydrophilic pocket lined by conserved histidines and a cysteine, suggestive of a metal-binding site that, being dominated by "soft" metal contacts to histidine nitrogens and cysteine sulfur, could account for the fact that *E. coli* RtcB requires manganese and is virtually inactive with magnesium (1). A water coordinated by the equivalents of *E. coli* RtcB side chains Asp-75, Cys-78, Asn-167, and His-168 is a potential mimic of the enzyme-bound metal (Fig. 4). Flanking the putative metal site in RtcB are two sulfate anions (potential mimetics of RNA phosphates) coordinated by basic amino acid side chains equivalent to *E. coli* RtcB residues Lys-298, His-168, and Arg-189 (Fig. 4).

Here we used the *Pyrococcus* RtcB structure to guide a mutational analysis of 11 conserved residues in *E. coli* RtcB that we thought might comprise an active site (Fig. 4). Recombinant RtcB and RtcB-Ala proteins were produced in bacteria purified from soluble lysates (supplemental Fig. S1). The proteins were tested for ligase activity with a broken tRNA-like substrate (1) modeled on the anticodon stem-loop of yeast $tRNA^{Glu(UUC)}$ (Fig. 4). Although RtcB and mutant H280A sealed ~80% of the stem-loop substrate *in vitro*, mutants D75A, C78A, H168A, R189A, H337A, and R341A were virtually inert, with <1% ligation (Fig. 4). Mutants N167A, H185A, R189A and K298A were severely impaired (sealing 3, 5, and 3% of the substrate, respectively), and R345A was modestly impaired (24% sealing). Each of the RtcB-Ala mutants was tested for *trl1*Δ complementation in yeast; only H280A was functional (Fig. 4).

Structure-activity relations at seven of the RtcB amino acids defined as essential by the alanine scan were probed by introducing conservative substitutions (supplemental Fig. S2). Replacing Asp-75 by either asparagine or glutamate inactivated RtcB, attesting to the requirement for a carboxylate at this position and the steric constraints on the main chain to carboxylate distance (supplemental Fig. S2). Changing Cys-78 to serine abolished ligase activity, signifying that the Sγ atom is critical. His-168 and His-337 were replaced by glutamine and asparagine; the H168N, H168Q, H337N, and H337Q mutants were catalytically inactive (supplemental Fig. S2). The mutational effects are consistent with roles for Asp-75, Cys-78, His-168, Asn-167, His-185, and His-337 in metal binding and/or RNA transesterification. Although replacing the sulfate-binding Lys-298 with glutamine phenocopied K298A, the arginine substitution restored ligation to one-fourth of the wild-type RtcB (supplemental Fig. S2), highlighting positive charge as the key property of this residue. By contrast, neither Arg-189 nor Arg-341 could be functionally substituted by lysine or glutamine, implying that the multivalent ionic and hydrogen-bonding contacts of these arginines seen in the RtcB crystal structure (Fig. 4) are indeed pertinent to enzyme activity, either via binding to the RNA phosphates (a putative function of Arg-189) or in stabilizing the active site conformation (a likely role of Arg-341). None of the conservative mutants complemented *trl1*Δ (not shown).

Further insights to the substrate specificity of RtcB were gained by varying the 3′ and 5′ termini of the broken stem-loop substrate and testing the capacity of a 5′-OH DNA strand to serve as the nucleophile for the sealing reaction. A 5′ ^{32}P-labeled 19-mer RNA with either a 2′,3′ cyclic phosphate end (R19>p) or a 3′-OH end ($R19_{OH}$) was annealed to an unlabeled 20-mer strand composed of all ribonucleotides (R20) or all deoxynucleotides (D20) to form the broken stem-loops depicted in Fig. 5. The unlabeled 20-mer strands had either a 5′-OH terminus ($_{HO}$R20 or $_{HO}$D20) or a 5′-PO_4 terminus (pR20). The results of the ligation assays established that: (i) 2′,3′ cyclic phosphate and 5′-OH ends are the only suitable reactants for *E. coli* RtcB among the combinations tested and

(ii) RtcB is adept at joining the R19>p "donor" strand to either RNA or DNA "acceptor" strands so long as they have a 5′-OH end. The versatility of RtcB with respect to the 5′-OH acceptor suggests practical applications for this enzyme in tagging and/or cloning mature RNAs or RNA processing intermediates that have 2′,3′ cyclic phosphate ends.

In summary, we have provided convincing genetic and biochemical evidence that RtcB can serve as a genuine tRNA splicing/repair enzyme in a eukaryal cell. Our findings here and previously (7) attest to the portability of viral, fungal, plant, and bacterial tRNA repair systems. The salient theme is that sealing by any of several distinct enzymatic/chemical pathways suffices for tRNA splicing and unconventional mRNA splicing *in vivo*. The candidacy of mammalian RtcB homolog as an agent of tRNA splicing by direct ligation is supported by our genetic results. However, the jury is still out as to whether RtcB is functionally redundant with a mammalian tRNA repair pathway via sequential end-healing and end-sealing steps (8, 10).

Our findings also fortify the case for the Trl1-associated ligase as a promising antifungal drug target for the following reasons: (i) Trl1 is present in all fungal proteomes; (ii) ligase-inactivating mutations in the active site of Trl1 are lethal *in vivo* (25, 26); and (iii) mammalian taxa encode no homolog of the Trl1 ligase domain. Thus, any ATP-dependent ligase involved in the putative mammalian healing-sealing pathway (8) must either belong to a different enzyme family or have diverged so far from a fungal-type ancestor as to be unrecognizable. In either event, one predicts that a mechanism-based inhibitor of the Trl1 ligase should selectively block fungal growth without affecting mammalian cells. By the same token, an antagonist of RtcB might be useful in transiently impeding the UPR for therapeutic benefit in human diseases involving endoplasmic reticulum stress (21). The availability of isogenic yeast strains with orthogonal tRNA splicing systems should enable differential cell-based screening for bioactive molecules that selectively inhibit growth by targeting Trl1 *versus* RtcB and vice versa.

REFERENCES

1. Tanaka, N., and Shuman, S. (2011) *J. Biol. Chem.* **286,** 7727–7731
2. Englert, M., Sheppard, K., Aslanian, A., Yates, J. R., 3rd, and Söll, D. (2011) *Proc. Natl. Acad. Sci. U.S.A.* **108,** 1290–1295
3. Popow, J., Englert, M., Weitzer, S., Schleiffer, A., Mierzwa, B., Mechtler, K., Trowitzsch, S., Will, C. L., Lührmann, R., Söll, D., and Martinez, J. (2011) *Science* **331,** 760–764
4. Filipowicz, W., and Shatkin, A. J. (1983) *Cell* **32,** 547–557
5. Laski, F. A., Fire, A. Z., RajBhandary, U. L., and Sharp, P. A. (1983) *J. Biol. Chem.* **258,** 11974–11980
6. Zofallova, L., Guo, Y., and Gupta, R. (2000) *RNA* **6,** 1019–1030
7. Schwer, B., Sawaya, R., Ho, C. K., and Shuman, S. (2004) *Proc. Natl. Acad. Sci. U.S.A.* **101,** 2788–2793
8. Zillmann, M., Gorovsky, M. A., and Phizicky, E. M. (1991) *Mol. Cell. Biol.* **11,** 5410–5416
9. Spinelli, S. L., Malik, H. S., Consaul, S. A., and Phizicky, E. M. (1998) *Proc. Natl. Acad. Sci. U.S.A.* **95,** 14136–14141
10. Weitzer, S., and Martinez, J. (2007) *Nature* **447,** 222–226
11. Ramirez, A., Shuman, S., and Schwer, B. (2008) *RNA* **14,** 1737–1745
12. Schwer, B., Aronova, A., Ramirez, A., Braun, P., and Shuman, S. (2008) *RNA* **14,** 204–210
13. Kato-Murayama, M., Bessho, Y., Shirouzu, M., and Yokoyama, S. (2005) *J. Mol. Biol.* **348,** 295–305
14. Jain, R., and Shuman, S. (2009) *RNA* **15,** 923–931
15. Brooks, M. A., Meslet-Cladiére, L., Graille, M., Kuhn, J., Blondeau, K., Myllykallio, H., and van Tilbeurgh, H. (2008) *Protein Sci.* **17,** 1336–1345
16. Torchia, C., Takagi, Y., and Ho, C. K. (2008) *Nucleic Acids Res.* **36,** 6218–6227
17. Harding, H. P., Lackey, J. G., Hsu, H. C., Zhang, Y., Deng, J., Xu, R. M., Damha, M. J., and Ron, D. (2008) *RNA* **14,** 225–232
18. Klassen, R., Paluszynski, J. P., Wemhoff, S., Pfeiffer, A., Fricke, J., and Meinhardt, F. (2008) *Mol. Microbiol.* **69,** 681–697
19. Sidrauski, C., Cox, J. S., and Walter, P. (1996) *Cell* **87,** 405–413
20. Gonzalez, T. N., Sidrauski, C., Dörfler, S., and Walter, P. (1999) *EMBO J.* **18,** 3119–3132
21. Hotamisligil, G. S. (2010) *Cell* **140,** 900–917
22. Amitsur, M., Levitz, R., and Kaufmann, G. (1987) *EMBO J.* **6,** 2499–2503
23. Nandakumar, J., Schwer, B., Schaffrath, R., and Shuman, S. (2008) *Mol. Cell* **31,** 278–286
24. Okada, C., Maegawa, Y., Yao, M., and Tanaka, I. (2006) *Proteins* **63,** 1119–1122
25. Sawaya, R., Schwer, B., and Shuman, S. (2003) *J. Biol. Chem.* **278,** 43928–43938
26. Wang, L. K., and Shuman, S. (2005) *RNA* **11,** 966–975

Supplemental Material

RtcB, a novel RNA ligase, can catalyze tRNA splicing and *HAC1* mRNA splicing *in vivo*

Naoko Tanaka, Birthe Meineke, and Stewart Shuman

From the Molecular Biology Program, Sloan-Kettering Institute, New York, NY 10065

Supplemental Figures S1 and S2.

Supplemental Figure 1

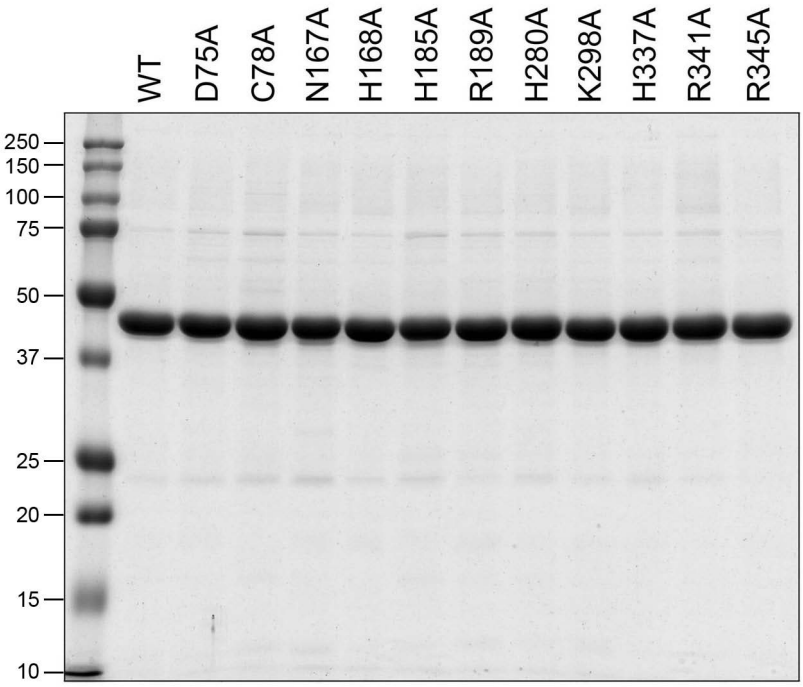

Fig. S1. **Alanine scanning mutagenesis of *E. coli* RtcB**. Aliquots (4.5 µg) of recombinant wild-type (WT) RtcB and the indicated RtcB-Ala mutants were analyzed by SDS-PAGE. The Coomassie blue-stained gel is shown. The positions and sizes (kDa) of marker proteins are indicated on the *left*.

Supplemental Figure 2

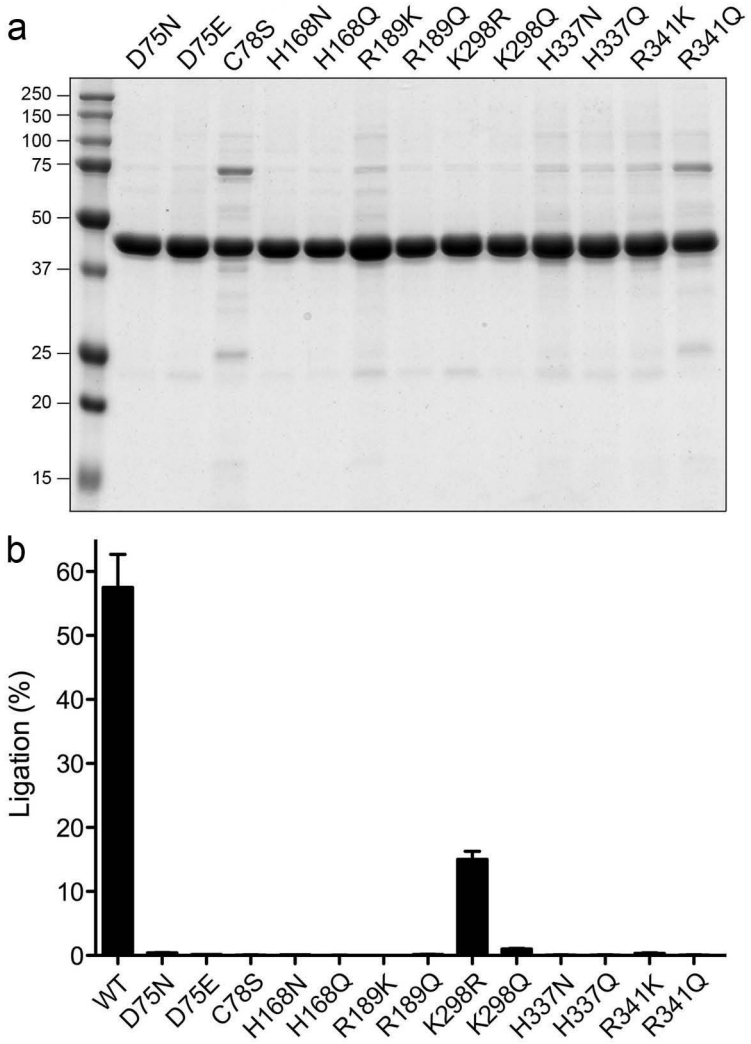

Fig. S2. **Effects of conservative mutations on RtcB activity**. (a) Aliquots (4.5 µg) of recombinant RtcB mutants as specified were analyzed by SDS-PAGE. The Coomassie blue-stained gel is shown. The positions and sizes (kDa) of marker proteins are indicated on the *left*. (b) RNA ligase reaction mixtures (10 µl) containing 50 mM Tris-HCl (pH 8.0), 2 mM $MnCl_2$, 100 µM GTP, 100 nM of 5'-^{32}P-labeled broken RNA stem-loop substrate, and 2 µM wild-type or mutant RtcB as specified were incubated for 30 min at 37°C. The extents of conversion of the radiolabeled 19-mer substrate strand into sealed 39-mer product (% ligation) are plotted. Each datum is the average of three separate ligation experiments ±SEM.